AN AUTOMATED OFF-LINE LIQUID CHROMATOGRAPHY/MASS SPECTROMETRY INTERFACE USING SOLID PHASE, TIME-OF-FLIGHT SECONDARY ION MASS SPECTROMETRY

A Thesis Submitted to

the Faculty of Graduate Studies

University of Manitoba

In Partial Fulfillment

of the Requirements for the Degree

Doctor of Philosophy

by

Ronald Charles Beavis

ISBN 0-315-37247-8

AN AUTOMATED OFF-LINE LIQUID CHROMATOGRAPHY-MASS SPECTROMETRY INTERFACE USING SOLID PHASE, TIME-OF-FLIGHT SECONDARY ION MASS SPECTROMETRY

BY

RONALD CHARLES BEAVIS

A thesis submitted to the Faculty of Graduate Studies of the University of Manitoba in partial fulfillment of the requirements of the degree of

DOCTOR OF PHILOSOPHY

This thesis is dedicated to my mother Anne Beavis.

ACKNOWLEDGEMENTS

I would like to thank my advisor, Dr. Ken Standing, for directing the research presented in this thesis. The concept for the work described was his: my part was the realization of the idea. He also provided me with a great deal of support, both materially and intellectually, during the work. Helpful advise and discussions on the chemistry involved in this thesis were provided by Drs. Dennis Main and John Westmore. Dr. Werner Ens provided me with a working mass spectrometer able to do the work. Without his data system and data analysis software, the actual taking of mass spectra and analyzing them would have been a much more laborious process. Drs. Bruno Schueler and Gerard Bolbach provided moral support.

I am greatful to Gail Imms for typing the longest (and most cryptic) manuscript she had ever worked on. The actual production of the manuscript was greatly assisted by the loan of an Atari 1040ST computer for use as a word processor, by Francois Lafortune.

Equipment and operating capital for the work described in the thesis was provided by the Natural Sciences and Engineering Research Council of Canada and the National Institutes of Health (USA). Financial assistance for myself was provided by the Natural Sciences and Engineering Research Council of Canada and the University of Manitoba.

I would also like to thank Gilles Roy for his frequent assistance in obtaining equipment for my experiments.

ABSTRACT

The design and construction of an automated off-line interface to couple a microbore high performance liquid chromatograph to the Manitoba TOF I secondary ion mass spectrometer is described. In particular, the details of adapting the electrospray sample deposition method to deposit the eluent of a microbore HPLC column are discussed.

While developing the interface, several changes were made to the electrospray method to improve sensitivity. A method of focussing the spray onto a small diameter spot on a substrate decreased the sample use for preparing targets for TOF SIMS by three orders of magnitude. A nitrogen flow past the spray needle increased the quasimolecular ion yields from deposits. The introduction of a hydrophilic aluminum hydroxide substrate (boehmite) greatly reduced the sensitivity of electrosprayed deposits to sodium contamination and increased the relative yield of protonated molecular ions in peptide samples.

The design of a microbore HPLC system is described, including details of the plumbing hardware and column packing procedures. Comments are made as to the reliability and efficiency of several column packing materials, in this application. The off-line interface was applied to the separation and identification of peptides produced by enzymatic (trypsin) cleavage of several parent peptides. The cleavage products expected were detected by the mass spectrometer. The fragment ions in the mass spectra were analyzed to give sequence information about the peptides. The amount of sequence information available was closely correlated with the stability of the

protonated molecular ion in the drift region of the spectrometer. The stability of a particular peptide appears to be a function of the residue sequence. The application of the interface to a fully protected peptide and to several steroid hormones is also discussed.

CONTENTS

CHAPTER I

Introduction

1.1) General Comments

This thesis details the development of an automated sample preparation system allowing the use of the total eluate of a high performance liquid chromatography column in the Manitoba time-of-flight mass spectrometer, without loss of chromatographic information. The meaning of this statement is the subject of this introductory chapter, while its realization is the subject of the subsequent chapters. The work carried out was based on preliminary discussions between Ken Standing and myself. Subsequent discussions and ideas were also provided by Dennis Main, Werner Ens and Bruno Schueler.

1.2) Development in the Mass Spectrometry of Organic Molecules

Over the last ten years there has been a great deal of interest in the mass spectrometry of organic molecules that were long thought to be incompatible with direct mass measurement. The mass spectrometry of smaller organic molecules has a long history, at least long in scientific terms. The salient point in this history (for the purposes of this thesis), was that up until twenty-five years ago, to be analyzed a molecule had to be volatilized into the gas phase at some stage prior to

ionization in a mass spectrometer's ion source. The limitation imposed by volatilization was that many molecules of interest to organic and biochemists are thermolabile, i.e. the molecules are destroyed by heating. This limitation, while being restrictive in the size of molecule examined, did not hold back the application of mass spectrometry to organic chemicals of many sorts. In fact, with the development of the chemical ionization method of ion production from gaseous organics, the mass spectrometry of such molecules must rank as one of the great success stories of modern applied science. The additional dimensionality produced by the use of gas chromatography in conjunction with mass spectrometry has revolutionized trace analysis because of the great dynamic range and sensitivity available in a conventional mass spectrometer and the enormous separatory power of gas chromatography. The purpose of this thesis is not, however, to detail the development of gas phase ion sources and ionization methods. Good reviews of these topics are easily obtainable [1,2,3].

The ionization methods relevant to this thesis were developed for use with solid phase samples. Ionization techniques using solid or liquid phase samples in the ion source eliminate the need for the volatilization of the molecule before ionization. The main requirement for a solid phase ionization technique to be useful in mass spectrometry is that the amount of energy transferred to the molecule by the ionization process must be relatively small. To see what small means in this context, it is necessary to distinguish between the three major types of energy that can be transferred to a molecule. These modes of energy are: 1) translational (ie. collective translation of the molecule;

2) vibration/rotational (v/r) motion, and 3) electronic excitation. When a molecule goes from the solid phase to the gas phase and is ionized, it is the translational energy that allows the molecule to leave the surface and it is electronic energy that ionizes the molecule. In addition to these mechanisms, electronic and vibrational energy can also lead to the dissociation of the molecule (fragmentation). A perfect solid phase ionization method would be one that ionized the molecule and added only a small amount of energy to the translational mode to volatilize the molecule. In reality, currently available solid phase ionization methods add energy into both the translational and vibrational modes. Therefore, there is a substantial amount of fragmentation.

The usefulness of a solid phase desorption/ionization technique can be assessed by the relative amount of energy put into the fragmentation producing channels. A qualitative description of the amount of fragmentation is frequently referred to as the "softness" of a technique. A "soft" ionization method leads to intense molecular ions and few fragments. A "hard" ionization technique produces copious fragments and few if any, molecular ions. The exact definition of "hard" and "soft" is not particularly important and in practice, any technique producing intact molecular ions as measured by a mass spectrometer is "soft" enough.

The first technique "soft" enough for large organic molecules was field desorption [3,4]. In this process, a very fine needle tip is coated with the sample of interest. The needle is then placed in the ion source of a mass spectrometer and the needle raised to a very high electrostatic potential. Due to the very small radius of curvature of the needle tip, the electric field strength at the tip is very large.

The needle is heated moderately and ions corresponding to the intact molecule are emitted from the tip into the gas phase and then enter the mass spectrometer. From the lack of fragment ions observed under these conditions, field ionization is considered to be one of the softest forms of desorption/ionization. The method has been used analytically but not widely. A problem with field ionization is the reproducibility of sample preparation. The fabrication of the needles required and loading sample onto these needles requires a technician who is "good at it" [5,6]. Even with such a technician, the reproducibility of the emitters is frequently low. This lack of reliability has discouraged the use of field desorption ionization and prevented it from becoming a fixture in the typical analytical laboratory.

The methods that have been successful in attracting wide attention and use are those involving different types of radiation to desorb and ionize molecules from a surface. The first radiation induced desorption method successfully applied to mass spectrometry used low energy ions (keV/u). Starting with discharge bombardment of electrodes [7] and developing into the use of focussed ion beams, primary ion bombardment has been used to desorb and ionize secondary ions characteristic of the atomic makeup of inorganic solid surfaces for many years [8,9]. The process by which secondary ions are produced from the surface is called sputtering. Under normal ion beam conditions (1 $\mu A/cm^2$), only atoms and small fragments of larger molecules are present as secondary ions. The use of primary ion beams to produce secondary ions and to erode solid surfaces for depth profile analysis is well accepted in the industrial community for the analysis of semiconductor materials, under the acronym of secondary ion mass spectrometry (SIMS).

A particle bombardment technique that has shown excellent results for organic materials is fission fragment bombardment. Macfarlane, et al. [10, 11] noticed that when an organic material was struck by a fission fragment from a spontaneously fissioning ^{252}Cf source, mass spectra of large (3,000 u) molecules have been observed. The spectrometer operates by using the recoiling fragment of the pair produced by fission as the start signal for time-of-flight electronics. The molecules and fragments desorbed from the sample surface are then accelerated by a uniform electric field and drift down a flight tube. Using fast timing electronics originally designed for nuclear physics, the flight time of the individual ions produced can be recorded. This experiment is repeated many times and the results of the experiments are histogramed to produce a mass spectra. Fission fragment mass spectrometry (also referred to as plasma desorption mass spectrometry) has shown itself to be a reliable method for the analysis of large (5,000 u) polar molecules. Instrumentation to perform an analysis using fission fragments has only recently come onto the market, developed by Bio-Ion, Inc. With the availability of a relatively inexpensive commercial instrument, fission fragment mass spectrometry may become a standard technique for the determination of the molecular weight of high mass peptides.

Another particle desorption method uses high energy ions, with energies on the order of 1 MeV/amu, produced by heavy ion accelerators [12, 13]. The results of using high energy ions are very similar to those produced by fission fragments (fission fragments are high energy ions) and are also qualitatively similar to those produced by low energy ions. While using high energy ions is of interest for basic experiments

where the ability to change the charge state and the energy of the primary particle is important, for practical analytical work fission fragments are superior because not every laboratory has a heavy ion accelerator at its disposal.

The use of SIMS for desorption of organic molecules was pioneered by Benninghoven [14]. He discovered that it was possible to produce ions characteristic of intact large organic molecules if the primary ion flux was kept very low ($\simeq 1$ pA/cm^2). The higher beam fluxes used in sputtering rapidly damaged the surface by well understood mechanisms of radiation damage, leading to a jumble of fragments on the surface before a mass spectrum could be accumulated. The use of very low flux primary ion beams was called static SIMS, to accentuate the fact that very little material was being sputtered off the surface. The higher flux mode was then referred to as dynamic SIMS.

A variation on the SIMS method of desorption has recently become very popular with mass spectrometrists using magnetic sector instruments. Introduced at the American Society for Mass Spectrometry's 1981 meeting in Minneapolis, Minnesota [15], this variant is called fast atom bombardment (FAB). FAB uses keV energy atoms as the primary particles in place of keV primary ions. The advantage of using atoms is that a typical sector mass spectrometer has magnetic and electric fields in and around the ion source. In order to pass an ion beam into the ion source it is necessary to either shield it from these fields or design a different primary ion source for each type of mass spectrometer. A beam of atoms, however, is undisturbed by the presence of these fields. So long as there is a line-of-sight access to the sample in the ion source it is possible to attach a standard type of atom beam source to any

commercial instrument. Such atom beam sources have been a great success from the commercial standpoint. Physically, there is little difference between bombarding the surface with an ion or an atom, as the primary particle gains an equilibrium charge state characteristic of its velocity almost immediately upon encountering the sample surface. The similarity in spectra obtained by SIMS and FAB confirm the similarity in mechanism.

A significant advance made with the introduction of FAB was the use of a liquid sample matrix [16], rather than a simple, dry solid. As mentioned above, the limitation on secondary ion production from a solid surface in SIMS is the radiation damage produced on the surface by the primary ions. Therefore, the molecular ion signal from a surface will decrease with time as the top few molecular layers become damaged. If the sample being studied is first dissolved (or at least suspended) in a viscous liquid with a very low vapour pressure, it is the surface of the solution (or slurry) that is analyzed. When the drop of liquid is placed in the primary beam, the surface layer will become damaged as in the solid case. The liquid surface layer will not, however, remain static; desorption, convection and evaporation quickly remove the damaged layer from the surface, exposing a fresh, undamaged surface to the beam. A result of the continual refreshing of the surface is that the limitation on primary beam current imposed by radiation damage is removed. Therefore, higher primary beam currents can be used, and concomitantly, higher secondary ion currents can be obtained. This increase in the number of secondaries produced by a single sample can be very important for applications involving sector field and quadrupole mass spectrometers

as these instruments require relatively large stable secondary ion currents. The application of FAB and liquid matrix methodology to organic mass spectrometry has become the subject of a large and steadily growing body of literature [17, 18, 19]. FAB has become the method of choice for small to medium sized biopolymers (100 - 5000 u) as well as many other organic molecules in this mass range.

In SIMS, FAB and fission fragment mass spectrometry, an important aspect of producing ions from a sample is the proper preparation of the material before it is placed in the mass spectrometer. The introduction of low levels of ionic impurities (eg. alkali metal cations at the ppm level) can distort relative intensities of the ions representative of the intact molecule and its fragments or can produce new ions due the cationization of the molecule that dominate the mass spectrum. Traces of particularly easily ionized organic molecules (eg. phthalate plasticizers; which are, for practical purposes ubiquitous) can also distort spectra by occulting the peaks of interest. Liquid matrix samples are also subject to the vagaries of preparation. The matrix used for a given molecule is dependent on the functional groups in that molecule. A fairly wide range of choice in liquid matrices classified as to what functional groups they are compatible with is available in the literature in "cookbook" form [20]. More will be said about sample preparation throughout this thesis.

A method related to particle induced desorption is laser induced desorption. A solid surface bombarded by photons, under the right conditions, will yield a large number of secondary ions. This effect has been used to develop commercial microanalysis machines, such as the LAMMA

500 and LAMMA 1000 [21, 22]. The LAMMA instruments use a short pulse of well focussed laser light to desorb organic and inorganic ions from a small area of a sample. The ions are then analyzed by time-of-flight, using transient recorder electronics. The main difference between laser ionization and particle induced desorption is the energy deposited in the secondary ions. Laser desorption produces ions with a larger amount of fragmentation and higher translational energies than particle induced desorption. It is therefore not as "soft" an ionization method. The problem seems to be that the amount of energy in the laser beam necessary to achieve desorption of neutral molecules is much lower than the energy necessary to desorb ions. The additional energy necessary to achieve ionization also seems to excite modes in the molecules that lead to fragmentation.

A recent development in the laser desorption field has rekindled interest in the use of lasers in mass spectrometry. Schlag, et al. [23, 24] have developed a unique system overcoming the lack of "softness" discussed above. A pulsed CO_2 laser is used to desorb molecules from a solid sample. The molecules desorbed are neutral; the photon flux used is too low to produce ionization. The desorbed molecules are then collisionally cooled in a supersonic gas jet that sweeps the molecules into the ion source of a time-of-flight mass spectrometer. The molecules are then ionized in a small region of space by a finely focussed laser beam from a tunable dye laser. The laser frequency is tuned to produce resonant ionization of a particular functional group in the molecule of interest. Using an ion mirror to remove to first order the effect of excess translational energy in the time-of-flight of the molecule [25],

mass resolutions of m/ m = 6,000 - 10,000 (FWHM) have been achieved. Resonance enhanced multiphoton post-ionization used in this manner show great promise for increasing the selectivity and dynamic range of desorption techniques and will certainly be a topic of intense research in the next few years.

1.3) Development of High Performance Liquid Chromatography

Liquid chromatography began as a slow, low resolution method of separating a dissolved mixture into its constituent components (see the excellent historical over view by L.S. Ettre for details [26]. The attraction of the method to chemists was that there was no other method available to do this. While liquid chromatography remained a relatively static field until the late 1960's, a related technique, gas chromatography, was developed in the late 1950's. In gas chromatography, rather than separating a mixture of components dissolved in a liquid, the approach was to separate a mixture of gases. A "carrier" gas and volatile analytes were forced down a thin tube under pressure. The walls of the tube (column) were coated with adsorbing material that had the effect of retarding the flow of those molecules in the gas stream that interacted with it. Therefore, if the volatile molecules to be analysed were added to the carrier gas flow as a "plug" of analyte would separate into several smaller plugs (or more properly, bands) due to the action of the adsorbant on the column walls. Providing that the column had sufficient resolution, each substance in the original mixture would

separate out as one band and come out of the end of the column at a characteristic time, referred to as the substance's retention time. If the end of the column was inside of a mass spectrometer's ion source, each of the eluting bands could be examined with the mass spectrometer and the molecules making up the bands could be identified. This wedding of gas chromatography to mass spectrometry (usually referred to as GC-MS) has been very successful in the analysis of complex mixtures of volatile chemicals and has allowed the detection limits for important environmental contaminants [27] (such as pesticides) to be greatly improved. However, many important classes of organic molecules are involatile and cannot be made volatile by derivatization. To examine involatile molecules, improvements in liquid chromatography were necessary.

Over the past twenty years, the development of high performance liquid chromatography has been little short of amazing. Starting out as a development technique, in response to the theoretical ideas of Giddings [28] and others in the early sixties, rapid improvements and changes were made by a range of eminent scientists, such as Cs. Horvath, J.J. Kirkland, R.P.W. Scott, L.R. Snyder, G. Guichon, B.L. Karger and J.H. Knox - to name a few. Due to their work, the low resolution technique of liquid chromatography in use up until that time was radically changed into a reliable technique with two orders of magnitude better resolution. Suddenly, organic chemists had at their disposal a methodology for separating high molecular weight, non-volatile molecules on the basis of hydrophilic interactions (reverse phase chromatography) or absorbent properties with respect to silanol (normal phase chromatography). The

ability to separate large, polar molecules on the basis of retention time has made high performance liquid chromatography an indispensable technique in many chemistry laboratories. The clinical applications of the technique are also broad, greatly improving the sensitivity and speed of blood and urine tests for trace substances.

High performance liquid chromatography's development paralleled the progress made in gas chromatography in the 1950's and early 1960's. A natural progression along this parallel would be the coupling of liquid chromatography with mass spectrometry, analogous to the coupling of gas chromatography to mass spectrometry. Gas chromatography-mass spectrometry has been very successful in making the rapid routine analysis of complex mixtures of volatile molecules a common procedure. Hopefully, liquid chromatography-mass spectrometry will allow the same analytical convenience for involatile molecules.

(1.4) Our Instrument and LC-MS

A mass spectrometer in use in our laboratory is the Manitoba TOF I time-of-flight mass spectrometer. The Manitoba TOF II mass spectrometer is now operational but was not designed initially for use with chromatographic eluent. Manitoba (I) has been thoroughly described in the literature [26, 27]. The primary ion gun is shown in Figure 1.1. A primary ion beam is produced by a filament coated with an aluminosilicate-alkali metal compound usually referred to as a beta-eucriptide. The ions are accelerated to approximately 20 keV, collimated and focussed onto a slit. By applying properly timed high voltage pulses to the deflection plates, the ion beam is rapidly swept

past the slit, producing a pulse of ions after the slit. The time width of the ion pulse produced is on the order of 3 nanoseconds. The pulse of ions passes through a field free region and then goes through the secondary ion acceleration grid (at ground) and is decelerated (or accelerated) by the secondary ion accelerating voltage. Therefore, the total energy of the primary ion when it impinges on the sample is the primary ion energy accelerating energy, plus/minus the secondary ion accelerating voltage. The deflection plates shown just after the slit allow the beam to be moved vertically on the sample.

The sample introduction system of the spectrometer is shown in Figure 1.2. The samples are mounted on flat metallic targets, approximately 1 centimeter in diameter, mounted on small cylinders that fit into an insulating ladder. The ladder has a central region made of machinable ceramic (Macor) and stainless steel end pieces for strength. The top and bottom of the ladder have brass rails and the top has a brass rack, driven by a brass pinion inside of the instrument. Five sample substrate/cylinder assemblies can be mounted onto the ladder at a time and loaded into a side arm on the main vacuum system. Using the rack and pinion described above, the ladder is slid into the main vacuum system and positioned so that the target of interest is in line with the ion beam. A spring loaded contact makes the high voltage connection to the cylinder from behind the ladder, allowing the voltage of the substrate to be raised to several kilovolts (practical maximum voltage is 10 kV). A 60% transmission nickel grid, permanently fixed approximately 3 millimeters from the target provides the ground electrode.

Figure 1.1

Detailed drawing of the pulsed primary ion gun in Manitoba I.

a) ceramic standoff
b) shield
c) filament
d) cathode plate
e) collimator
f) einzel lens
g) vertical deflection plates
h) horizontal deflection plates
i) slit
j) vertical positioning plates
k) acceleration grid
l) sample on substrate

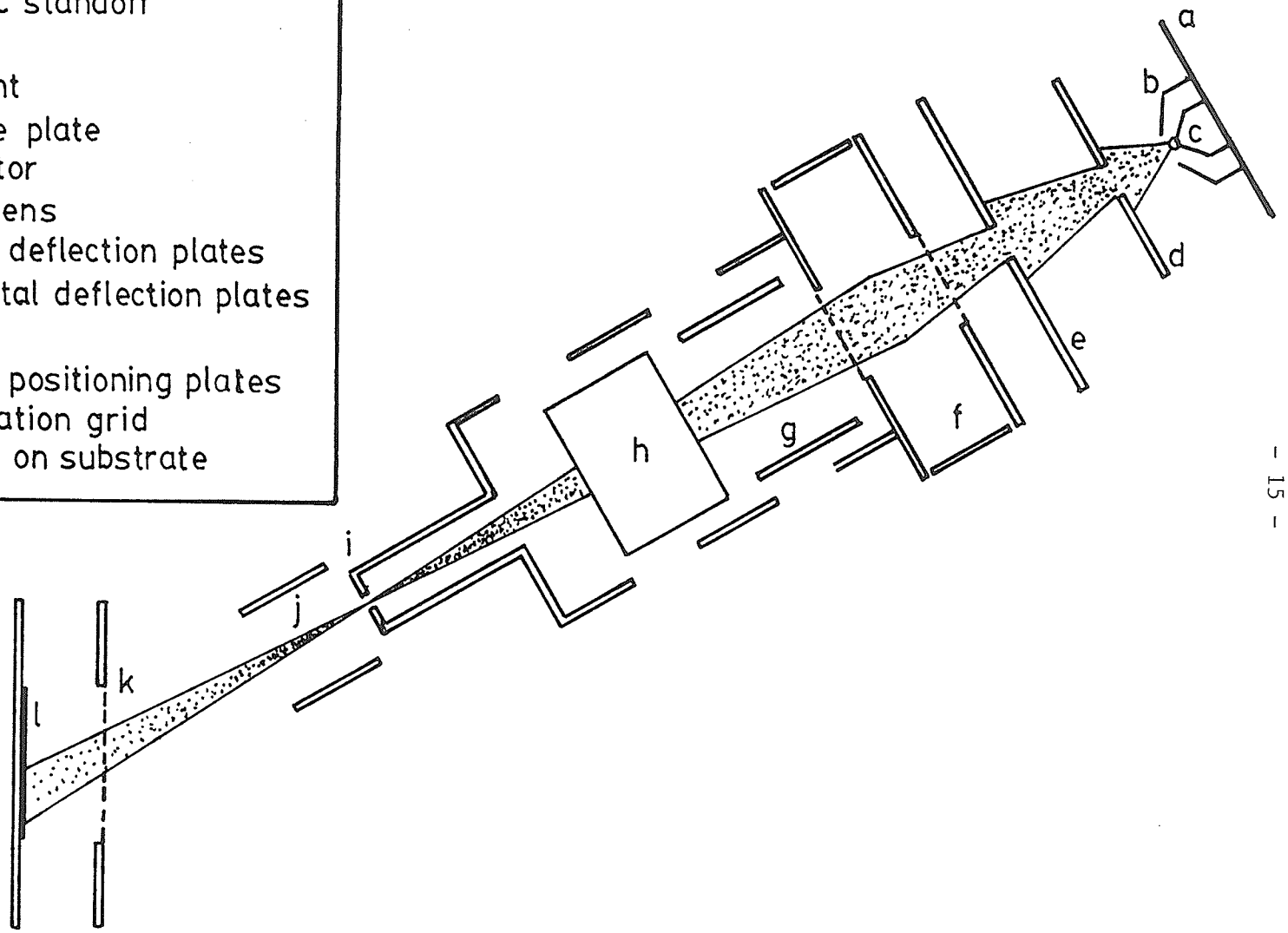

An overview of the electronics used in the spectrometer is shown in Figure 1.3 [33, 34]. A clock signal from a quartz controlled oscillator starts the sequence. A pulse is sent to the shield surrounding the filament source allowing the beam to be extracted for several microseconds. The beam is then pulsed, using the primary pulsing plates shown in Figure 1.1. The pulse strikes the selected sample, causing the desorption of neutral and charged particles. The charged particles selected by the high voltage polarity on the sample are accelerated towards the nickel grid, pass through and drift down the flight tube. It is important to note that after an ion has passed the grid no further active changes are made to an ion's velocity. Therefore, if an ion dissociates into two daughter ions in the flight tube - as is often the case for large organic molecules - the two daughters continue down the flight tube with the same center-of-mass velocity as the parent. On reaching the end of the flight tube, the ions are detected by an assembly, of two microchannel electron multiplier plates, (configured in the"chevron" pattern), and a collector plate. The output pulse produced is impedance matched by a fast preamplifier and converted into a NIM standard pulse by a constant fraction discriminator. The discriminator pulse is used as the stop pulse for a time-to-digital convertor with the possibility of 8 stop signals per start. After the experiment (i.e. the events caused by one initial ion pulse), the ion transit times recorded by the digitizer are moved into a fast preprocessor (both digitizer and preprocessor are resident on a CAMAC bus) and histogramed. The histogram is then available to the main controller computer, an LSI PDP 11/23. There the histogram can be displayed and stored. The experiment

Figure 1.2

Front and end view of the introduction mechanism in Manitoba I.

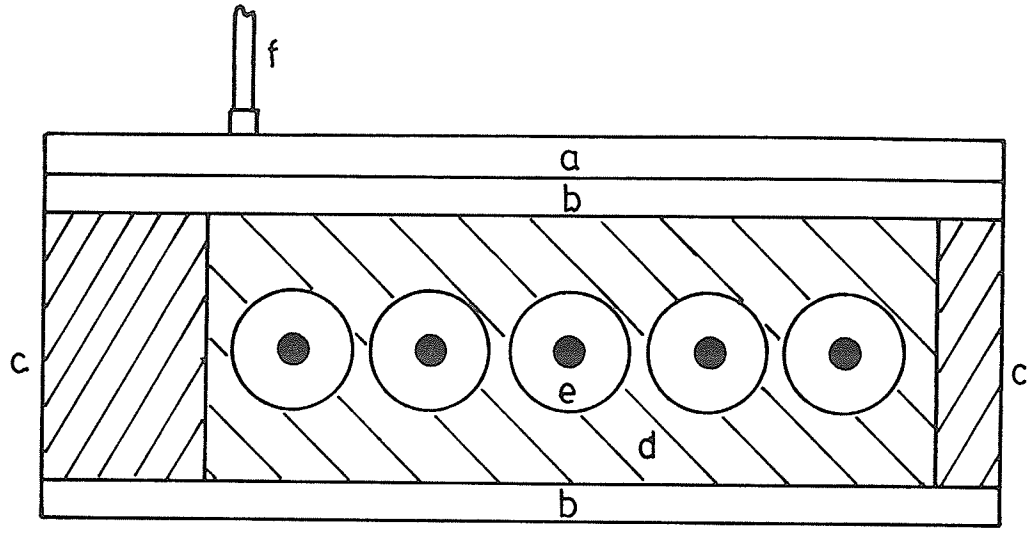

Front View

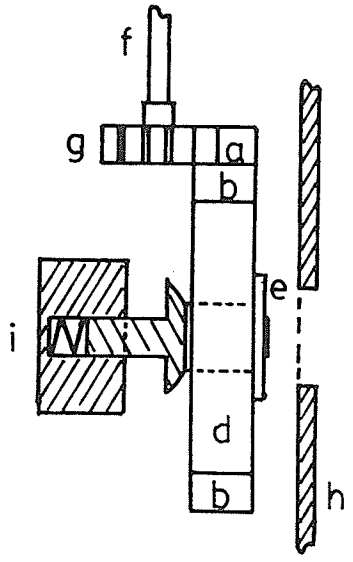

End View

a) rack
b) brass rail
c) stainless steel insert
d) ceramic (Macor)
e) sample holder
f) drive shaft
g) drive gear
h) acceleration grid (X-section)
i) high voltage contact assembly (X-section)

described above is repeated many times to accumulate a good mass spectrum, at the rate of 2,000 experiments per second.

The mass spectrometer described above clearly has requirements that differ from a conventional magnetic mass spectrometer. The method of sample introduction suggested to us a rather simple methodology for introducing chromatographic eluent:

i) deposit the eluent from a chromatograph in fractions along the centre of a strip of conductive material;

ii) mount the strip onto a modified sample ladder;

iii) using the rack and pinion drive described above, position the fractions on the strip into the ion beam sequentially;

iv) record mass spectra of each of the fractions.

If the current secondary ion source geometry was maintained, only slight modification of the instrument would be necessary to accommodate the "strip" of conductive foil. Therefore, the major problem is making the off-line interface becomes depositing the chromatographic eluent in a form compatible with SIMS, rather than how to introduce the eluent into the mass spectrometer. The problems of sample deposition and chromatograph design are discussed in detail in Chapters 2 and 3.

1.5) Off-line Versus On-line Interfaces

Interfaces to combine liquid chromatography with mass spectrometry can be broadly categorized into two distinct types, on the basis of the way in which the temporal information given by HPLC retention time is maintained in the process. One method of maintaining temporal

Figure 1.3

Overview block diagram of the electronics for Manitoba I.

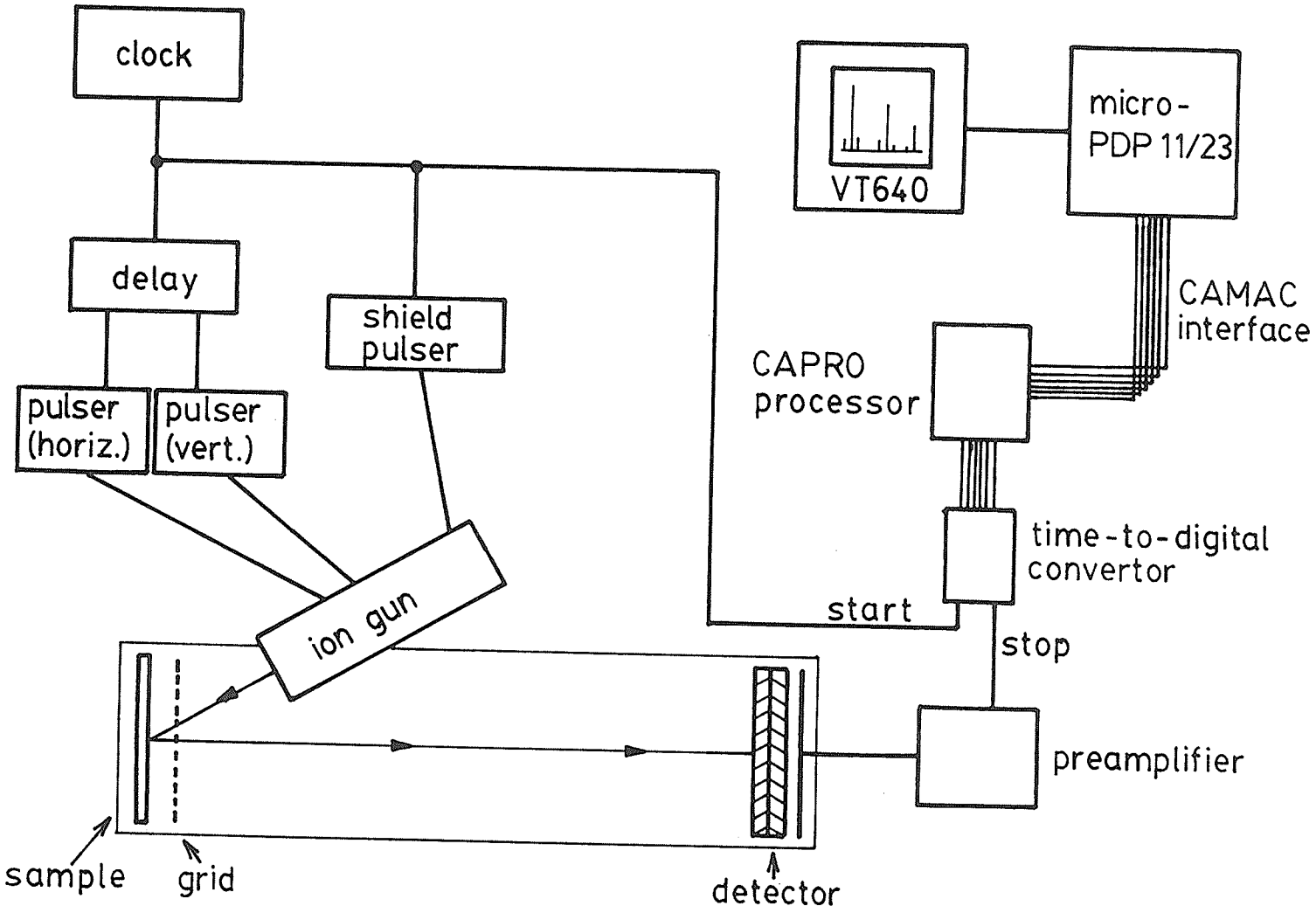
clock
delay
shield pulser
pulser (horiz.)
pulser (vert.)
ion gun
sample
grid
detector
start
stop
VT640
micro-PDP 11/23
CAMAC interface
CAPRO processor
time-to-digital convertor
preamplifier

information is to use the mass spectrometer as an outlet flow detector for the HPLC column, i.e. the eluent is analyzed in real time as the HPLC run progresses. There may be some small time delay between elution and mass analysis, but in general the mass spectrometer and the chromatograph are synchronous. A system operating in this way is called an on-line system. The methods described in Section 2.2 are on-line interfaces.

The other method of maintaining the temporal information available from an HPLC column involves the collection of fractions. Discrete portions of the chromatograph eluent are collected separately, in a location remote from the mass spectrometer. These fractions are then treated to make them compatible with the mass spectrometer, usually by the removal of volatile solvents. Therefore, in this mode the HPLC column and the mass spectrometer operate separately and the data rate of the two devices are decoupled, implying that one type of analysis can take longer than the other. The term assigned to this type of interface is off-line.

There has been considerable debate about the practicality of on-line interfaces versus off-line interfaces for LC/MS. The current ideal in the research community is the on-line interface [29]. Contributing to the preference for an on-line technique is the success of on-line gas chromatography - mass spectrometry. It was initially hoped that a similar success in the analysis of non-volatile organic compounds would be produced by the development of an on-line LC/MS interface. The analogy between the two techniques is only skin deep, unfortunately. Even the best HPLC columns only achieve on the order of twenty thousand theoretical plates when used routinely (one million plates has been

achieved, but the retention times are measured in days rather than minutes [30]). As well, the solvents used as the mobile phase in HPLC contain many more impurities than the carrier gases used in gas chromatography, leading to contamination and signal-to-noise problems. Another problem, of no small consequence, is that the vacuum systems of most mass spectrometers are not capable of handling the introduction of milliliters of solvent per minute without special pumping alterations. Thus, the marriage of liquid chromatography with a mass spectrometer is not as simple as was the marriage of gas chromatography.

The case for on-line interfaces was posed by Karger and Vouros [29] in a recent paper. The main points in their argument were that on-line interfaces, as opposed to off-line interfaces, have the following advantages:

i) convenience, particularly for multi-component mixtures;

ii) higher speed of analysis (important for clinical applications);

iii) reduced sample loss, or at least the reduced possibility of sample loss;

iv) easier deconvolution of partially resolved chromatographic peaks;

v) reliable evaluation of chromatographic peak purity over the entire peak;

vi) accurate quantitation using isotopically labelled internal standards.

It is worth noting that only points (i) and (ii) are specific to on-line interfaces. The other points (iii) - (vi) apply to LC/MS interfaces generally.

A case can also be made for off-line interfaces. Using the particular example of the interface that is the subject of this thesis, ie. an off-line interface involving deposition of fractions onto a metallic substrate and then sequential analysis of these deposits by SIMS, the following advantages can be listed:

i) inexpensive;

ii) compatibility with solid phase SIMS, particularly time-of-flight SIMS;

iii) no changes in vacuum systems are required;

iv) no high temperatures required to achieve evaporation, reducing damage to thermolabile molecules;

v) no loss of sample (all non-volatile material deposited);

vi) samples available for further analysis after SIMS.

Clearly, because our laboratory is engaged in time-of-flight SIMS, point (ii) would seem to be almost a sufficient argument for our choice of off-line LC-MS. However, our method (described in the previous section) takes advantage of point (v) as well, i.e. no sample loss. The use of microbore HPLC (see Chapter 2) and the deposition of the entire involatile portion of the eluent should result in increased sensitivity, hopefully approaching the very high sensitivity of static SIMS when applied to pure materials (0.1-10 picomoles). This sensitivity would allow the application of the technique to samples of limited size, which can be very important for biological applications where the "world supply" of a chemical may be one or two micrograms.

In addition to points (i) - (vi), our method of LC-MS has the feature of decoupling the data rate of the HPLC and the mass spectrometer. On-line techniques are limited to the mass spectrometer running syncronously with the HPLC. This enforces a limitation on the MS techniques that can be applied: not only must one be able to collect and store mass spectra as quickly as HPLC peaks elute, but there is no possibility of re-examining an interesting chromatographic band under different MS conditions (e.g. higher mass resolution or larger mass range). Our method of off-line analysis removes the restriction of the HPLC and the MS running at compatible rates. This is to our advantage, as time-of-flight MS usually takes several minutes to collect and store spectra. Spectra can, however, be run in as little as thirty seconds. Therefore, a preliminary scan of a chromatogram can be done quickly and interesting fractions re-examined at leisure, to accumulate better spectra of important components.

CHAPTER II

Our Approach to LC/MS

2.1) General Comments

The discussion given above (Section 1.4) demonstrated the interest in liquid chromatography combined with mass spectrometry (LC/MS). When we became interested in the possibility of adding HPLC capability to our laboratory, several decisions had to be made about the type of HPLC hardware to purchase, the columns to be used and the method of combining the HPLC eluent with the particular needs of our mass spectrometer. The rest of this chapter discusses how these decisions were made, and the results of the decisions. The arguments that are presented are in a few cases the product of hindsight, rather than those originally set forward, but for the purposes of this thesis the final, better considered arguments are presented.

Our laboratory became interested in liquid chromatography as a possible method of purifying organic and biological samples for subsequent mass spectrometry. Important samples, particularly those derived from biological sources, usually are unsuitable for the direct application of mass spectrometry. These materials must go through several stages of purification after production (or extraction) in order for them to be in a pure enough form to be useful for mass spectrometry. If impurities are present, the mass spectra that result may be significantly different from those of the pure compound. The changes in

a mass spectrum are not merely a linear superposition of the mass spectra of each component of a mixture taken separately. The presence of an impurity, in rather small concentrations, may totally suppress the secondary ion yield of the compound of interest, or may produce adduct ions making the interpretation of the spectrum difficult. Therefore, it would be advantageous for a laboratory analyzing such materials to have some capability for removing impurities. Liquid chromatography would seem to be a natural method for separating sample from impurity. Samples sent to the laboratory for analysis could then be re-purified before analysis. As well, it would provide a standard method for sample preparation, by which soluble biochemicals could be prepared reproducibly. The importance of this point will become clearer after the discussion in Chapter 4 on sample deposition.

2.2) On-line LC-MS Interfaces

Two different strategies have been pursued for the development of on-line LC-MS interfaces. The first type developed involved the deposition of a sample from solution onto a substrate (a metal wire/or ribbon) and then rapidly moving the substrate into the ion source of a mass spectrometer through a region of differential pumping. The deposited sample would then be heated and the evaporated sample examined by electron impact [35, 36]. Further development of this type of interface led to the use of primary ion beams [37] and primary atom beams [38] for desorption and ionization. Commercial interfaces based on mechanical transfer into standard electron impact ion sources are available [39]. The main drawback of moving belt interfaces has been

that the desorption/ionization methods employed have not allowed the use of truly involatile materials in the eluent (except for [38]).

The second type of interface developed involves volatilizing the molecules directly from the liquid eluent and introducing the gas into the ion source. The most successful of the many such interfaces reported in the literature (see [40] for a review of these methods) are:

1) direct liquid introduction (DLI) - a split of the eluent is passed through a heated pin hole into the ion source [41];
2) monodisperse aerosol generation (MAGIC) - eluent is nebulized by a carrier gas at atmospheric pressure and swept into a atmospheric pressure ion source [42];
3) thermospray - the rapid heating of the eluent in a tube near an outlet nozzle, causing a rapid volatilization of the eluent and a spray into a rapidly pumped ion source [43];
4) electrospray - the eluent is made into a charged aerosol by passing it out of a needle set at a high potential. The aerosol is then dried and the ions introduced into the ion source [44].

All of the above methods are based on the production of a very fine aerosol which can be rapidly dried in the ion source vacuum.

There has been considerable success using the above four types of introduction for the analysis of large molecules. Direct liquid introduction has been used for drug analysis [42, 43] and commercial apparatus is available. MAGIC has only recently become available commercially and little practical application work has been done. Thermospray, since its introduction, has become the favorite method of LC-MS coupling and new papers on its applications are published every

month. There are several models of commercial thermospray equipment on the market. Electrospray is perhaps the most exotic of the techniques. Only one interface capable of accepting chromatographic eluent has been produced [44] and the results from the apparatus have been very promising.

Any technique that introduces milliliters per minute of chromatographic eluent directly into the ion source of a mass spectrometer has problems associated with vacuum pumping. The MAGIC interface, where the aerosol formation is done at atmospheric pressure and enters the mass spectrometer through a rather large hole directly into the vacuum system, requires very large, high capacity cryopumps. Thermospray requires sufficient pumping to remove almost a milliliter per minute of liquid water from the eluent flowing in. To put this in perspective, one milliliter of water corresponds to approximately 20,000 liters of saturated vapour at 0.05 mbar pressure. Direct liquid introduction and electrospray both use substantially less eluent, on the order of 10 ul/minute.

A mechanism involved in ion formation from these evaporated aerosols has been proposed. As the droplet decreases in size, the surface charge density increases until field ionization of the molecules of interest takes place at the surface [45]. Another mechanism determining the ions seen in the mass spectrometer appears to be ion-molecule reactions in the high pressure source region of the source [46]. Thermospray sources frequently use an electron beam passing through the spray jet after the aerosol has been largely volatilized to produce the same effect as the electron beam in a chemical ionization source. Electrostatic fields are also set up by a repeller plate, perpendicular to the extraction field, to trap ions near the extractor.

The trapping produces a region of high concentration of reactive ions to form just below the extraction orifice. The use of an electron beam (referred to in thermospray literature as the "filament on" condition) is necessary for many classes of compounds which do not yield significant amounts of pseudo-molecular ions without it [47].

Note: For a more complete listing of the many excellent papers on on-line LC/MS, see Appendix C.

2.3) Column Type: Wide Versus Narrow Bore

Chromatography columns are generally classified on the basis of internal diameter (bore). The somewhat arbitrary names usually assigned are given in Table 2.1, along with the inside diameter and current uses of the different column types. The practical differences in operating the various types of column are the amounts of solvent flow necessary and the amounts of sample used to produce a given separation.

Before discussing the selection of the HPLC column diameter to be used for our interface, it would seem appropriate to include a brief discussion of the principles on which HPLC is based. A liquid chromatography column is generally a tube containing some type of particulate packing material. A solvent (referred to as the mobile phase) is run through this packing tube, (the packing material being referred to as the stationary phase). If a small amount of a sample mixture is introduced into the solvent flow at the inlet (or top) of the column, the sample mixture is swept through the column by the solvent and arrives at the outlet of the column as a "plug" or band (analogous to the discussion of gas chromatography in Chapter I). The large surface area of the packing material allows the sample mixture intimate contact with

the packing's surface. In the simplest case, if there is some adsorption of sample molecules to the surface of the packing, those adsorbed molecules will be slowed with respect to unadsorbed molecules in the initial band of sample and will form a new band that elutes from the column later than the band of unadsorbed material. The time it takes an unadsorbed band to elute is termed the "void time" of the column. The time it takes for a partially adsorbed bank to elute is the "retention time" of the particular chemical in that band. Therefore, a mixture of chemicals in the original sample will be separated by the column into many bands on the basis of a chemical's adsorption behavior. This type of chromatography is called elution analysis normal phase chromatography. The adsorbants (packings) used for this application are stable, polar surfaces such as silanol (Si-OH) and the mobile phases are stable, non-polar solvents such as hexane or benzene. The "high performance" in HPLC refers to the use of high pressures (10 MPa) and small diameter porous packing materials to improve the resolution of the analysis.

Normal phase HPLC cannot be applied to highly polar analytes, however, because rather than elute, these materials are permanently adsorbed to the polar stationary phase. A new type of packing material was developed to use for polar molecules. The highly adsorbant silanol surface was coated with long, non-polar hydrocarbon chains. Therefore, the surface became hydrophobic rather than hydrophilic. Such packing materials are called reverse phase packings. If an aqueous mobile phase was used, mixtures of polar molecules could be separated using these packings. It is important to note that the interaction between the reverse phase packing material and the analyte molecules is not adsorption. The aqueous solvent prefers to exclude the hydrophobic portion of a large analyte molecule from the mobile phase to reduce the

entropy of the solvent surrounding the molecule. Therefore, it is favoured to have the analyte in the non-polar environment of the stationary phase surface. The competition between the solvation of the polar portion of the analyte molecule and the entropy reduction produced by excluding the molecule from the solvent determines the retention time.

To understand the criteria for choosing a column diameter for our work, it is necessary to understand the basic parameters that are important in quantifying an HPLC column's behavior. The early development of HPLC theory used a simplistic model that divided the length of a column into a large number of identical cells, referred to as theoretical plates. Assuming a simple time delay on each plate, caused by adsorption, a model can be developed producing separated bands at the end of the column, with each band having a Gaussian concentration profile. The early success of this simplified model has led to the use of its parameters in practical discussions of column behavior. The most basic parameter is the column efficiently, i.e. the ratio of analyte retention time to band width. This is related to the number of theoretical plates (N) necessary to produce such an efficiency by:

$$N = 16\ (t_r/w)^2 \qquad (2.1)$$

where t_r is the retention time and w is the base width of the peak. The resolution of a column (as opposed to the efficiency) refers to the ability to resolve a particular mixture of two compounds with relatively close retention times.

Another parameter frequently used in HPLC is the "capacity factor"

TABLE 2.1

Types of HPLC columns, classified by internal diameter

Column i.d. (mm)	Common Name	Purpose
>10.0	Preparative	Refining large quantities of sample
4.6	Analytical	Refining small quantities of sample/ analysis of samples
2.0	Small Bore	Analysis of samples (used to reduce solvent use)
0.25 - 1.0	Microbore	Analysis of samples (experimental)
0.25	Capillary	Experimental use only

(k') for an analyte. This is simply the difference between the retention time of a particular substance and the void time (t_0), normalized to the void time:

$$k' = \frac{t_r - t_0}{w} \qquad (2.2)$$

It is usually the capacity factor for a compound that is quoted in the literature rather than the retention time, because the capacity factor is, at least to first order, independent of the solvent flow rate and the column length.

The parameters discussed above are independent of the column on which the parameters were measured, i.e. none of the physical dimensions of the column have been taken into account. In order to relate these parameters to the resolution, the column efficiency must be expressible in terms of measurable physical variables. The efficiency, or number of theoretical plates, is not normally used in such calculations. It is much more convenient to use the height equivalent of the theoretical plate, H:

$$H = L/N \qquad (2.3)$$

where L is the length of the column bed. In order to reduce the number of constants in the expression relating H and the linear velocity of the eluent u ($u = L/t_0$), a set of "reduced" parameters is used:

$$h = L\,(Nd_p)^{-1} = H / d_p \qquad (2.4)$$

$$\nu = (L/t_0)(d_p/D_m) = u(d_p/D_m) \qquad (2.5)$$

where d_p is the diameter of the packed particle and D is the diffusion constant of the solute in the eluent. The particle diameter is typically 1×10^{-5} m and D_m is typically 1×10^{-9} m^2 s^{-1}. It should be noted that both the reduced plate height h and the reduced linear velocity are dimensionless.

The reduced parameters h and ν in Eqns. (2.4) and (2.5) are related to each other by a simple phenomenological equation:

$$h = A\,\nu^{1/3} + (B/\nu) + C\,\nu \qquad (2.6)$$

The first term (coefficient A) represents the contribution from anisotropy in solvent flow through the column. As the solvent follows its tortuous route through the packed column bed, dispersion results. The second term (co-efficient B) represents axial diffusion. While the molecules are being swept down the column bed, a zone containing the molecules broadens slowly due to simple diffusion along the axis of the column. This term is inversely proportional to the linear velocity; the longer the zone is in the column bed, the more diffusion possible. The final term (coefficient C) represents the results of slow mass transfer between the mobile and stationary phases. As discussed above, the principle on which chromatography is based is that the molecules of interest will spend a given amount of time in the mobile phase and another fraction of the time in the stationary phase. The exchange between phases does not lead to much dispersion at low velocity, where the mobile and stationary phases are at approximate equilibrium. As the linear velocity of the mobile phase

increases, molecules in the stationary phase will fall behind those in the mobile phase, leading to dispersion of the chromatographic band. The results of these three mechanisms are shown in Fig. 2.1 and the combination of the three (h in Equation 2.6) is shown as the solid line.

From these considerations, the most important parameter controlling the efficiency of a column, assuming that the column is well packed, is the linear velocity of the solvent through the packed bed. In our situation, the maximum volume flow rate allowed by the deposition method chosen (see Section 2.4) was approximately 5 µl/minute. Table 2.2 shows the estimated reduced linear flow rates for 10 um packing material for the various column bores commonly used, assuming 5 µl/minute volume flow rate. Comparing the reduced linear velocities in Table 2.2 and reduced plate heights in Figure 2.1, it is clear that 10 mm diameter columns are too large for our application. Similarly, columns of less than 0.5 mm diameter also gives rise to undesirably large values for h. In the region between 4.6 mm and 0.5mm however, the case is not quite so clear. The coefficients used to produce Figure 2.1 are only typical values; frequently the minimum in the curve is shifted over to the right in curves measured for real columns. The minimum can be over a range from $\nu = 2 - 20$. Therefore, the 4.6mm diameter column is probably too large, but the 0.5 mm diameter column may perform quite well under these conditions.

The fourth column of Table 2.2 is the void time for the column. The void time is a practical indication of how long a particular separation may take. For the analysis of large organic molecules, the retention time for a given molecule will be on the

Figure 2.1

Performance curve for a typical HPLC column showing contributions of peak broadening from diffusion, mass transfer and flow anisotropy ($h = A\,\nu^{1/3} + (B/\nu) + C\,\nu$).

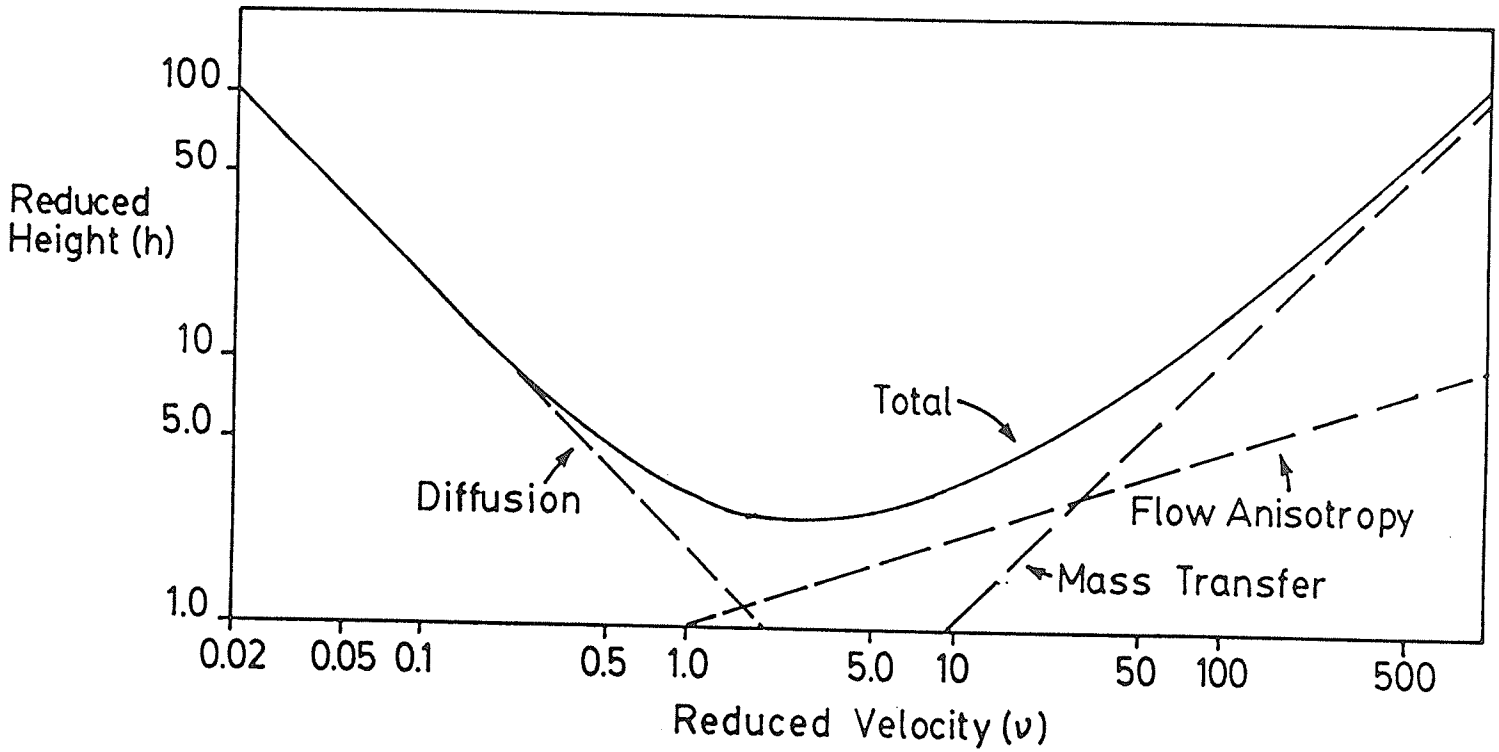
100
50
10
5.0
1.0
Reduced Height (h)
Total
Diffusion
Flow Anisotropy
Mass Transfer
0.02
0.05
0.1
0.5
1.0
5.0
10
50
100
500
Reduced Velocity (ν)

TABLE 2.2

Column parameters for a volume flow rate of 5 µl/minute.

Column i.d. (mm)	Linear Velocity (u, cm/sec)	Reduced Velocity (ν)	Void Time (t_0, min)
10.0	2.1×10^{-4}	0.2	1575
4.6	1.0×10^{-3}	1.0	333
2.0	5.3×10^{-3}	5.3	63
1.0	2.1×10^{-2}	21.2	16
0.5	8.5×10^{-2}	84.8	3.9

FIGURE 2.2

a) Typical Electrospray Apparatus

b) Focussed Electrospray Apparatus

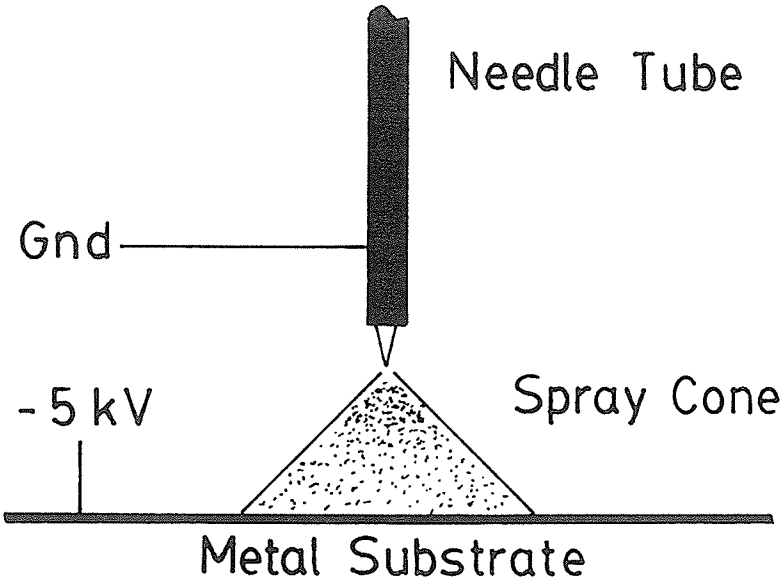
Needle Tube
Gnd
-5 kV
Spray Cone
Metal Substrate

(a)

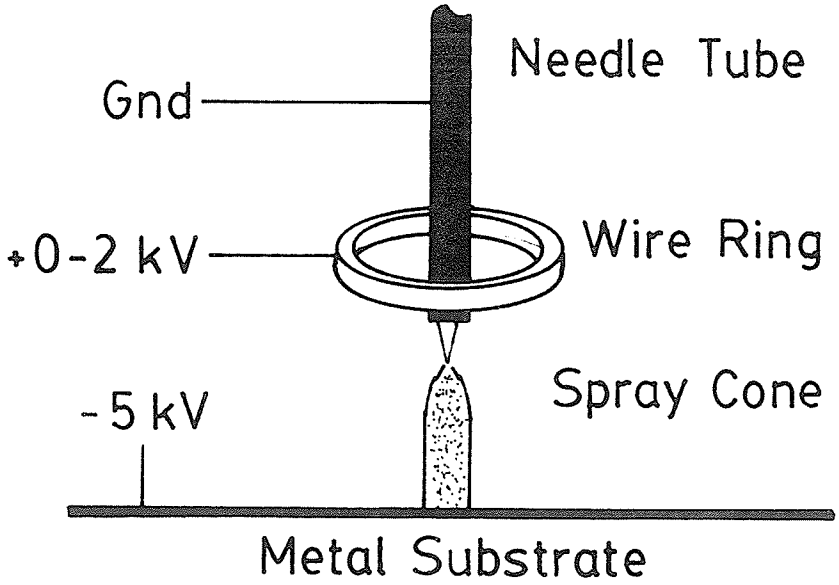
Needle Tube
Gnd
+0-2 kV
Wire Ring
Spray Cone
-5 kV
Metal Substrate

(b)

order of 1 - 20 column volumes. For a process to be practical, the time for analysis should also be practical; on the order of a few hours at most. Simple inspection of Table 2.2 shows that column diameters of greater than 1.0 mm can be rejected as impractical on the basis of elution time. Combining the results of the examining resolution and speed of analysis, the best diameter column to use in our application is between 0.5 and 1.0 mm. A column of this type is referred to as a "microbore" column.

2.4) Sample Deposition

The HPLC system described in this thesis was built around the electrospray sample deposition method (not to be confused with electrospray ionization [44]). The reason for using electrospray to deposit the HPLC eluent on a metal backing (the form necessary for time-of flight SIMS) was simple: it was proven effective. The production of efficient samples for SIMS has always been a problem. Simply spotting a metal foil with an organic compound will not, in general, produce intense molecular ion signals. Spotting the same compound on specially etched and cleaned silver will produce intense spectra. Electrospraying the same compound onto the foil will also usually produce intense spectra. Therefore, because electrospray was a proven method of sample preparation from dilute solutions of polar organic solvents and water, it seemed to be suitable for HPLC.

The electrospray process itself is very simple. The layout

of a simple electrospray is shown in Figure 2.2 (a). A polar organic solvent, or water/solvent mixture slowly flows through the needle tubing to the tip. The needle is held at several kilovolts DC with respect to the conductive (metallic) deposition substrate. The drop that forms at the end of the needle is torn up into small charged droplets that fly to the substrate. If the voltage and flow rate are chosen properly, no liquid beads form on the substrate. If there is a solute contained in the liquid , a macroscopically uniform coating is laid down on the substrate.

The phenomenon of electrostatic breakup of drops in high electric fields has been studied for a long time. The first systematic study was undertaken by Zeleny in 1914 [48]. Many studies of this phenomenon followed, mainly using the approach of isolating an individual drop in a high field and photographically following its distortion and instability. The excellent pictures due to Macky [49] clearly show that a drop is distorted in the direction of the field, resulting in a long thin "streamer" of liquid being pulled off of one end of the oblong drop. If the field is high enough, this streamer then breaks up into a number of very small drops that continue off in the direction of the electric field. Vonnegut and Neubauer [50] showed that by forming a drop on the end of a glass capillary and then subjecting it to a high electric field, the same effect could be produced. They also observed that the droplets formed in this way were uniform in size (monodisperse). An additional property of these droplets was that by increasing the electric field above the droplet formation threshold, the monodisperse droplets could

be further atomized into very small (on the order of microns) diameter droplets, referred to as "smoke". (Note: This observation had been made by Zeleny [48] thirty years previously). The "smoke" flared out in a cone from the point of formation.

The very finely atomized particles in the "smoke" described above suggested a method of making thin films to Carswell and Milsted [51]. Nawab and Mason [52] also decided to use the same technique. By dissolving some of the intended film material in a polar organic solvent such as methanol and producing the "smoke" type of atomization, the charged particles of solution could be accelerated towards a substrate by the electric field. Because of the very small size of the individual solution particles, when the solvent evaporated, a very uniform deposit was formed. An unexpected, but welcome, effect due to electrospray atomization was that the particles were so small, and the volume flow rate so low that the solute was deposited on the substrate as a dry film. The absence of solvent on the film allowed the production of very uniform layers.

The possibility of using films made by electrospray as samples for solid phase particle desorption ionization was first described by Krueger [53] and confirmed by McNeal, et al. [54] for fission fragment desorption. Our laboratory began using electrospray on the advice of Ron Macfarlane and it has been the standard method of sample preparation for large, polar organic molecules since.

CHAPTER III

Development of a Microbore HPLC System

3.1) General Comments

This chapter discusses the finished product: a microbore HPLC system compatible with the electrospray method of sample deposition described in Section 2.4. The actual process of development and results obtained during this developmental stage is in Chapter 4.

An obstacle to the development of our off-line LC-MS interface was that there were no available commercial microbore HPLC systems at the time we began our project. Therefore, rather than applying a commercial system to the problem, first the microbore system had to be built. The papers of Scott and Kucera [55] and Ishii [56] were the blueprints on which the system was assembled. These papers gave a good outline of how to pack microbore columns and how to adapt existing hardware to microbore's specifications. The modifications to hardware (plumbing) necessary for our application are described below. Additional information on the hardware aspects of microbore HPLC was gleaned from informal discussions and workshops at American Society of Mass Spectrometry conferences.

Note: When describing the practical layout of a chromatography system, it was convenient to use inches (") as the units for tubing dimensions. Small tubing available in North America is manufactured in inches. Therefore, throughout the text to follow, frequent mention was made of tubing outside diameter (o.d.) and inside diameter (i.d.) in inches. Where it was important or conventional, the measure in SI units were also included.

3.2) Hardware Considerations

The primary obstacle to constructing a microbore HPLC system from hardware originally designed for normal bore (4.6 mm i.d.) columns was dead volume. Dead volume, in chromatographic parlance, refers to any unpacked volume in the system that the analyte may pass through. The presence of even relatively small amounts of dead volume in key locations will greatly reduce the chromatographic efficiency of a system by providing mixing volumes. Analyte passing through the column will be delayed by entering these mixing volumes and then diffusing back out of them. If the analyte has several of these hidden reservoirs, the trailing edge of the chromatographic peaks resulting will be greatly lengthened (referred to as peak tailing). The method used in microbore HPLC to avoid this problem is to use 1/16" o.d. tubing for the HPLC column and standard 1/16" o.d. connectors and fittings used in normal HPLC. If these fittings are modified to make sure that the tubes and connectors butt up against each other as tightly as possible, systems with very low dead volumes can be achieved.

The hardware components common to any HPLC system are:

1) a high pressure pump (with appropriate flowrate control);
2) a injection mechanism to introduce sample onto the column;
3) a column;
4) a column endfitting that serves both to hold in the column bed and to connect the column to the outlet tubing;
5) outlet tubing;
6) tubing to connect the injection valve to the pump.

In the microbore system first designed the pump used was the Eldex A-30-S (reciprocating piston type). This pump has a flowrate adjustable by means of a micrometer limiting the travel of the pump piston. This pump was only barely adequate for the very low flowrates used (1-5 ul/min). Improved performance and reliability were obtained later using a Isco ulC-500 Micropump (syringe type, worm screw drive) with its flowrate controlled from the front panel using digital meters resulting in a very finely controllable flowrate from less than 1 ul/min to 1.5 ml/min and the capacity to run in a constant pressure mode.

The injection mechanism chosen was a high pressure injection valve. The purpose of an injector is to apply a small amount of the sample of interest onto the top of the HPLC column, without interrupting the eluting solvent flow or introducing any additional volume to the system. The simplest type of injection valve has two small loops of tubing attached to a flat stator and acts as a simple flow switching valve. The operation of the stator is shown in Figure 3.1. Between injections, the stator is set in the normal position (Figure 3.1(a)) and the solvent flows through the shunt tube. When the sample is injected, the length of

Figure 3.1

A flow schematic diagram of the Rheodyne 7410 injection valve.

a) Normal flow

b) Inject sample

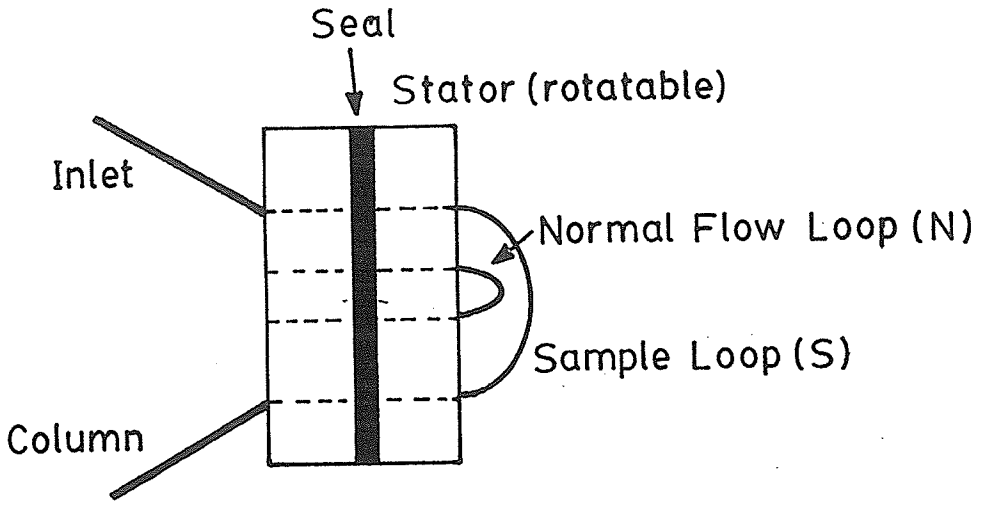

Side View of the 7410 Valve
(Inject Position)

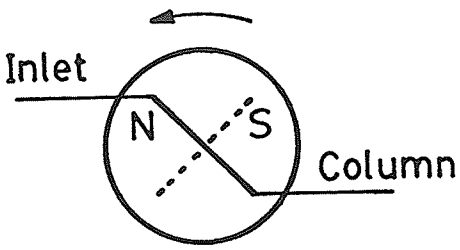

(a)

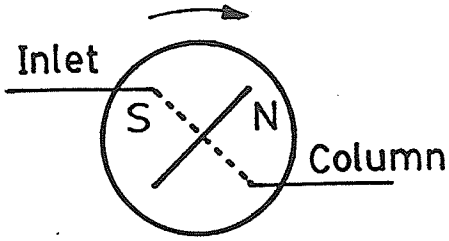

(b)

tubing containing the sample is inserted into the flow stream by rotating the stator (Figure 3.1(b)). After the injection is complete, the stator is rotated back to the normal flow position (Figure 3.1(a)). The injection valve installed in the HPLC system was the Rheodyne 7410, with a 500 nanoliter internal sample loop.

The column blanks chosen were 1/16" o.d., with i.d. of from 0.25 mm to 1.0mm (0.010" - 0.040"), made of either 316 stainless steel or nickel. The reason for the range of column i.d. was that experimentation was necessary to determine the i.d. that was practical for our application (described in Section 4.3). The most successful column i.d. turned out to be 0.5mm (0.020") nickel, as a trade-off between resolution, flowrate and analysis time. The subject of column blanks and what goes in them will be dealt with in more detail in Section 3.3. The connection between the injection valve and the inlet of the column was simple: the column was directly attached to the outlet (1/16" o.d. female tubing connection), using a stainless steel ferrule and bushing to make a high pressure joint, with essentially no dead volume. The column endfitting was a particular problem. The endfitting had to contain a filter to hold the column packing in the column blank against 70 MPa packing pressure and also make a low dead volume connection between the 1/16" o.d. column blank and a 32 gauge (0.0095" o.d., 0.0040" i.d.) needle tube that ended in the electrospray tip. Two different designs of endfitting were used (Figures 3.2 and 3.3).

The first design that was successful is shown in Figure 3.1. The main body of the fitting is a Swagelok 1/16" female-female "zero dead volume" connector (316 stainless steel). The body of the connector was not altered. An inlet of the endfitting was chosen and a 1/16" diameter

Figure 3.2

An endfitting for microbore HPLC columns using a modified Swagelok 1/16" union.

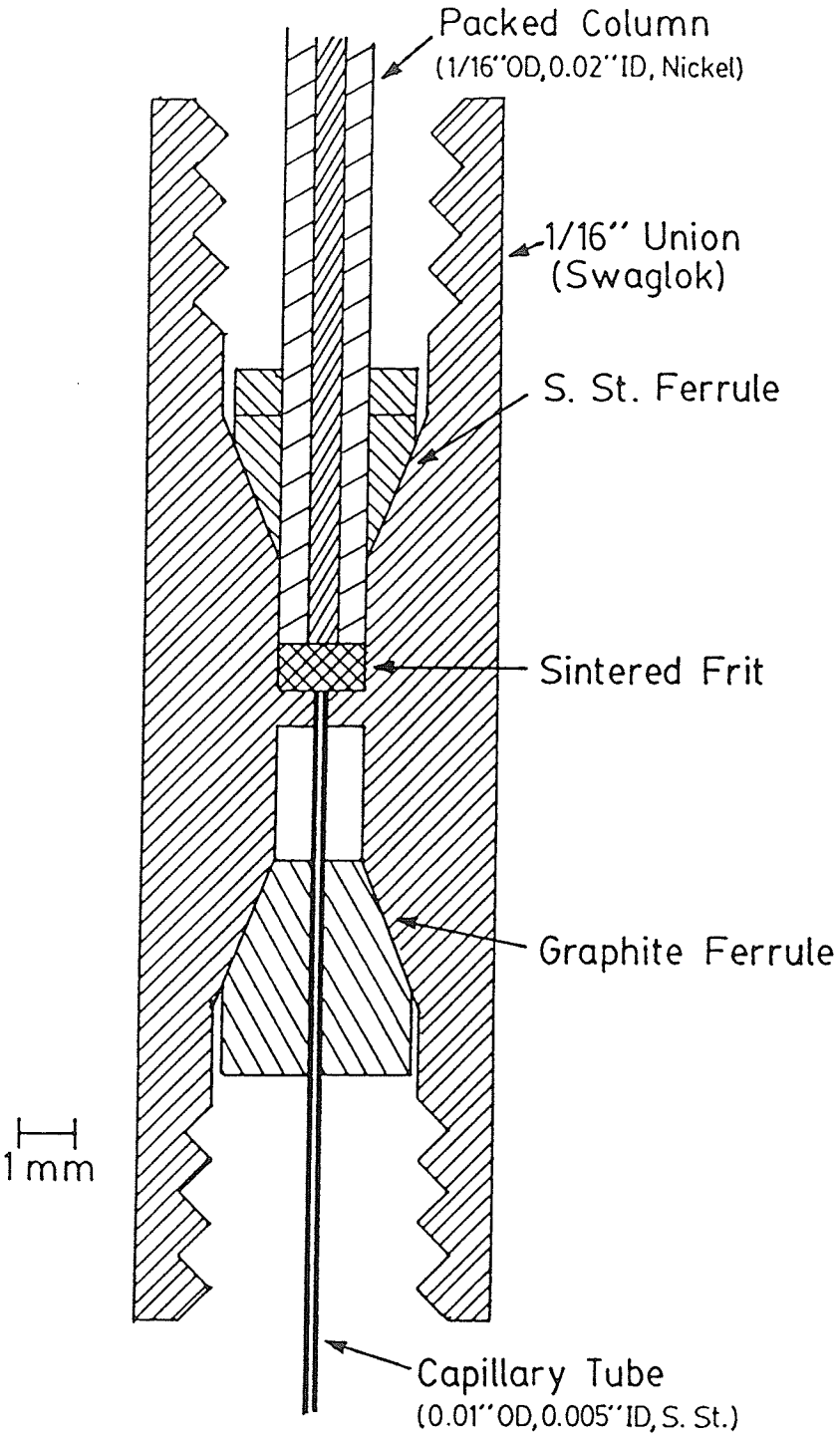
Packed Column
(1/16"OD, 0.02"ID, Nickel)
1/16" Union
(Swaglok)
S. St. Ferrule
Sintered Frit
Graphite Ferrule
1 mm
Capillary Tube
(0.01"OD, 0.005"ID, S. St.)

column was butted as tightly as possible to the frit. The column was attached to the endfitting by a Swagelok 2-piece ferrule and a 1/16" bushing. A ferrule is a small conical piece (usually metal) has a center bore the i.d. as the tubing. The bushing presses the ferrule into the fitting and it is compressed against both the tube and the fitting, making metal to metal high pressure (70 MPa maximum) seals. At the outlet side, a 3.5 cm length of 32 gauge needle tubing was inserted into the narrow passage between the inlet and outlet compartments (this passage was originally present in the fitting). A graphite (or Vespel) ferrule (normally used for capillary gas chromatography) was placed over the needle tubing and a 1/16" bushing tightened against the ferrule.

The second design is shown in Figure 3.3. The main body of this endfitting is a Valco 1/16" female-female "zero dead volume" connector (316 stainless steel). The connector was altered in this design by drilling a 1/16" hole through the center of the fitting and removing the narrow gauge separating channel. The column blank was then inserted into one end of the connector and the high pressure connection made with a Valco stainless steel ferrule and bushing. The blank was inserted to the half way point of the 1/16" o.d. channel in the connector. The filter element was then inserted from the other end of the fitting. Either a screen (316 stainless steel, 2 um porosity) or a frit (316 stainless steel, 0.5 um or 2 um porosity, 1 mm thick) was used as the filter element, but screens seem to be superior in practice. Using the screens made it necessary to carefully press the screen down into the fitting to make sure it was butted up against the column blank and was sitting flat in the channel. The key to attaching the needle tubing to

Figure 3.3

An endfitting for microbore HPLC columns using a modified Valco 1/16" union.

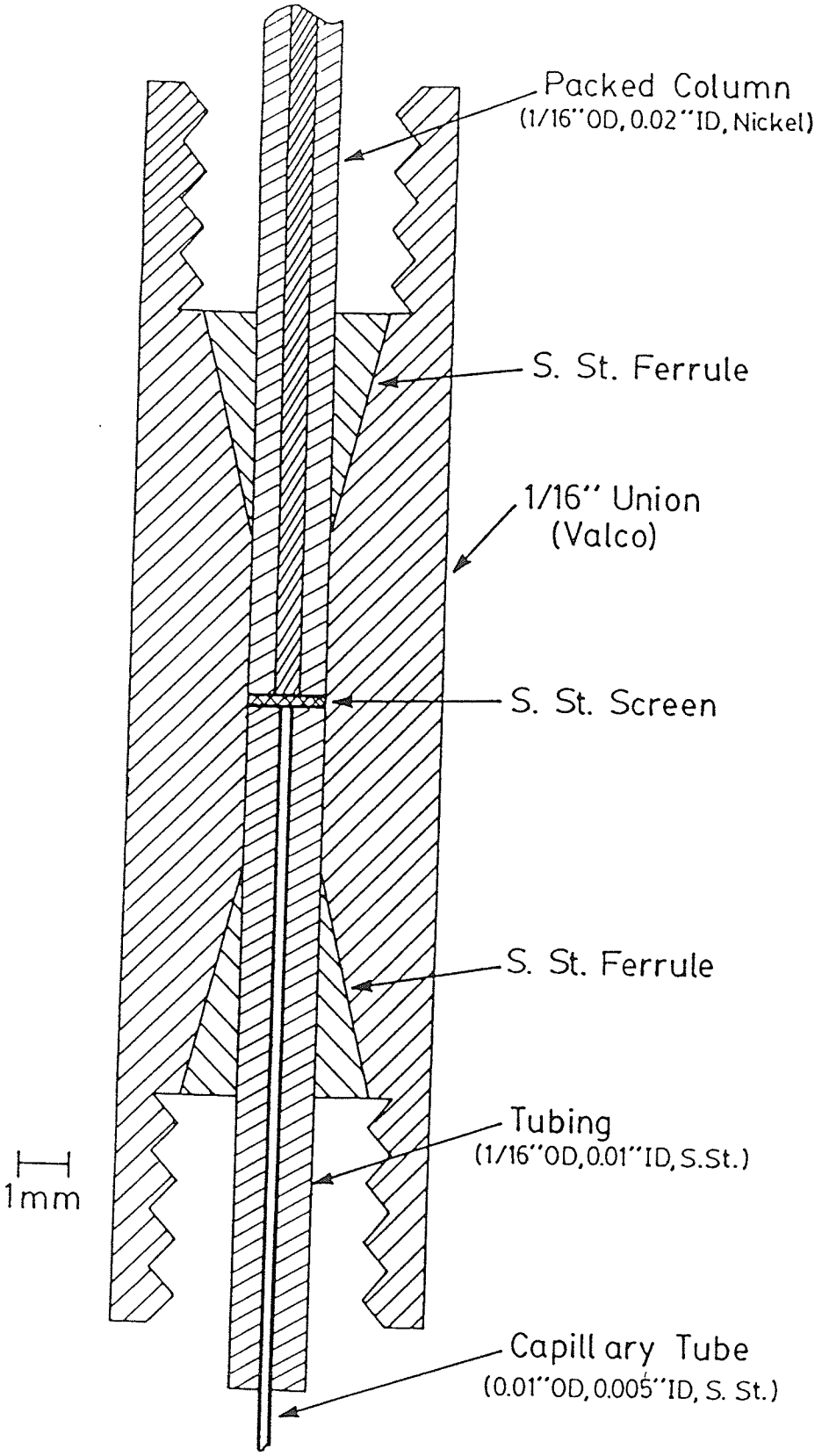
Packed Column
(1/16"OD, 0.02"ID, Nickel)
S. St. Ferrule
1/16" Union
(Valco)
S. St. Screen
S. St. Ferrule
Tubing
(1/16"OD, 0.01"ID, S.St.)
1mm
Capill ary Tube
(0.01"OD, 0.005"ID, S. St.)

this type of endfitting was to secure the needle tubing into a short piece of 1/16" o.d. stainless steel tubing as follows: a short length of 1/16" o.d., 0.010" i.d. tubing (approximately 2 cm) was cut, the ends squared and the bore carefully cleared and washed with acetone to remove any oil. A length of 32 gauge (0.0095" o.d., 0.0040" i.d.) stainless steel needle tubing (approximately 3.5 cm) was cut and the ends cleared. The needle tubing was then reduced in o.d. by electropolishing in phosphoric acid (making the needle an electrode in a phosphoric acid bath and placing approximately 6 VAC through the bath) until it just fit into the inside bore of the 1/16" tubing. The needle tubing was then carefully washed and dried to remove any traces of phosphoric acid. After the needle tubing dried, it was inserted a short way into the 1/16" tubing. A small drop of freshly mixed quick setting epoxy glue was then applied to the end of the 1/16" tubing with the needle tubing sticking out. The needle was then carefully worked down into the 1/16" tubing so that a layer of epoxy was carried down into the space between the needle and 1/16" tubing, without any of the epoxy entering the inside bore of the needle tubing. When the needle tubing was flush with the end of the larger tubing, the assembly was set aside until the epoxy hardened. Then the needle assembly was inserted into the connector channel, butted up against the filter and fastened in place using a Valco ferrule and bushing. This second type of endfitting may seem to be more complicated than the first one described, but in practice it was much easier to manipulate the needle tubing when sheathed with 1/16" tubing. It was not trivial to insert the needle tubing into the first type of endfitting and swage down on the Vespel ferrule without moving the tubing out of the

very short central passage in the housing, or accidently bending the tubing. Disassembling the first type of endfitting was also difficult, as the Vespel ferrule was difficult to remove and cannot be reused. The second type of endfitting gets around these problems by making the needle tubing more robust with a thick casing and by using a solid ferrule-tubing assembly that can be reused.

For either type of endfitting described above, the fine 32 gauge stainless steel tubing that serves as the column outlet tubing at one end and as the electrospray needle at the other had to be cut and the ends finished. This operation was refined through experimentation and the method that evolved was reasonably quick and reproducible. First, the length of tubing necessary was measured out from a longer piece of tubing stock and cut off using a pair of sharp diagonal cutters or scissors. To open the ends of the tubing, one end at a time was rubbed against a flat piece of unglazed, fine grained ceramic, until the pinched portion of the tubing had been removed. The bore of the tubing was then opened with the sharp point of a scalpel. Burrs formed on the outside of the tubing were removed by gentle rubbing with the ceramic. The resulting tube ending was not suitable for electrospray, however. To produce a good electrospray ending, tubing must be electropolished by inserting the needle tip into a phosphoric acid bath. The needle tubing was then carefully cleaned and washed to remove any acid. When treated in this way, the tube end served as an excellent electrospray tip.

Connections between the pump and the chromatography system were made using 1/16" o.d., 0.040" i.d. 316 stainless steel chromatography high pressure tubing, with the high pressure joints made with ferrules and bushings. The tubing was cut using a jeweller's coping saw and a jig to

make straight cuts. The burrs on the outside and inside of the tubing were removed using a scalpel blade tip and a flat piece of unglazed ceramic as an abrasive. Care was taken not to damage the finish of the tubing in the area that the ferrule was to swage to. Column blanks were also cut using the jeweller's saw and jig. The ends of the column blanks were more carefully squared, using the flat piece of ceramic and a fine toothed flat file. The tubing was also carefully cleaned with organic solvents to remove any oil in the bore.

3.3) Packing Microbore Columns

The first piece of apparatus that had to be acquired for packing our microbore columns was a pump with sufficient capacity and speed to achieve rapid flow rates at very high pressures (70 MPa). Examination of the literature and discussions with chromatographers led to the purchase of a Haskel high pressure pneumatic amplifier pump. This class of pump uses relatively low pressure gas to drive a reducing piston that in turn drives the fluid being pumped at a much higher pressure. The amplification of pressure is determined by the area reduction ratio of the piston. The pump purchased was the Haskel MCP-110, with an amplification ratio of 126 and special Teflon and Kel-F seals for maximum resistance to solvent corrosion. The MCP-110 has been in use for approximately 5 years and has never given any problems.

Once the pump was in place, the reservoir for the slurry to be packed had to be constructed. Several designs were tried, but the

Figure 3.4

A slurry reservoir for packing 0.5mm (0.02") i.d. microbore HPLC columns.

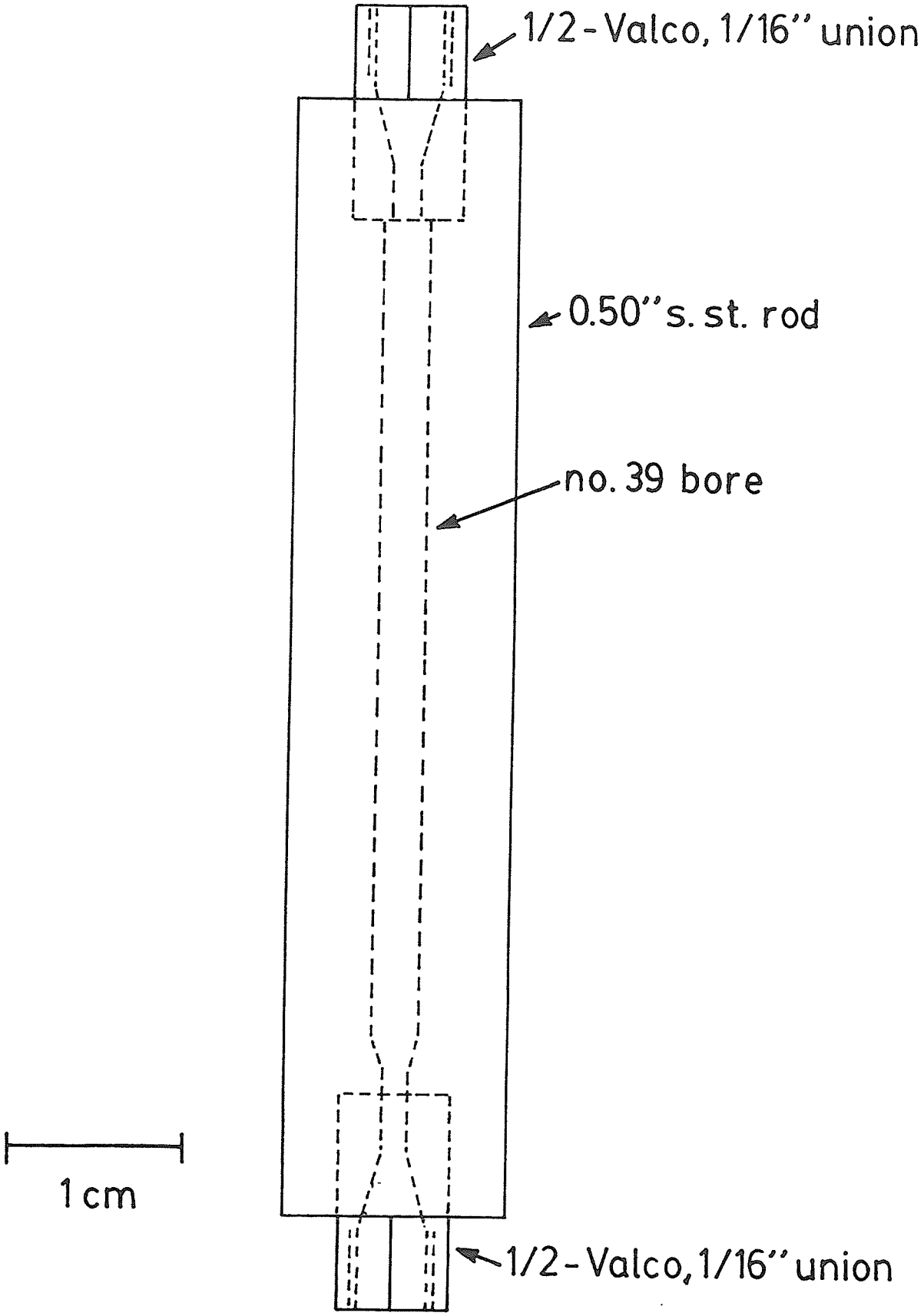
1/2 - Valco, 1/16" union
0.50" s. st. rod
no. 39 bore
1 cm
1/2 - Valco, 1/16" union

Figure 3.5

The block diagram of the column packing system.

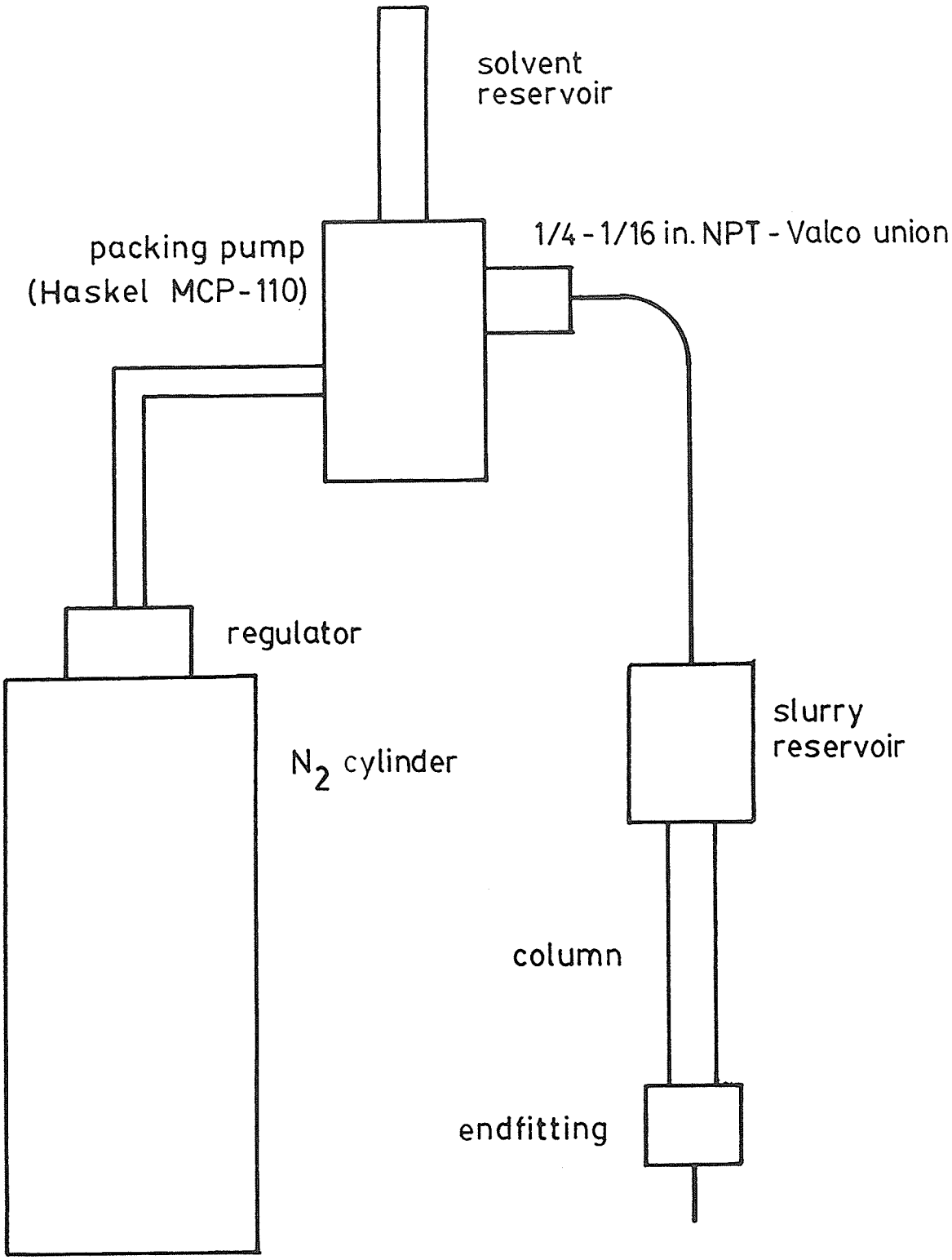
solvent
reservoir
packing pump
(Haskel MCP-110)
1/4 - 1/16 in. NPT - Valco union
regulator
N_2 cylinder
slurry
reservoir
column
endfitting

simplest one, which has proven both reliable and easy to use, is shown in Figure 3.4. The main body of the reservoir was a rod of 316 stainless steel. The dimensions of the central cavity were chosen so that the total free volume of the reservoir would be 1 milliliter. The endfitting to attach the column and the inlet tubing was simply one half of a Valco female-female 1/16" connector, with the central passage drilled out to 1/16". Drilling out the passage was particularly important to decrease the flow resistance of the fitting.

The description of exactly how the columns were packed will be given in point form (i.e. as a recipe). The individual steps are the result of much experimentation (see Section 4.3) and reading [55, 56, 57, 58]. The physical layout of the packing system is shown in Figure 3.5. A detailed description of the procedures is given in Appendix A.

3.4) Choosing the Stationary Phase

The stated objective of the LC-MS system that we developed was to help in the identification of peptide mixtures, or more generally, mixtures of relatively large (100 - 3000 u) polar organic molecules. The objective makes the choice of stationary phase simple: reverse phase silica. There are a range of choices within reverse phase silica:

1) Particle size (3 - 20 μm diameter);

2) Particle shape (irregular or spherical);

3) Reverse phase coating (propyl, octyl or octadecyl).

Particle size determines the resolution per meter of the column. It also determines the back pressure that the column will have for a given flow rate; the smaller the particle the higher the back pressure and the

higher the resolution per meter. Using the very low flow rates that were useful for electrospraying, the back pressure was not a particularly important consideration, made even less so by the addition of the Isco syringe pump. To test the system, 10 μm diameter porous silica was chosen mainly because it was the most widely used type of silica available at that time and it had been used successfully in microbore applications [58]. The final type of analytical column developed was a 3 um silica column.

Particle shape was a less tangible problem. Columns have been packed using both irregular and spherical material by several authors [60, 61] and the spherical material produced more reproducible column resolutions, on average. In these investigation it was not clear as to whether the problem was with the irregular shape of the silica or that irregular silica should be packed under somewhat different conditions from spherical silica. Therefore, as a first attempt, irregular silica was tried, due to its low cost. The silica chosen for this first set of experiments was RSil 10 μm irregular silica (Alltech Associates, Deerfield, Illinois, USA) with either propyl silane (C3) or octadecyl silane (ODS or C18) reverse phase groups attached. These particles were useful in setting up packing procedures and initial experimentation, but the columns packed with them were of widely variable efficiency. In addition, the column material was not very stable to attack by the solvents and buffers used.

Due to the problems discovered using irregular silica, spherical silica was tried. Altex Ultrapack (Anspec Company, Ann Arbor, Michigan, USA) 10 um spherical silica, with either octyl (OS or C8) or octadecyl

silane were used with very encouraging results. However, the best results were obtained using another spherical material, Shandon MOS-Hypersil (Anspec Company, Ann Arbor, Michigan, USA) 3 µm silica, with a special high load octyl silane bonded phase. To use the very fine grained 3 um silica without clogging the endfitting's filter, it was found that first packing a few milligrams of 10 µm Ultrapack OS material into the column, followed by the 3 um Hypersphere material produced superior results both in reproducability and efficiency for 0.5 mm i.d. columns.

The logic behind the choice of octyl silane bonded phases as opposed to octadecyl silane bonded phases hinged on one simple fact: smaller bonding groups lead to more stable silica [62]. The reason smaller groups give rise to more stable material is that the larger the group attached to the silica surface, the greater the steric inhibition to very dense bonding at the silica surface. Therefore, octadecyl silane bonded particles carry a smaller percentage of their total surface area covered than do octyl silane bonded particles. The large groups also interfere with the process of "endcapping" the materials -- bonding a smaller silane (C3 or C2 usually) to the free silanol groups left after the large silane was attached -- resulting in some free silanols left on the material surface. In our application, it was of paramount importance to keep the amount of column bleeding, i.e. loss of column material due to solvation, to a minimum to reduce background in the mass spectra of the fractions obtained. With the above in mind, octyl silanes were the preferred materials.

3.4) The Automated Fraction Collection System

Once the microbore HPLC column was packed and attached to the rest of the chromatographic system, the problem of how to collect the eluent efficiently and automatically still remained. The additional constraint of having to use electrospray as a sample deposition method implied that the eluent must be sprayed onto a conductive medium. The secondary ion source of the Manitoba time-of-flight mass spectrometer added the constraint that the backing material must be flat (when in the mass spectrometer) and it was convenient if the material was at least 2 cm wide. Originally, the material chosen was 0.001" thick aluminized polyester sheet (chosen because it was our usual sample substrate). The sheet was cut into strips 35 cm long and 2.5 cm wide. The strip of material was mounted on a drum 10.5 cm in diameter and positioned so the center of the strip of material was aligned with the spray needle on the end of the column endfitting (see Figure 3.6). The drum was mounted on an insulating shaft connecting to a motor. To collect fractions, a stepping motor was used.

The stepping motor was controlled by a clock (Ortec 719 time base) and a control unit allowing the number of steps per clock pulse to be varied. The Ortec 719 time base provided one output pulse a given time after an input pulse, the time interval being variable from a front panel mounted rotary switch. The control unit was designed and constructed to be used with the 719 time base. It is shown in Figure 3.7. Its purpose was to receive the pulse generated by the 719 at the end of its timing cycle, send a given number of pulses to the stepping motor control chip (IC3) resulting in the same number of steps from the stepping motor and

Figure 3.6

The electrospray apparatus for collection of microbore HPLC fractions.

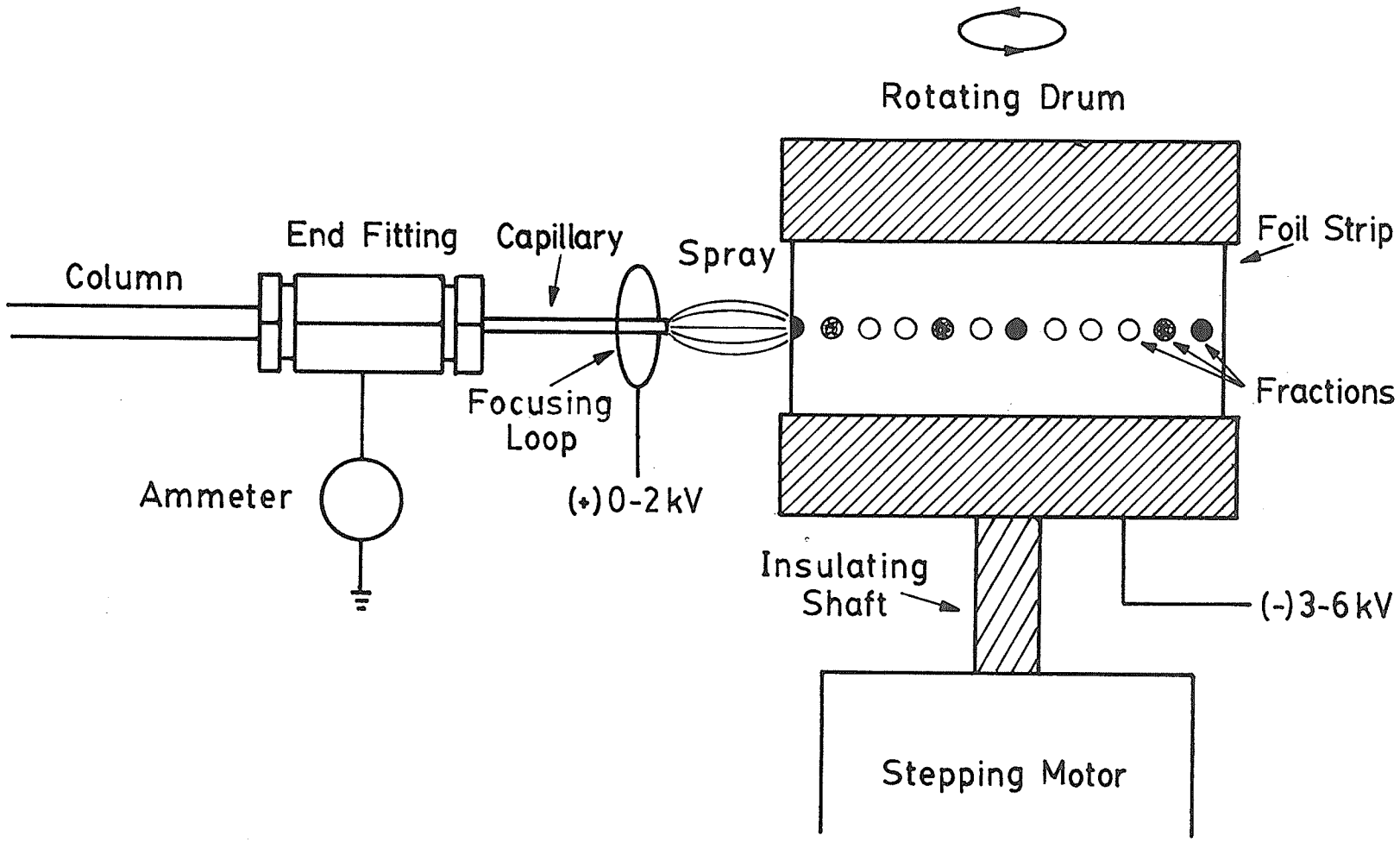
Rotating Drum
Foil Strip
End Fitting
Capillary
Spray
Column
Fractions
Focusing
Loop
Ammeter
(+)0-2 kV
Insulating
Shaft
(-)3-6 kV
Stepping Motor

Figure 3.7

The schematic diagram of the stepping motor control (designed by R.C.B.).

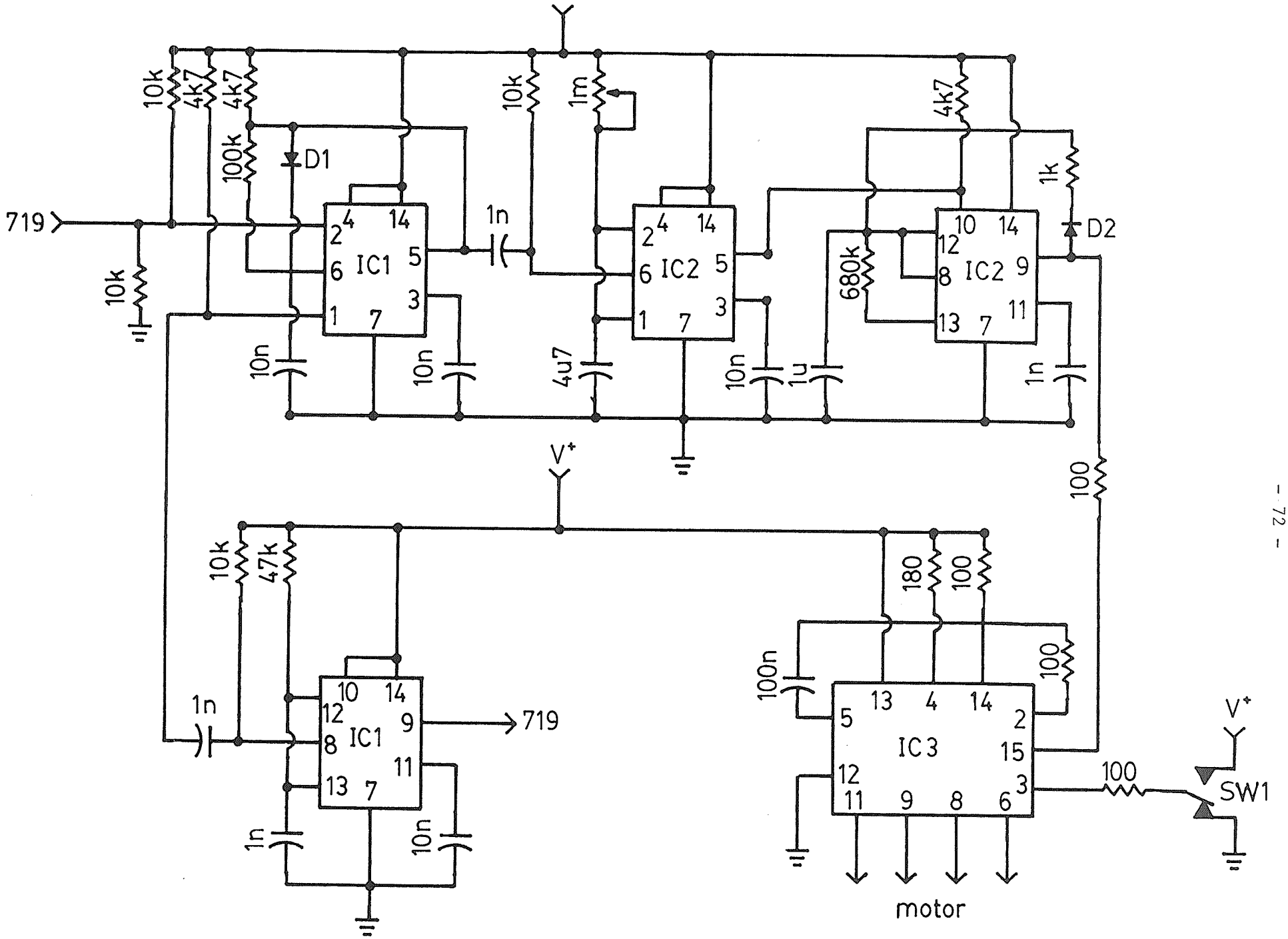
V+
10k
4k7
4k7
100k
D1
719
10k
IC1
1n
10n
10n
10k
1m
IC2
4u7
10n
1u
4k7
1k
D2
680k
IC2
1n
100
V+
10k
47k
IC1
1n
719
1n
10n
180
100
100
100n
IC3
100
SW1
V+
motor

then to send a pulse back to the 719 to restart the timing cycle. The direction of the step (clockwise or counterclockwise) was set by the position of SW1. The system operated as follows:

1) The 719 was started using an external panel switch.

2) When the end of the 719 timing cycle was reached, the motor controller was activated, moving the drum 1/200th of a revolution per step. In normal operation, one step per cycle was used.

3) The 719 was restarted by the controller, repeating the cycle.

When the chromatograph operating and the electrospray voltages attached as in Figure 3.5 the cycle described above had the effect of collecting a fraction at a given location on the strip for the time interval set on the 719 timer and then advancing the strip to a new position, collecting a fraction for the same time interval, advancing the strip,..., et cetera. The resultant chromatogram was a series of small spots down the centre of the strip of backing material, each spot corresponding to a fraction from the chromatograph. Each spot was then available for mass spectrometric examination. The spot deposits formed on the strip were mechanically stable; electrospray deposits can only be removed by scraping. Therefore there was no problem in transporting the backing material or mounting it in the mass spectrometer.

To insert the strip bearing the chromatogram into the mass spectrometer, a special "ladder" had to be constructed. The ladder is shown in Figure 3.8. The general design of the ladder was a modification of the sample ladder already in use with the mass spectrometer. The basic function of the ladder was to hold the strip of conductive backing material taut and to isolate the strip from ground. The geometry of our

Figure 3.8

Sample holder for the Manitoba I time-of-flight mass spectrometer, modified to hold foil substrate strips.

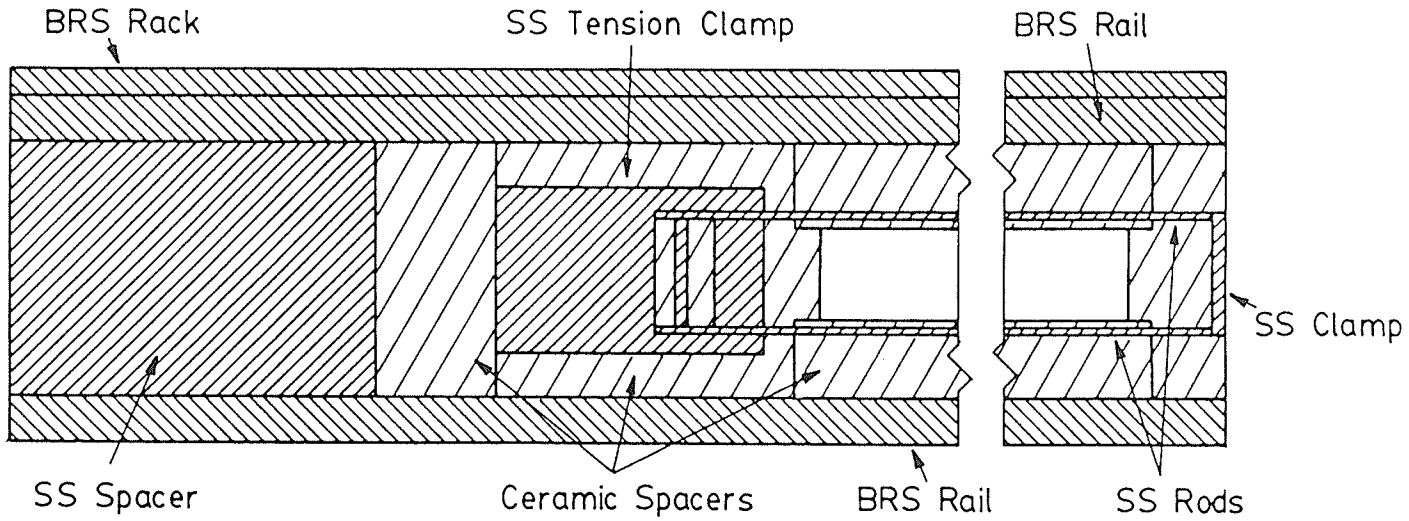
BRS Rack
SS Tension Clamp
BRS Rail
SS Clamp
SS Spacer
Ceramic Spacers
BRS Rail
SS Rods

time-of-flight instrument was such that the sample backing must be held at high voltage (5 - 10 kilovolts) with respect to a parallel grid placed several millimeters in front of the sample. The distance between the sample and the grid must remain constant and, in order for the ions produced at the surface to have a flight path normal to the grid, the sample and the grid must be parallel to a rather high degree of precision. The ladder shown in Figure 3.8 has the strip of backing material clamped at both ends, with a spring loaded tension device at one end to maintain a constant tension in the strip. The clamps were attached to ceramic inserts in the ladder, isolating them from the body of the spectrometer. Long ceramic inserts down the sides of the ladder's body kept the edges of the strip from making contact with the ground. The edges of the strip were held in place with two long stainless steel rods. These rods also served to reduce sparking from the sharp edges of the strip. The high voltage contact to the strip was made using a sliding contact that also flattened the portion of strip material directly in front of the grid. The slide was clamped in position by a spring loaded contact fixed in place behind the ladder track holding the slide directly in front of the grid at all times during a measurement. The contact is the same one illustrated in Figure 1.2 for use with the old individual sample holder ladder.

After several trials, it was found that aluminized polyester was not a suitable material to be used in the strip ladder. With a strip of aluminized polyester mounted on the ladder and set in the mass spectrometer, it was not possible to increase the voltage on the strip to

higher than 2 kV without sparking. The electrostatic attraction between the strip and the grounded secondary ion source housing (minimum clearance = 3 mm) caused the strip to stretch and make contact with the housing, resulting in the sparking. Our usual substrate holders keep the aluminized polyester under much higher tension than the strip holder, so the electrostatic attraction does not cause this problem. A more rigid material was clearly required. Because aluminum was our normal metallic substrate for electrospray (in the form of aluminized polyester) and the availability of various thicknesses of aluminum in the laboratory, aluminum foil was tried as a substitute substrate. The mechanical properties of the aluminum made it a far better material for use with the strip target ladder. Once the foil was mounted, running the slide up and down the central track of the ladder formed the foil around the edge restraining rods, producing a flat surface. The foil was also much less prone to damage from sparking in the electrospray procedure, something that could happen if a high concentration of ionic salts suddenly flows out of the column. The greater rigidity of the foil allowed the operation of the mass spectrometer at secondary acceleration voltages of up to 8 kilovolts on a routine basis -- sufficient for good MS resolution and efficiency for any of the molecules examined.

3.6) Practical Considerations in Using a Focussed Electrospray

The method of focussing an electrospray plume was described previously (Section 2.4). The reason for focussing the plume was to increase the ratio of sample surface/backing surface exposed to the primary ion beam and to match the size of the primary ion beam and the deposit to make the use of sample as efficient as possible (see Section

4.2). Using the simple wire ring method shown in Figure 2.2(b), deposits of approximately 1 mm in diameter were routinely made. The formation of a deposit of these dimensions has one major drawback: sample wetting. For electrospray to be effective as a sample preparation method, the deposit formed on the substrate must be dry, i.e. no droplets of liquid should form on the surface. The matter of why the deposit must be dry is dealt with in more detail in Section 4.6 As the area onto which the electrospray plume is sprayed decreases, the ratio of surface area to liquid sprayed onto the surface decreases as the square of the deposit diameter. Using an aluminum backing (hydrophobic), droplets of liquid form readily on the surface, rather than spreading out. Therefore, in order to keep the deposit dry as it is being sprayed, the aluminum substrate must be heated to increase the eluent evaporation rate.

Heating the aluminum substrate had several difficulties associated with it. One difficulty was heating the aluminum strip when it is at -5 kilovolts with respect to ground; using an infrared heat lamp to heat the drum solved any isolation problems. Another problem was that even with heating, eluent flow rates of greater than 2 µl/minute produced wet deposits and unreliable results. Low flow rate meant that the analysis times for strongly retained substances on a 0.5 mm i.d. column could become unpractically long (void volume elution times ≃ 15 minutes). Clearly, for practical work, this flow rate restriction made analysis difficult. However, several good results were obtained using the heat lamp and aluminum foil and are described in the Chapter 4.

To relax the flow rate restriction imposed by sample wetting, a fruitful approach was the modification of the surface properties of the substrate. The formation of droplets on the surface of the substrate was, at least in part, due to the hydrophobic nature of the surface. If

a single electrospray droplet lands on a hydrophobic surface and is not completely dry, then the droplet will form a roughly spherical drop on the surface, to minimize its contact area with the hydrophobic substrate. These microscopic drops dry slowly, due to the small area: volume ratio of a sphere. If more droplets impact the surface adjacent to the original droplet before it dries, the droplets coalesce into a larger drop, with a further decrease in the area: volume ratio and a slower evaporation rate. Clearly, this process rapidly produces large drops on the surface. To stop the formation of these drops, the process must be halted at the first stage: each droplet must evaporate before the next adjacent droplet arrives.

One method to effect rapid drying of the spray droplets was to heat the surface, as described above. Another method was to make the surface that the droplets were sprayed onto hydrophilic, rather than hydrophobic. A hydrophilic surface allows a droplet on the surface to spread out on the surface, greatly increasing the area/volume ratio of the liquid in the drop. The increased area leads to increased evaporation, producing rapid drying of the droplet.

Unfortunately, most metal surfaces are hydrophobic. Aluminum can be made hydrophilic by the addition of an electrochemically generated oxide layer (a process called anodization [63]). The simplest method of producing an anodized surface on an aluminum foil strip was to make the foil the anode in a dilute sulfuric acid bath (10% sulfuric acid by volume) and slowly increase the voltage between the electrodes to approximately 35 VDC. Going beyond 35 VDC caused the strip to be etched. Strips of foil were produced using this method and some improvement in the surface properties of the foil was observed. Surface films of oxide

of greater than 500 nm in thickness were easily produced in this way; the thickness could be estimated from the interference colors produced on the foil surface. These oxide films are called "porous films" because of small (10 nm) pores in the surface caused by the anodization process. These are thought to allow the formation of thick layers of oxide without disruption of the surface. Unfortunately, the hydrophilic properties of these thick oxide layers do not seem to be stable: the layers become increasingly hydrophobic as they are mildly heated (40 C), presumably due to loss of absorbed water.

A refinement to the aluminum oxide layers was to convert the surface from Al_2O_3 to (AlO)OH, a material called "boehmite" (named after a naturally occurring form of aluminum ore [63]). Porous, anodized aluminum oxide layers were converted into boehmite by simply placing them into boiling water for ten to twenty minutes. The surface layer produced by this process was very hydrophilic. A 0.5 ul drop of water spread out rapidly on an aluminum foil strip prepared in this way (i.e. with a boehmite layer), forming a circle approximately 1 cm in diameter. The same drop placed onto untreated aluminum foil stays in a spherical ball on the surface and takes approximately six times longer to evaporate (at room temperature in still air). It was the use of boehmite films that made higher flow rates (up to 5 µl/minute) possible. It should be noted that a thin boehmite layer can be produced on aluminum that has not been anodized, by simply boiling the material. The thin layer of oxide on the aluminum surface is converted into boehmite. However, the very thin layer of boehmite produced is not mechanically stable and can be removed by light abrasion (e.g. gently stroking the surface with a small camel

hair paint brush). The fragile nature of the surfaces produced on non-anodized aluminum makes them difficult to work with and nonuniform. For this reason, the additional step of anodizing a thick layer of aluminum oxide onto the foil before producing boehmite on the surface was found to be the most satisfactory from an operational standpoint.

CHAPTER IV

Results of the Microbore, Reverse Phase HPLC-MS Interface

4.1) General Comments

The following chapter details the main results of research into the applicability of the microbore HPLC, electrospray sample deposition, time-of-flight MS system described in the first three chapters. The work described occurred over the period May 1981 to April 1987 and is laid out in roughly chronological order.

4.2) Electrospray and Focussing

The first problem to be overcome was to decrease the radius of an electrosprayed deposit. A description of electrospray deposition was given in Section 2.4. The reason for decreasing the radius of the deposit was to match the area of the deposit to the area analyzed by the primary ion beam ($\simeq$ 1 mm^2). A major criticism of the electrospray method of sample preparation was the large amount of material used to prepare a sample - on the order of 100 ug - of which only a small fraction would eventually be examined by the ion beam [64]. The sensitivity of such a method was obviously limited by the great waste of sample involved. If an HPLC interface was to be developed, sensitivity must be an important issue. A system that could not use samples smaller

than 100 ug would be of little practical use for solving problems involving biological molecules where only a few nanomoles of material may take a researcher months to produce. The limitation of using microbore HPLC (see Section 2.3) also restricts the amount of sample that can be applied to the top of the column. The maximum injection volume for a microbore column of the type proposed was about 1 µl. Therefore, if 100 µg of sample were necessary, the sample would have to be very soluble in the mobile phase just to be applied to the column and would saturate column material producing undesirable peak tailing.

Clearly, if the diameter of the electrosprayed deposit could be reduced from 25 mm (a typical value for samples dissolved in methanol sprayed from a 26 gauge needle) to 1 mm, the amount of sample required could be reduced by a factor of 625, hopefully without changing the intensity of the quasi-molecular ions produced. The amount of sample needed would then be approximately 100 ng, a more useful level of sensitivity, allowing a microbore column to function without sample saturation.

The first approach to focussing the electrospray was to treat the charged electrospray droplets as if they were ions or electrons and use normal ion optics to focus them into a smaller spot. The first lens tried was an einzel lens. An einzel lens consists of an entrance plane held at ground, a central cylinder held at high voltage and an exit plane also at ground. It was found that the electrospray droplets did not traverse this type of lens but rather deposited on the entrance electrode. The reason why the droplets did not enter the lens is simple: the assumption that an electrospray droplet was equivalent to an ion in a vacuum was invalid. Electrosprayed droplets do not continue in a

straight line when they pass into a field-free region. Rather, they slow rapidly due to the frictional force of air on the approximately spherical droplets. The introduction of an important frictional resistance into the consideration of lens type to be used leads to the conclusion that the droplets must always be kept moving under the influence of an electric field; there can be no field free region in the optics.

A type of lens that has no field free region is an immersion lens, the type used in electron guns in television picture tubes. Immersion lenses have two cylindrical electrodes, one above the point of electron production, and one below. By analogy, the electron source was replaced with the electrospray needle. It proved difficult to set the lens voltages so that a stable electrospray was possible. Figure 4.1 shows an example of the results obtained using an immersion lens. From Figure 4.1, it was clear that it was possible to focus the electrospray using an immersion lens. However, it was also observed that the deeper the needle tip was in the lens, the greater the amount of sample was being deposited on the electrodes of the lens, implying that the decrease in deposit diameter produced was at least in part due to the loss of droplets with a large radial velocity to the lens electrodes. Clearly if the object of focussing the spray was to increase the amount of sample being deposited on a small area, any attenuation of sample caused by the lens was undesirable.

Experimentation with various types and configurations of electrodes resulted in several simple, but effective, configurations for focussing the electrospray. The easiest method for decreasing the deposit diameter proved to be the addition of an electric field parallel to the substrate

Figure 4.1

Electrospray plume focussing characteristics

of an immersion lens.

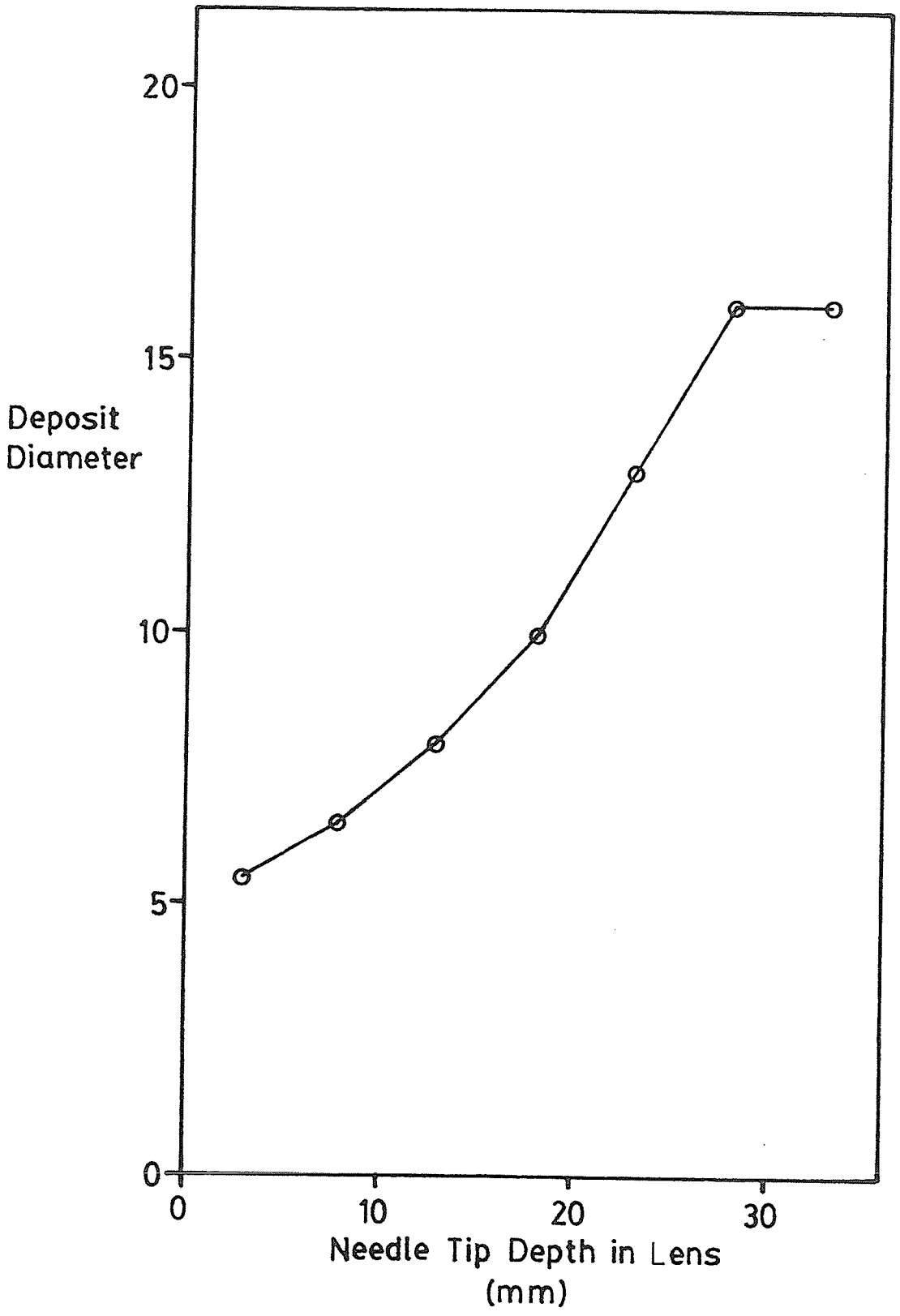
20
15
10
5
0
Deposit
Diameter
0
10
20
30
Needle Tip Depth in Lens
(mm)

plane. The electrosprayed droplets follow electric field lines, so the superposition of a field normal to the substrate with the divergent field created by the needle had the effect of "flattening" the off-axis electric field lines. This field "flattening" reduced the deposit diameter by a factor of 2 - 3. While this reduction was promising, it was still not a large enough factor to give the increase in sensitivity required.

As was mentioned in Section 2.4, the electrode configuration that produced the necessary reduction in deposition diameter was a conductive wire ring, concentric with the spray needle. The ring originally used was made of 14 gauge copper wire and had a radius of 25 mm. With the sample backing surface held at negative high voltage (-3 to 5 kV) and the needle held at ground, the ring was attached to a high voltage supply allowing the ring to be placed at either positive or negative voltage with respect to the needle. For positive voltage on the ring, the effect was to decrease the sample deposit's diameter. For negative high voltage, the effect was to increase the deposit's diameter. By selecting a ring voltage between ground and +2 kV the deposit diameter could be easily reduced to 1 to 2 mm. The additional effect produced by the parallel plate field described above was used initially but was found to be less important than originally thought with the substitution of a smaller ring (5 mm diameter, 20 gauge wire).

After the focussing properties of the ring electrode were discovered, it was necessary to determine if the focussing properties were caused by attenuation, as was the case with the immersion lens. Simply spraying a sample with the ring in place did not produce a noticeable deposit on the ring and the spray plume (made visible by

shining a laser through the plume) appeared to travel only towards the sample backing, without any component going to the ring. To be positive that no attenuation was occurring, a known quantity of CsI was sprayed onto a piece of aluminum foil from a methanol solution, both with and without the focussing ring. The deposit was then redissolved in a carefully measured quantity of deionized water; then the solutions were assayed for iodide content spectrophotometrically using the reaction of toluidine with iodide to produce a yellow product. The results showed that the sample sprayed with the focussing ring contained the same amount of iodide as the sample sprayed without the ring.

With a method for focussing the electrospray plume established, the next question was whether deposits made by focussed electrospray would produce quasimolecular ions in the same abundance as deposits that were sprayed unfocussed. Because the theoretical reason why electrosprayed deposits worked was not completely understood (i.e. why an electrosprayed deposit produces quasimolecular ions and a deposit produced by drying a solution on the same surface does not), it was not clear that focussing the electrospray plume would not have some effect on the subtle mechanism which produces "good" samples. Initial experiments were encouraging. The sample material chosen was phenylalanine ($C_9H_{11}O_2N$) because it gave strong quasimolecular ions at m/z = 166 u, a fragment ion (M-COOH) at m/z = 120 u and a "tropyllium" ion at m/z = 91 u. The results are shown in Figure 4.2. The graph demonstrates that the quasimolecular ion yield increases (for a sample of 0.5 ug) as the diameter of the spot decreases. The curve corresponding to Al^+ cation (m/z = 26.98) showed that the

Figure 4.2

Quasi-molecular ion intensity versus deposit diameter for phenylalanine.

(Sample size = 0.5 μg)

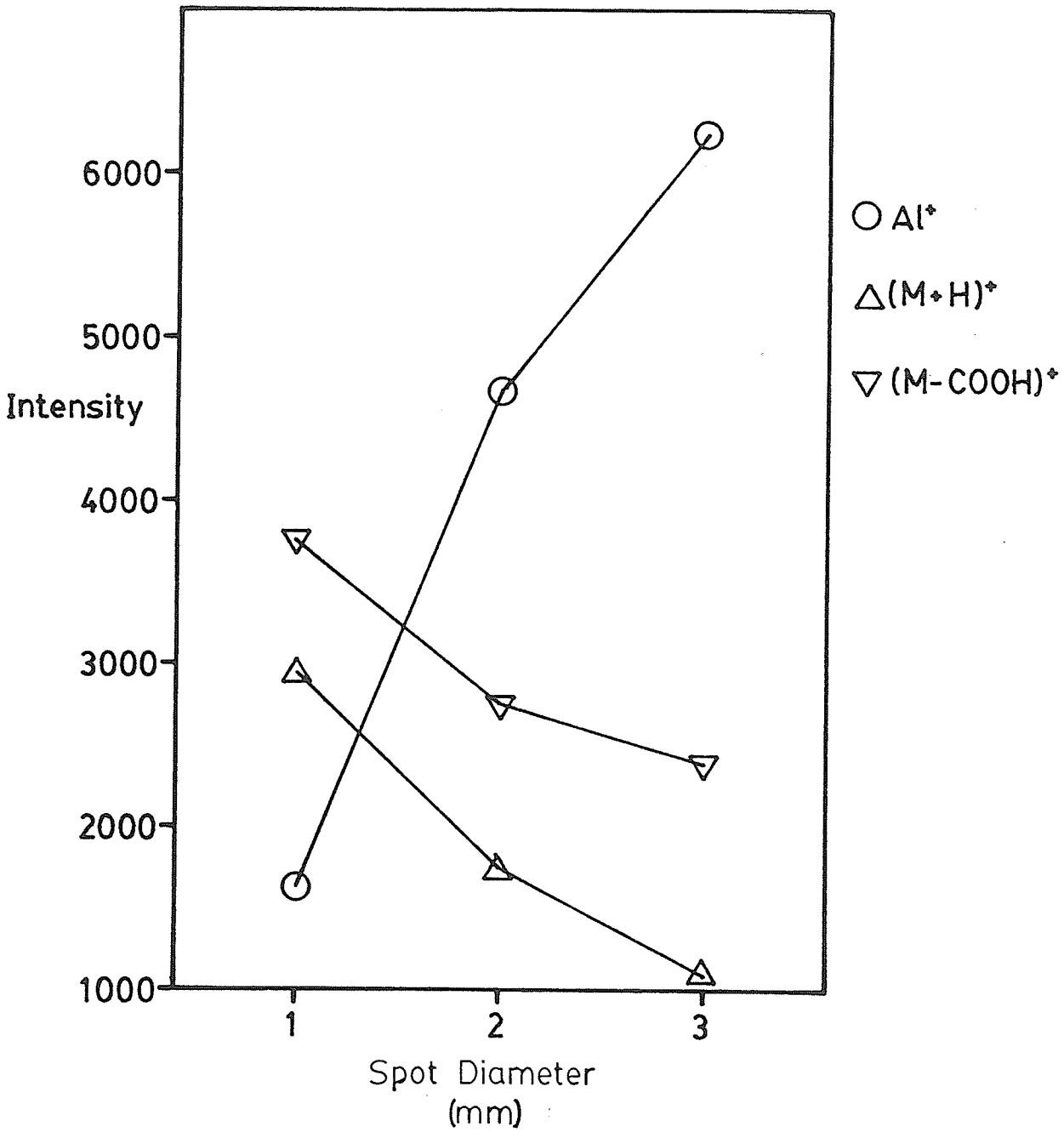
6000
5000
4000
3000
2000
1000
Intensity
1
2
3
Spot Diameter
(mm)
Al+
(M+H)+
(M-COOH)+

substrate was being covered by the sample to a greater extent as the deposit diameter decreased.

Once it became clear that focussing the electrospray plume was possible and the focussing did not interfere with the formation of quasimolecular ions in the mass spectrometer, it was necessary to investigate the behavior of electrospray with respect to an important parameter in HPLC: flowrate. The initial experiment was done using the HPLC eluent deposition apparatus with a C18 column, 1.0 mm diameter, 0.5 ul injection volume, an aluminized polyester substrate and methanol eluent. Phenylalanine was injected onto the column with the column running at various flowrates and the eluent electrosprayed onto the aluminized polyester. The spray apparatus was slightly different from that described in Section 3.4. The spray was vertical rather than horizontal and the strip of substrate was slowly dragged past the spray in a continuous motion. The results of these experiments were shown in Figure 4.3. These results demonstrated that the yield of quasimolecular ions from a sprayed deposit was strongly dependent on the flowrate of the HPLC, with the best SIMS yields being obtained from very low flowrates, approximately 1 µl/minute (the lowest flowrate achievable with the Eldex piston pump). These results were reported at the American Society for Mass Spectrometry's 31st Conference on Mass Spectrometry and Allied Topics in Boston, May 1983 [62].

The limitation of flowrate to 1 ul/minute was a serious handicap for the development of an HPLC system incorporating electrospray deposition of the entire eluent. The theoretical discussion given in Section 2.3 shows that for a flowrate of 1 µl/minute, the maximum column diameter allowable, without loss of resolution, was approximately 0.25 mm (0.01").

Figure 4.3

Quasi-molecular ion intensity versus electrospray fluid flowrate of a phenylalanine sample.

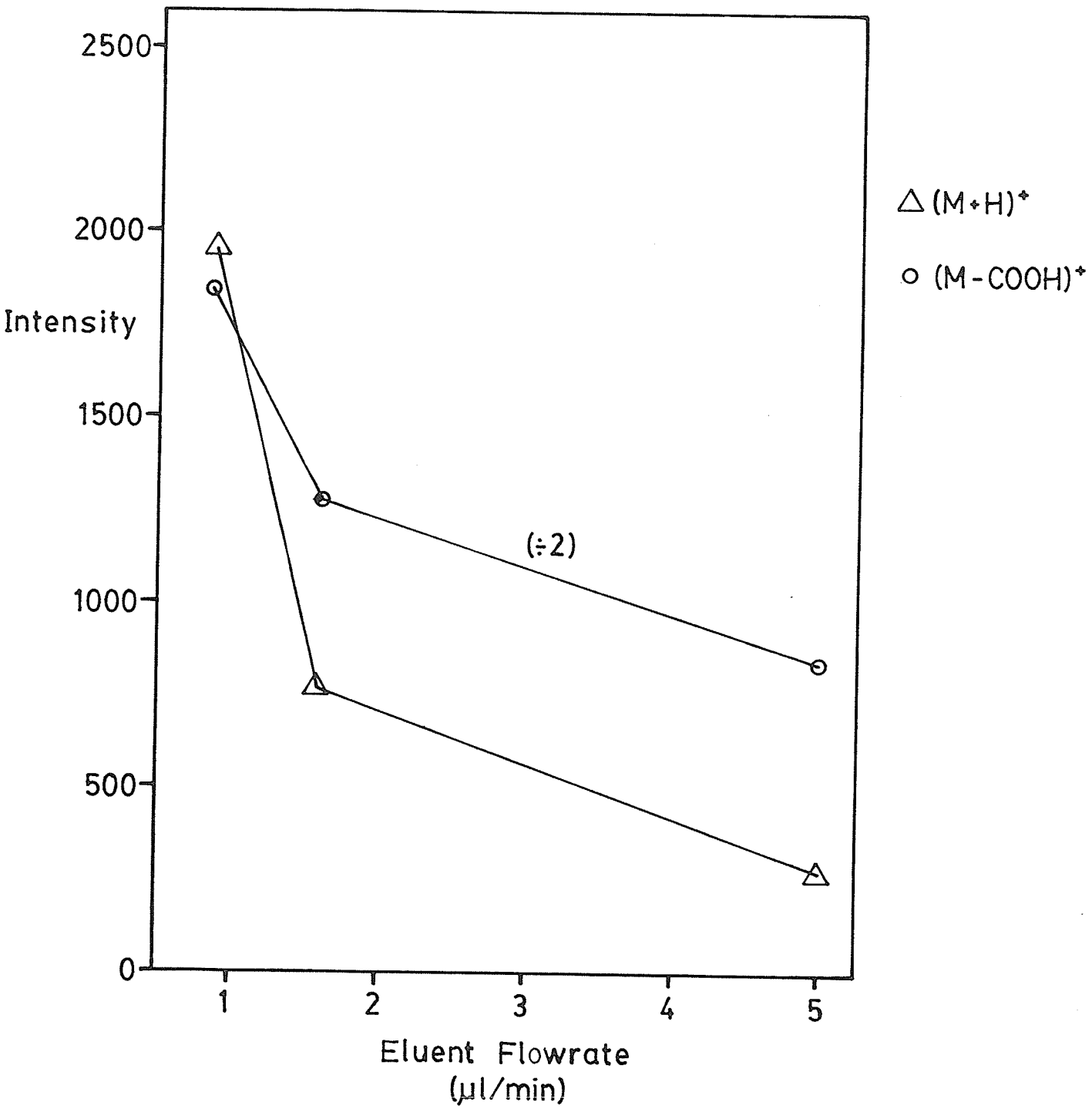
2500
2000
1500
1000
500
0
Intensity
1
2
3
4
5
Eluent Flowrate
(µl/min)
(÷2)
△ (M+H)+
○ (M-COOH)+

At the time this limitation was discovered, successful columns of such small internal diameters had not been reported in the literature and it was not clear that such a column could be packed.

4.3) Early HPLC Results

The first column diameter attempted was 1.0 mm (0.04") i.d., 1/16" o.d., packed with 10 um particles. These parameters were selected to reproduce the results of Scott and Kucera [65, 66]. The packing system used was similar to the one described in Section 3.3, with a packing reservoir of 10 ml capacity. The column blank was 50 cm long. The slurry solvent was 70:20:10 acetonitrile:methanol:hexane. The slurry contained 10 ml of solvent mixture and 0.75 g of RSil (Alltech) 10 um irregular reverse phase silica. The column was packed at 65 MPa for 90 minutes, using methanol as the packing solvent. The column endfitting consisted of a drilled through Valco 1/16" female coupling, with a 1/16" diameter, 1 mm thick, 2 μm porosity stainless steel frit pressed between the end of the column and a section of 0.01" i.d. stainless steel tube (5 cm long) with a 26 gauge needle soldered onto the end for electrospraying.

The first column showed some promise. Several amino acids injected onto the column produced "spots" on the aluminized polyester substrate as it was moved past the electrospray. The mechanism for moving the substrate past the electrospray is shown in Figure 4.4. The chromatogram on the substrate was not very good, demonstrating an efficiency of no more than 500 plates. The substrate also showed a continuous visible deposit, somewhat intensified where the amino acids were deposited. It

Figure 4.4

The original electrospray/substrate advance apparatus.

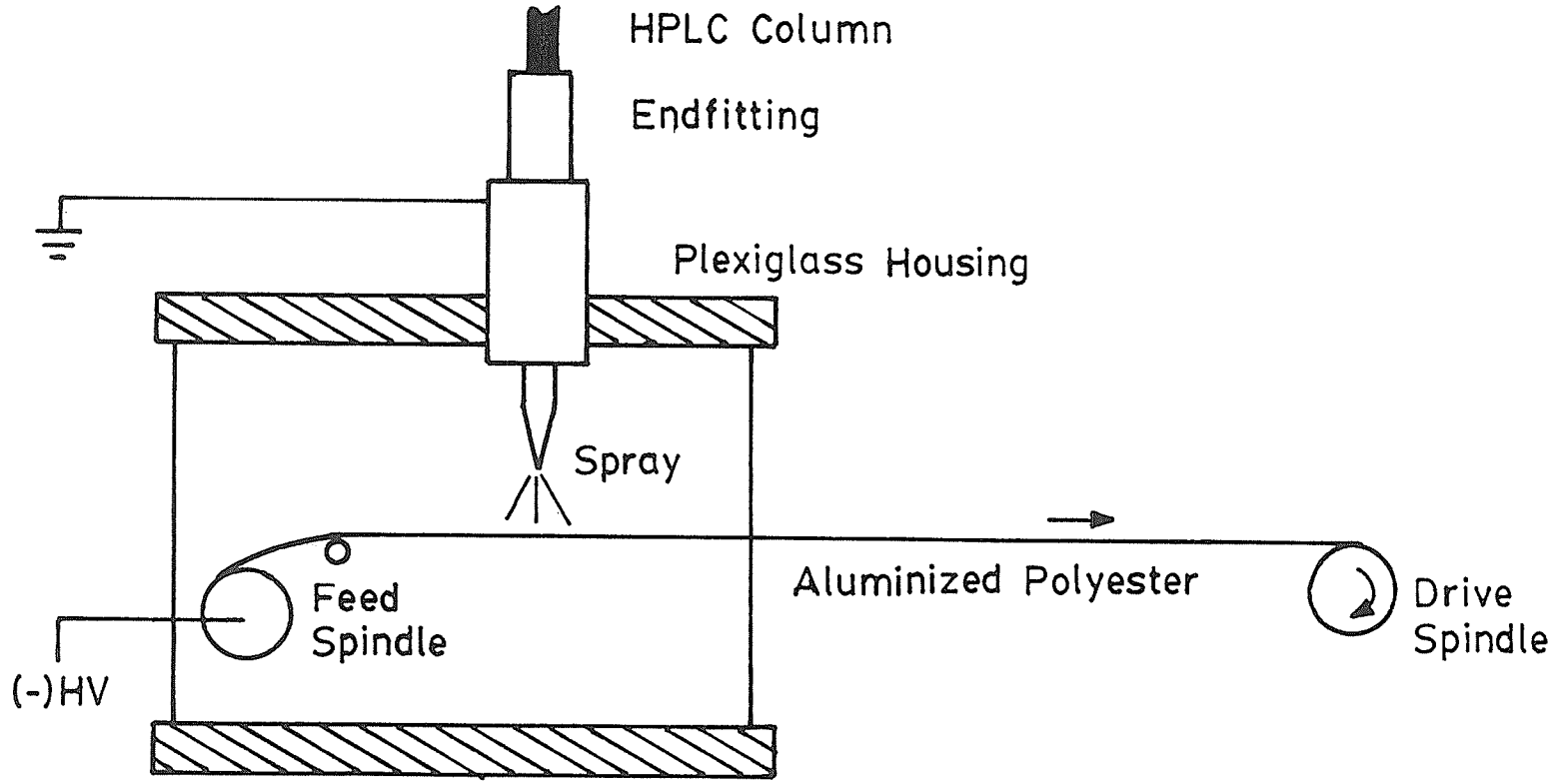
HPLC Column
Endfitting
Plexiglass Housing
Spray
Aluminized Polyester
Feed
Spindle
(-)HV
Drive
Spindle

was difficult to spray any solvent mixture containing water (as little as 20%) and the addition of water to the solvent mixture dramatically increased the visible deposit on the substrate. The strip sample holder described in Section 3.4 (see in particular Figure 3.8) was not yet built; (because of problems in the machine shop, the holder was not completed until August, 1984) so any deposit on a substrate strip had to be cut out of the strip and carefully mounted on an individual sample holder of the type normally used in the mass spectrometer (Figure 1.2). The spots corresponding to amino acids on these early strips showed very poor quasimolecular ion yields for the amino acids and a large number of background ion peaks.

The high backgrounds observed were of particular concern. A frequently mentioned subject in discussions of the coupling of HPLC to MS was the high levels of impurities present in HPLC eluent [67, 68]. In our application, a surface active impurity present in the solvent would totally extinguish quasimolecular ion yields by creating a surface layer of impurity shielding the molecules of interest from the primary ion beam. Techniques that examine the bulk of the eluent (such as UV absorption or thermospray ionization MS) may not be as sensitive to these contaminants as static SIMS. Because the range of the primary ions in an organic material is quite short (on the order of 5 - 10 nm), even monolayer coverage of the electrosprayed deposit results in a substantial reduction of secondary ion yields. For this reason, it was necessary to establish a regimen to minimize the amount of contamination present in the HPLC solvents before worrying too much about the resolution of the HPLC column.

The most obvious source of contamination of the HPLC solvents was the solvents themselves. Initially it was thought that HPLC grade

solvents would be ideal for our application. Therefore HPLC grade water (Fisher), HPLC grade acetonitrile (Caledon Laboratories) and spectrophotometry grade methanol (Caledon Laboratories) were used. All of these solvents left substantial deposits on the substrate when electrosprayed. The HPLC grade water was particularly contaminated, leaving a very strong deposit at relatively low (10% by volume) concentrations in the eluent.

The reason for the contamination problem with these solvents was the difference in requirements for conventional HPLC using a ultraviolet absorbance detector and our detection system. Solvents manufactured for use with ultraviolet absorbance detectors must not contain impurities that absorb in the ultraviolet (i.e. wavelengths between 185 and 300 nm) and are rigorously refined and tested to assure that they do not. However, in our application, not only were we interested in solvents without ultraviolet absorbing material dissolved in them, but the solvents had to be low in all types of dissolved materials, including alkali metal cations and plasticizers. From testing HPLC grade solvents, it was apparent that the amount of dissolved solid, particularly sodium and potassium salts, was too high to be used. To minimize the level of dissolved solids, various brands of solvent were tested. Caledon Laboratories Distilled-in-Glass grade solvents appear to give the best results for organic solvents such as methanol, acetonitrile and 2-propanol. Water, being an excellent and aggressive solvent for alkali metal cations, was originally distilled using a simple distillation apparatus and later using a sub-boiling quartz still to remove dissolved material. The best type of commercial water proved to be Fisher W-2 grade water, purchased in 20 liter polyethylene carboys. In the last

year, water obtained from the University of Manitoba Department of Chemistry's Instrumentation Laboratory, produced by reverse osmosis and a four cartridge water finishing system, has been available and has proved satisfactory.

The second important source of contamination in the HPLC eluents used was the buffers. A buffer is a mixture of acid and base solutions that is used to maintain the pH of a solution within certain bounds. Buffers are used in peptide chemistry to maintain the charge balance between basic groups (e.g. amines) and acidic groups (e.g. carboxylic acids) found in any peptide's structure [69]. In order to carry out HPLC on peptides, it is necessary to keep the peptide molecules in one charge state as they travel down the column. For many types of peptides, the fully protonated form produces the best chromatographic resolution. Typical buffers for HPLC are composed of ortho-phosphoric acid, trifluoroacetic acid, acetic acid or formic acid and triethylamine, ammonium hydroxide or pyridine. Frequently, a relatively low concentration of trifluoroacetic acid (TFA) (e.g. 0.1% TFA v/v) or ortho-phosphoric acid (e.g. 0.05 M) is used neat in the eluent to protonate the peptides. When highly positively charged peptides are being examined, it has been found to be necessary to include a counterion for the acid, such as triethylamine (TEA) [69]. For reasons that are not fully understood, these positively charged peptides (those containing lysine or arginine residues) can become bound to the column if these basic counterions are not present.

It was decided to try to use volatile buffers in our system. Buffers based on ortho-phosphoric acid are not volatile at room temperature and so such buffers were automatically eliminated from consideration. Desiderio [70] suggested the use of TEA/formic acid

buffers in conjunction with mass spectrometry. These buffers are easily evaporated and do not interfere with the mass spectrometry. Following Desiderio's lead, the initial work done using our microbore columns used a TEA/formate buffer, with $3.0 \leq pH \leq 7.0$ at a concentration of approximately 0.1% v/v. The addition of this buffer system to the HPLC eluent improved the characteristics of the HPLC column, but produced a large increase in the amount of involatile material left on the substrate after spraying. A thorough washing of the column with the buffer eluent decreased the amount of the deposit somewhat, however the level of contamination was still unacceptable. The TEA and formic acid were both obtained from Fisher and were reagent grade.

A simple distillation of the liquids decreased the visible deposit. With respect to volatile buffers, it was found that even with redistilled buffers a deposit was still left on the substrate, but the deposit would eventually disappear, presumably by evaporation. Some reflection pointed out the problem. What were referred to as "volatile" buffers in the literature were buffers easily removed by lyophilization (vacuum freeze drying), a definition that did not necessarily imply that the buffer salts rapidly evaporated at room temperature. These organic salts, such as triethylammonium formate, have decomposition points over 100° C, but will spontaneously decompose in the presence of water and the individual components evaporate slowly at room temperature. Experimentation showed that if the substate was held at 40° C, no deposit from the buffered eluent was left on the surface. Raising the substrate temperature also proved helpful when spraying eluents with higher water loads (above 20% water), allowing the electrospray droplets to dry quickly on the surface and not coalesce into larger droplets (see the discussion in Section

3.6). The heating of the substrate was done using an infra-red heat lamp (200 W) set near the substrate holder. The use of a lamp rather than a direct electrical heater made the high voltage isolation of the substrate very simple. Care had to be taken to keep the temperature of the substrate down to the minimum necessary to evaporate the buffer; high temperatures encourage the oxidation of certain amino acid side chains, particularly methionine residues.

Even with the substrate heated, it was important to keep the concentration of buffer to as low a concentration as possible. After experimentation with TEA/formate buffers, TEA/TFA buffers were tried. The high dissociation constant of TFA (pK = 0.5) with respect to formic acid (pK = 3.75) meant that a lower concentration of TFA would have the same effect as a higher concentration of formic acid. TEA/TFA buffers also have their greatest buffering capacity at $2 \leq pH \leq 4$, the range of greatest importance in peptide work. The use of TEA/TFA buffers allowed the routine use of buffer concentrations of 0.01% to 0.05%, with good recovery of peptide from the column. The TFA (Aldrich) had to be redistilled before use.

After the contaminant concentration had been reduced to a reasonable level, further research into packing efficient columns was conducted. As was stated above, the first column packed was 1.0 mm i.d. x 50 cm length had a low plate count, poor (and variable) recovery and a very long t_0. Several variations of packing procedure produced no improvement so it was decided to attempt to pack a column with a 0.25 mm (0.010") i.d., also using RSil C18HL 10 um particles. Substantial effort was put into packing 0.25 mm columns and results were uniformly poor. These narrow diameter columns proved to be substantially worse with low resolution and rapid column failure. By analyzing the system theoretically, using the

tools set out in Section 2.3, it became apparent that the two problems of greatest importance for such small i.d. columns were the critical importance of any small dead volume, and the small mass handling capacity of a column containing so little packing material (a 0.25 mm i.d. x 30 cm column bed contains only 15 ul of packing). Therefore, the injector necessary for the proper use of such a column would have at most 0.10 µl injection volume, rather than the minimum of 0.5 µl injection volume available with our injection value. At the time, no injection valve of such a low volume was available commercially.

The most successful column diameter was 0.5 mm (0.020") i.d., both from the theoretical standpoint of Section 2.4 and from the practical viewpoint. Shortening the column from 50 cm to 20 cm made analysis times more reasonable, although because of the flowrate limit imposed by secondary ion yields (1 - 2 µl/min) the t_0 for the column was still 15 - 20 minutes for a typical chromatogram. The injection valve used was adequate for 0.5 mm i.d. columns and did not contribute a great deal to chromatographic band broadening.

Experience using RSil 18HL irregular silica demonstrated a lack of consistency in packing the columns and in the lifetime of the columns packed. The packing slurry solvent most frequently used was acetonitrile, but the slurry was not very stable and had to be rapidly loaded into the packing reservoir before the particles settled. On the suggestions of Dr. Jim Owen (a visiting chromatographer) 2-propanol was tried as a slurry solvent and much better slurry stability was achieved. The viscosity of 2-propanol (2.4 Pa.S) was approximately 6 times the viscosity of acetonitrile (0.38 Pa.S), enabling the slurried particles

to remain in suspension longer. Also on Dr. Owen's suggestion, silica with a shorter reversed phase coating was tried, RSil 10 μm C4 reverse phase irregular silica. The shorter coating group was suggested for three reasons: increased resistance to column bed attack by solvents (see Section 3.4); decreased retention times for large molecules of low polarity; and increased recovery of peptide from the column bed with low concentration buffers.

The results of using Dr. Owen's suggestions were encouraging. Packing a 0.5 mm i.d. column using RSil C4 material suspended in 2-propanol produced a column of greater stability. When using the C18HL material, even with the best solvents, there was still a light continuous deposit left on the substrate. The column bed had a tendency to shrink in the column, which limited its practical usefulness to about one week after packing. Presumably some of the column material was being attacked by the solvents because of incomplete endcapping of the silica. A column packed with C4 material showed a much reduced background. The butyl-silane used to cover the surface of the C4 material has little steric inhibition of more butyl-silane attacking the silica close to it, while the octadecyl-silane used in the C18 material strongly inhibits nearby reactions [62]. Therefore, the C4 material was more completely protected against the solvents. However, the change to C4 material did not eliminate the problem of column bed shrinkage; it was only slowed down.

The column shrinkage problem was improved by the removal of fines from the column packing material before packing. Irregular silica supports have the tendency to break off small projections on the material in the course of normal handling. These smaller particles are called

fines and because of their small size are not retained by the endfitting's frit. As the fines were slowly washed out of the column bed, the bed shrank, leaving a gap at the top of the column of several millimeters. This gap provided an unacceptably large mixing volume on the top of the column, broadening the chromatographic bands. The fines were removed by sedimentation rate in 2-propanol. A gram of packing material was suspended in 100 ml of 2-propanol and then placed in a graduated cylinder. The silica separated into a fast sedimenting and slow sedimenting fraction. By discarding the slow sedimenting fraction and repeating the operation on the pellet left on the bottom of the cylinder several times, the fines were effectively removed. A column bed packed with the fast sedimenting material remained stable for over a month and showed little deposited background.

The selection of the mobile phase system to be used for separating peptides was the final important problem to resolve. The first experiments with our packed columns were done using acetonitrile as the organic modifier in the eluting solvent. Acetonitrile is the most commonly used solvent in the HPLC literature and has several advantages for use in conventional HPLC equipment [71, 72]. If ultraviolet absorption is used as the detection method, acetonitrile is ideal, because of its low (185 nm) UV cutoff point. Most other organic solvents have cutoff points over 200 nm and many, such as dimethylformamide or acetone, have UV cutoff points above 250 nm. The most important UV range for the detection of peptides is 200 - 260 nm (many single wavelength detectors are set at a nominal 254 nm to detect the amide bonds in a

peptide). In addition, when using gradient elution methods to increase the resolution of a column for a complex mixture of peptides, the mobile phase composition changes with time during the course of the chromatogram. Figure 4.5 showed the viscosity of acetonitrile/water mixtures as a function of water content. The graph shows a near linear increase in viscosity as the percentage of water in the mixture increases, with a maximum viscosity at approximately 20% acetonitrile. During a gradient run, the column back pressure therefore decreases slowly (after 20% acetonitrile) and nearly linearly with an increase in acetonitrile content, making it easy for the pumping system to deliver an accurate gradient. The viscosity of methanol/water mixtures has a very different profile, with a maximum viscosity at approximately 60% water, as shown in Figure 4.6. The maximum is almost twice the viscosity of pure water. Therefore, during a gradient run, the back pressure developed across the column bed would increase sharply and then decrease, making it difficult for the pumping system to keep up an accurate gradient and flowrate. For these two reasons, acetonitrile is the organic modifier of choice for conventional HPLC peptide analysis.

In our HPLC system, the normal reasons for choosing acetonitrile as the organic modifier were not germane. There was no ultraviolet detector (or detector of any kind) at the outlet end of our HPLC column, therefore ultraviolet cutoff was not a factor. Also, because of the low flowrates involved, gradients were not used, so the unusual viscosity behaviour of alcohol/water mixtures was not a limiting factor. What was important was that alcohol/water mixtures electrosprayed more easily than acetonitrile/water mixtures. Mixtures of up to 80% water electrosprayed

Figure 4.5

Fluid viscosity as a function of organic content for acetonitrile/water mixtures.

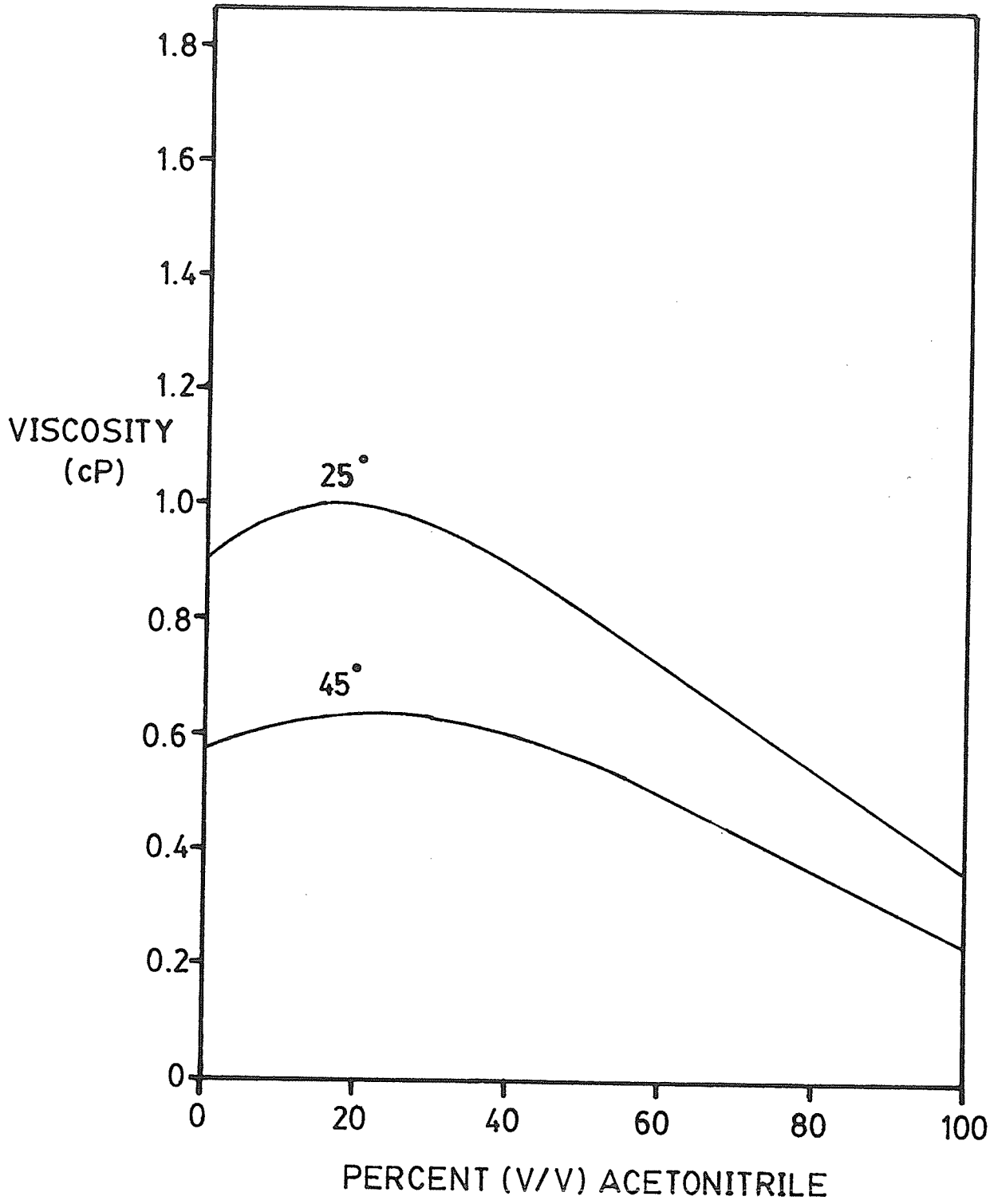
1.8
1.6
1.4
1.2
VISCOSITY
(cP)
25°
1.0
0.8
45°
0.6
0.4
0.2
0
0
20
40
60
80
100
PERCENT (V/V) ACETONITRILE

Figure 4.6

Fluid viscosity as a function of organic content for methanol/water mixtures.

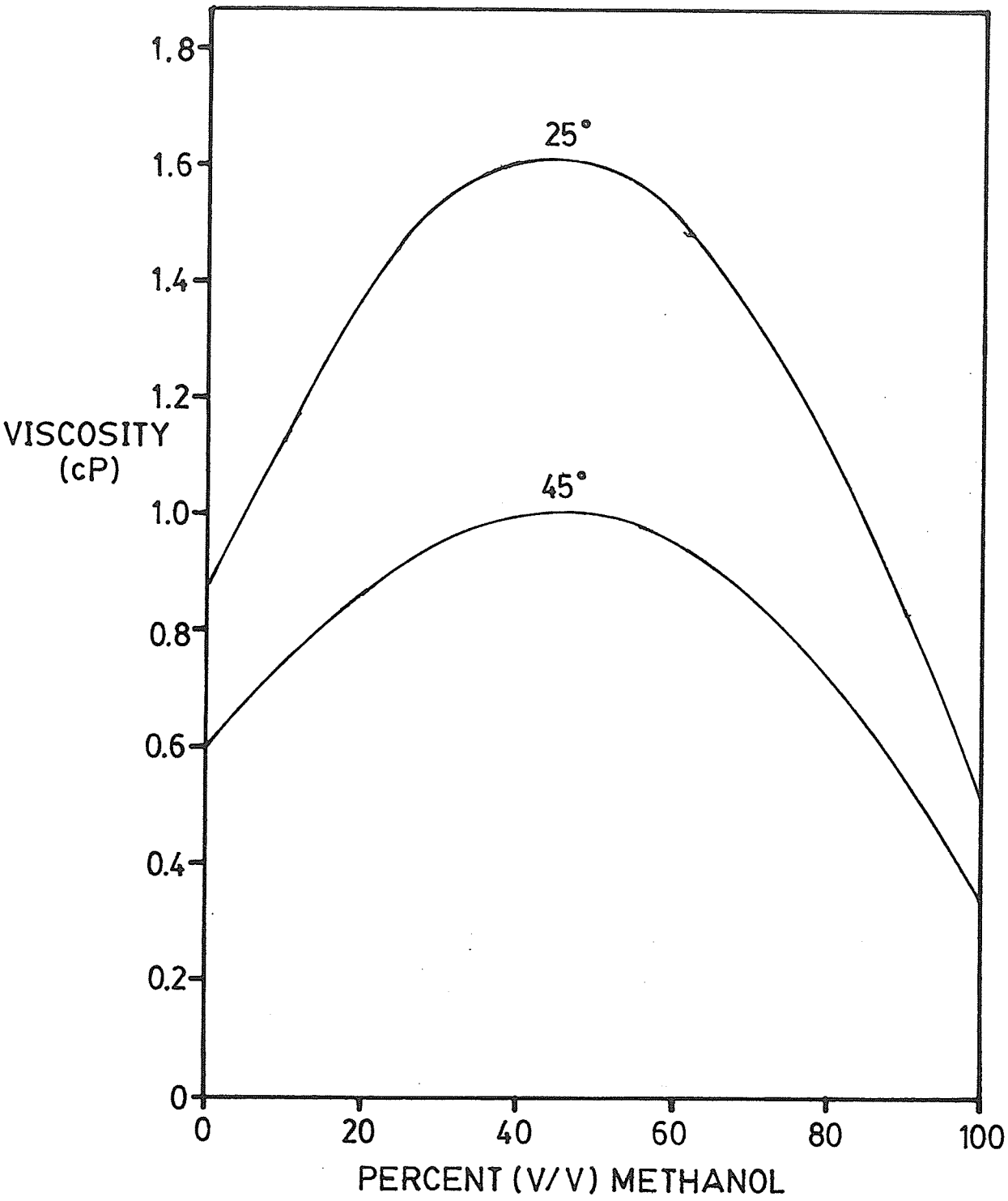
1.8
1.6
1.4
1.2
1.0
0.8
0.6
0.4
0.2
0
VISCOSITY
(cP)
25°
45°
0
20
40
60
80
100
PERCENT (V/V) METHANOL

quite well when using 2-propanol as the organic modifier, but were very difficult to spray using acetonitrile. Methanol was also a satisfactory organic solvent with respect to its electrospraying compatibility. Difficult to spray mixtures of water and either acetonitrile or methanol were made much more tractable by the addition of 5-10% 2 - propanol.

From the standpoint of chromatography, 2-propanol had good characteristics for our microbore system. The relatively high viscosity of 2-propanol/water mixtures allowed the microbore columns to be run at low flowrates with reasonably high back pressures. The typical retention times in a 2-propanol/water reverse phase silica system were not too long for small peptides (initially our interest was in enkephalin-like peptides with 4 - 6 amino acid residues) and did not vary sharply with 2-propanol concentration, as was the case with methanol or acetonitrile [72]. The mass spectra of samples sprayed from 2-propanol/water mixtures were at least as good as those sprayed from methanol, usually better. Therefore, 2-propanol was the organic modifier of choice for use in our microbore HPLC.

4.4) Initial LC-MS Results

The first positive results of the use of the system described above were reported at the American Society for Mass Spectrometry 33rd Annual Conference on Mass Spectrometry and Allied Topics in San Diego, California in May 1985 [73]. An expanded version of that material was presented at the Fifth Annual Conference on the HPLC of Proteins. Peptides and Polynucleotides in Toronto, Ontario in November 1985 [74].

The primary impetus for the development of an LC-MS system was to separate mixtures of peptides obtained from biological sources. The peptides of main interest were neurotransmitters, in particular the endogeneous opiates. The class of peptides selected as a model system for developing procedures for handling these compounds was the naturally occurring and synthetic analog enkephalins. Enkephalins were chosen because the are simple, well characterized peptides, that have been used to determine the mass spectral fragmentation pathways for peptides [75]. The enkephalins are small peptides (typically 5 amino acid residues) so that a great deal of structural information can be determined from the secondary ion mass spectra. Our experience with enkephalins had demonstrated had shown that they produce quasimolecular ions relatively easily, so that if an LC-MS technique would not work with the enkephalins it was not going to be suitable for peptide work. Another important consideration was that a large range of structurally modified enkephalins were available commercially at reasonable cost, allowing for a large amount of experimentation in the separation of structurally similar peptides without the expense involved if a more "exotic" class of peptides had been chosen. Note: Frequent references to amino acids in peptides will be made during the rest of the thesis using standard abbreviations, both three letter and one letter, as defined in Appendix B.

For the rest of this chapter, frequent reference is made to spectra reproduced in figures. All the spectra shown in this thesis (unless otherwise stated) were taken using the Manitoba TOF I time-of-flight mass spectrometer [29], using the time-to-digital convertor based data system and software designed by Werner Ens [23]. All of the spectra

were analyzed using the program TOFMA (designed by Werner Ens) and have been converted from a linear time abscissa to a linear mass abscissa by a simple algorithm. The titles of the spectra usually consist of a spectrum number of the type "Hxxxx.BIN" and either a number (the position of the spot being analyzed on the original substrate strip) or a description of the sample. The numbers on the right hand side of an individual histogram give the number of nanoseconds per channel in the data recorded on disk in the format "1ch=Xns" and the number of channels added together in a bin - this number forms a single bar in the histogram in the format "bin=Xch". The left hand side of the spectrum shows the absolute number of counts (individual ions recorded) in one bin. Unless otherwise stated, all the spectra were scaled so that the most intense peak in the histogram was full scale. Therefore, when a large spectrum is split up into several sections for clarity, care must be taken by the reader to check the left hand ordinate for scale factor changes.

The spectrum in Figure 4.7 was produced from a spot on the aluminum foil substrate sprayed with eluting solvent only. The solvent was 40:50 2-propanol:water, with 0.01% TFA, with a flowrate of 1 ul/minute. The deposit was approximately 1 mm in diameter and was collected for 4 minutes. The spectrum was typical of those obtained from any fraction not containing sample. The most intense ion in the spectrum is m/z = 23 u, corresponding to the sodium cation, Na^+. The next most intense peak is m/z = 27 u, a combination of the aluminum cation, Al^+ and $C_2H_3^+$. The peak m/z = 39 u is mainly due to the potassium cation K^+. Most of the other peaks in the spectrum correspond to organic contaminants in the solvents. It must be remembered that this spectrum was taken using the best solvents available. Above m/z =

Figure 4.7

Mass spectrum obtained from an HPLC eluent fraction sprayed onto aluminum foil containing only eluent contaminants. (Note vertical scale changes)

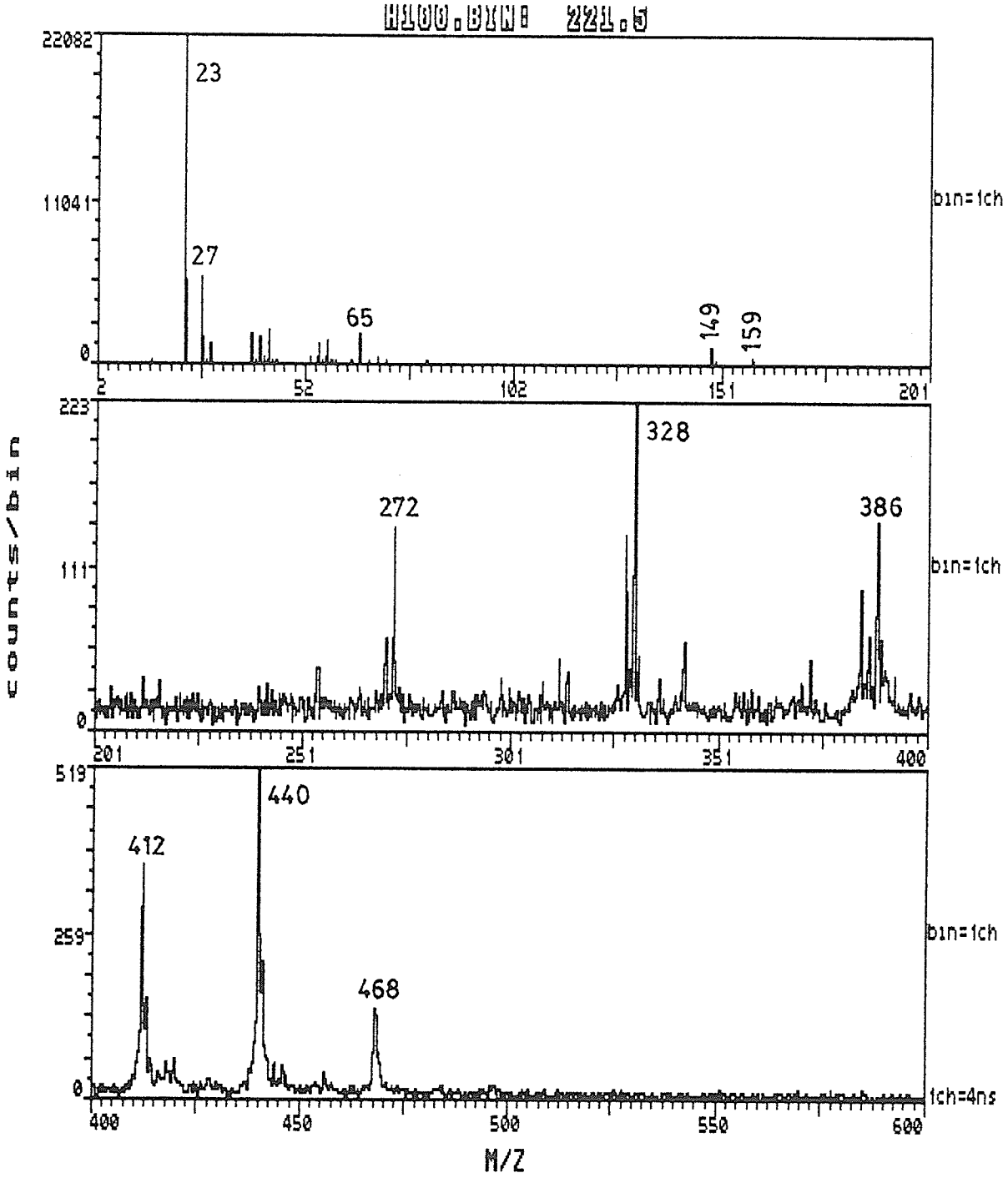
H100.BIN: 221.5
22082
11041
0
23
27
65
149
159
2
52
102
151
201
bin=1ch
223
111
0
328
272
386
201
251
301
351
400
bin=1ch
519
259
0
440
412
468
400
450
500
550
600
bin=1ch
1ch=4ns
counts/bin
M/Z

100 u, the most intense peak is m/z = 149 u, assigned to a stable fragment of phthalate plasticizer, a seemingly ubiquitous compound in mass spectrometry [68]. The higher mass peaks m/z = 412, 440 and 463 u are common to all spectra taken using these solvents and were due to contaminants in the water (spectra taken with the pure organic solvents did not show these peaks).

The spectrum shown in Figure 4.8 was taken from a section of unwashed aluminum foil that had not been electrosprayed. The most intense peak in this spectrum was m/z = 27 u (Al^+), but strong ion signals were also present for a large number low mass organic fragment ions. Also present were m/z = 6 and 7 u (Li^+), 23 u (Na^+) and 39 u (K^+). The most intense ion above m/z = 100 u was again m/z = 149 u (phthalate fragment) and much less intense ions were observed up to m/z = 900 u.

Obviously, it would have been to our advantage to have a substrate that produced fewer characteristic ions on its own, however it was found that washing procedures not only failed to reduce the number of contaminant peaks in the spectrum but usually added several new, intense peaks. It was decided that the foil, as it stood, was as good (or bad) as what was obtained after washing. Therefore it was used without modification as the sample substrate.

The simplest biological compound of interest for our purposes was phenylalanine. Not only was phenylalanine one of the amino acids present in most enkephalin peptides, but it served as a simple benchmark for determining the properties of a column. Figure 4.9 was the spectrum obtained from a fraction containing phenylalanine. The conditions were the same as for Figure 4.7, except that 50 ng of phenylalanine were

Figure 4.8

Mass spectrum obtained from bare, unwashed aluminum foil.

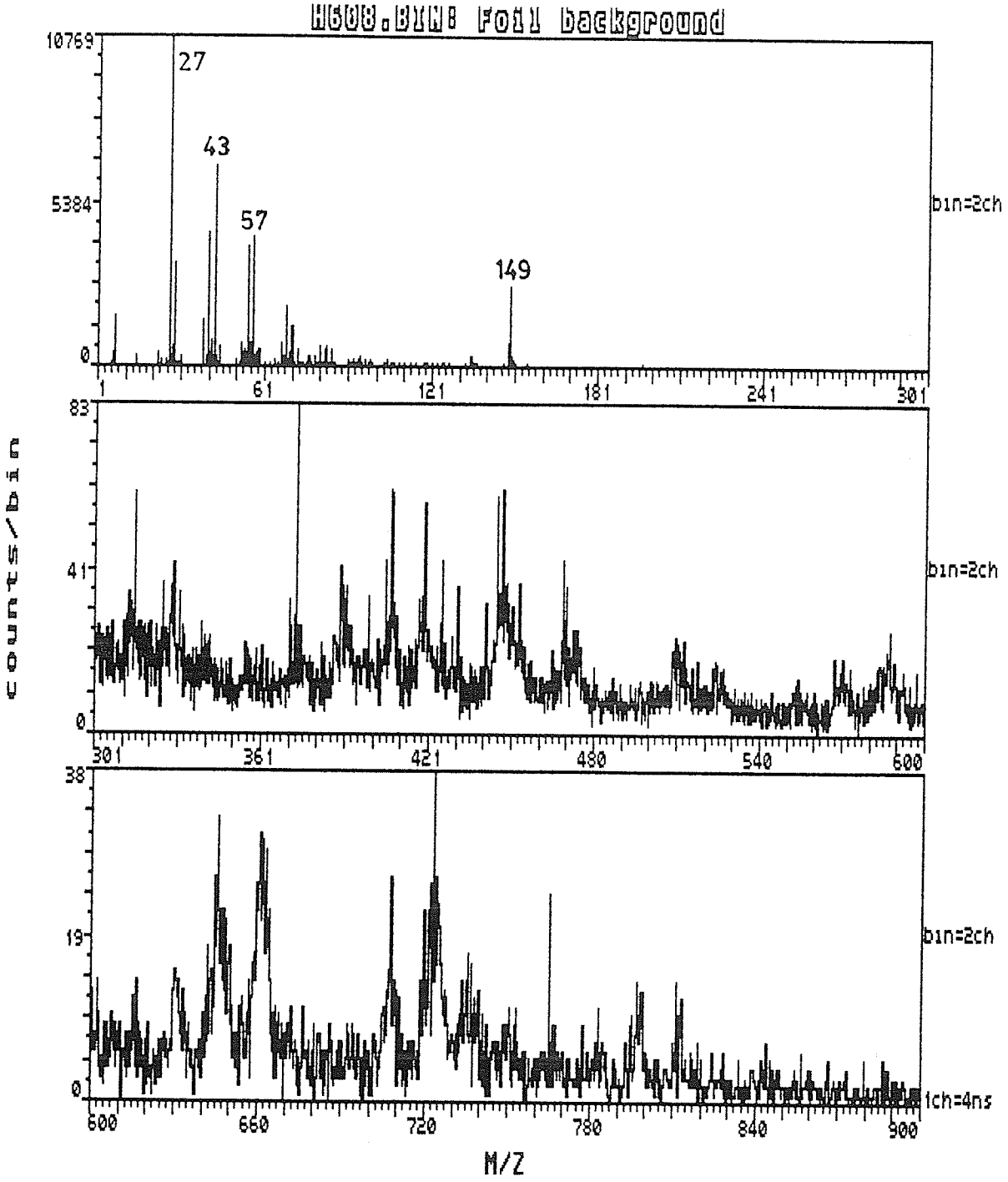
H608.BIN: Foil background
10769
27
43
57
149
5384
0
1
61
121
181
241
301
bin=2ch
83
41
0
301
361
421
480
540
600
bin=2ch
38
19
0
600
660
720
780
840
900
bin=2ch
1ch=4ns
COUNTS/BIN
M/Z

Figure 4.9

Typical mass spectrum of a phenylalanine containing HPLC fraction.

(0.5 µg injected)

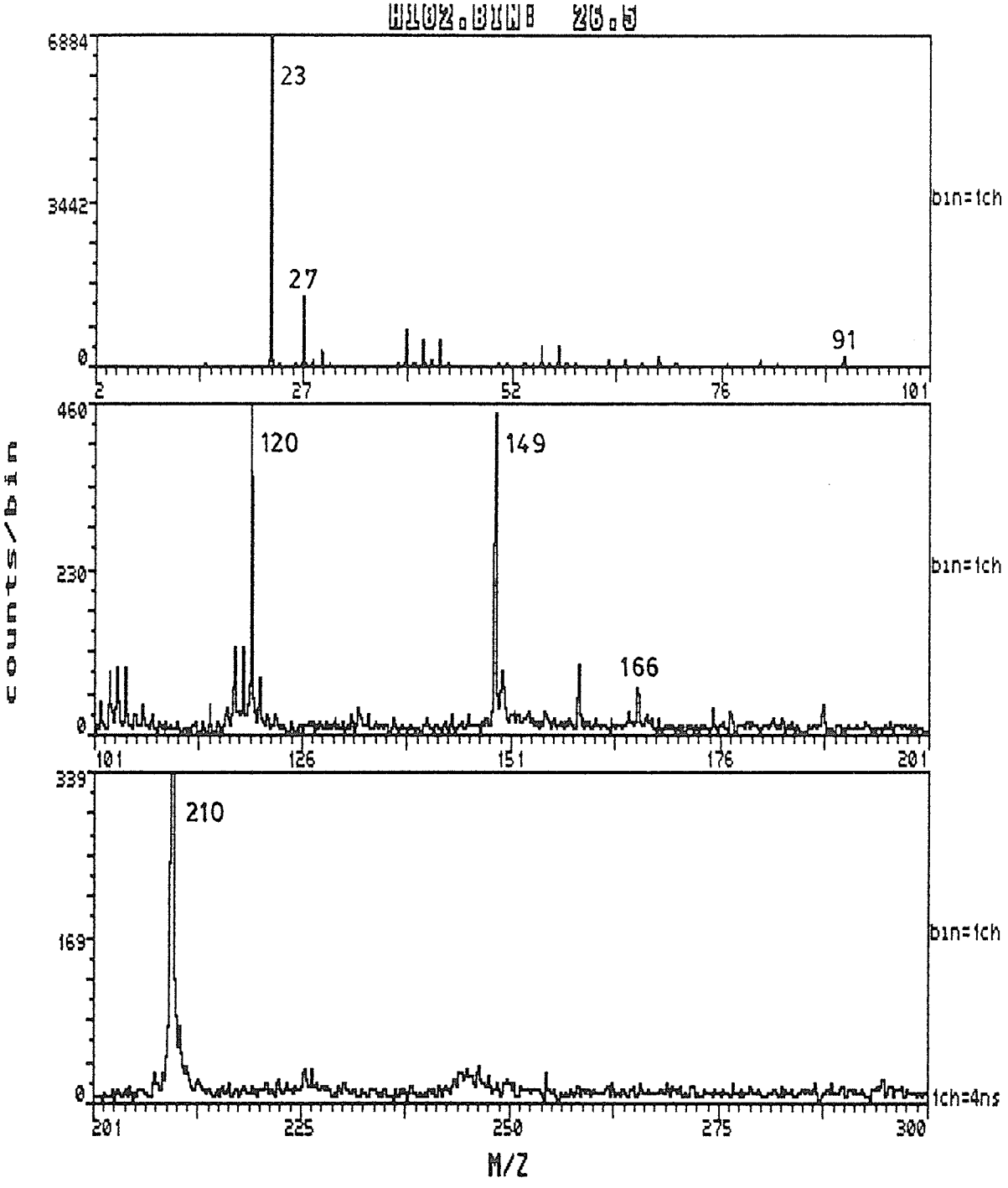
H102.BIN 8 25.5
6884
3442
0
23
27
91
2
27
52
76
101
bin=1ch
460
230
0
120
149
166
101
126
151
176
201
bin=1ch
339
169
0
210
201
225
250
275
300
bin=1ch
1ch=4ns
counts/bin
M/Z

injected onto the column and the fraction containing the eluted phenylalanine was examined. The fraction containing the sample was easily determined by visual examination of the strip; electrosprayed deposits of very small amounts (as low as 10 ng) of material were visually observable as a white spot on the highly reflective aluminum foil. The dominant ion in Figure 4.9 was m/z = 23 u (Na^+), the same as for the solvent only. The predominance of sodium cations and cationization in samples prepared from the HPLC system was a general feature of all spectra obtained. The spectrum has been split into 3 histograms (note scale changes). The phthalate fragment ion at m/z = 149 u was a major peak, as it was in the neat solvent case. The ion corresponding to the intact, hydrogen adduct cation was m/z = 166 u ($(M+H)^+$). The major fragmentation pathways for phenylalanine were loss of COOH, m/z = 120 u, and the formation of a tropyllium ion, m/z = 91 u. The most prominent quasimolecular ion present in the spectrum was the di-sodium adduct ($(M+2Na-H)^+$), m/z = 210 u (no other quasimolecular ions were present). The addition of two sodium atoms to the phenylalanine molecule was a consistent feature of samples prepared by spraying from aqueous solvents. The dominant presence of sodium in the spectra indicated that at the surface of the electrosprayed deposit there was a relatively high concentration of sodium, which presumably could complex with the phenylalanine, either on the surface or in the so-called selvedge region formed during the primary ion impact.

Figure 4.10 shows the spectrum of a fraction containing leucine enkephalin (Tyr-Gly-Gly-Phe-Leu, YGGFL), prepared in the same way as the sample shown in Figure 4.9. The low mass portion of the spectrum is again dominated by the sodium cation. Above mass m/z = 100 u the most

Figure 4.10

Mass spectrum of a leucine enkephalin fraction (two pages).

Sample injected on column = 0.25 μg.

(Note changes of vertical scale.)

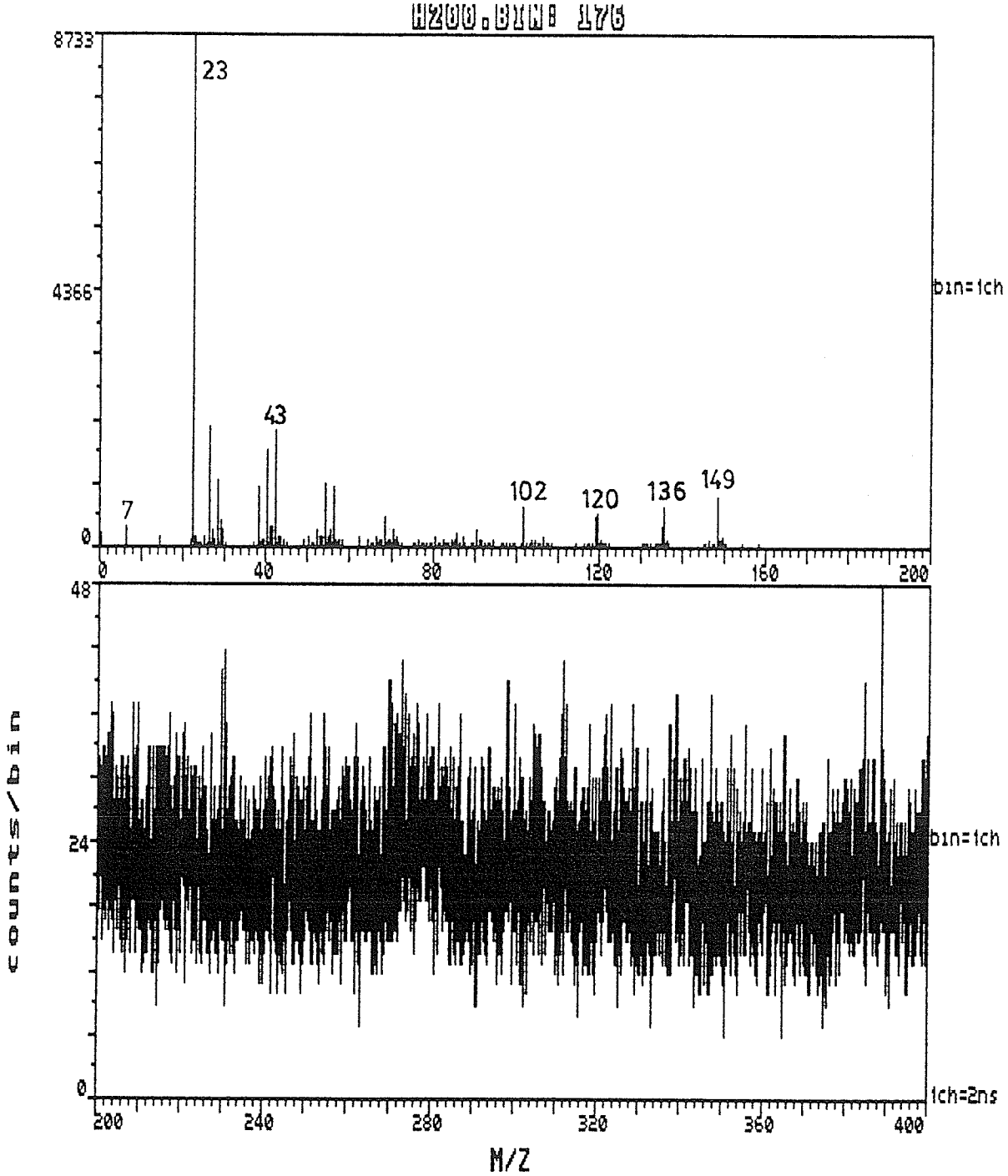
HZ00.BIN: 176
8733
4366
0
23
43
7
102
120
136
149
0
40
80
120
160
200
bin=1ch
48
24
0
counts/bin
200
240
280
320
360
400
M/Z
bin=1ch
1ch=2ns

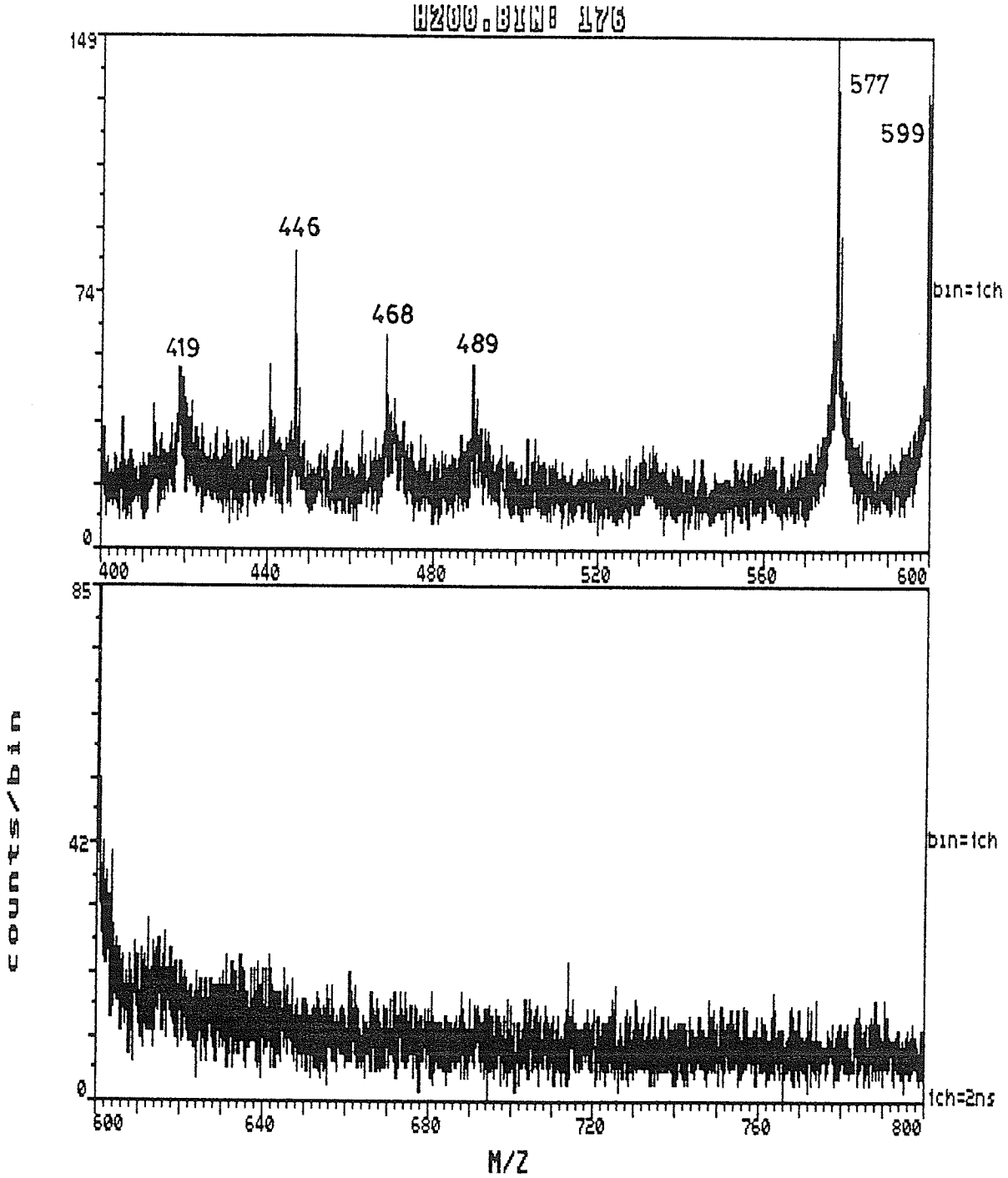
H200.BIN: 176
149
74
0
577
599
446
468
419
489
400
440
480
520
560
600
bin=1ch
85
42
0
600
640
680
720
760
800
bin=1ch
1ch=2ns
counts/bin
M/Z

intense ion was again the phthalate fragment ion. The spectrum shows intense ions at m/z = 120 u and m/z = 136 u, fragments characteristic of the amino acid residues phenylalanine and tyrosine respectively. The formation of these ions is shown in Figure 4.11. This process normally produces characteristic fragment ions for phenylalanine and tyrosine residues. A related fragment ion appears at m/z = 30 u, corresponding to glycine. Above m/z = 200 u, the spectrum was relatively featureless, except for the quasimolecular ions at m/z = 577 and 599 u, $(M+Na)^+$ and $(M+2Na-H)^+$ respectively. The cluster of ions between 400 u and 500 u were contaminants due to the eluting solvents (see Figure 4.7). As in the case of phenylalanine, the intense quasimolecular ions were sodium cationized species, with little or no evidence of the hydrogen adduct ion at m/z = 556 u.

Figure 4.12 is the spectrum of methionine enkephalin (Tyr-Gly-Gly-Phe-Met, YGGFM). The sample was treated in the same way as the leucine enkephalin (YGGFL) sample in Figure 4.10 and contained the same amount of peptide. The low mass portion of the spectrum shows once again the domination of the spectrum by the sodium cation and the range m/z = 100 - 200 u is again dominated by the phthalate fragment (m/z = 149 u) and the tyrosine and phenylalanine characteristic fragments (m/z = 136 and 120 u respectively) are quite intense. However, by comparison with Figure 4.10, the quasimolecular yield was low. The most intense quasimolecular ion for YGGFM is the potassium cationized species, $(M+K)^+$, followed by the $(M+Na)^+$ species. The hydrogen adduct ion was not observed. The contaminant ions between m/z = 400 - 500 u were consistent with those observed in Figure 4.7 and 4.10.

Figure 4.13 is the spectrum of 250 ng of proenkephalin

Figure 4.11

Probable mechanism for the formation of fragment ions characteristic of amino acid residues in a peptide.

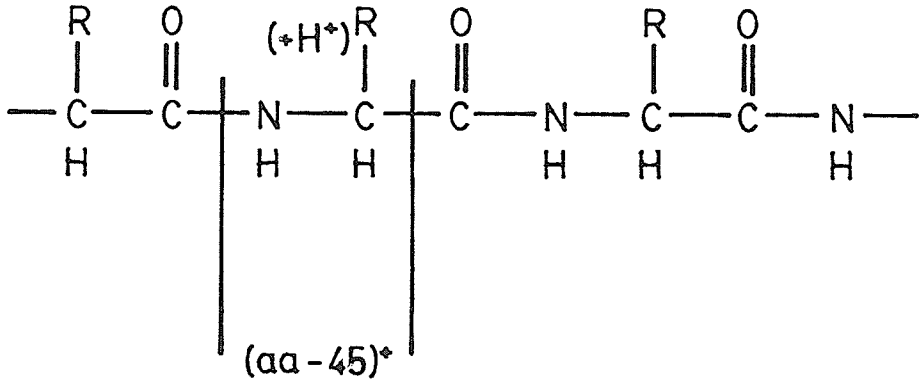
R
O
(+H+)R
O
R
O
C
C
N
C
C
N
C
C
N
H
H
H
H
H
H
(aa-45)+

Figure 4.12

Mass spectrum of a methionine enkephalin fraction (two pages).

Sample injected on column = 0.25 µg.

(Note changes at vertical scale.)

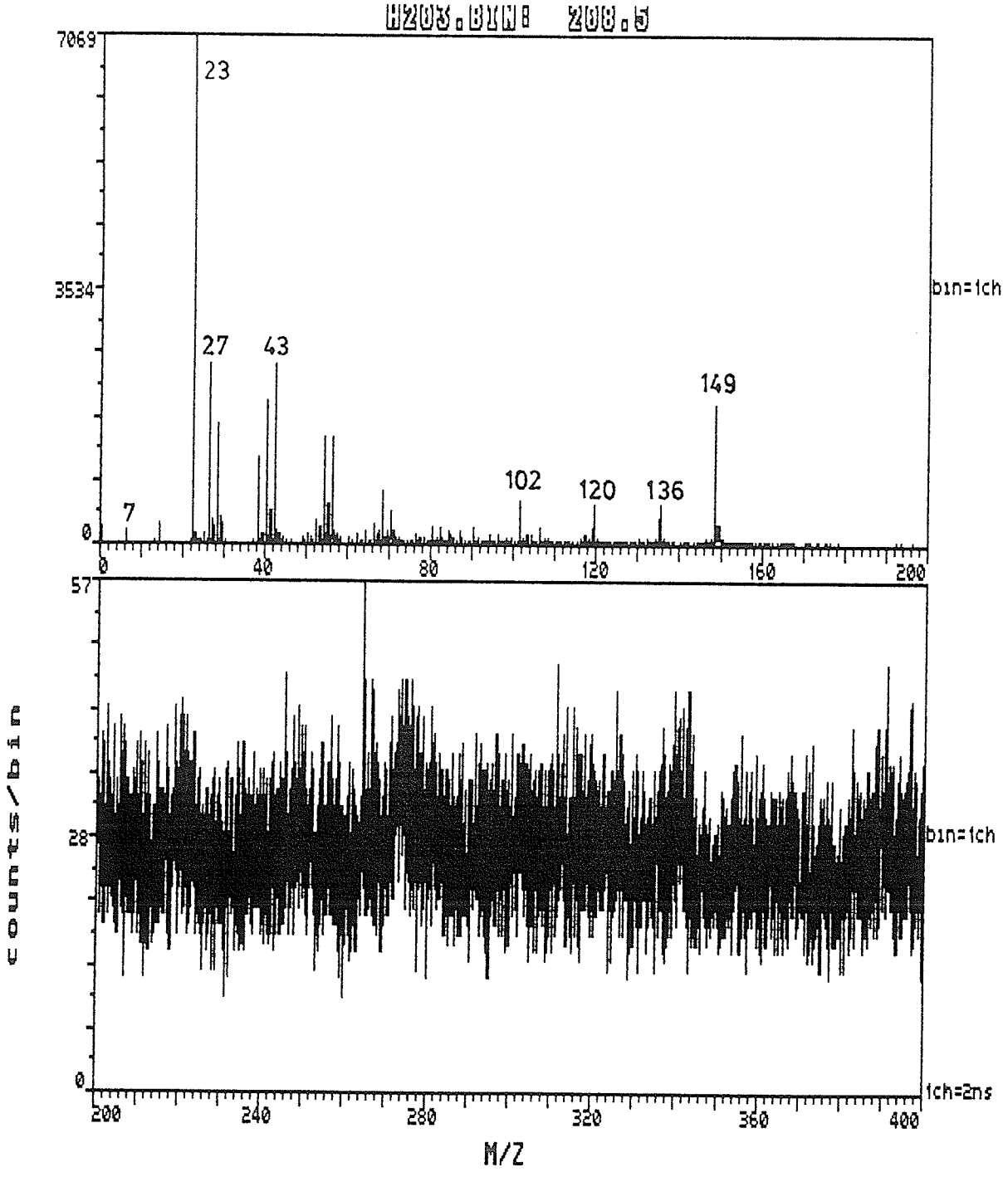
H203.BIN: 208.5
7069
3534
0
23
27
43
7
102
120
136
149
0
40
80
120
160
200
bin=1ch
57
28
0
200
240
280
320
360
400
bin=1ch
1ch=2ns
counts/bin
M/Z

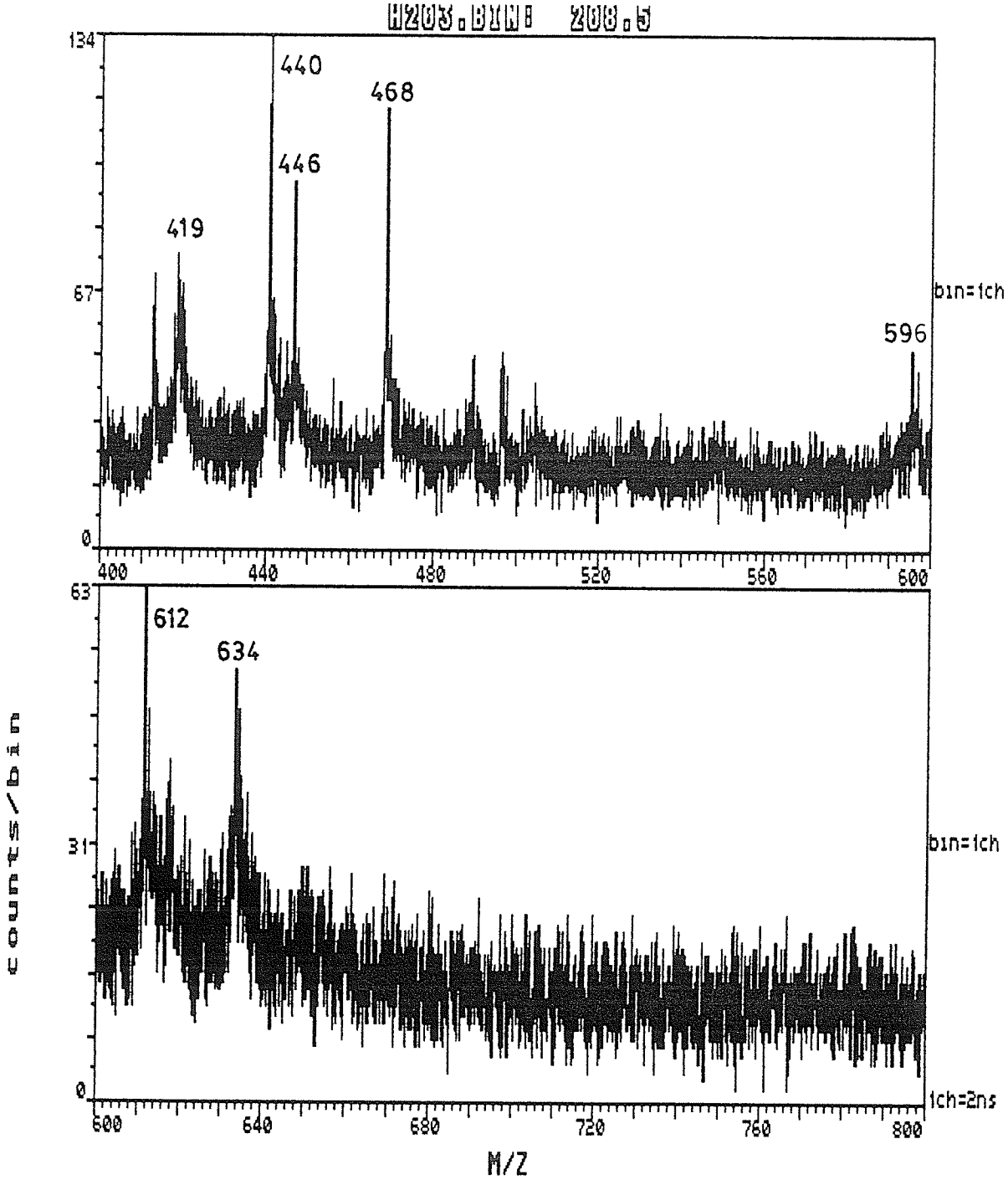
H203.BIN: 208.5
134
67
0
440
468
446
419
596
bin=1ch
400
440
480
520
560
600
63
31
0
612
634
bin=1ch
1ch=2ns
600
640
680
720
760
800
M/Z
counts/bin

(Tyr-Gly-Gly-Phe-Met-Arg-Gly-Leu, YGGFMRGL), a methionine enkephalin precursor [76], prepared in the same manner as the enkephalin above. The Na^+ ion was again intense, as was the K^+ and phthalate fragment. The phenylalanine and tyrosine characteristic ions were present. The hydrogen adduct quasimolecular ion, (M+H)+, was observed for YGGFMRGL, as were the sodium and potassium cationized species.

The spectra shown in Figures 4.7 - 4.13 are typical of the spectra obtained using the LC-MS system. Figures 4.14 and 4.15 are chromatograms produced using the system. In both cases, mixtures containing approximately equal amounts of synthetic peptides (purchased from Sigma) were dissolved in water and injected onto the HPLC column (sample concentrations were approximately 0.1 µg/µl of each peptide). The eluting solvent in both cases was 40:60 2-propanol:water, with 0.02% TFA/TEA buffer, with a flowrate of 1 µl/min (using the Eldex HPLC pump) and an electrospray deposit diameter of 1 mm. The fractions were collected for four minutes in both cases. The chromatogram in Figure 4.14 was made using an RSil C18HL 10 µm silica column bed, 30 cm long, 0.5 mm i.d.(0.02"). The chromatogram in Figure 4.15 was made using an RSil C4 10 um silica column bed, 15 cm long, 0.5 mm i.d. (0.02"). In both cases, the phenylalanine peak eluted close to the void volume of the column.

The preliminary results given in Figure 4.7 - 4.15 demonstrate that the system that had been made to achieve off-line coupling of the Manitoba I mass spectrometer with HPLC had promise. The spectra obtained showed that electrospraying the eluent from an HPLC column could be used to make samples compatible with low flux primary ion bombardment ionization. Quasimolecular ions characteristic of intact

Figure 4.13

Mass spectrum of a proenkephalin containing fraction.

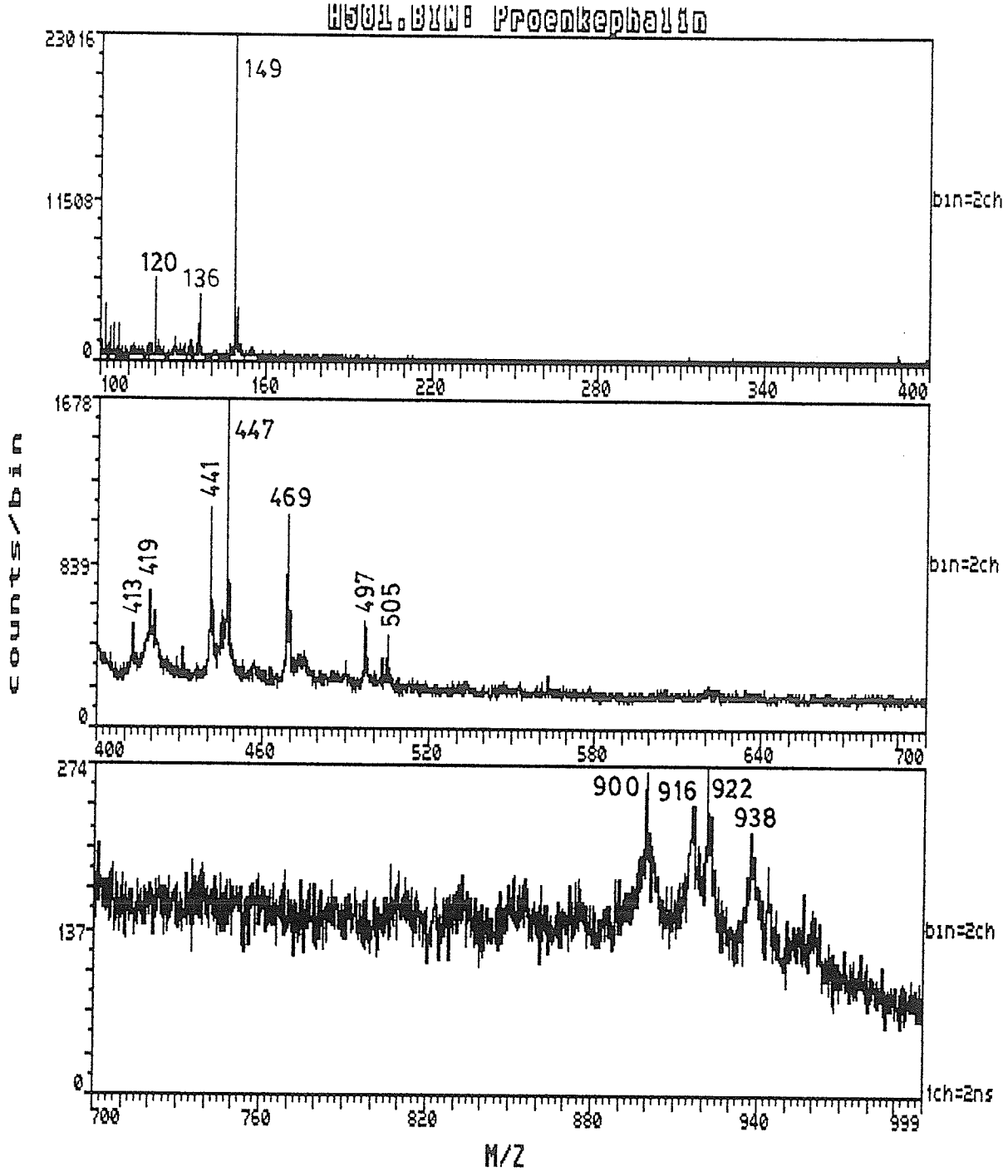
H90U1.BIN: Proenkephalin
23016
11508
0
149
120
136
100
160
220
280
340
400
bin=2ch
1678
839
0
447
441
469
419
413
497
505
400
460
520
580
640
700
bin=2ch
counts/bin
274
137
0
900
916
922
938
700
760
820
880
940
999
bin=2ch
1ch=2ns
M/Z

Figure 4.14

Chromatogram of a peptide mixture produced by integrating the quasimolecular ion intensities in the mass spectra of deposited fractions.

Components:

1) Phe

2) Tyr-Gly-Gly-Phe

3) Tyr-(D-Ala)-Gly-Phe-Met

4) Tyr-Gly-Gly-Phe-Met

5) Tyr-(D-Ala)-(D-Ala)-Phe-Met

6) Gly-Gly-Phe-Leu

7) Tyr-Gly-Gly-Phe-Leu

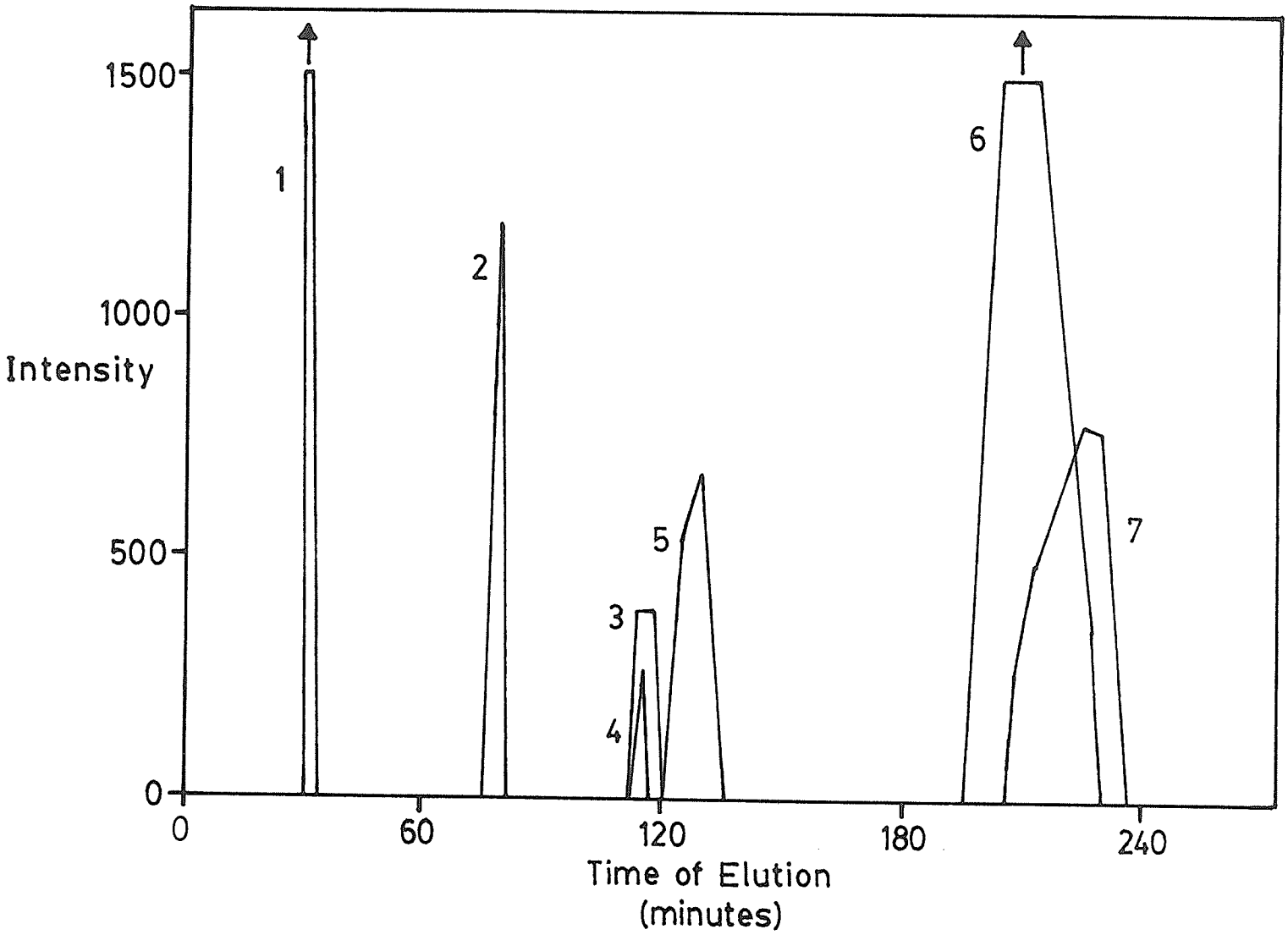
1500
1000
500
0
Intensity
1
2
3
4
5
6
7
0
60
120
180
240
Time of Elution
(minutes)

Figure 4.15

Chromatogram of a peptide mixture produced by integrating the quasimolecular ion intensities in the mass spectra of deposited fractions.

Components:

1) Phe

2) Tyr-Gly-Gly-Phe-Met

3) Tyr-Cys-Gly-Phe-Cys

4) Gly-Gly-Phe-Leu

5) Tyr-Gly-Gly-Phe-Leu

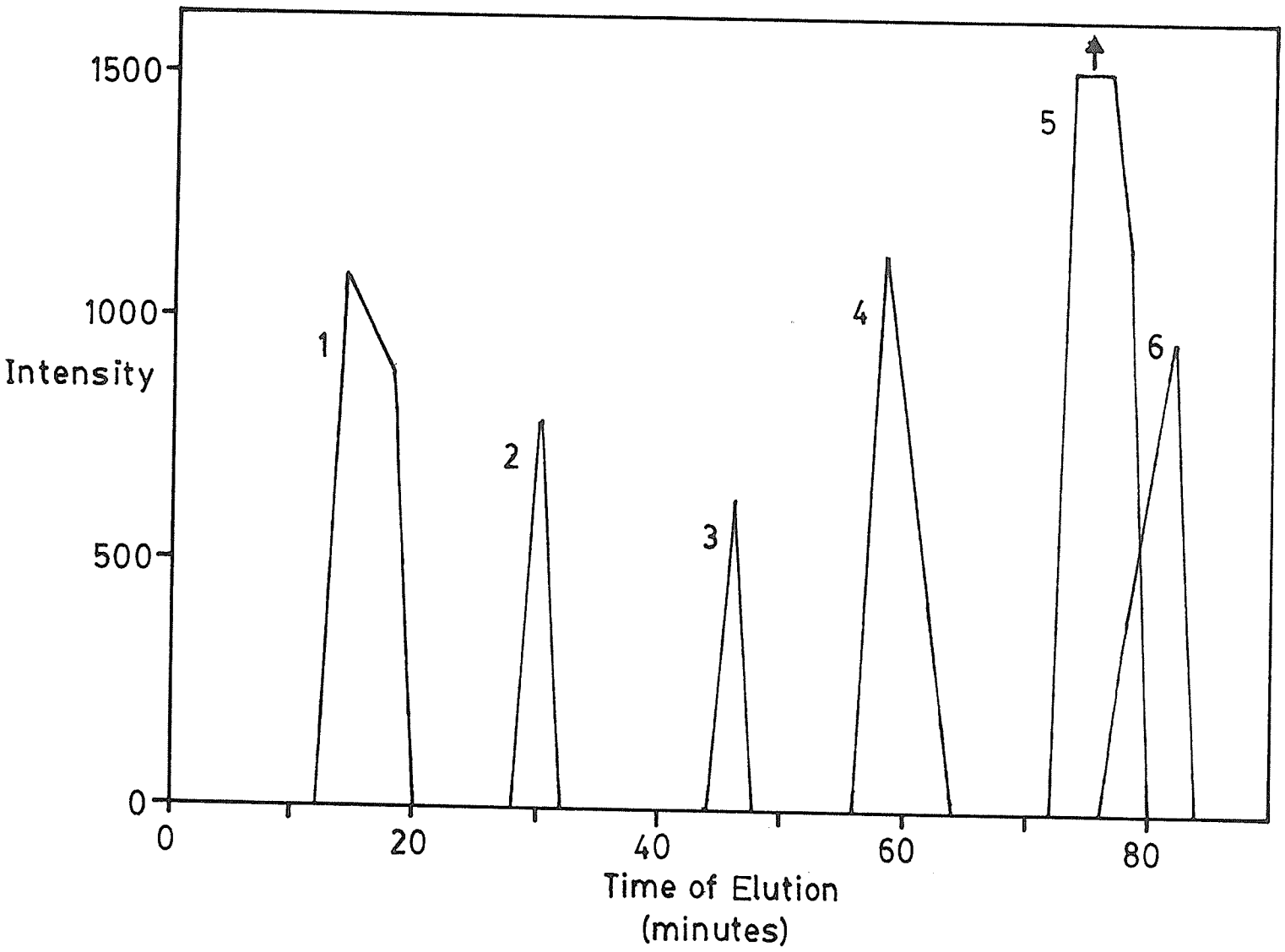
1500
1000
500
0
Intensity
1
2
3
4
5
6
0
20
40
60
80
Time of Elution
(minutes)

peptides were produced and some structure related fragments were present in the mass spectra. The sensitivity of the technique also appeared promising. As little as 40 picomoles of leucine enkephalin produced quasimolecular ions ($(M+Na)^+$) that were easily observed.

The results also pointed to several problems with the system as it stood. The most serious problem was still contamination. The very high yield of the sodium cation in all spectra showed that a "large" amount of sodium was present in the solvents, i.e. there was a high surface concentration of sodium on the deposits produced by electrospraying the HPLC eluent. The high surface concentration of sodium (SIMS spectra only give a reflection of the surface; the bulk is not necessarily the same) had a negative effect on the peptide mass spectra produced: sodium cationized species dominated the quasimolecular ion region, with the exception of proenkephalin (YGGFMRGL). In the case of phenylalanine, the doubly cationized species was by far the most intense quasimolecular ion. While these intense, relatively stable cationized species were easily observed in the spectrum, the high intensity of singly and multiply cationized species and the variability of the intensity pattern of these species (compare the quasimolecular ions for YGGFL and YGGFM) would make the mass determination of an unknown molecule difficult. The reliable presence of observable hydrogen adduct ions in the peptide spectra would have been desirable for the unambiguous determination of the parent molecule's mass. The presence of the somewhat variable contamination peaks in the m/z = 400 - 500 u mass range was not desirable. Most peptides containing four amino acid residues are in this mass range, making the interpretation of spectra

difficult for these compounds. The presence of these large contaminant peaks would also make the interpretation of the structurally related fragment peaks difficult.

A particularly troubling problem with the system was the lack of structurally related fragments in the mass spectra. Our laboratory's previous work with enkephalin peptides [75] had indicated that the amino acid residue structure of some of these peptides could be inferred from the fragmentation of the peptide at specific bonds in the peptide chain. Part of the expected information from the LC-MS system was partial determination of the structure of a peptide after HPLC separation of a mixture had allowed unambiguous linking of a fragment ion to a single parent peptide (something not possible for a mixture of peptides in a SIMS sample). The spectra shown above (Figures 4.10, 4.12 and 4.13) do not contain observable structural fragment ions, except for the amino acid characteristic ions (Figure 4.10).

The characteristics of the HPLC system were not as good as was hoped. The very long elution times caused by the slow flowrates necessary to produce reliable SIMS samples meant that the chromatographic efficiency of the columns was compromised by axial diffusion of a chromatographic band as it progressed down the column. Increasing the flowrate or decreasing the column internal diameter would minimize the problem, but neither of these alternatives had proven feasible. The reliability of the columns produced was quite low; only one out of three columns packed proved to be efficient enough for use. The columns that did have a sufficiently high plate count did not have very predictable retention times, i.e. each column had very different retention time characteristics. The results obtained with these columns

for positive charged peptides (e.g. dynorphin) were poor: the charged peptides were strongly retained by the column and in many cases appeared to bind to the column under our elution conditions.

4.5) Improvements to the HPLC System

The comments at the end of the last section indicate that there were very real problems with the microbore HPLC eluent deposition system that had been developed up to that point. The low flowrate imposed by the results in Figure 4.3 and the lack of success achieved in packing 0.01" i.d. column beds limited both the efficiency and the speed of the chromatography achievable from 0.5 mm (0.02") i.d. columns. The lack of reproducibility from one column to another was also disappointing.

The pace of research into improving HPLC columns and procedures was greatly improved by the purchase of the Isco µLC 500 Micropump (syringe type). As mentioned above (Section 3.2), the Isco uLC 500 was much easier to operate in the flowrate range in which our microbore columns were operated. The continuously variable flowrate adjustment, easy and reproducible settings from 0.02 µl/minute to 1.6 ml/minute, and digital readout of both pressure and flowrate, replaced the fussy micrometer adjustment on the Eldex pump. The Eldex pump was prone to stalling at low flowrates; a small gas bubble lodged in the piston cylinder would stop the solvent flow. The pump would then have to be disassembled, the bubble flushed out, the pump reassembled and reattached. No such problems existed with the Isco syringe pump.

The initial approach taken to overcome the drawbacks in the system's HPLC characteristics was to pack relatively short columns with

very high efficiency reversed phase silica. To produce higher efficiency, more reliable columns, spherical silica was tried. The material first obtained was 7 μm diameter Nucleosil C8 reversed phase spherical silica. This particular material was difficult to suspend in a slurry for any length of time using 2-propanol as the slurry solvent. Experimentation with various solvents indicated that dimethylsulfoxide (DMSO) produced the best slurries. Packing the Nucleosil material into short (10 cm long, 0.02" i.d., nickel) columns achieved better chromatographic results than the longer columns packed with irregular silica. The stability and reproducibility of using Nucleosil in columns proved to be worse than the irregular silica, however. Nucleosil silica was a bit too fragile to be reliably packed at 70 MPa (the pressure rating for the material was 60 MPa). Packing columns at such a high pressure collapsed the pores in the rather fragile silica spheres, greatly reducing the surface area exposed to the mobile phase. Packing the columns at somewhat lower pressure (50 MPa) reduced the problem of pore collapse but the column was not packed as well.

The experience with Nucleosil packing suggested that spherical material was better than irregular, so a more robust type of silica, Altex Ultrapak 10 μm C8 spherical reversed phase, was obtained. Altex silicas were available in 1 gram quantities, a considerable economy compared to most materials that were only available in 10 gram quantities. Columns made using Ultrapak material were easy to pack (2-propanol was a good slurry solvent for Ultrapak) and consistent. The column length was extended to 20 cm, in order to make the physical layout of the system better; with the 10 cm column the sample collection drum was too close to the injection valve. The Ultrapak column beds

were of only moderate resolution, however, and had very low column back pressures. At 2 ul/minute, using a 2-propanol/water mobile phase, the column backpressure was 0.2 MPa.

To improve resolution, 3 um diameter Hypersil MOS C8 silica was tried. The MOS material was a special type of octyl reverse phase silica with a very high load of organic surface coating. The packing instructions given in Section 3.3 describe the technique settled upon for packing columns with either the Ultrapak or Hypersil MOS material. Columns packed with the MOS material were of higher efficiency than those packed with Ultrapak, but the column bed had a tendency to shrink. Packing a few milligrams of Ultrapak (10 um) material into the column bed first, and then packing the rest of the column bed with Hypersil (3 um) material produced a very good column, with excellent stability. The Hypersil silica was not as fragile as the Nucleosil silica; it was not crushed by packing.

Use of the Ultrapak and Hypersil columns was still limited by the flowrate restrictions discussed above. Chromatograms could be run using higher flowrates (3 - 5 ul/minute) and good efficiencies could be obtained, but when these chromatograms were analyzed in the Manitoba I time-of-flight instrument the spectra produced had low quasimolecular ion yields. The failure to produce good spectra cancelled a presentation to the ASMS meeting in Cincinnati in May, 1986. Therefore, to exploit the additional resolution of the new column beds and to increase the speed of the chromatography, something had to be done to improve the quasimolecular ion yield from deposits electrosprayed at a flowrate of higher than 1 ul/minute.

4.6) Modification to the Substrate's Physical Properties

The substrate used for our electrospray deposition had always been aluminum, whether as a film on a polyester backing or a solid foil. Aluminum substrates worked well enough for electrospray deposition, but some substrates, such as nitric acid etched silver [77], do not need electrospray deposition to produce quasimolecular ions under static SIMS conditions. Acid etched silver produces good mass spectra if a small amount ($\simeq$ 1 µl) of dissolved material is dropped onto the surface. The etching process produces a very rough, hydrophilic surface on which the drop of sample rapidly spreads out and quickly dries. Strong silver adduct quasimolecular ions of the sample are observed from very small amounts (picomoles) of peptide. The use of etched silver as an electrospray substrate seemed to be very attractive, but there were several drawbacks to its direct application in the LC-MS system as it stood. A strip of silver foil 35 cm by 2.5 cm would be necessary to be compatible with the substrate sample holder shown in Figure 3.7. Even assuming that the strip was reusable, i.e. it could be satisfactorily cleaned after use, the cost of strips of silver would be considerable. For individual samples, the silver is normally cut into small (1 cm diameter) disks and then placed in a 50° C, 1 N nitric acid bath until the surface loses its sheen and becomes dull white. Adapting this rather crude process to the production of uniform long thin strips was obviously not going to be simple. Also, the silver stock used to produce the individual sample disks was much too thick to be used with the strip substrate holder. Thinner silver

could not be used because the etching process completely dissolved a thin piece of silver before it was adequately etched. Therefore, to use etched silver would mean altering the design of the substrate holder. To avoid the problems associated with using etched silver as the substrate for electrospray deposition, it was decided to attempt to modify the properties of the aluminum foil surface to mimic those of the etched silver. It is not completely understood how the etched silver surface interacts with a deposited sample to produce a good secondary ion source. Therefore, there was no a priori reason why aluminum could not serve the same purpose.

The two most obvious physical properties of an etched silver target are the increased surface area because of the extremely rough texture of the etched surface, shown in Figure 4.16 and the hydrophilic nature of the surface, i.e. aqueous solvents rapidly spread out over the surface. The first attempt to produce a similar aluminum surface was to simply treat the aluminum in the same way as the silver. Unfortunately, the aluminum quickly perforated and dissolved in the nitric acid bath. Etching the aluminum surface with a basic solution (10% NaOH) produced a rough surface, but did not leave it hydrophilic. Several different acid and base solutions were tried, but the surfaces produced did not have the properties desired.

From the metallurgical literature [63], a possible treatment for producing a hydrophilic surface was anodization. Anodization is simply making the aluminum the anode in an acid bath and applying DC voltage. If the acid bath concentration and the voltages applied were kept in the appropriate range (see Section 3.6), a thick layer ($\simeq$ 100nm) of aluminum oxide was formed on the surface. A 10% sulfuric acid bath

Figure 4.16

Scanning electron micrograph of nitric acid etched silver foil (magnification = 9.8 kX, bar = 1 μm).

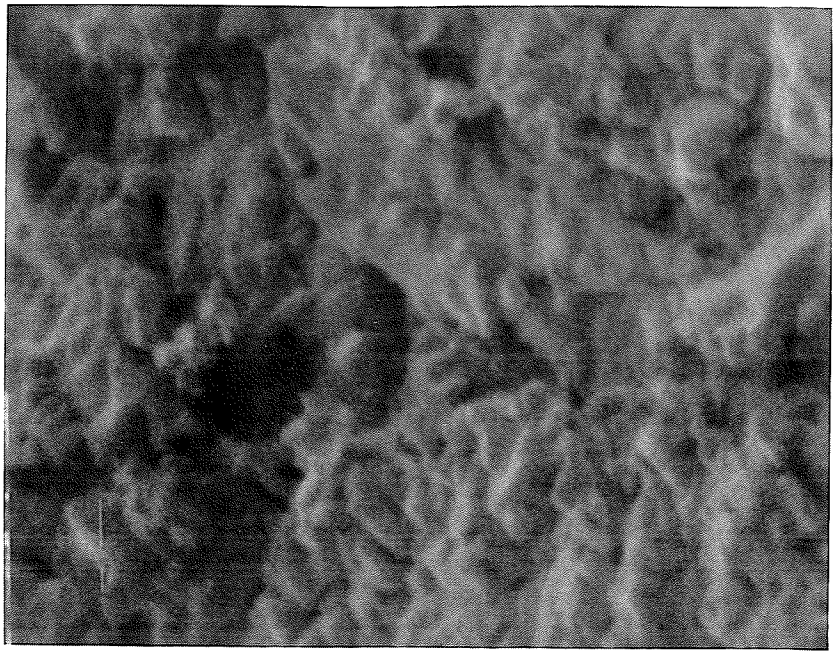

produced a flat, unetched surface while a 10% nitric acid bath produced an etched surface. Both surfaces were hydrophilic. The additional step of placing the anodized foil in boiling deionized water for ten to fifteen minutes produced a very hydrophilic surface that was stable to heating. The boiling water converted the surface from being normal aluminum oxide (Al_2O_3) to a hydroxide form called boehmite ((AlO)OH).

The results of using boehmite surfaces as electrospray deposition substrates were very promising. Figure 4.17 is a comparison of the mass spectra of the bare boehmite and aluminum foil. Both the boehmite and aluminum foil have a strong Al^+ ion (m/z = 26.98 u). The boehmite has fewer and less intense organic peaks, relative to the aluminum foil. The mass spectrum above m/z = 200 u showed that the boehmite was free of high mass contamination in the region of most interest for peptide work.

The result in Figure 4.17 showed that boehmite surfaces were free of most contaminants, but would it work for electrosprayed samples? Figure 4.18 shows the comparison of spectra obtained for phenylalanine on aluminum and boehmite substrates. A sample containing 100 ng of phenylalanine was injected onto the HPLC column, with the elution solvent 60:40 2 - propanol:water, 0.05% TFA/TEA buffer (pH = 3.0), and a solvent flowrate of 3.0 µl/minute. The eluent was sprayed onto aluminum and then the experiment repeated on boehmite. Both samples were prepared in exactly the same way. At a flowrate of 3.0 µl/minute, the results on the aluminum foil were quite poor as expected. The only significant quasimolecular ion was the $(M+2Na-H)^+$ ion at m/z = 210. The sodium cation was five times more intense than any other ion in the spectrum. The sample sprayed onto the boehmite produced very different results. The sodium cation in this spectrum was eight times smaller

Figure 4.17

Mass spectra obtained from bare aluminum foil (upper) and boehmite (lower) surfaces. The vertical scales (upper vs. lower) are relative only.

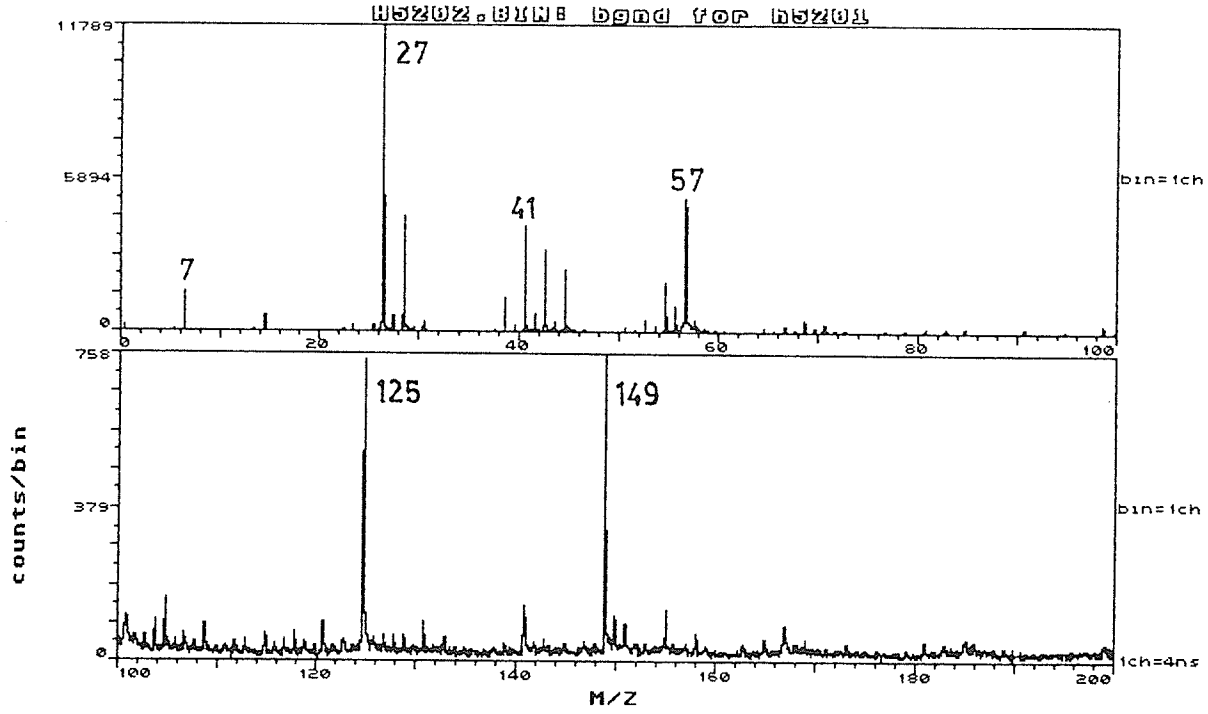
11789
5894
0
27
41
57
7
0
20
40
60
80
100
bin=1ch
758
379
0
125
149
100
120
140
160
180
200
1ch=4ns
counts/bin
M/Z

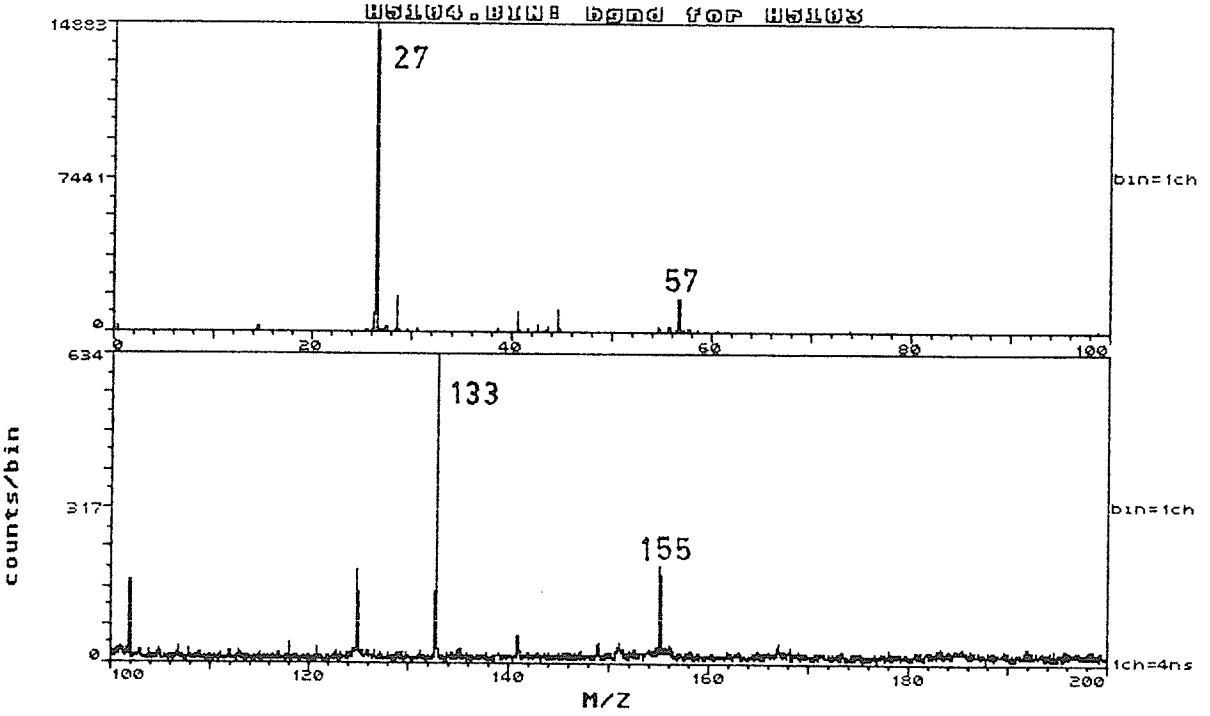
14883
7441
0
27
57
0
20
40
60
80
100
bin=1ch
634
317
0
133
155
100
120
140
160
180
200
1ch=4ns
counts/bin
M/Z

Figure 4.18

Mass spectra comparing a phenylalanine deposit on aluminum foil (upper) and boehmite (lower) surfaces. The vertical scales (upper vs. lower) are relative only.

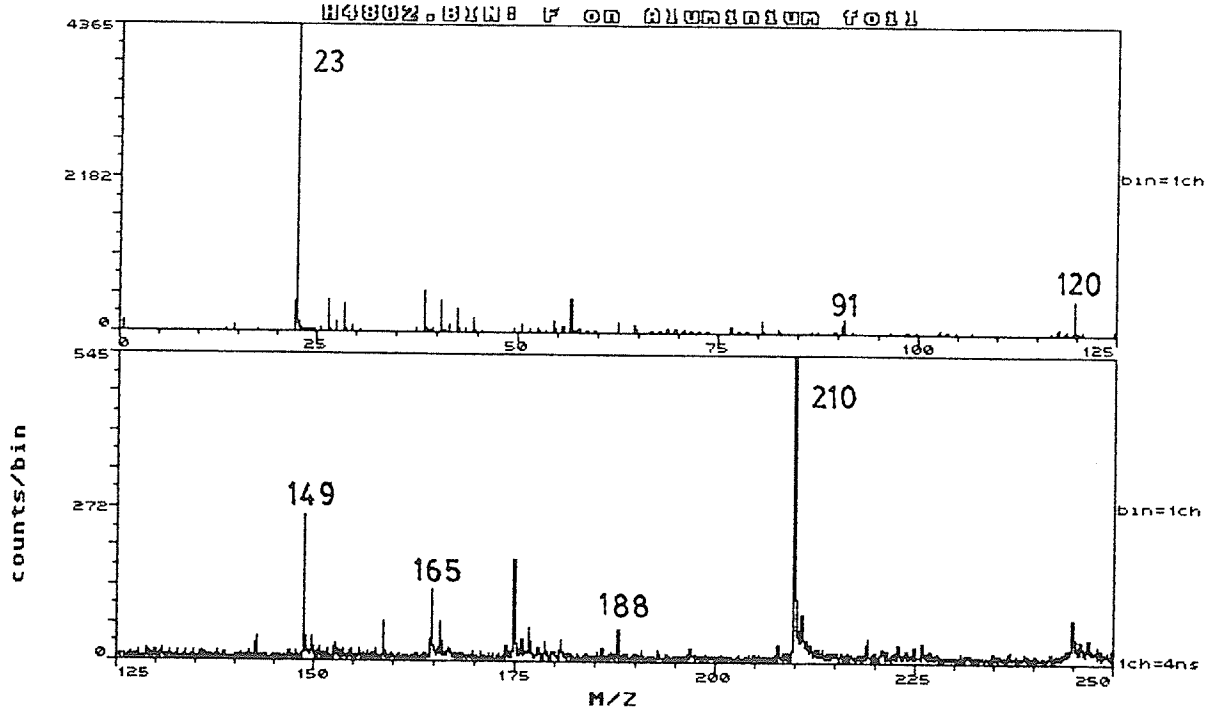
4365
2182
0
23
91
120
bin=1ch
545
272
0
149
165
188
210
bin=1ch
125
150
175
200
225
250
1ch=4ns
counts/bin
M/Z

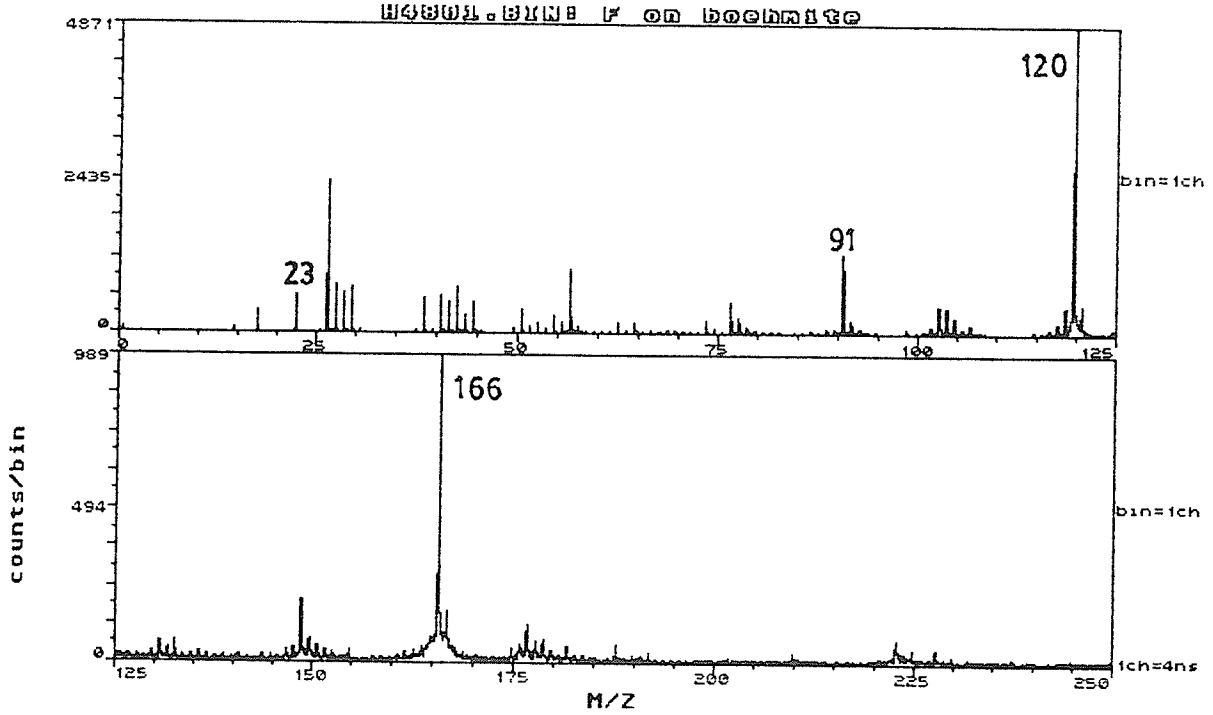
4871
2435
0
23
91
120
bin=1ch
989
494
0
166
bin=1ch
125
150
175
200
225
250
1ch=4ns
counts/bin
M/Z

than the most intense ion. The most intense ion was the $(M-COOH)^+$ structural fragment of phenylalanine. The hydrogen adduct cation $(M+H)^+$ was the only observable quasimolecular ion; there was no evidence of sodium cationization.

Is the effect shown in Figure 4.18 limited to phenylalanine? Figure 4.19 is the same sort of comparison, using leucine. The leucine samples were treated using the same method as was the phenylalanine sample above. The sample sprayed onto aluminum has a hydrogen adduct quasimolecular ion, m/z = 132, an $(M-COOH)^+$ fragment ion at m/z = 86 and the sodium cation is the third most intense ion in the spectrum. The most intense ion in the spectrum sprayed onto boehmite is the hydrogen adduct cation, with an increase in relative intensity, compared to the spectrum on aluminum, of approximately one order of magnitude. The sodium cation was the sixteenth most intense ion.

The spectra in Figure 4.18 and 4.19 show that boehmite is a much superior substrate to bare aluminum foil for electrospraying from our HPLC system. The large increases in hydrogen adduct quasimolecular ion yields meant that unambiguous interpretation of spectra would be possible for unknown samples. An unexpected feature of these spectra was the large decrease in the intensity of the sodium cation and sodium adduct quasimolecular ions. Because the samples were prepared in exactly the same way, using the same batch of solvent and under the same electrospray conditions, the only possible reason for the decrease in the sodium related signals was some interaction between the substrate and the electrosprayed deposit. The presence of an interaction between the deposited sample and the substrate also implied that the electrospray plume still contained solvent when it landed on the

Figure 4.19

Mass spectra comparing a leucine deposit on aluminum foil (upper) and boehmite (lower) surfaces.

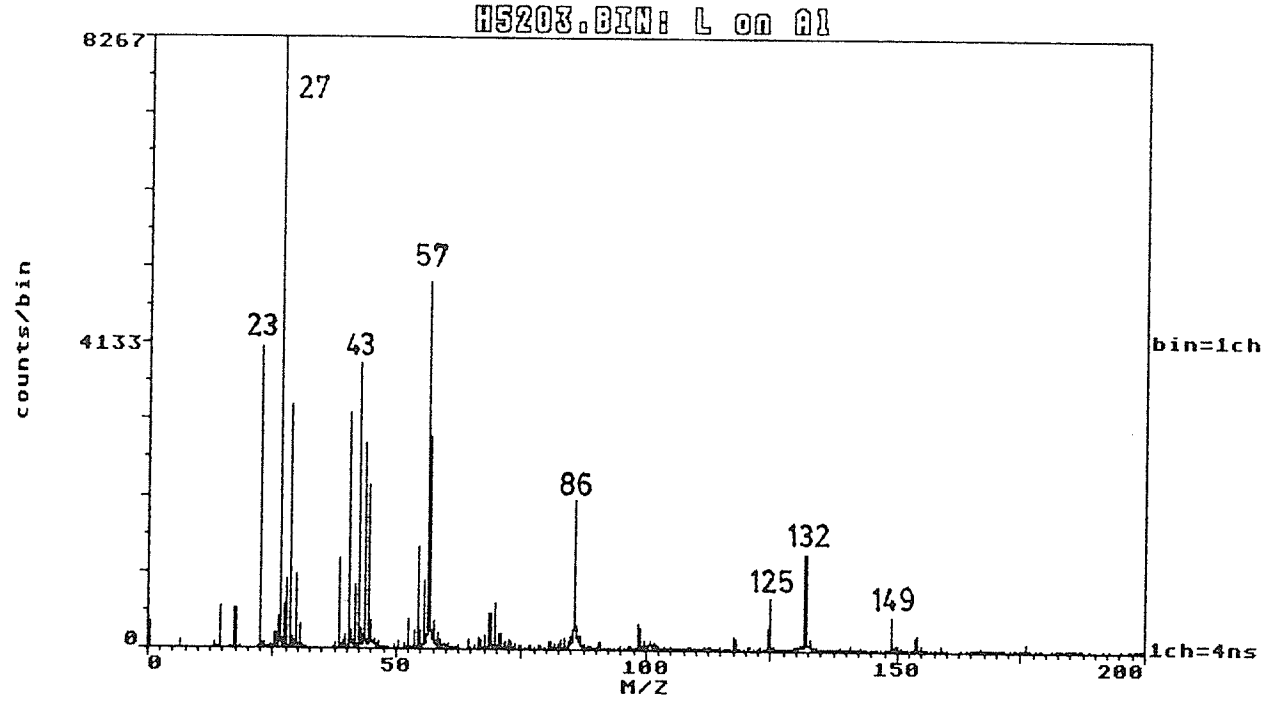
H5203.BIN: L on Al
8267
4133
0
counts/bin
27
23
43
57
86
132
125
149
bin=1ch
1ch=4ns
0
50
100
150
200
M/Z

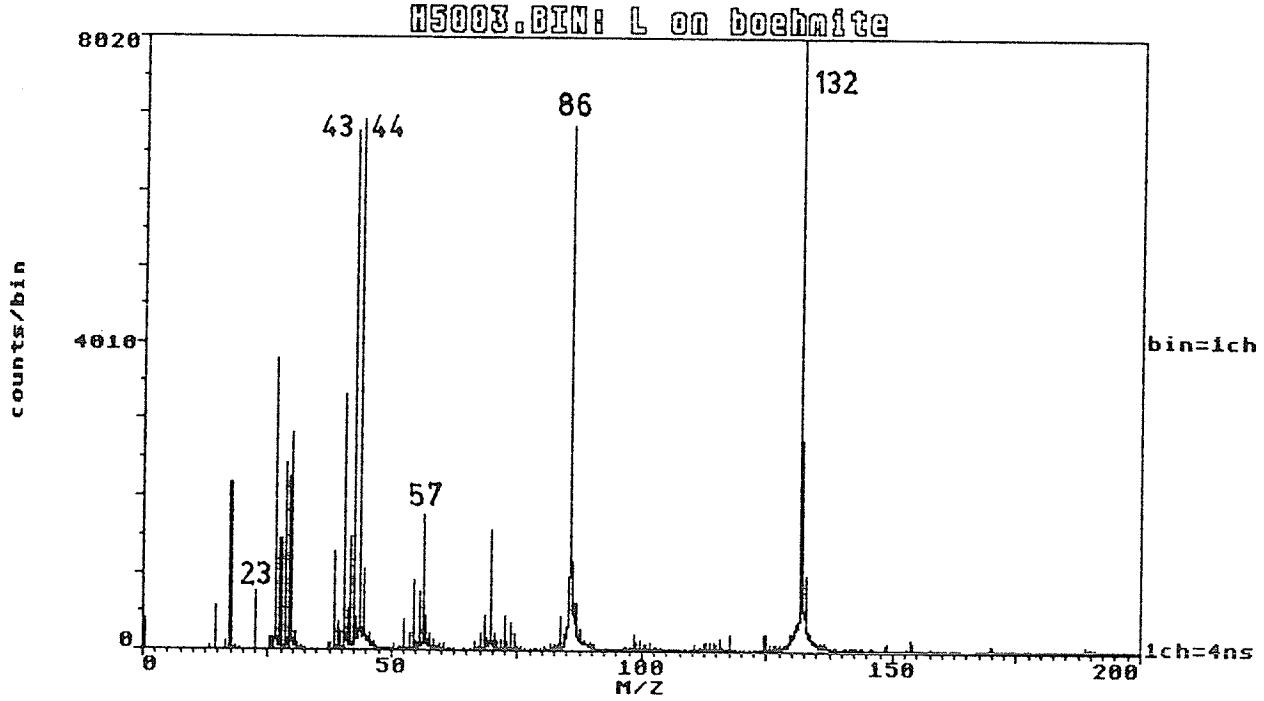
H5003.BIN: L on boehmite
8020
4010
0
counts/bin
43
44
86
132
57
23
bin=1ch
1ch=4ns
0
50
100
150
200
M/Z

substrate. If the plume contained only dried particles of sample when they hit the substrate, it would be difficult to see how the substrate could affect the surface of these dry particles in such a way as to inhibit sodium ion production.

The decrease in sodium cation intensity in the SIMS spectra of electrosprayed sample deposited on boehmite surface could be caused by two separate mechanisms. The first mechanism is the alteration of the drying process in an electrosprayed droplet on a hydrophilic surface as compared to a hydrophobic surface. As mentioned in Section 3.6, an aqueous, wet droplet landing on a hydrophobic surface will form itself into a spherical bead to minimize the liquid's contact area with the surface. As the particle dries, the solvent evaporates from the bead's surface in contact with the air. The least soluble components of the droplet will begin to come out of solution, forming a "wet snowball" [54] of slurried sample/solvent. If sufficient drying occurs in the electrospray plume before impact, the initial deposit on the surface will be in this "wet snowball" form. Further drying of the "snowball" produces a net flow of solvent from the interior to the exterior of the particle. Sodium salts are very soluble in aqueous solvents and will remain in solution until almost all the solvent has evaporated. Therefore, the sodium that would be deposited in the bulk of the particle if there were no solvent flow, is drawn to the surface and forms a crust as the solvent is completely evaporated. The SIMS spectrum of such a deposit would then show a much larger ion signal from highly soluble contaminants in the solvents than would be expected from the bulk concentrations of these materials.

A wet droplet (or "snowball") landing on a hydrophilic surface would spread out, maximizing the contact area between the surface and the droplet, forming a thin "pancake" on the substrate. As the solvent evaporates from the surface exposed to the air -- a surface which is much larger than the surface area of a beaded drop on a hydrophobic surface -- the same effect occurs, i.e. highly soluble contaminants come to the surface. In the case of a thin "pancake" however, the surface area is larger and therefore the surface concentration of the contaminants is lower than in the beaded case. Therefore, while in the beaded case a nearly complete (or complete) crust of contaminant is formed on the surface, in the "pancake" case, there will not be enough of the contaminant in the bulk to cover the larger surface area. Clearly, it is also assumed that the bulk concentration of these highly soluble contaminants is quite low. This hypothesis implies that electrospraying wet droplets onto a hydrophilic surface will decrease the secondary ion yield due to high solubility, trace eluent contaminants and increase the relative yield of lower solubility eluent components (in our case, the peptide sample).

Direct microscopic evidence of the difference between sample sprayed on hydrophobic and hydrophilic aluminum surfaces is unfortunately difficult to present for this thesis. Figure 4.20 is a micrograph of phenylalanine sprayed onto an untreated aluminum foil surface from a 60:40 water:2-propanol eluent. The surface shows small lumps of material that have not spread out. In many cases, individual droplets seem to have coale ed to form chains or patches of connected lumps. This observation supports the arguments put forward both above and in Section 3.6. Electron micrographs of the same material sprayed

Figure 4.20

Scanning electron micrographic of a phenylalanine electrospray deposit on aluminum foil (magnification = 10 kX, bar = 1 μm).

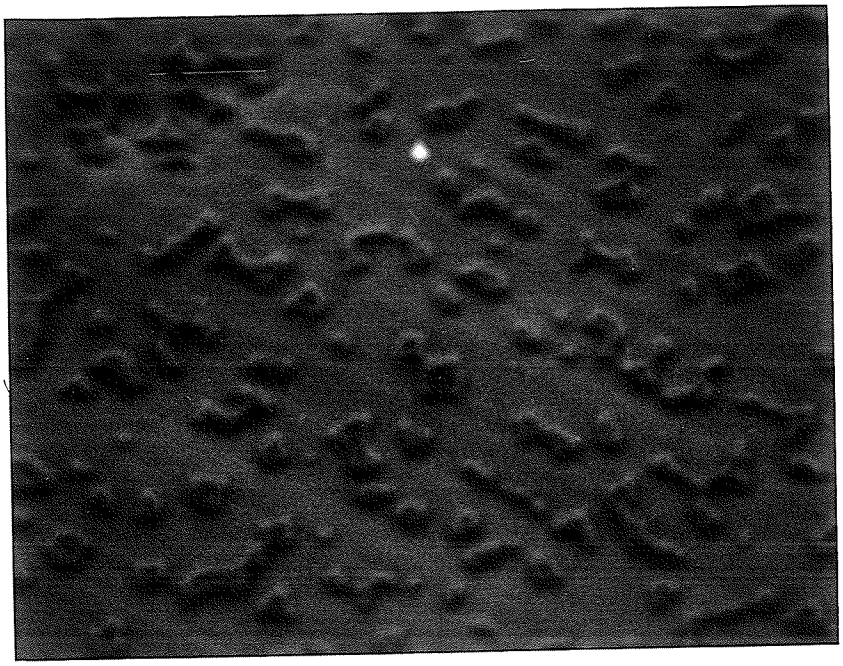

onto boehmite could not be obtained, however. Even using a very low energy primary electron beam (2 keV), the surface was damaged almost instantaneously by the electron beam, too quickly to produce photographs. The brief view of the deposit possible before it was completely beam damaged showed an almost featureless surface that appeared very similar to the adjacent boehmite surface. The only difference observable was the darkening of the deposit covered surface as the electron beam damaged the surface (see Figure 22 (a) for an example of beam damage on a more robust sodium chloride deposit). The rapid damage to the surface implied that the layer must have been thin, as expected from the spreading model proposed above.

Another hypothetical mechanism to explain the very low alkali metal cation yield was that some property of the boehmite suppressed the yield of these cations. To test this hypothesis, a 500 nl drop of water containing 50 ng of NaCl was applied to a hydrophobic aluminum surface (untreated aluminum foil) and an identical drop applied to a hydrophilic aluminum surface (anodized foil, boehmite surface). The drop on the hydrophobic surface dried in 6 minutes and did not spread across the metal surface, leaving a roughly circular deposit, 1.5 mm in diameter. The deposit is shown in Figure 4.21(a). The deposit contained large (75 μm) crystals of NaCl and highly organized crystalline structures on a much smaller scale (1 μm) shown in Figure 4.21(b). The drop placed on the hydrophilic surface spread out rapidly over a roughly circular area 10 mm in diameter and the deposit dried in 45 seconds. The deposit is shown in Figure 4.22(a). The dark lines and rectangles on the photograph are caused by damage to the surface from scanning electron microscope's electron beam. No similar damage was

Figure 4.21

Scanning electron micrograph of the deposit left by drying a 0.5 µl drop of water containing 50 ng of NaCl, on a bare aluminum surface.

a) Magnification 65 X.

b) Magnification 4200 X.

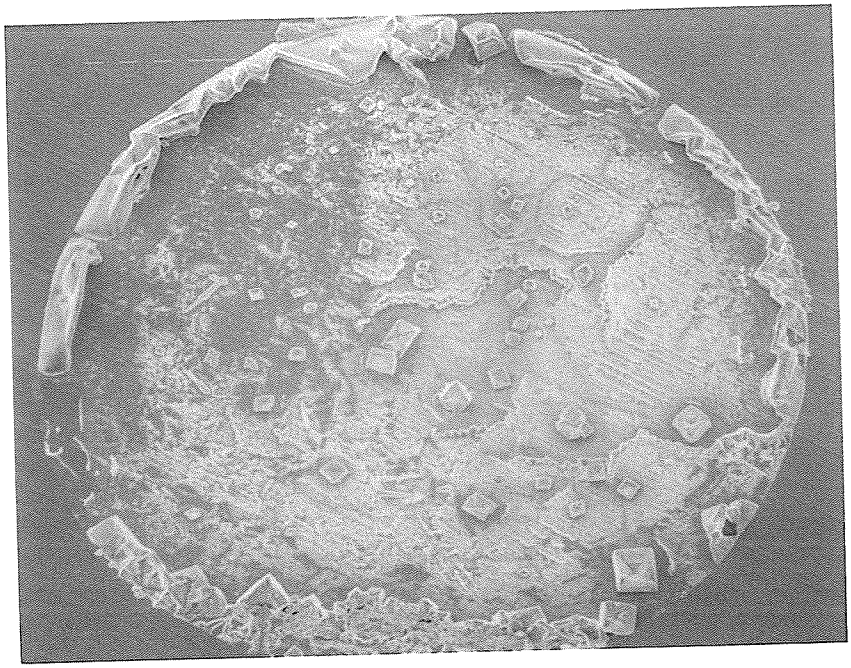

a

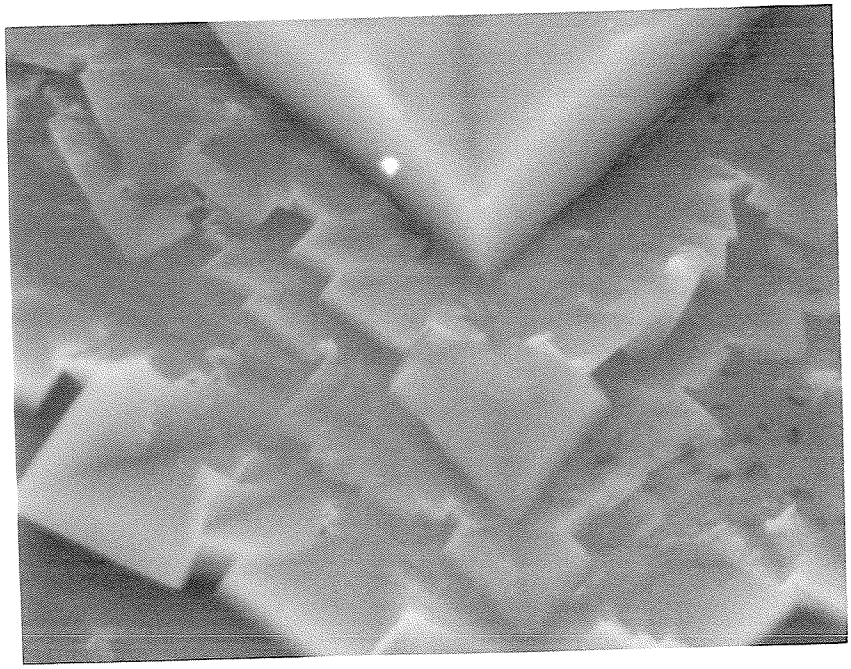

b

Figure 4.22

Scanning electron micrograph of the deposit left by drying a 0.5 µl drop of water containing 50 ng of NaCl, on a bare boehmite surface.

a) Magnification 23 X.

b) Magnification 4200 X.

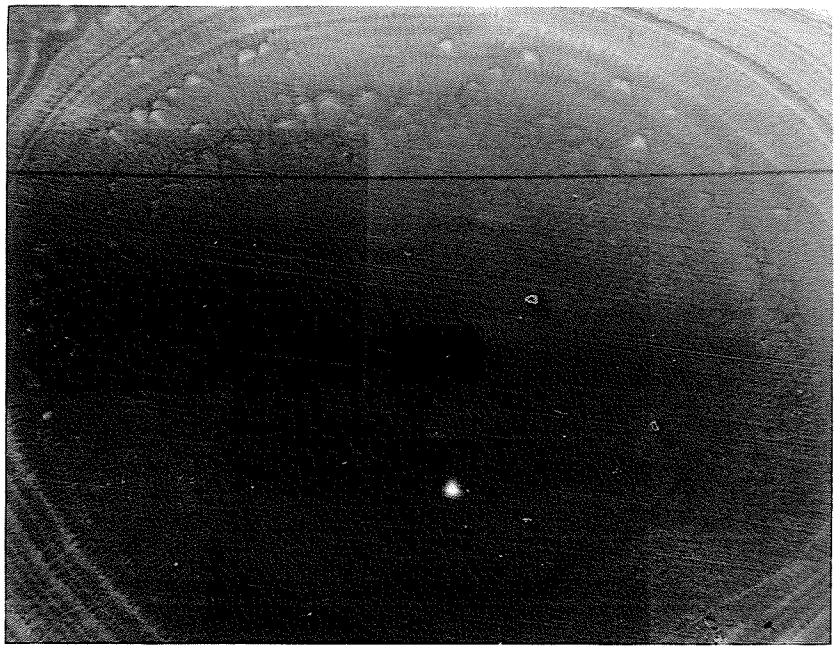

a

b

observed in Figure 4.21(a), even though the samples were analyzed using the same intensity and energy electron beam. Figure 4.22(a) shows that on the boehmite surface, no large crystalline structures formed; in fact little organization of the deposit is shown at all. The only systematic structures in the deposit seem to be concentric rings, presumably caused by the deposit drying from the edges towards the center. Examination of Figure 4.21(a) showed that in the hydrophobic case, there were none of these concentric features, except at the outside edge of the deposit, where a ring of large, crystalline structures formed giving the appearance of a walled fortress. The crystalline steps formed inside of the outer edge were not concentric, but were linear and in the same direction as the milling scratches on the aluminum foil that were barely visible in the apparently featureless region outside of the deposit. The more highly magnified view of the hydrophilic substrate sample is shown in Figure 4.22(b), at the same magnification as Figure 4.21(b). The structure observed at this scale is highly ordered in the hydrophobic case but is very nearly unordered in the hydrophilic case. No crystalline features were observed in the deposit, although there were hints of some organization, such as the "V" shapes in the upper half of the micrograph. The rest of the material appeared quite amorphous at this magnification (4200 x) and was difficult to distinguish at higher magnifications. It should be noted that in both deposits there was good surface coverage of the substrate so that SIMS analysis of the surfaces would produce mass spectra characteristic of the deposited material, with a small contribution from the bare substrate.

The mass spectra of the NaCl deposits described above are shown in Figure 4.23. The difference in sodium cation (m/z = 23) yield is striking. For the deposit on untreated foil, the base peak in the spectrum is the sodium cation. The other ions in the spectrum are typical of bare aluminum foil contaminants. The deposit on the boehmite surface has the aluminum cation (m/z = 27) as the base peak, with the sodium cation peak intensity 40 times lower than the aluminum peak. The ratio of yields (boehmite deposit Na^+)/(bare foil deposit Na^+) is approximately 0.025. This result is surprising in view of the micrographs in Figure 4.21 and 4.22 that show good surface coverage for both deposits. Therefore, the yield of the sodium cation does not depend only on the amount of sodium chloride surface exposed to the primary ion beam.

In order to explain the lack of correlation between surface exposure to the primary ion beam and secondary ion yield, the physical structure of the deposit must have some effect on the secondary ion yields. The idea that the local structure of a deposit (including the sample's interaction with a substrate) strongly influence secondary ion yields is not new: all the successful methods of preparing organic molecules for SIMS depend on unusual types of local surface structures. Electrospray from neat organic solvents produces many small deposits of relatively amorphous material. Deposition on etched silver produces a thin layer of sample over a large, rugose metal surface. By sample area arguments, the layer of sample on the silver surface must be at most a broken monolayer and in many instances, consist of isolated molecules. Surface absorption of sample molecules onto polymer substrates such as Naphion [78, 79] and nitrocellulose [80, 81] also produces unusual, composite surface with isolated sample molecules held onto a surface by

Figure 4.23

Mass spectra produced by the deposits shown in Figures 4.21 (upper) and 4.22 (lower).

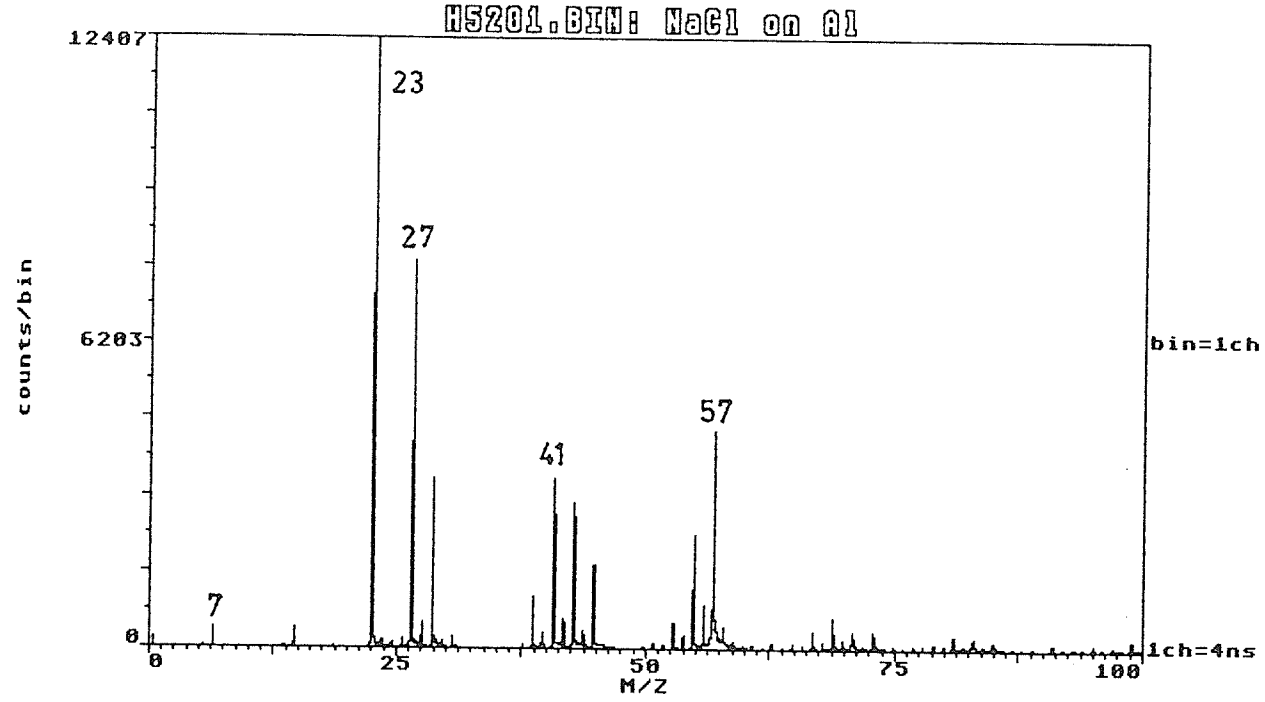
H5201.BIN: NaCl on Al
12407
6203
0
counts/bin
23
27
41
57
7
0
25
50
75
100
M/Z
bin=1ch
1ch=4ns

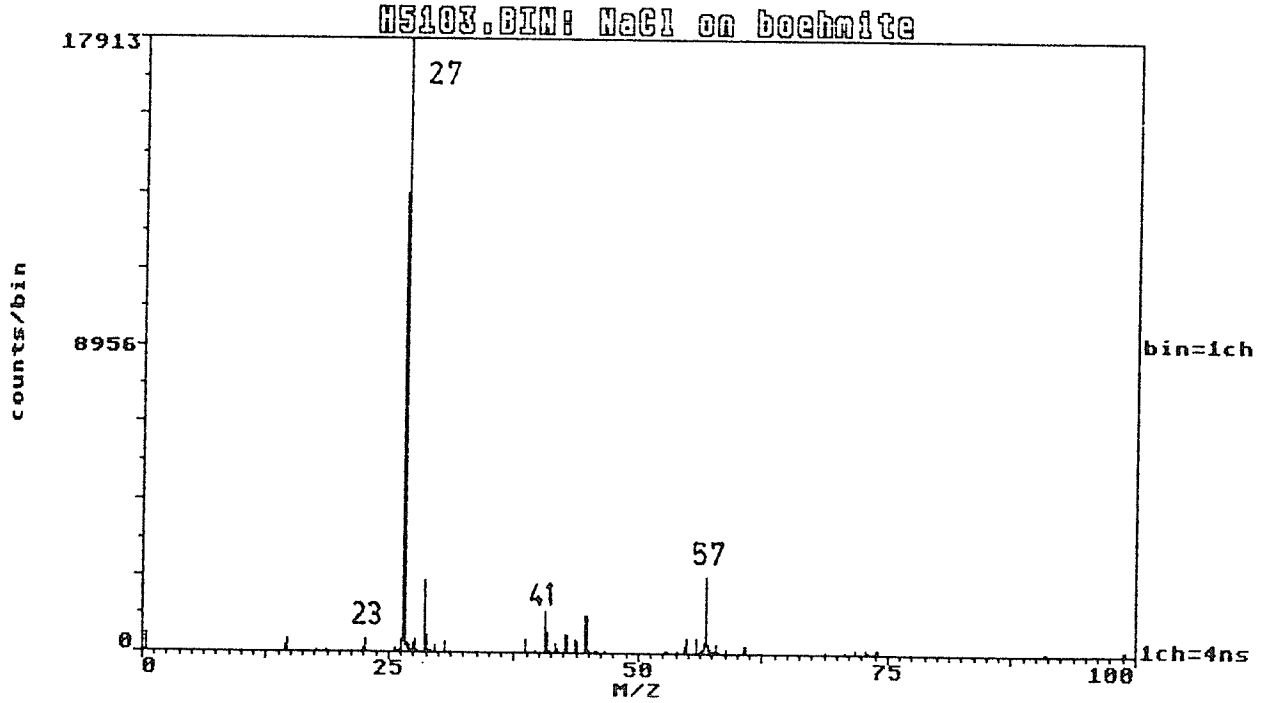
H5103.BIN: NaCl on boehmite
17913
8956
0
counts/bin
27
57
41
23
0
25
50
75
100
M/Z
bin=1ch
1ch=4ns

rather weak forces. Simple crystalline organic samples do not have significant ion yields.

The lack of crystalline structures in the deposit formed on the boehmite surface indicated that there is an interaction between the salt and the polar boehmite surface. Assuming that the surface is completely covered with sodium chloride, simple surface area/volume considerations show that 50 ng spread over a 1.5 cm diameter circle would produce a layer of sodium chloride 0.13 nm thick. Clearly Figure 4.22(b) shows the layer of sodium chloride to be thicker than 0.13 nm, at least locally, but the layer is thin, on the order of the range of primary ions in the material. Therefore, the interaction between the boehmite and the salt is probably important in suppressing the sodium cation yield. A much thicker layer made by depositing 25 μg of sodium chloride on boehmite (a nominal deposit thickness of 650 nm) produced the spectrum shown in Figure 4.24. The only significant ion peak in the spectrum is the sodium cation. The presence of the strong sodium cation yield for a thick deposit demonstrated that rapid drying in itself did not suppress cation yields; the proximity of the boehmite surface to the deposit surface was important.

With the introduction of boehmite as a sample substrate, it became possible to use much higher flowrates for the HPLC eluent. The higher flowrates, however, meant that the spray conditions were somewhat more difficult to set up. The problem was that for some solvent mixtures, containing either large amounts of water or high buffer concentrations, all of the eluent did not spray off of the needle tip. A small amount of eluent would stay on the needle and gradually build up a drop on the side of the needle. When the drop became a critical size, the

Figure 4.24

Mass spectrum of a deposit left by drying a 0.5 µl drop of water containing 25 µg of NaCl, on a boehmite surface.

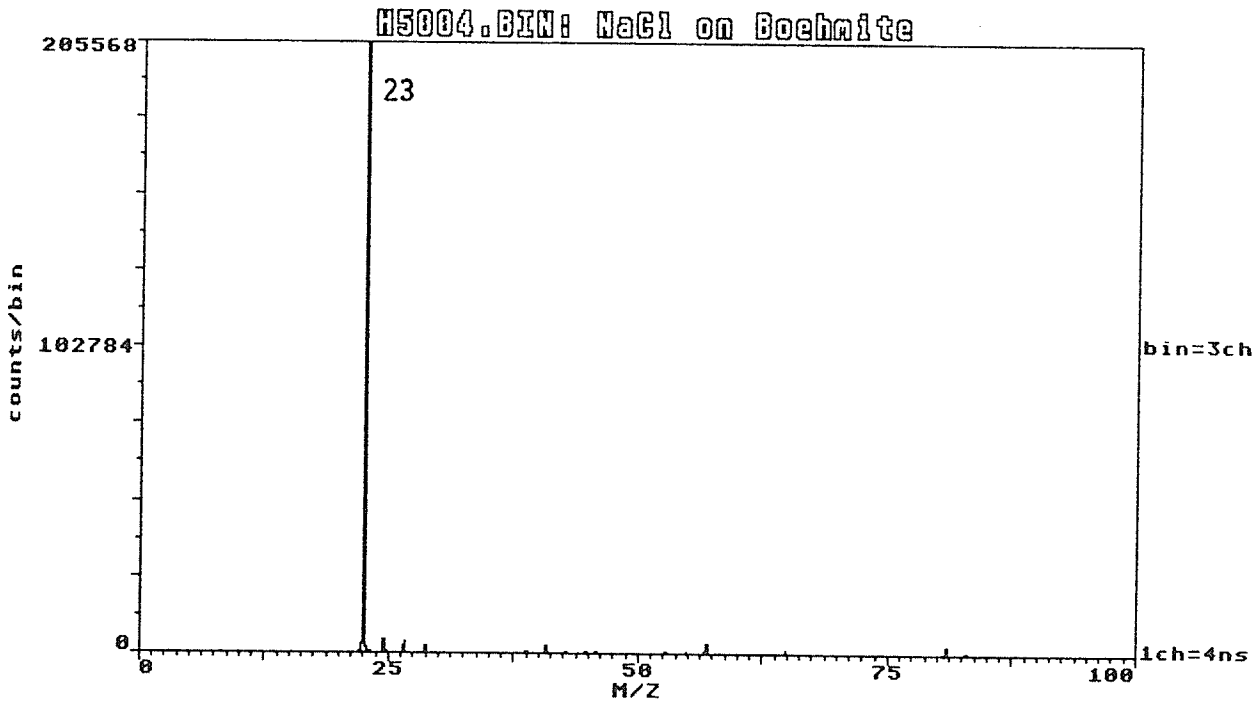
H5004.BIN: NaCl on Boehmite
205568
102784
0
counts/bin
23
bin=3ch
1ch=4ns
0
25
50
75
100
M/Z

electrostatic attraction of the substrate would overbalance the surface tension holding the drop to the needle, the drop would leave the needle and land on the substrate. These large drops would disrupt the deposit on the substrate.

In an effort to eliminate the formation of drops on the electrospray needle, an attachment for the electrospray needle was made, allowing gas to flow past the needle from behind. The apparatus is pictured in Figure 4.25. The attachment was made from the barrel of a plastic syringe. The gas used was dry nitrogen. The nitrogen flow removed the difficulty of having drops form on the needle at high flowrates. An unanticipated benefit of the gas flow was that the additional forward momentum the gas flow gave to the electrosprayed droplets decreased the diameter of the electrosprayed deposit, without changing the electrospray electric fields. Previous experience had shown that an improvement in the appearance of the electrosprayed deposit did not necessarily imply an improvement in its SIMS characteristics in our mass spectrometer. However, Figure 4.26 shows the spectrum of proenkephalin (Try-Gly-Gly-Phe-Met-Arg-Gly-Leu, YGGFMRGL) prepared by injecting 260 ng of sample onto the HPLC column and examining the fractions. The flowrate was 3.00 µl/minute, with nitrogen flowing and using a boehmite substrate. Comparison of Figures 4.26 and 4.13 clearly demonstrates that the addition of nitrogen gas flow past the spray needle did not suppress secondary ion yields.

To explore the effect of nitrogen gas flow on secondary ion yields, two simple experiments were carried out. In the first experiment, the eluent flowrate was kept constant at 3.00 µl/minute and the rate of nitrogen flow was varied. For each nitrogen flowrate a

Figure 4.25

Nitrogen flow assisted electrospray apparatus.

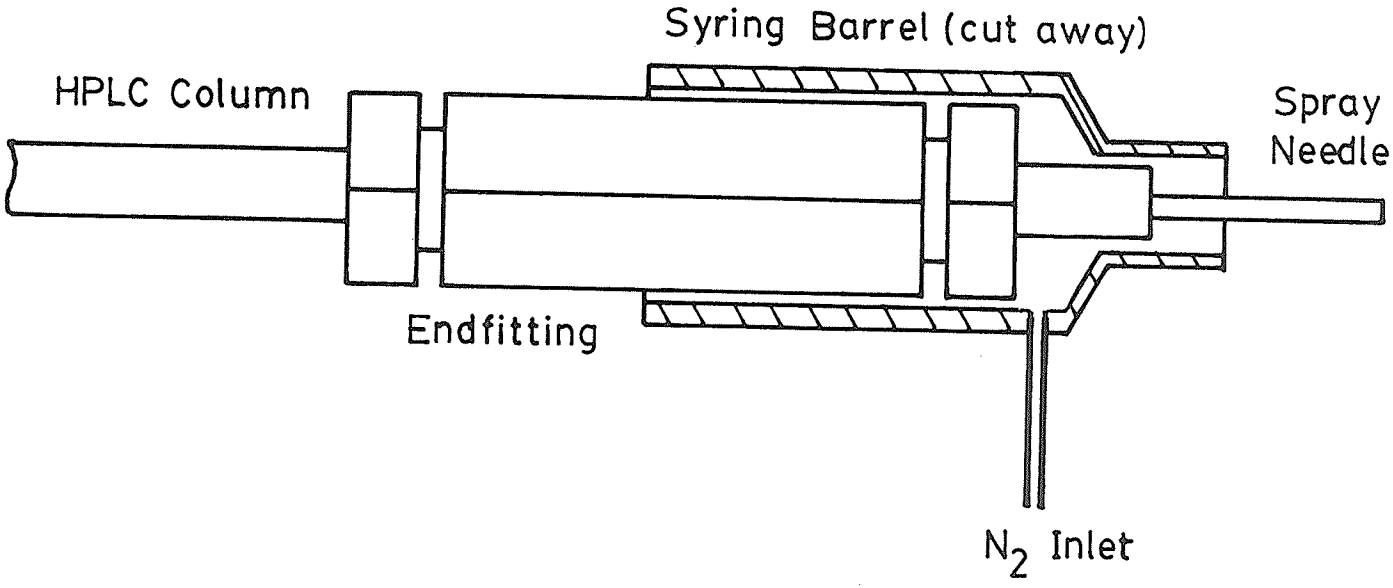
Syring Barrel (cut away)
HPLC Column
Spray
Needle
Endfitting
N_2 Inlet

Figure 4.26

Mass spectrum of a fraction containing proenkephalin (Tyr-Gly-Gly-Phe-Met-Arg-Gly-Leu, YGGFMRGL), 0.1 µg injected on column.

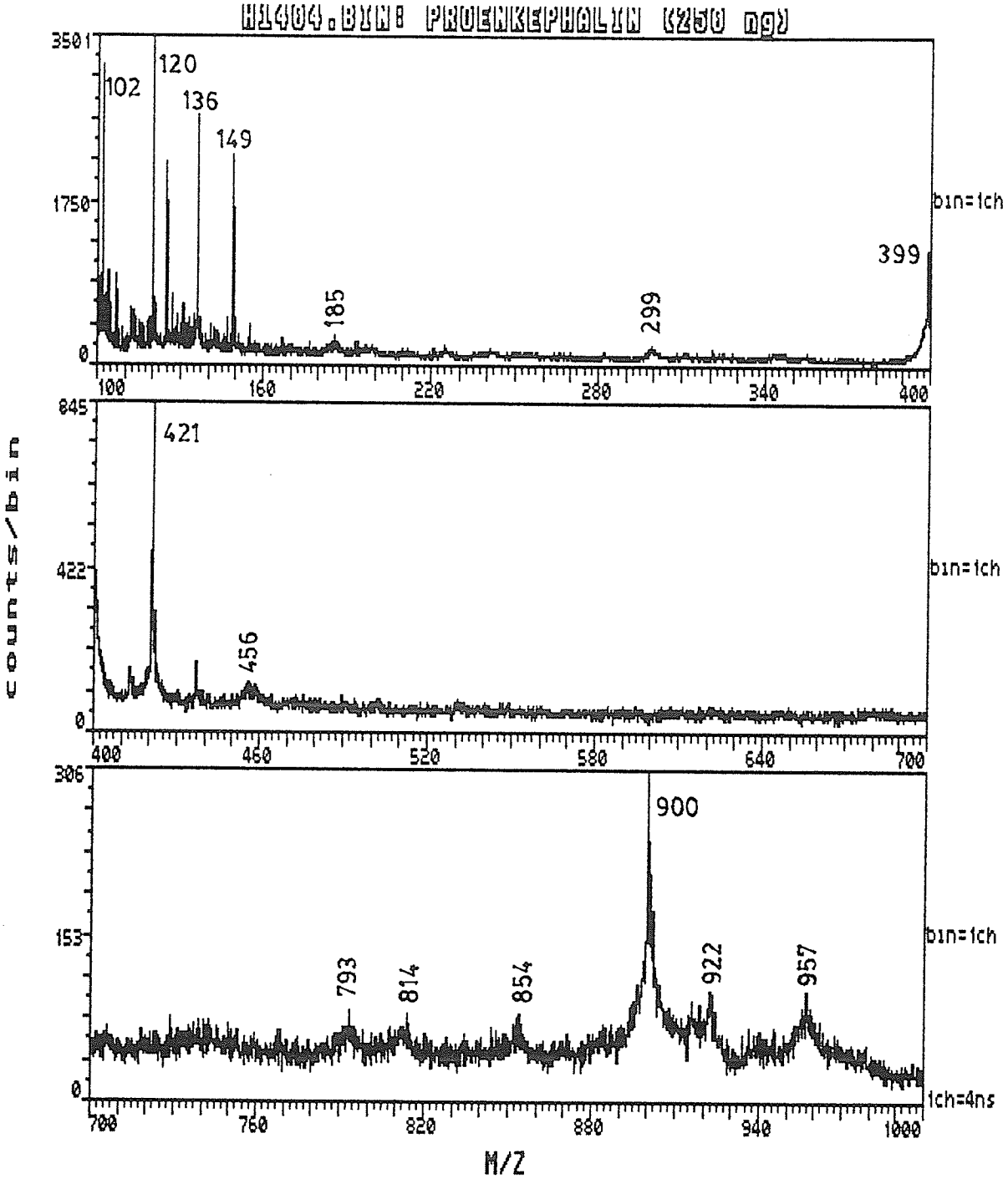
H1404.BIN: PROENKEPHALIN (250 ng)
counts/bin
M/Z
bin=1ch
bin=1ch
bin=1ch
1ch=4ns
102
120
136
149
185
299
399
421
456
793
814
854
900
922
957

sample of (D-Ala)^2-methionine enkephalinamide (100 ng) was injected onto the column. The fractions containing the peptide, deposited at five different nitrogen flowrates, were SIMS analyzed and the integral intensity of the quasimolecular ion determined. Figure 4.27 is the histogram obtained for ion intensity as a function of nitrogen flowrate. The nitrogen flowrates indicated increase from 1 to 5, but the exact values for the flowrates was not known because of the crude regulation used (the nitrogen flowrate was varied by turning the valve on a normal, low pressure nitrogen pressure regulator). The flow at a value of 1 was barely perceptible and the flow at 2 was just audible and by 5 had a backpressure of 5 p.s.i. when the gas inlet tubing was blocked. From Figure 4.27 flowrate = 2 produced the highest quasimolecular ion yields for the peptide and the yield leveled off at a somewhat lower plateau for higher flowrates.

The other experiment done to investigate the effect of combining boehmite substrates with nitrogen gas flow for improved electrospray was to maintain a constant gas flow and to change the eluent flowrate. The nitrogen gas flow was maintained at a level barely audible (i.e., at 2 in Figure 4.27) while the eluent flowrate (60:40 2-propanol:water, 0.05% TFA/TEA buffer) was increased from 2 µl/minute to 5 µl/minute. (D-Ala)^2 methionine enkephalinamide was again used as the test compound, injecting 100 ng onto the column. The fractions containing the peptide were examined by SIMS and the secondary ion yields versus eluent flowrate are shown in Figure 4.28. Comparing the relative intensities in Figures 4.28 and 4.3, the characteristics of the new deposition system are an improvement over the original system. Secondary quasimolecular ion yields were not only higher for the boehmite substrate, but the yields increased with eluent flowrate. These results

Figure 4.27

Secondary ion yield of (D-Ala)^2 methionine enkephalin as a function of nitrogen flow rate. The units of nitrogen flow were arbitrary, but the rate increase as the number increases (boehmite substrate).

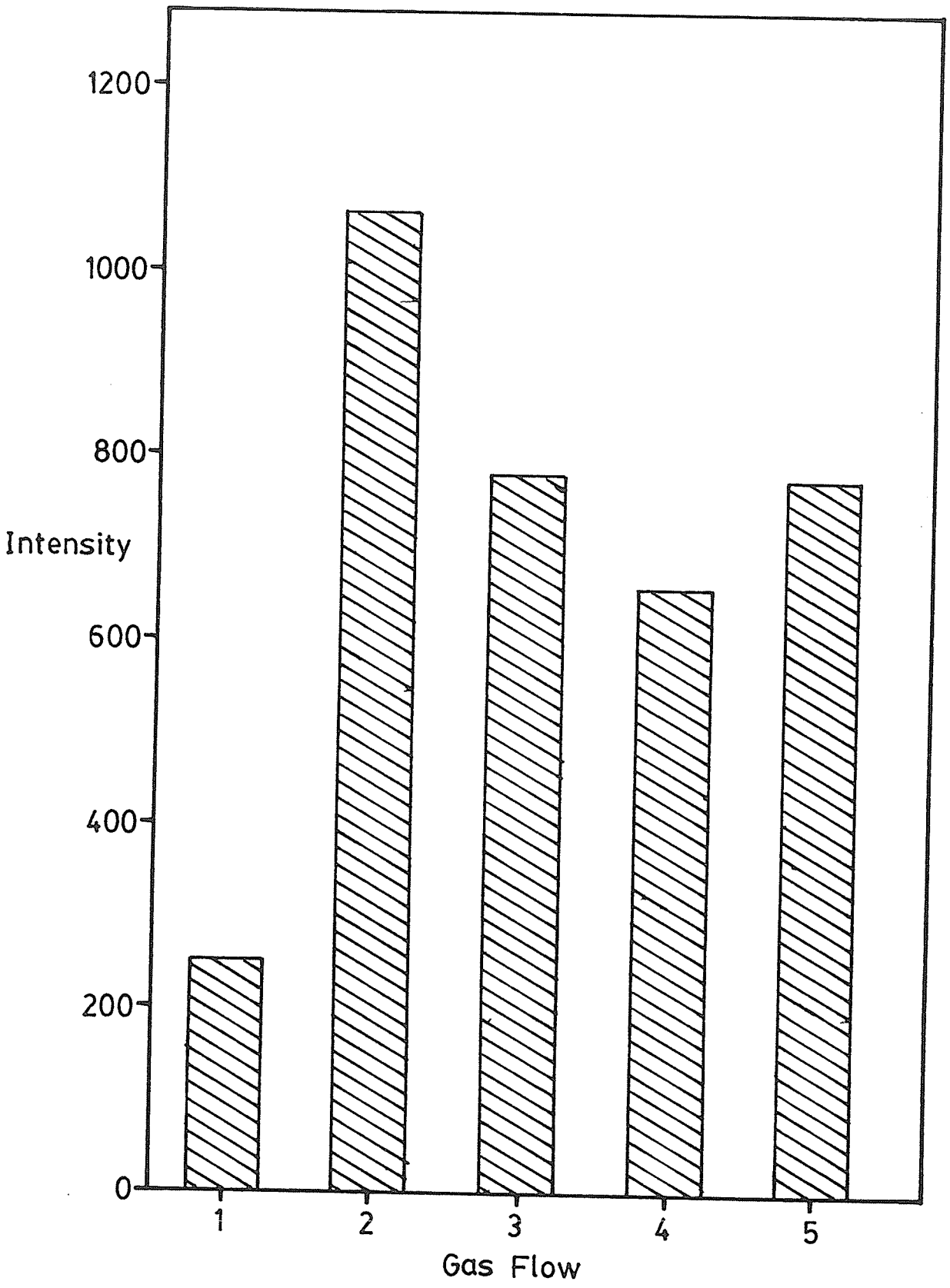
1200
1000
800
600
400
200
0
Intensity
1
2
3
4
5
Gas Flow

Figure 4.28

Secondary ion yield of (D-Ala)^2 methionine enkephalinamide as a function of eluent flowrate, with a nitrogen flow(boehmite substrate).

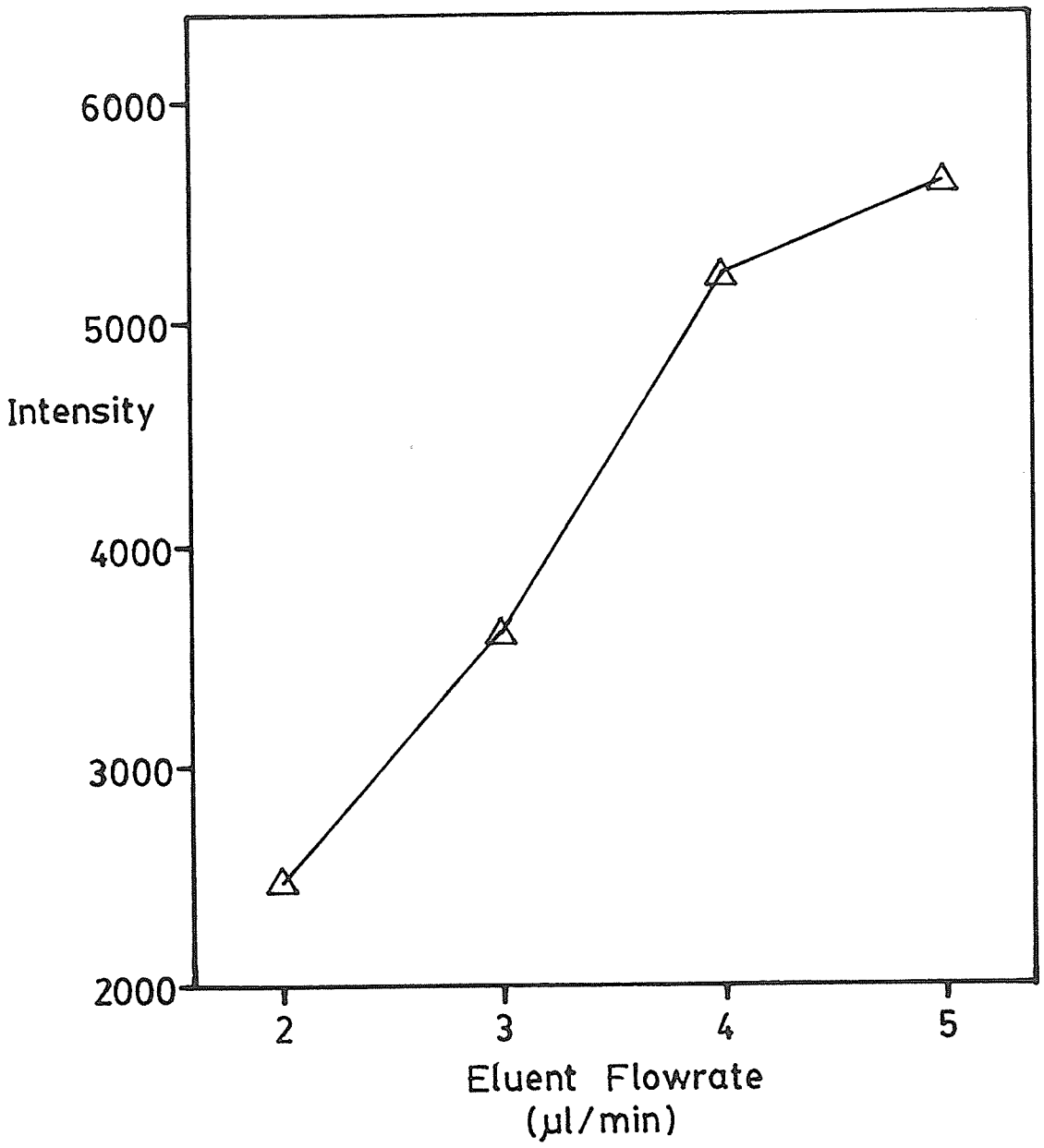
6000
5000
Intensity
4000
3000
2000
2
3
4
5
Eluent Flowrate
(µl/min)

demonstrate that the flowrate restriction imposed by the old spray/substrate system had been removed by using the combination of concentric gas flow past the spray needle and the use of a hydrophilic substrate (boehmite).

4.7) LC-MS Results for Peptide Digests

The improvements to the LC-MS system outlined in Section 4.5 and 4.6 allowed the application of the system to samples of medium sized peptides. The difficulty in obtaining good samples from positively charged peptides was eliminated by using the new packing materials and higher buffer concentrations. Therefore, in order to demonstrate the usefulness of the system as a practical method of peptide analysis, it was important to use peptide mixtures that were "real world" samples. The mixtures of synthetic peptides used in Section 4.4 were interesting for initial purposes but samples that were not completely characterized before LC-MS would be much more convincing examples.

An important class of peptide mixtures are enzyme digests of large peptides. The technique of sequencing a peptide by examining SIMS/FAB spectra alone becomes increasingly difficult as the size of the peptide increases [82, 83]. The smaller the peptide the more sequence information is usually available from the mass spectrum. Therefore, if one starts with a large polypeptide, reducing the size of the molecule in a predictable fashion increases the amount of SIMS/FAB information available from mass spectra alone. The simplest method for achieving a reduction in peptide length is to cleave the peptide backbone at well defined places using endopeptidases. Enzymatic cleavage leaves a

mixture of smaller peptides that could then be separated into individual components by using HPLC and each individual component is then analyzed in the mass spectrometer. In these experiments, we used two endopeptidases: trypsin and chymotrypsin.

Trypsin proved an excellent choice for these purposes. Trypsin is a well characterized endopeptidase, found in the pancreas of mammals [84]. The enzyme cleaves polypeptides at positively charged amino acid residues (arginine and lysine) only, leaving the arginine or lysine as a C-terminus. No side reactions occur regardless of reaction time. The only exception to the cleavage specificity listed in the literature [85] was for the sequence (Xxx-Lys-Pro-Xxx) where the presence of proline following lysine inhibits the action of the enzyme completely. Trypsin is readily available in pure form and is very stable in both the solid form and in solution. The pH range for trypsin (pH = 7.0-9.0) is wide and therefore easy to maintain. Trypsin is also compatible with a volatile buffer system (formic acid/triethylamine), allowing the removal of buffer by lyophylization before HPLC analysis. The very specific nature of the enzyme had the advantage for our purposes of producing few cleavages in medium sized (1000 - 3000 u) polypeptides, because polypeptides of this size usually contain only a few arginine or lysine residues. The small number of cleavages should therefore leave significant portions of the peptide intact to be sequenced by mass spectrometry .

Experiments with chymotrypsin were not as successful as with trypsin, mainly due to the lack of specificity of the chymotrypsin cleavage. The main sites of attack for chymotrypsin are the aromatic residues (tyrosine, tryptophan or phenylalanine), leaving the aromatic

residue as the C-terminal end. The rate of attack at these sites is dependent on the adjacent amino acid residues. In addition, chymotrypsin also attacks any residue with a bulky, non-polar side chain, such as leucine or methionine if the reaction time is too long. Therefore, it is not assured that an aromatic residue would be the C-terminus. One might think that the lack of specificity should not be a problem; the structural information produced from the mass spectra would be the same for both cases. This analysis of the situation would be naive. Even if chymotrypsin only attacked aromatic residues, because aromatic residues are quite common in medium sized neuropeptides, the number of cleavages produced by chymotrypsin would be larger than for trypsin, producing more single amino acids and dipeptides. The production of a large number of small fragments with unpredictable C-terminal residues makes the task of determining the original peptide's structure much more difficult. If a peptide was cleaved by trypsin into 3 sections (non-overlapping) that could be sequenced by SIMS, there would be 3! = 6 possible sequence combinations of these sections; only two combinations are possible if one of the cleaved peptides did not have either arginine or lysine as the C-terminal residue because that peptide must have been the C-terminus originally. If a peptide was cleaved by chymotrypsin into 5 non-overlapping sections that could be sequenced by SIMS, there would be 5! = 120 possible sequence combinations of these sections and because of the lack of specificity of the cleavage, the peptide containing the original C-terminus could be only identified for very favourable cases, i.e. if the C-terminal residue was strongly polar. To reduce the complication of the chromatographic and mass spectra analysis of neuropeptide structure, trypsin was clearly the endopeptidase of choice for producing easily

interpreted cleavages.

The method used to produce the neuropeptide digest was simple. The peptide was dissolved in 0.05 M formic acid/triethylamine buffer (pH = 8.0); typically 250 μg of peptide and 0.5 ml of buffer was used. The trypsin was added to the solution, in an amount approximately 1% of the peptide being cleaved (2.5 μg). The solution was placed into a small conically bottomed vial (Reactivial) that had a tight fitting top, usually with a Teflon seal and contained a small Teflon stir bar. The vial was then transferred to a stirred water bath maintained at 40 C for 60 minutes. After 60 minutes, the vial was removed from the bath. The contents (less the stir bar) were transferred to a wider vial and quickly frozen with liquid nitrogen. The frozen sample was placed into a vacuum system and lyophilized for several hours to remove the solvent and buffer. The pellet formed in the vial was then dissolved in a water/alcohol mixture and frozen for storage.

Before dealing with the results of analyzing trypsin digests of neuropeptides, the fragmentation patterns characteristic of a peptide's structure obtained from SIMS/FAB mass spectra should be discussed. Early work in applying primary particle bombardment techniques to the examination of peptides showed that many fragment ions appeared in the mass spectrum of a small peptide (such as leucine enkephalin, YGGFL) [86]. The fragment ions were assigned to breaking bonds along the peptide "backbone", with the addition or subtraction of hydrogen, or with the removal of sidechains. The fragments produced by breaking single bonds in the peptide backbone were of the greatest interest as it was these ions that gave the best structural information about the peptide. The nominal mass of the peptide $(M+H)^+$ ion did not help in

determining the sequence of a peptide, only in confirming a proposed structure.

The nomenclature of the fragment ions produced has varied considerably from paper to paper, usually naming the fragments with letters and/or numbers with some indication of proton transfers to the fragment ion. The nomenclature scheme chosen for this thesis was that of Roepstorff and Fohlman [87] (referred to here as the RF scheme). The basic features of the RF scheme are shown in Figure 4.29. The fragments labeled A, B and C retain the positive charge on the fragment containing the N-terminus while the fragments labeled X, Y and Z retain the positive charge on the fragment containing the C-terminus. Transfers of protons to the fragments shown in Figure 4.29 are denoted by the addition of the apostrophe after the letter (e.g. $Y_1 + H = Y_1'$, $C_2 + 2H = C_2''$) and the removal of a hydrogen from the fragment denoted by an apostrophe before the letter (e.g. $Y_1 - H = {}'Y_1$, $C_2 - 2H = {}''C_2$). A simple recursive algorithm for generating the masses of the RF fragments is given in Table 4.1.

Alpha-endorphin was the first peptide on which the trypsin digestion method was attempted. This is a polypeptide containing methionine enkephalin as part of its structure. The amino acid sequence of alpha-endorphin: Tyr-Gly-Gly-Phe-Met-Thr-Ser-Glu-Lys-Ser-Gln-Thr-Pro-Leu-Val-Thr or alternately YGGFMTSEKSQTPLVT. By inspection, the only trypsin cleavage point was between Lys^9 and Ser^{10}, leading to two cleavage products: YGGFMTSEK and SQTPLVT. The trypsin digestion was carried out as described above and the digest products were redissolved in water to a concentration of approximately 250 picomoles/microliter. The HPLC eluent was 60:40 2-propanol:water with 0.01% TEA/TFA buffer,

Figure 4.29

Roepstorff-Folmann peptide fragmentation nomenclature.

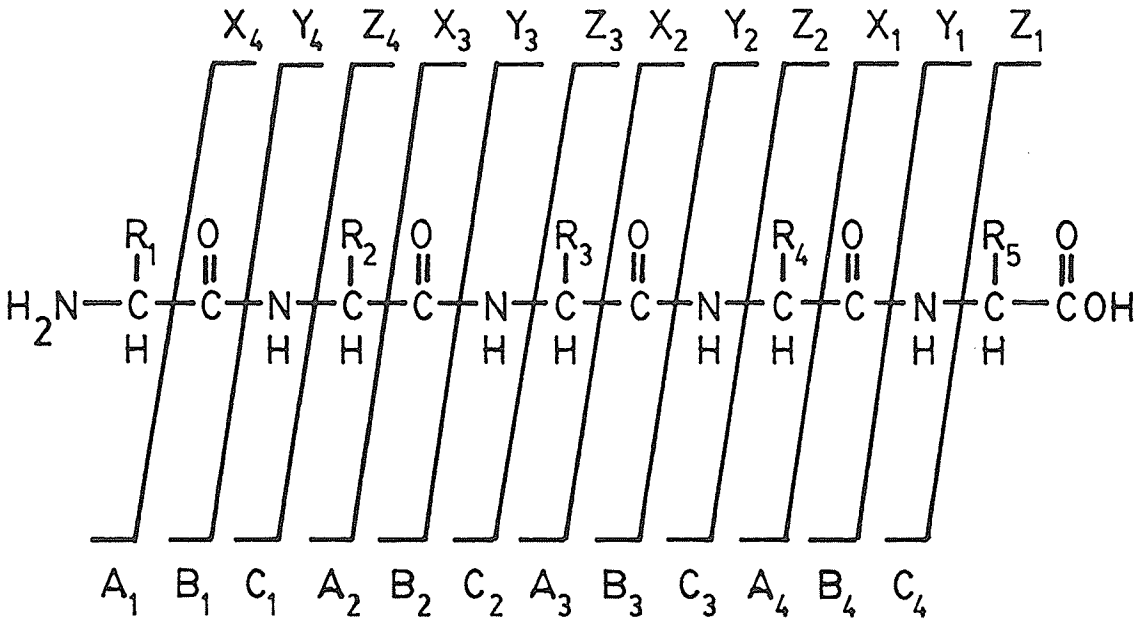
X4 Y4 Z4 X3 Y3 Z3 X2 Y2 Z2 X1 Y1 Z1
R1 O R2 O R3 O R4 O R5 O
H2N C C N C C N C C N C C N C COH
H H H H H H H H H H
A1 B1 C1 A2 B2 C2 A3 B3 C3 A4 B4 C4

Table 4.1

A recursive procedure for calculating the masses of RF-type peptide fragment ions.

$A_1 = R_1 + 29$	$B_1 = A_1 + 28$	$C_1 = B_1 + 15$
$A_2 = C_1 + R_2 + 13$	$B_2 = A_2 + 28$	$C_2 = B_2 + 15$
. . .	. . .	. . .
$A_N = C_{N-1} + R_N + 13$	na	na

$Z_1 = R_N + 58$	$Y_1 = Z_1 + 15$	$X_1 = Y_1 + 28$
$Z_2 = X_1 + R_{N-1} + 13$	$Y_2 = Z_2 + 15$	$X_2 = Y_2 + 28$
. . .	. . .	. . .
$Z_{N-1} = X_{N-2} + R_2 + 13$	$Y_{N-1} = Z_{N-1} + 15$	$X_{N-1} = Y_{N-1} + 28$

flowrate = 3 µl/minute. The substrate material was boehmite and the nitrogen gas flow was on. The electrospray voltages were adjusted so that the deposit diameter was approximately 1.5 mm. Two separate components were obtained from the mixture, well separated from each other. The mass spectra of the two components ware shown in Figure 4.30 (a) and (b). The number in the spectrum title refers to the position of the fraction being analyzed on the substrate strip, as read from a vernier dial on the pinion drive.

The first peptide to elute was the cleavage product SQTPLVT as shown in Figure 4.30 (a). The protonated molecule is observed at m/z = 745 u, a sodium adduct at m/z = 767 u, and a potassium adduct at m/z = 784 u.

Table 4.2 gives the predicted fragments for the molecule. Comparing the spectrum with Table 4.2, the important structural fragments are A_1, B_2, B_3, and C_4. There are, however, a large number of other fragment ions present in the spectrum. The high abundance of the sodium adduct quasimolecular ion suggested that there could be sodium addition to the fragments, and using this hypothesis, the fragments (C_4 + Na), (C_5 + Na) and (C_6 + Na) were assigned. Such ions have been reported as daughter ions produced by collisional activation of $(M+Na)^+$ ions [88] and also in reflected TOF mass spectra [89]. However, recent results in our laboratory [90] suggest that the correct assignment is Bn + 17 + Na. Examination of the remaining fragments showed a family of ions that could be assigned to (C_n - 22) ions. These ions are indicated in the spectrum by the addition of a tilde (~) over the C designation. A similar ion at $(M - 22)^+$ was observed as well. As a

Figure 4.30

Mass spectra of the two cleavage products of an alpha-endorphin trypsin digest. The spectra were obtained from HPLC fractions sprayed onto boehmite (see text for HPLC conditions). Primary ion energy = 10 keV; secondary ion energy = +8 keV.

a) Ser-Gln-Thr-Pro-Leu-Val-Thr, SQTPLVT.

b) Tyr-Gly-Gly-Phe-Met-Thr-Ser-Glu-Lys, YGGFMTSEK.

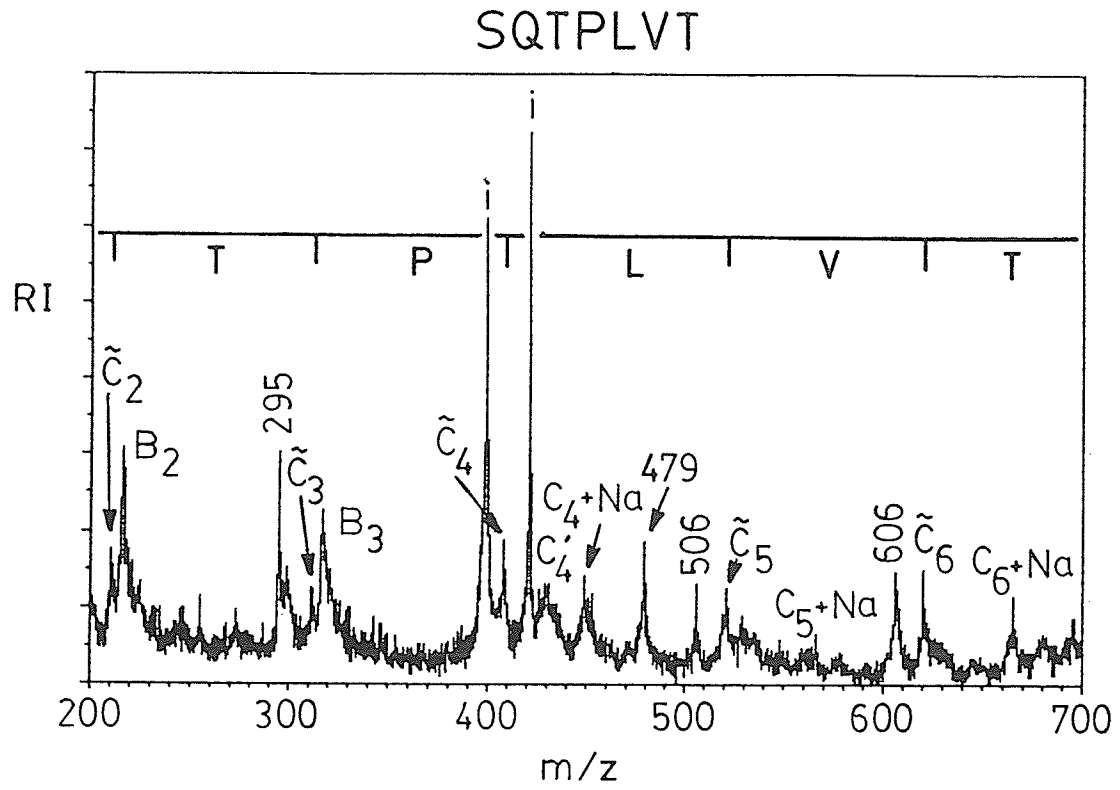
SQTPLVT
RI
T T T P T L T V T T
i
i
$\tilde{C}_2$
B_2
295
$\tilde{C}_3$
B_3
$\tilde{C}_4$
C_4+Na
C_4'
479
506
$\tilde{C}_5$
C_5+Na
606
$\tilde{C}_6$
C_6+Na
200
300
400
500
600
700
m/z

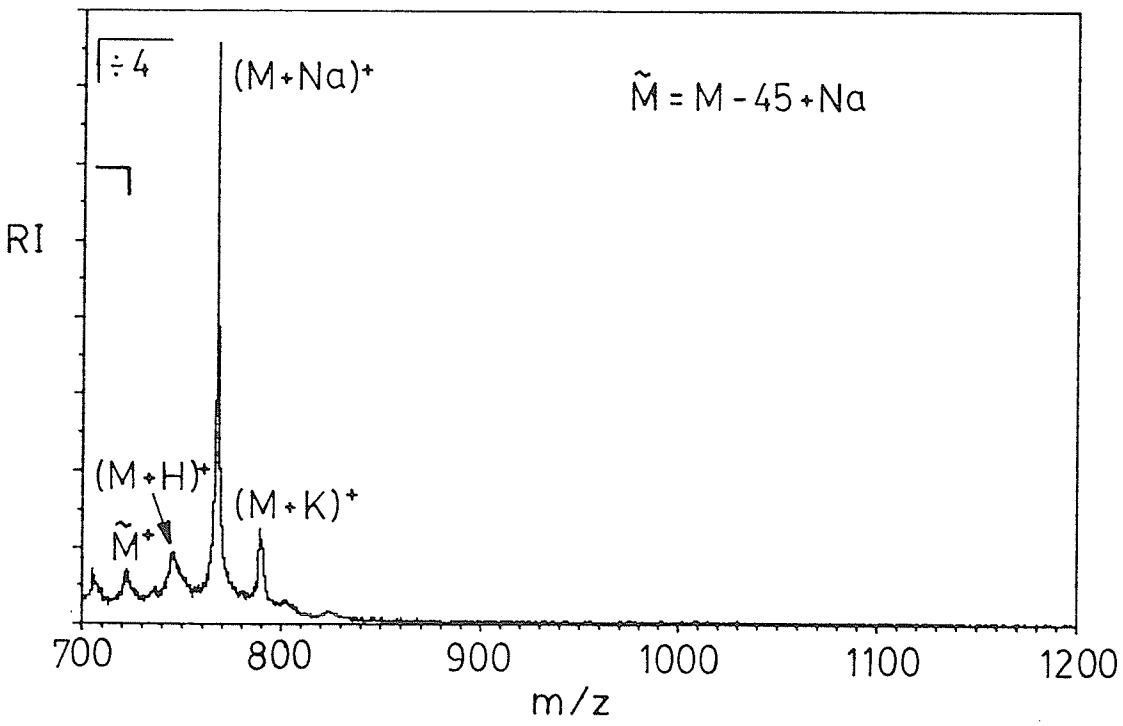
÷4
RI
$(M+Na)^+$
$\tilde{M}$ = M - 45 + Na
$(M+H)^+$
$\tilde{M}^+$
$(M+K)^+$
700
800
900
1000
1100
1200
m/z

(a)

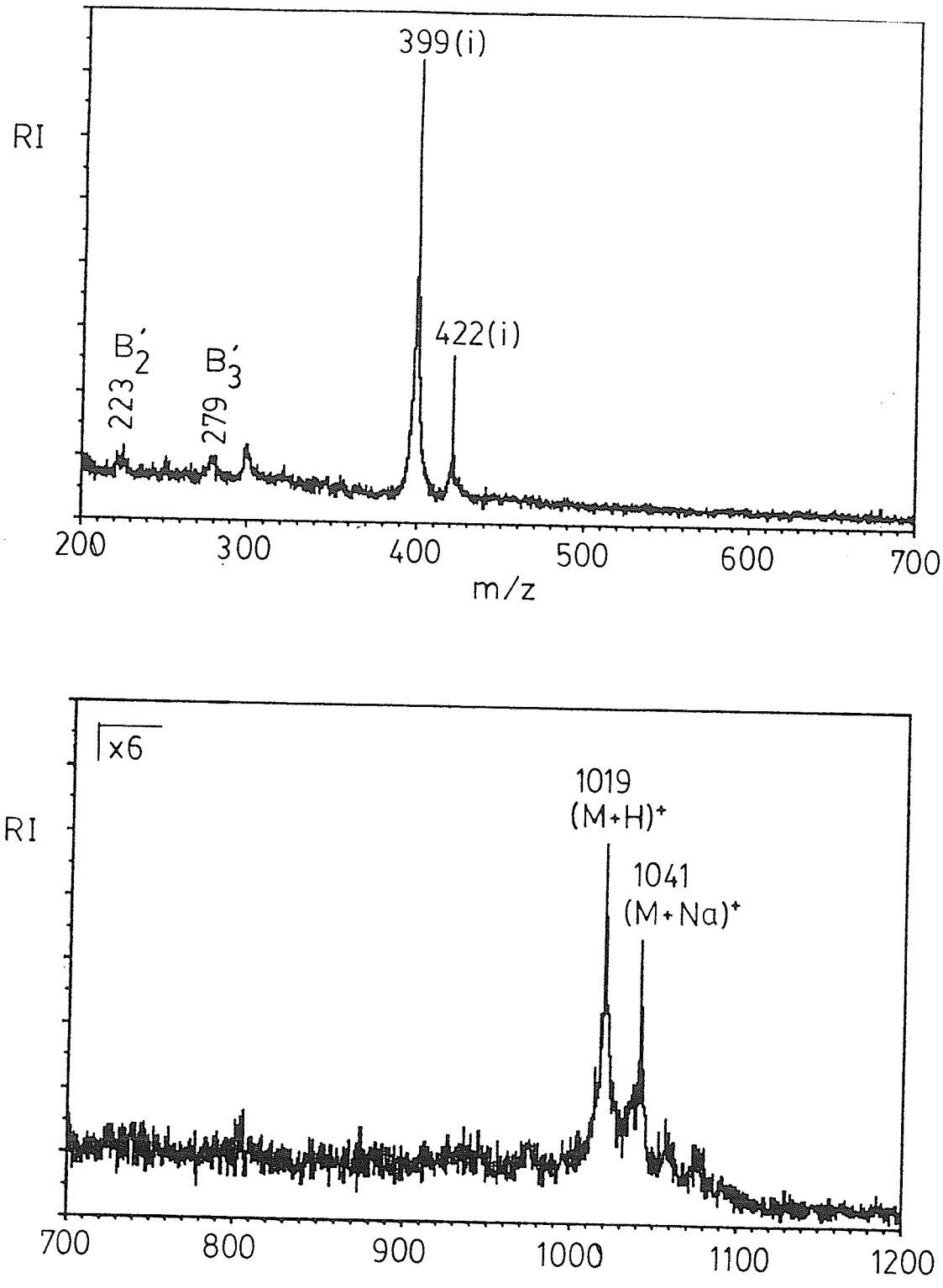
YGGFMTSEK
399(i)
RI
422(i)
B2'
223
B3'
279
200
300
400
500
600
700
m/z
x6
1019
(M+H)+
1041
(M+Na)+
RI
700
800
900
1000
1100
1200

(b)

Table 4.2

The RF-type fragments and nominal masses, predicted for the peptide SQTPLVT.

n	a.a	m(R)	A_n	B_n	C_n
1	S	31	60	88	103
2	Q	72	188	216	231
3	T	45	289	317	332
4	P	40	385	413	428
5	L	57	498	526	541
6	V	43	597	625	640
7	T	45	698	-	-

n	a.a	m(R)	Z_n	Y_n	X_n
1	T	45	103	118	146
2	V	43	202	217	245
3	L	57	315	330	358
4	P	40	400	414	442
5	T	45	500	515	543
6	Q	72	628	643	671

working hypothesis, this M - 22 ion was assigned to $(M - 45 + Na)^+$. The loss of COOH (M - COOH) from the C terminal end of the molecule could not explain the loss of 45 u from the molecule, because the fragments were C-type, with the charge retained on the N-terminal end. Therefore the most probable mechanism for explaining the loss of 45 u would be the loss of formamide ($HCONH_2$) from the glutamine side chain at position 2 in the molecule. The sodium ion would have to have been attached close to the N-terminal end of the molecule because C-tilde fragments were observed for n 2. The presence of the C-tilde fragments allowed the sequencing of the molecule, as shown in Figure 4.30 (a). The peaks marked i, m/z = 399 u and 422 u were common to all spectra taken from deposited fractions and were assumed to be the hydrogen adduct and sodium adduct ions of a water contaminant molecule, mass 398 u.

The spectrum of the fraction containing the second eluting material is shown in Figure 4.30 (b). A hydrogen adduct ion, m/z = 1019 u, and a sodium adduct ion, m/z = 1041 u, as predicted for the second trypsin cleavage product YGGFMTSEK. Table 4.3 shows the fragment ions calculated for the peptide. The only structure related fragments were A_1, B_2' and B_3'.

The mass spectra in Figure 4.30 demonstrate several phenomena which are generally applicable to SIMS spectra produced from HPLC eluent deposits. Firstly, the peptide SQTPLVT has a greater affinity for sodium than does YGGFMTSEK. The sodium adduct ion dominates the quasimolecular ion region of Figure 4.30 (a), while the sodium adduct ion is a minor component in Figure 4.30 (b). The amount of sodium

Table 4.3

The RF-type fragments and nominal masses, predicted for the peptide YGGFMTSEK.

n	a.a	m(R)	A_n	B_n	C_n
1	Y	107	136	164	179
2	G	1	193	221	236
3	G	1	250	278	293
4	F	91	397	425	440
5	M	75	528	556	571
6	T	45	629	657	672
7	S	31	716	744	759
8	E	73	845	873	888
9	K	72	973	-	-

n	a.a	m(R)	Z_n	Y_n	X_n
1	K	72	130	145	173
2	E	73	259	274	302
3	S	31	346	361	389
4	T	45	447	462	490
5	M	75	478	593	621
6	F	91	725	640	768
7	G	1	782	797	825
8	G	1	839	854	882

present in both fractions due to the eluting solvent is obviously the same so SQTPLVT either carried the additional sodium down the column with itself or the peptide had a much greater tendency to form sodium adduct ions than did YGGFMTSEK (or both possibilities occurred).

Another feature of these spectra is the difference in fragmentation pattern: SQTPLVT produced strong fragment ions from several peptide bonds, while YGGFMTSEK only produced fragment ions characteristic of the first three peptide bonds. A possible explanation for this phenomenon is that the quasimolecular ions of YGGFMTSEK are more stable than those of SQTPLVT. In fact, this difference in stability seems to be the case.

In time-of-flight SIMS, there are two components in any ion peak. One component is produced by ions that remained intact during their flight through the field free region, producing a sharp peak. The other component is produced by ions that undergo unimolecular decomposition in the field free region of the spectrometer. The daughter fragments of the decomposition still have the same center of mass velocity as the intact parent ion, so they appear in the mass spectrum at the same time (mass) as the parent, but the peak produced is broadened by the energy released in the decomposition. Unimolecular decays of this type are conventionally referred to as "metastable decays", or alternatively, the parent ions that undergo the decay are called "metastable ions". The physics of these metastable ion decays, including time constant measurements and the identity of the daughter fragments produced has been dealt with by our group [91] and by Chait and Field [92] for selected parent molecules. Figure 4.31 compares the hydrogen adduct ions of SQTPLVT and YGGFMTSEK. The resolution of the spectrometer was

Figure 4.31

Comparison of the hydrogen adduct quasimolecular ion regions of SQTPLVT (upper spectrum) and YGGFMTSEK (lower spectrum).

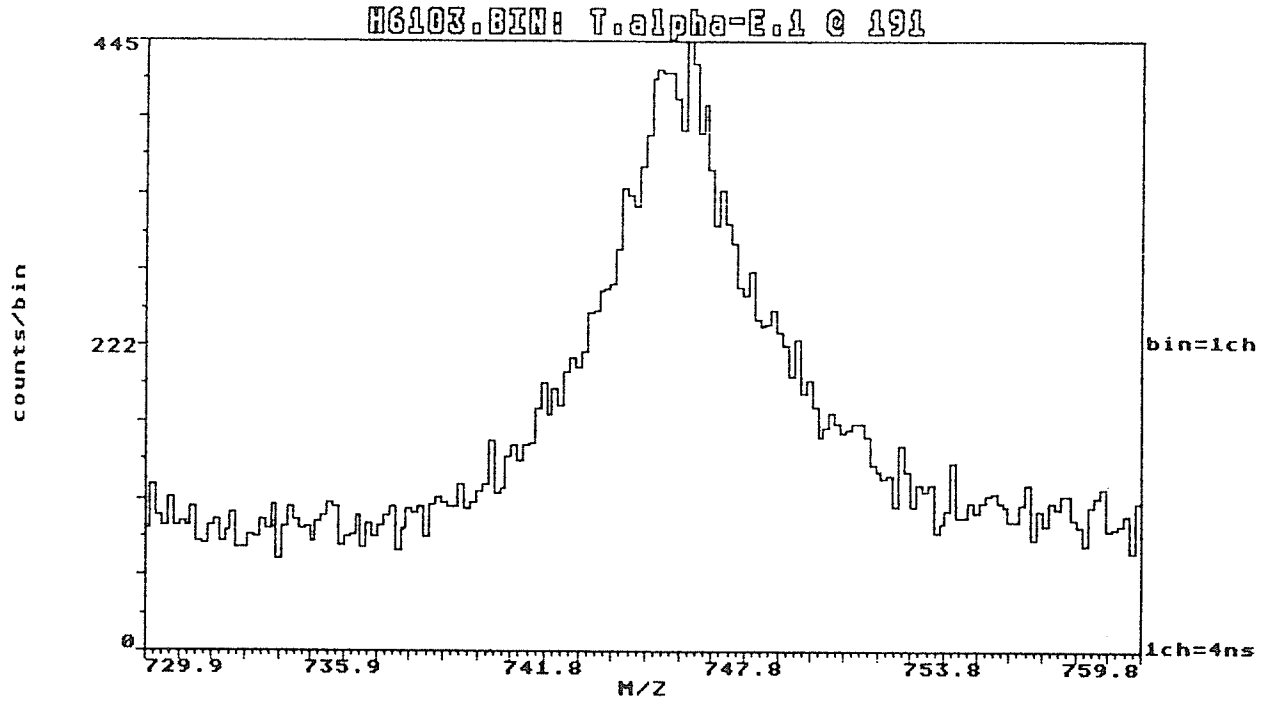
H6103.BIN: T.alpha-E.1 @ 191
445
222
0
counts/bin
bin=1ch
1ch=4ns
729.9
735.9
741.8
747.8
753.8
759.8
M/Z

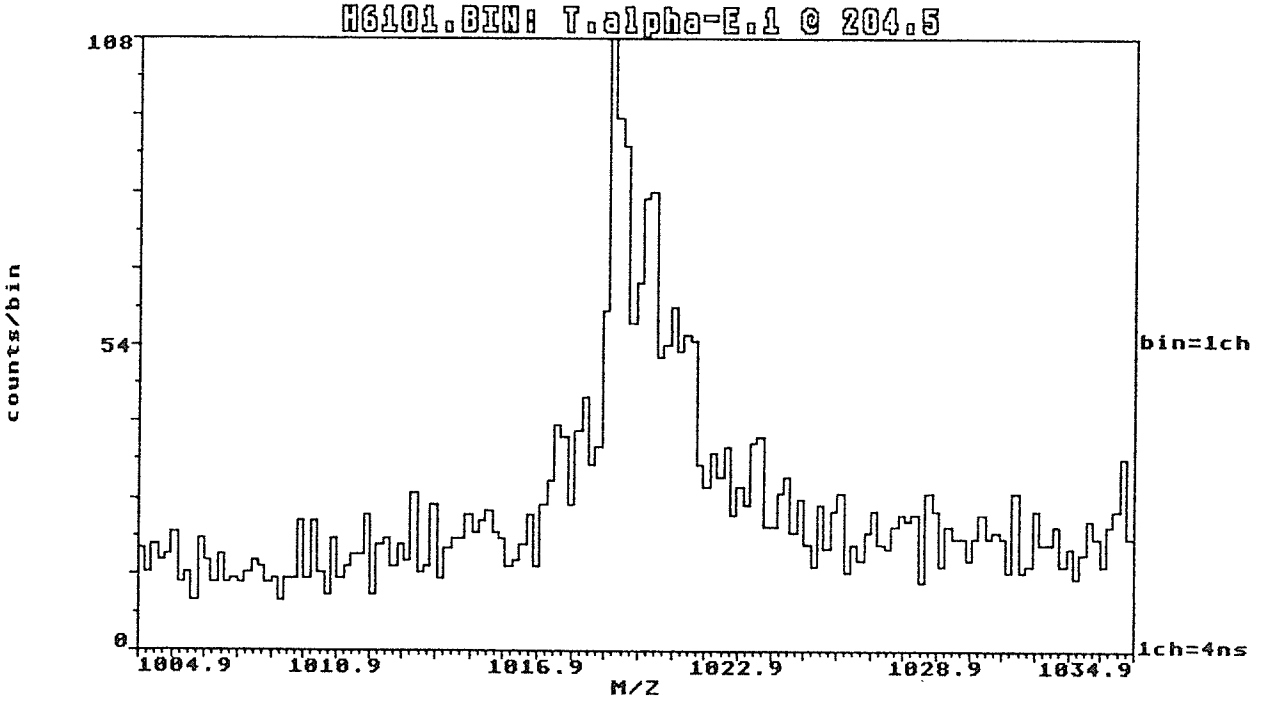
H6101.BIN: T.alpha-E.1 @ 204.5
108
54
0
counts/bin
bin=1ch
1ch=4ns
1004.9
1010.9
1016.9
1022.9
1028.9
1034.9
M/Z

approximately 2000 (full-width-half-maximum definition). The hydrogen adduct ion of SQTPLVT (upper spectrum) is an almost featureless broad peak, showing little if any resolution of the carbon-13 isotope pattern of the parent molecule. The broad nature of the peak indicates that the hydrogen adduct ion is unstable on the time scale of field free flight path of the spectrometer (approx. 40 μs), i.e. the ion was metastable. The hydrogen adduct peak of YGGFMTSEK (lower spectrum) is quite different. The carbon-13 isotope pattern is clearly evident, with only a small amount of broadening at the base of the cluster of peaks caused by metastable decay. Assuming that the above interpretation of peak shapes is correct, the desorbed SQTPLVT hydrogen adduct ion is unstable, while the YGGFMTSEK adduct is relatively stable. Therefore, assuming that the structurally related fragment ions are produced by a unimolecular decay of the parent ion very soon after desorption, it seems reasonable that the more stable parent ion (YGGFMTSEK) should produce fewer structurally related fragments. Unfortunately, there is no theoretical method of predicting the stability of hydrogen adduct quasimolecular ions. An interesting and perhaps related fact is that the sodium adduct of SQTPLVT is much more stable than the hydrogen adduct ion (compare the two spectra in Figure 4.32) and only one fragment containing sodium, i.e. $(M-COOH+Na)^+$, was observed. The enhanced stability of sodium adduct quasimolecular ions has been frequently observed in the past both by ourselves [93] and others [94]. The enhanced stability of the sodium (and potassium) adduct ion has been exploited in applying Fourier transform-ion cyclotron resonance mass spectrometry to the examination of peptide molecules, because quasimolecular ions stable for time periods of greater than a millisecond

Figure 4.32

Comparison of the hydrogen adduct (upper spectrum) and sodium adduct (lower spectrum) quasimolecular ions of SQTPLVT.

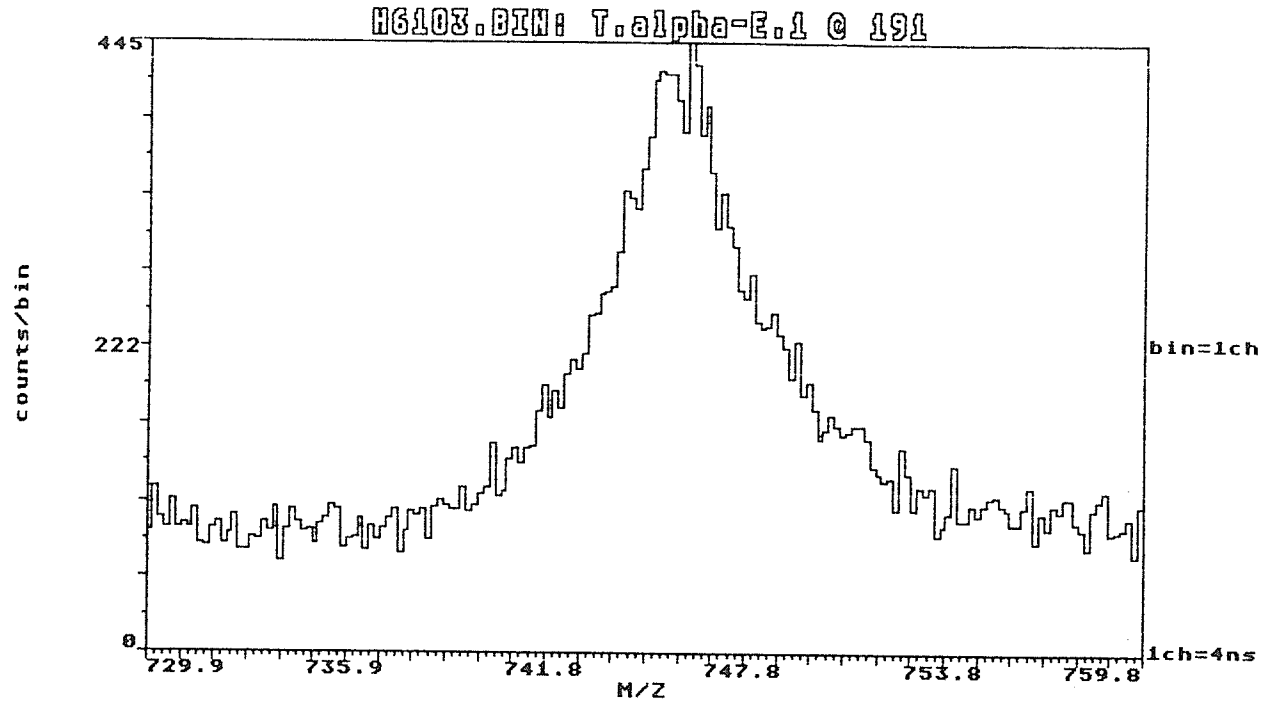
H6103.BIN: T.alpha-E.1 @ 191
445
222
0
counts/bin
bin=1ch
1ch=4ns
729.9
735.9
741.8
747.8
753.8
759.8
M/Z

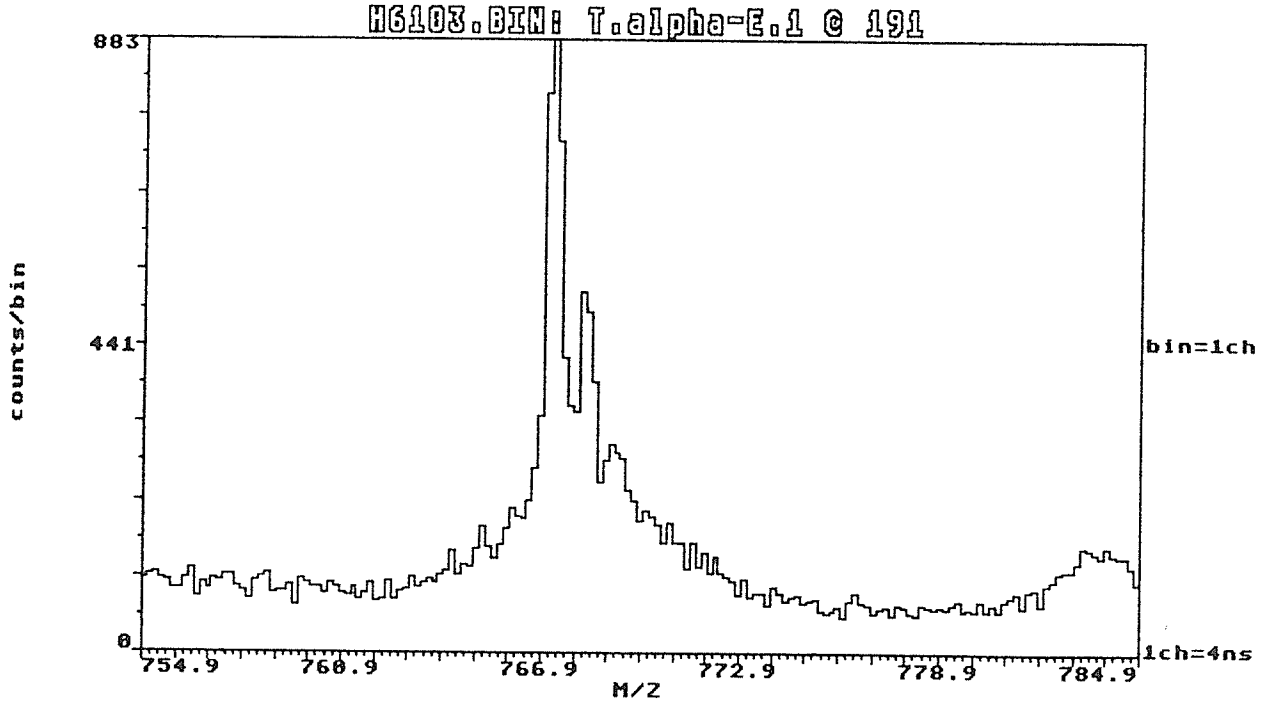
H6103.BIN: T.alpha-E.1 @ 191
883
441
0
counts/bin
bin=1ch
1ch=4ns
754.9
760.9
766.9
772.9
778.9
784.9
M/Z

are necessary to produce signals in this type of instrument [95].

The pattern of fragmentation from SQTPLVT is in itself, quite interesting. Of the possible structural fragments given in Table 4.2, only fragment ions containing the N-terminus of the peptide are observed. In addition, only one of the three possible fragment ion types (A, B, or C) is observed for bond fissions between the peptide units. All of the fragment ions for both enzymatic cleavage products (except the A_1) showed the addition of one hydrogen to the simple structure shown in Figure 4.29. Fast atom bombardment spectra of simple peptides show a different pattern of fragmentation [96]. In general, the FAB spectra were more complex, containing significant peaks corresponding to A, B, C, X, Y and Z fragments between peptide units, although the presence or absence of these fragments was by no means predictable. Also, the A and B type fragments observed in FAB did not have a hydrogen added, while the C type fragments had two hydrogens added.

It is unwise, however, to infer too much from a single observation (even though the above discussion is the product of hindsight). Another neuropeptide that was available and would be a good candidate for demonstrating the information available from examining a trypsin digest using the LC-MS combination was neurotensin. Neurotensin is a tridecapeptide with the structure: pyro-Glu-Leu-Tyr-Glu-Asn-Lys-Pro-Arg-Arg-Pro-Tyr-Ile-Leu, or pELYENKPRRPYIL. This molecule is interesting for several reasons. The peptide structure indicates that there should be two cleavages: 1) between Arg^8 and Arg^9: and 2) between Arg^9 and Pro^{10}. The bond Lys^6 and Pro^7 should remain intact, because as was mentioned above, proline following lysine inhibits the action of

trypsin. The presence of arginine in the digest would indicate unambiguously the presence of either an -Arg-Arg- or -Lys-Arg- sequence in the original peptide. The N-terminal amino acid residue is also of interest. The presence of a glutamic acid residue on the N-terminus of a peptide normally leads to the cyclization of the side chain, i.e. formation of a pyroglumatic acid residue. The ability to detect an N-terminal pyro-glutamic acid would be of practical importance. From the standpoint of ion fragmentation patterns, it would be interesting to observe whether changing an N-terminal amino group into an amide has an effect on the observed fragmentation pattern.

The trypsin digest of neurotensin was performed in the same manner as was outlined above for alpha-endorphin. The lyophilized digest was redissolved in 1 ml of water and 0.5 ul injected onto the HPLC column, with a mobile phase of 50:50 2-propanol:water + 0.05% TFA/TEA buffer, a flowrate of 3 ul/minute. Boehmite was used as the substrate. The HPLC results were not as expected. Only two components were separated, with no visually observable component at the retention time expected for arginine. The strip containing the chromatogram was placed into the mass spectrometer and analyzed. The masses of the two components showed that the expected cleavage between Arg^{9} and Pro^{10} did not occur. The two cleavage products were pELYENKPR and RPYIL. Presumably, under the conditions of our digest, the proline residue inhibited the action of trypsin on the arginine-proline bond, as proline does when following lysine.

The mass spectrum of the second component is shown in Figure 4.33 (a). The hydrogen adduct quasimolecular ion of RPYIL is m/z = 661 u.

Figure 4.33

Mass spectra of the two cleavage products of a neurotensin trypsin digest. The spectra were obtained from HPLC fractions sprayed onto boehmite (see text for HPLC conditions). Primary ion energy = 10 keV; secondary ion energy = +8 keV.

a) Arg-Pro-Tyr-Ile-Leu, RPYIL.

b) pyro-Glu-Leu-Tyr-Glu-Asn-Lys-Pro-Arg, pELYENKPR.

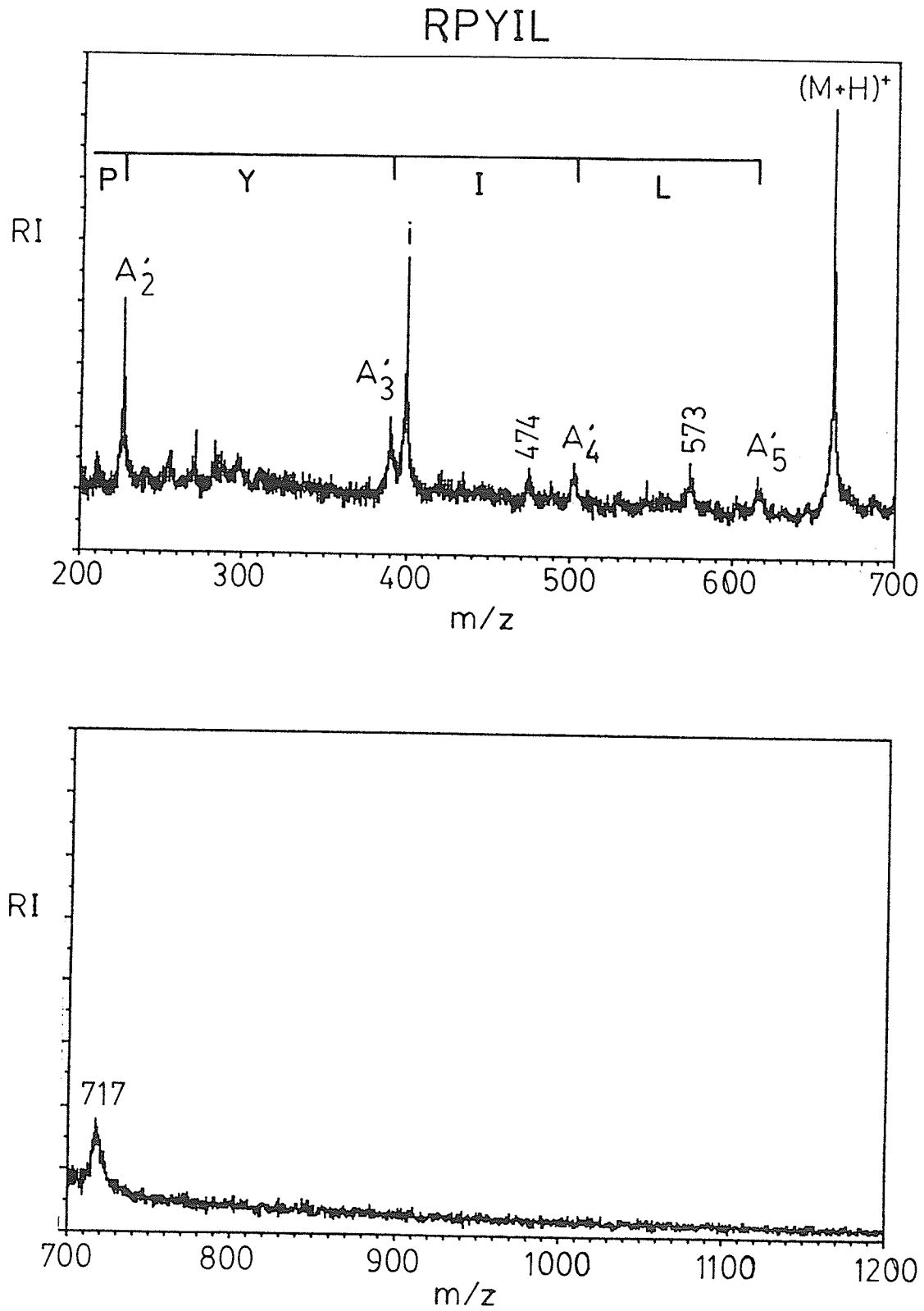
RPYIL
(M+H)+
P
Y
I
L
RI
i
A'2
A'3
474
A'4
573
A'5
200
300
400
500
600
700
m/z
RI
717
700
800
900
1000
1100
1200
m/z

(a)

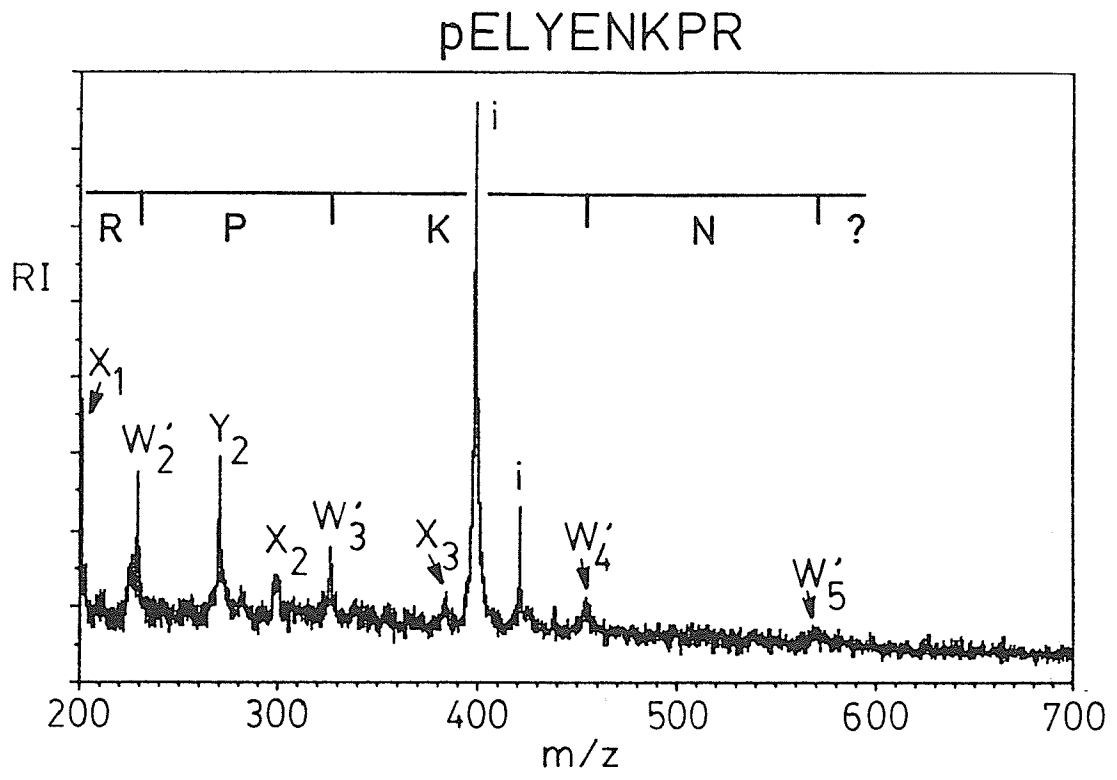
pELYENKPR
RI
R
P
K
N
?
i
X_1
W'_2
Y_2
X_2
W'_3
X_3
i
W'_4
W'_5
200
300
400
500
600
700
m/z

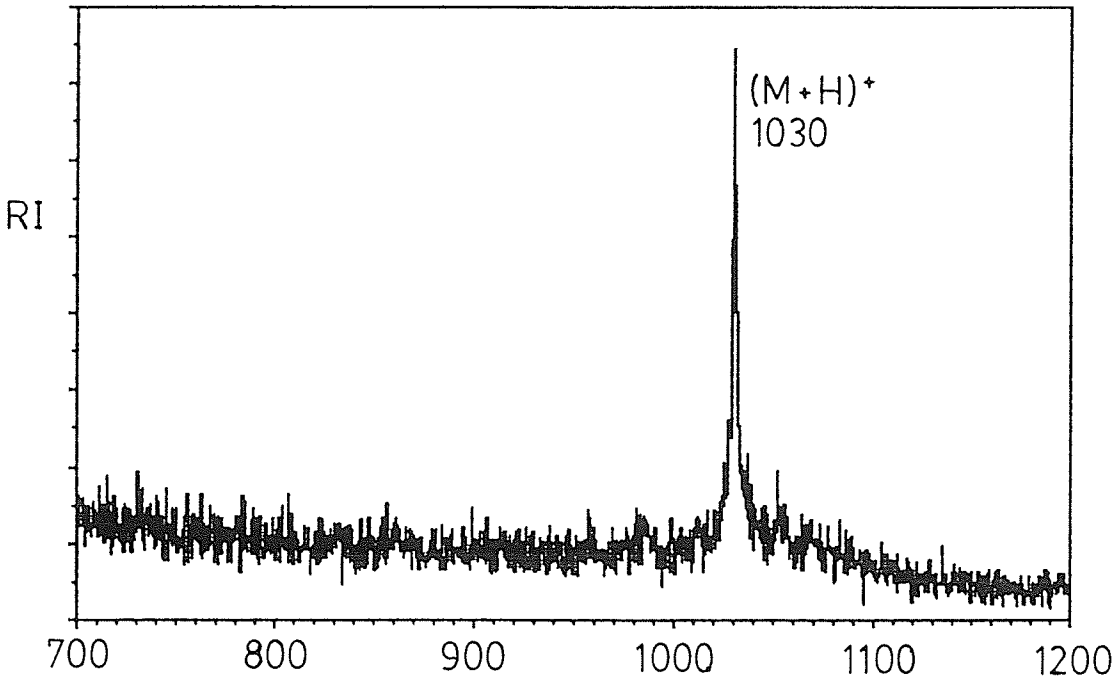
RI
$(M+H)^+$
1030
700
800
900
1000
1100
1200

(b)

The fragments for RPYIL is given in Table 4.4. Comparing the fragments with the mass spectrum, the observed sequence specific fragments are A_1', A_2', A_3', A_4', A_5', B_2 and X_2. Two other structural fragments are m/z = 573 u (loss of the isopropyl portion of the leucine sidechain from A_5') and m/z = 474 u (loss of the ethyl portion of the isoleucine side chain from A_4'). This fragmentation pattern is different from the pattern observed for the alpha-endorphin cleavage product SQTPLVT, in which the B type fragments were the most abundant. Also, RPYIL showed very little tendency to form a sodium adduct quasimolecular ion, while SQTPLVT formed a strong sodium adduct. After fragmentation the end of the molecule retaining the charge remained the same, however. Almost all of the significant fragments corresponded to the charge being retained on the N-terminal end of the molecule.

The very regular fragmentation pattern of RPYIL is demonstrated that in some cases, at least, the complete structure of a peptide can be determined from the fragmentation pattern. All of the A' type fragments were clearly present in the spectrum, with very few other types of fragmentation interfering with its interpretation. A similar fragmentation pattern was found previously in the SIMS spectra of methionine and leucine enkephalin by Westmore, et al. [86], but in that case, fragments corresponding to other fragmentation pathways were also present.

The component of the digest that eluted first had a hydrogen adduct molecular ion, m/z = 1030, corresponding to pELYENKPR, with the mass spectrum shown in Figure 4.33 (b). The fragments for this molecule are given in Table 4.5. The only structurally significant fragment ions

Table 4.4

The RF-type fragments and nominal masses, predicted for the peptide RPYIL.

n	a.a	m(R)	A_n	B_n	C_n
1	R	100	129	157	172
2	P	40	225	253	268
3	Y	107	388	416	431
4	I	57	501	529	544
5	L	57	614	-	-

n	a.a	m(R)	Z_n	Y_n	X_n
1	L	57	115	130	158
2	I	57	228	243	271
3	Y	107	391	406	434
4	P	40	487	502	530

Table 4.5

The RF-type fragments and nominal masses, predicted for the peptide pELYENKPR.

n	a.a	m(R)	A_n	B_n	C_n
1	pE	55	84	112	127
2	L	57	197	225	240
3	Y	107	360	388	403
4	E	73	489	517	532
5	N	58	603	631	646
6	K	72	731	759	774
7	P	40	827	855	870
8	R	100	983	-	-

n	a.a	m(R)	Z_n	Y_n	X_n
1	R	100	158	173	201
2	P	40	254	269	297
3	K	72	382	397	425
4	N	58	496	511	539
5	E	73	625	640	668
6	Y	107	788	803	831
7	L	57	901	916	944

observed from this scheme are X_1, X_2 and Y_2'. Another type of fragmentation must also have occurred in this molecule, to explain the fragment ions at m/z = 229 u, 326 u, 454 u and 568 u. A simple explanation of this type of fragment ion is demonstrated in Figure 34. A hypothesized mechanism is first the formation of a Z' fragment. The Z' fragment then undergoes a fission of the beta - gamma carbon bond adjacent to the first bond broken. This fission removes the residue sidechain, less the beta carbon. Calling these fragments "W" ions, the ions m/z = 229 u, 326 u, 454 u and 568 u correspond to W_2', W_3', W_4' and W_5', respectively. There has been considerable debate about the mechanism forming these ions. CAD studies [97] indicate that the ions form directly from the protonated molecular ion, while other work [98] suggests that the fragments form via the Z' ion.

On the basis of these results, it would appear as though the modification of the N-terminal amine to form a cyclic amide interferes with the formation of N-terminus containing charged fragments, i.e. A, B or C fragments. This has the clear implication that the charge on the quasimolecular ion precursor of N-terminal fragments is on the N-terminal amine. The absence of an N-terminal amine would appear to change the fragmentation pattern so that the positive charge resides on the C-terminal side of a fragmentation (in this case on the arginine side chain). This influence of pyroglutamic acid on the fragmentation pattern of the peptide may be of practical interest in demonstrating the presence of pyroglutamic acid on the N-terminus, or alternately, in interpreting the spectra of such peptides. The generalization of this finding to all peptides containing a pyroglutamic acid N-terminus is, however, speculation. More work has to be done using such peptides to

Figure 4.34

Proposed W-type fragmentation scheme.

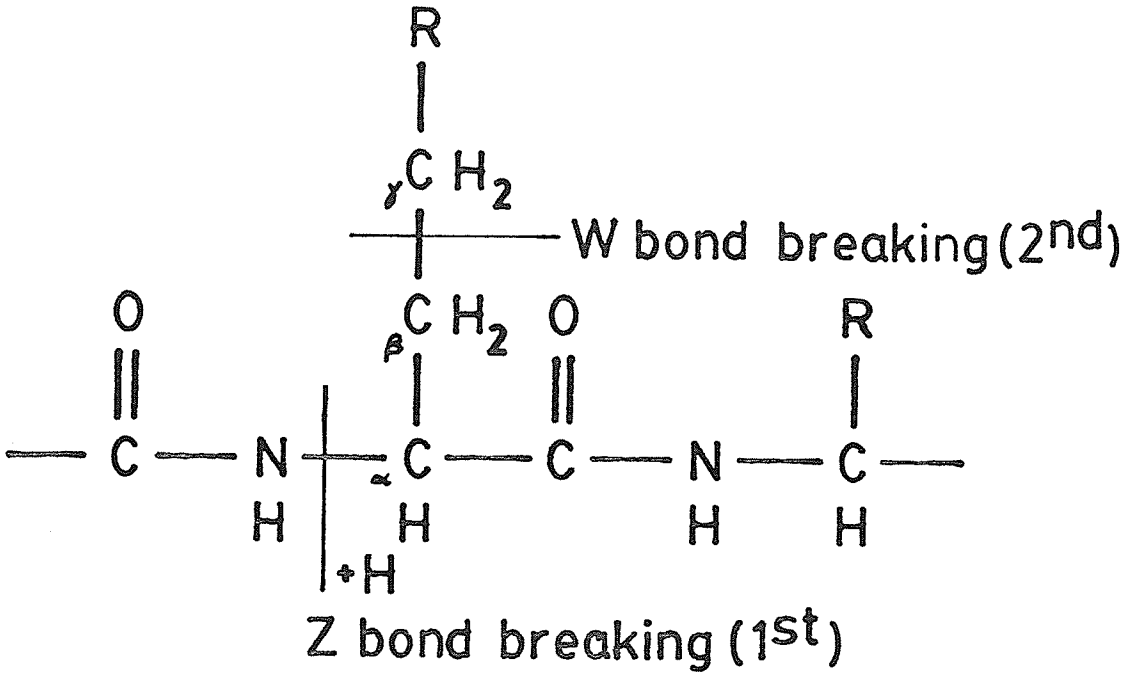
R
γCH2
W bond breaking (2nd)
O
βCH2
O
R
C
N
αC
C
N
C
H
H
H
H
+H
Z bond breaking (1st)

ensure that this change in fragmentation pathways is generally true and not the result of an unusual sequence of residues in this particular case.

The final example of a neuropeptide that was trypsin cleaved and analyzed is the dynorphin related peptide, dynorphin A (1-9), Tyr-Gly-Gly-Phe-Leu-Arg-Arg-Ile-Arg (YGGFLRRIR). Therefore, there should be three trypsin cleavages, yielding YGGFLR, R, and IR. The trypsin digest was performed using the same method as described above. The chromatography was done using a mobile phase of 60:40 2-propanol:water + 0.05% TFA/TEA buffer, a flowrate of 3 ul/minute and a boehmite substrate. The chromatogram had two sets of deposits. The first set of deposits contained only one fraction, while the second set of deposits contained 5 fractions. The strip bearing this chromatogram was analyzed in the mass spectrometer.

The first deposit, as expected from the retention time, was arginine. The spectrum of this fraction is shown in Figure 4.35 (a). The hydrogen adduct ion, m/z = 175 u, is clearly present. Note: No sodium addition was observed for any sample of arginine run under any HPLC conditions.

The first fraction in the second set of deposits is shown in Figure 4.33 (b). Assuming that the prominent peak at m/z = 288 u is a hydrogen adduct ion, the fraction is identified as containing the cleavage product Ile-Arg. The fragments are shown in Table 4.6. The fragment ions are A_1, A_2, and X_1. The relatively strong fragment ion at m/z = 229 u could be tentatively assigned to the loss of the isoleucine side chain from $(M+H)^+$.

Figure 4.35

Mass spectra of the three cleavage products of a dynorphin A(1-9) trypsin digest. The spectra were obtained from HPLC fractions sprayed onto boehmite (see text for HPLC conditions). Primary ion energy = 10 keV; secondary ion energy = +8 keV.

a) Arg, R.

b) Ile-Arg, IR.

c) Tyr-Gly-Gly-Phe-Leu-Arg, YGGFLR.

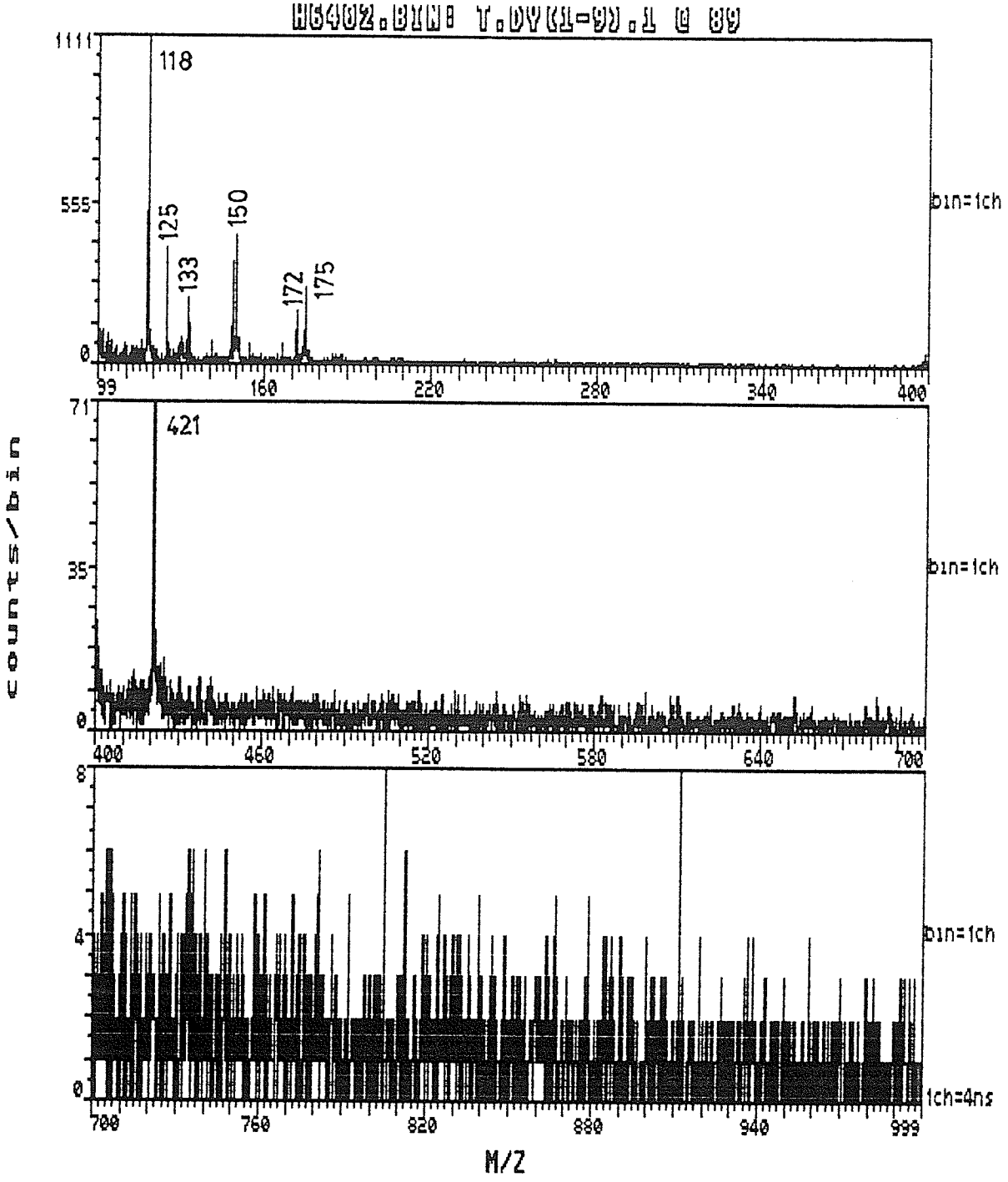
118
125
133
150
172
175
421
counts/bin
M/Z
bin=1ch
bin=1ch
bin=1ch
1ch=4ns

(a)

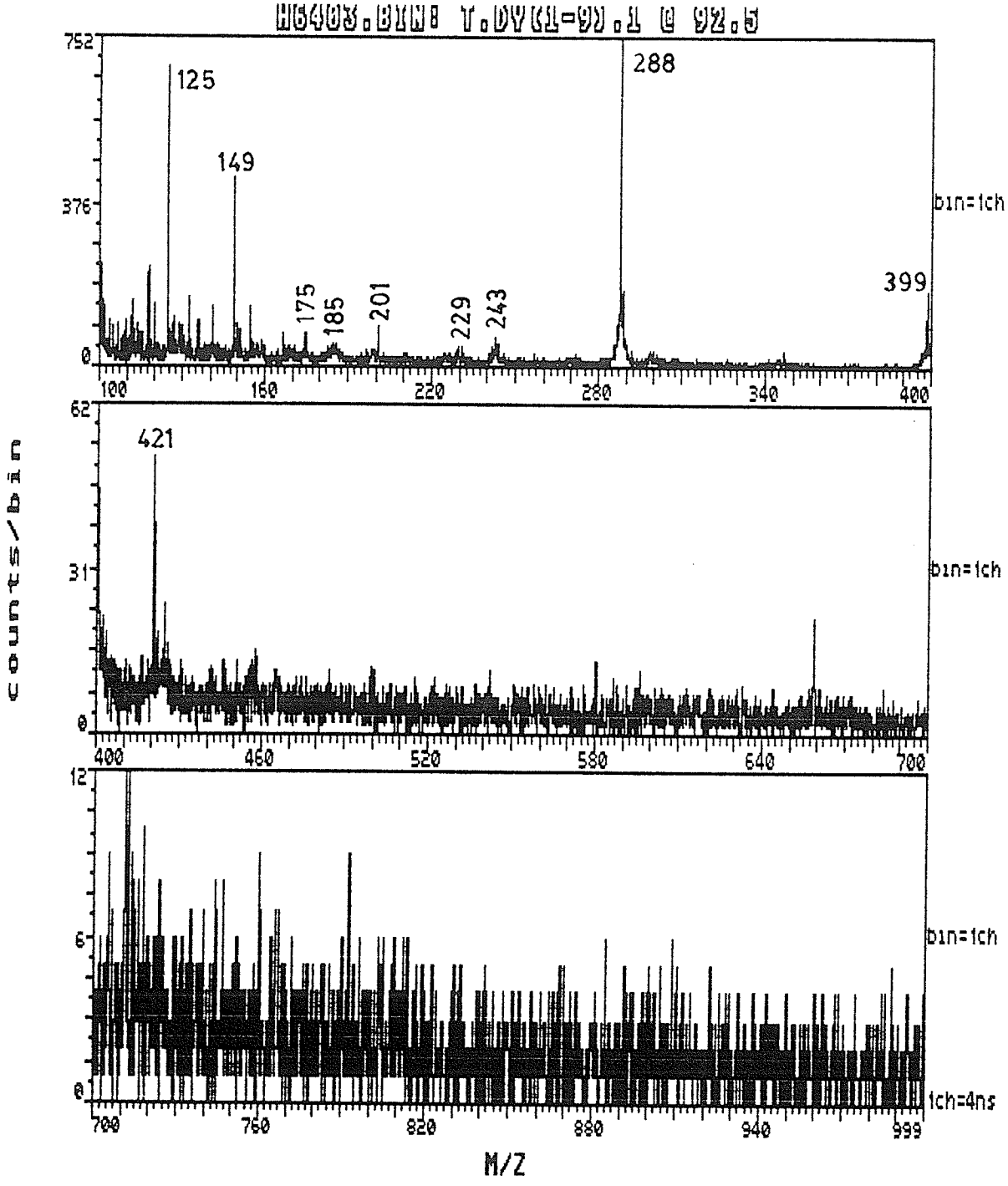
752
125
149
288
376
175
185
201
229
243
399
bin=1ch
100
160
220
280
340
400
62
421
31
bin=1ch
400
460
520
580
640
700
12
6
bin=1ch
1ch=4ns
700
760
820
880
940
999
M/Z
counts/bin

(b)

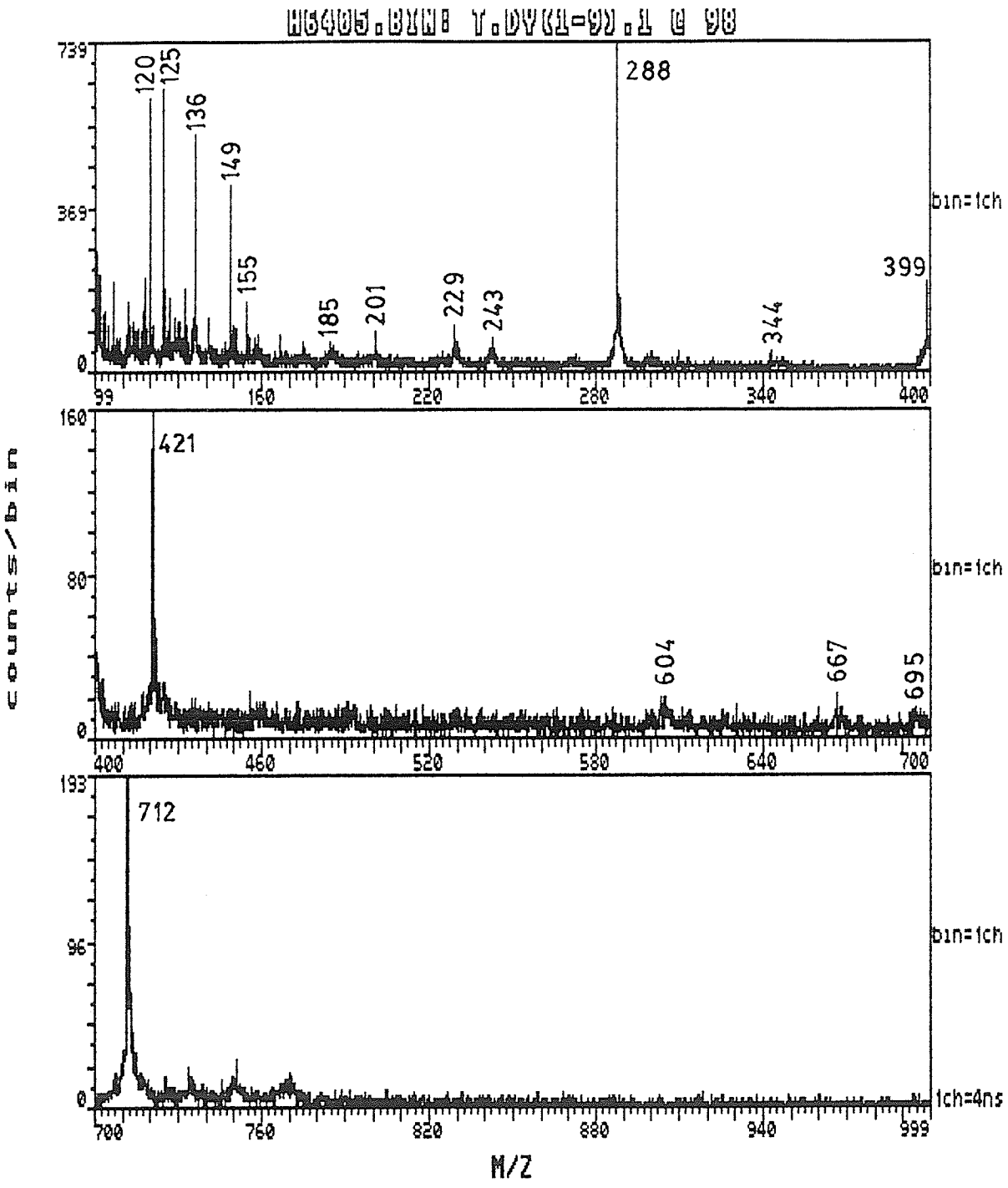
739
369
0
120
125
136
149
155
185
201
229
243
288
344
399
bin=1ch
99
160
220
280
340
400
160
80
0
421
604
667
695
bin=1ch
400
460
520
580
640
700
counts/bin
193
96
0
712
bin=1ch
1ch=4ns
700
760
820
880
940
999
M/Z

(c)

Table 4.6

The RF-type fragments and nominal masses, predicted for the peptide IR.

n	a.a	m(R)	A_n	B_n	C_n
1	I	57	86	114	129
2	R	100	242	-	-

n	a.a	m(R)	Z_n	Y_n	X_n
1	R	100	158	173	201

Table 4.7

The RF-type fragments and nominal masses, predicted for the peptide YGGFLR.

n	a.a	m(R)	A_n	B_n	C_n
1	Y	107	136	164	179
2	G	1	194	221	236
3	G	1	250	278	293
4	F	91	397	425	440
5	L	57	510	538	553
6	R	100	666	-	-

n	a.a	m(R)	Z_n	Y_n	X_n
1	R	100	158	173	201
2	L	57	271	286	314
3	F	91	418	433	461
4	G	1	475	490	518
5	G	1	532	547	575

The mass spectrum obtained from the third fraction in the second set of deposits is shown in Figure 4.33 (c). The observed ions indicate that there are two distinct quasimolecular species produced by the deposit: the hydrogen adduct ion of the dipeptide IR, m/z = 288 u; and the hydrogen adduct of the hexapeptide YGGFLR, m/z = 712 u. Therefore, these two peptides were not completely resolved by the column. The possible fragments for YGGFLR is given in Table 4.7. Unfortunately, only two fragment ions are unambiguously present: A_1 and B_6. Two other reasonably strong fragmentation pathways were the loss of the propyl group from the leucine sidechain $(M - 43)^+$, m/z = 668 u, and the loss of the tyrosine sidechain $(M - 107)^+$, m/z = 605 u. The lack of structural fragmentation in the molecule appears to be caused by the high degree of stability of the hydrogen adduct ion, implied by Figure 4.36. The same argument holds for this case as was already made in discussing Figure 4.31, i.e. the sharpness of the hydrogen adduct quasimolecular ion peak (and carbon-13 satellites) indicates that the ion is quite stable and is not expected to produce many fragments.

The mass spectra obtained from the dynorphin A (1-9) cleavage products are the least informative of the three examples. The presence of arginine in the digest indicated that there must be either a -Arg-Arg- or a -Lys-Arg- sequence in the peptide. The dipeptide could be sequenced. The only conclusions that were possible about the m/z = 712 u quasimolecular ion werethat it was due to a hexapeptide, probably with tyrosine as the N-terminus, containing phenylalanine in the structure (the m/z = 91 u and 120 u fragment ions characteristic of phenylalanine) and perhaps also containing a leucine or isoleucine

Figure 4.36

Hydrogen adduct quasimolecular ion region of the YGGFLR spectrum.

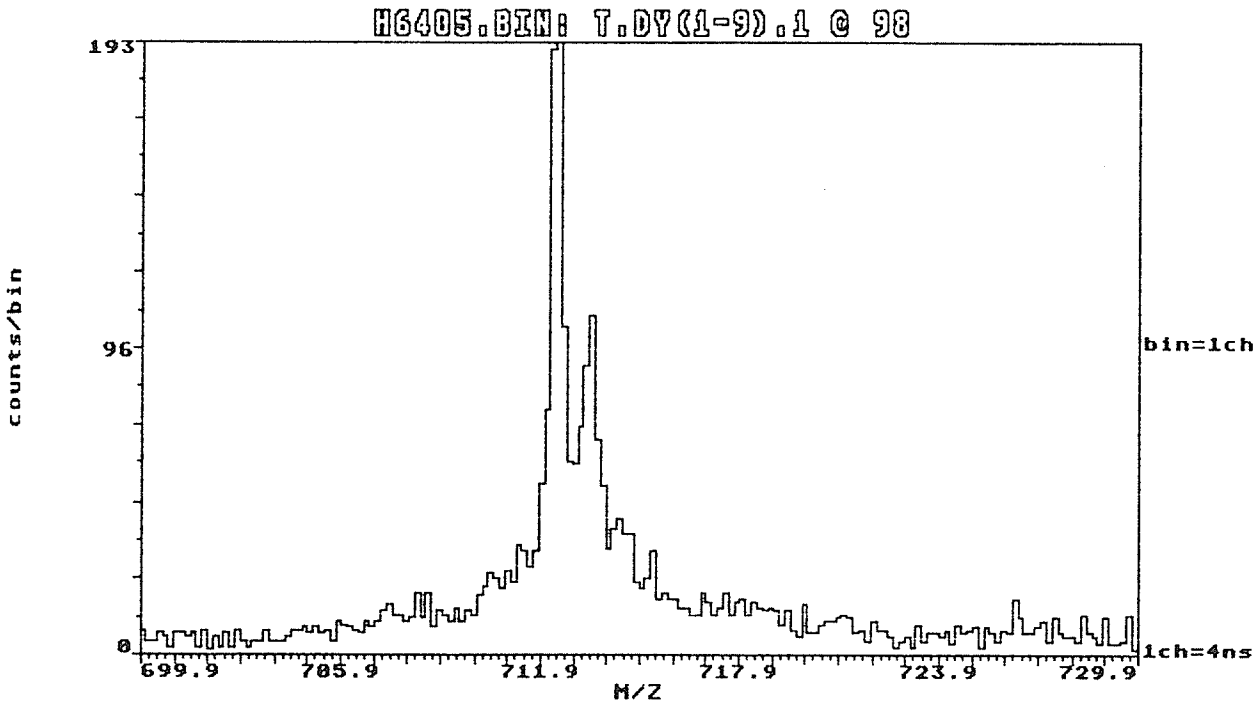
H6405.BIN: T.DY(1-9).1 @ 98
193
96
0
counts/bin
bin=1ch
1ch=4ns
699.9
705.9
711.9
717.9
723.9
729.9
M/Z

residue. While this information would clearly be helpful in confirming the structure of a peptide determined by other means, the information would not allow the sequencing of the peptide, even though it was cleaved into relatively small pieces.

4.8) LC-MS Results for Non-Peptide Samples

All of the results shown up until this point have dealt with the application of the LC-MS interface described in Chapter 3 to either amino acids or peptides. Peptides are not the only class of biologically interesting molecules that are amenable to the technique however. The majority of the time and effort taken in developing the LC-MS system was used to develop methods for dealing with peptides, but some testing was done to demonstrate the applicability of the methods to non-peptide samples.

One special case application was to improve the spectrum of a contaminated sample. Dr. Brian Chait, a colleague at Rockefeller University in New York, N.Y., sent our lab a sample of a fully protected heptapeptide; the suggested structure is shown in Figure 4.37, (m.w = 1531 u). Dr. Chait sent us the material because his PDMS time-of-flight instrument showed two separate families of quasimolecular ions that were interpreted as being due to two different molecules in the sample. The

Figure 4.37

Proposed structure of the fully protected oligopeptide referred to as "Peptide X".

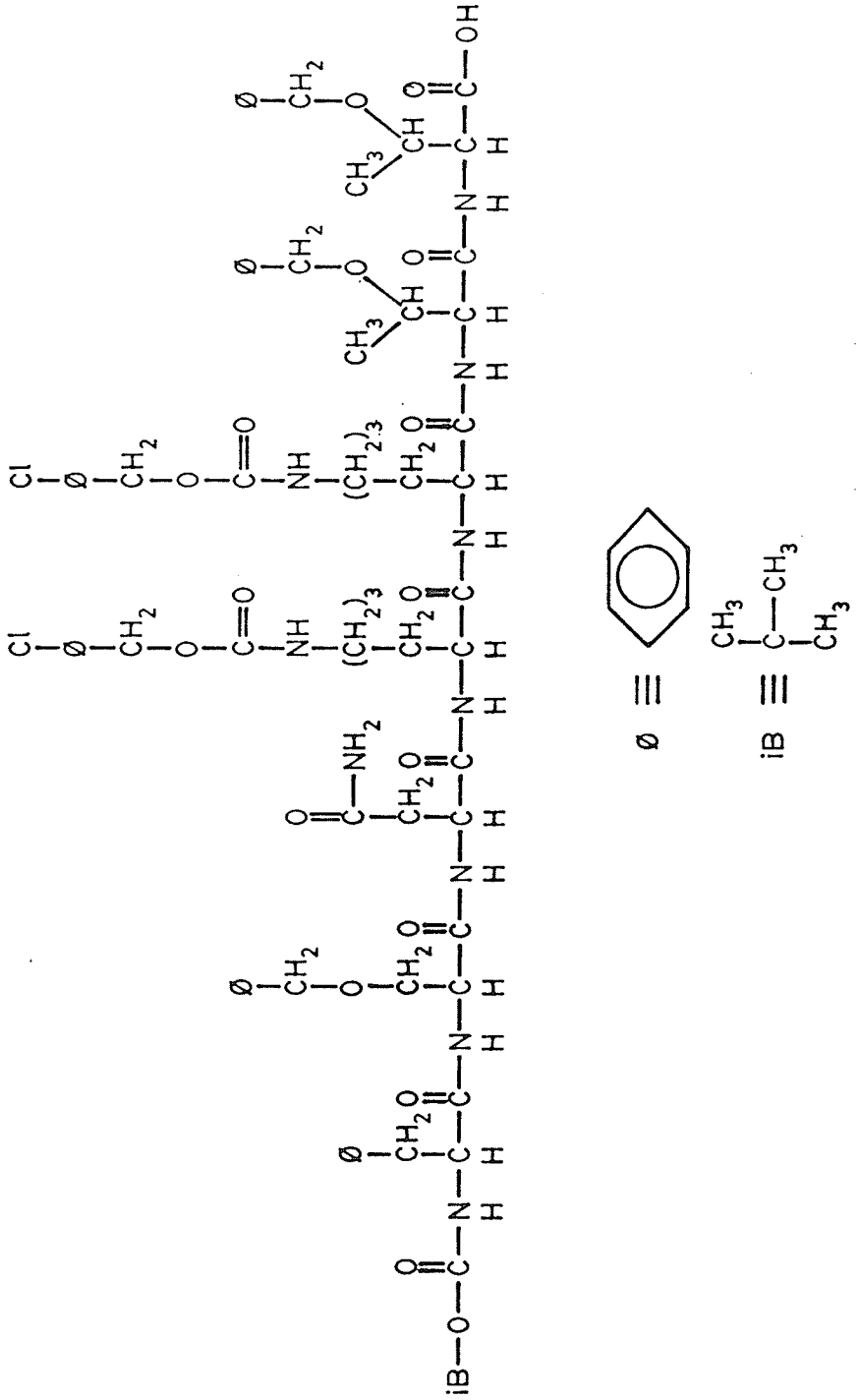

molecular ion region of Dr. Chait's spectrum is shown in Figure 4.38. The sample sent to us was mass analyzed using the Manitoba II secondary ion time-of-flight mass spectrometer and a portion of this spectrum is shown in Figure 4.39 (lower spectrum). The Manitoba II TOFSIMS instrument is equipped with an electrostatic ion mirror [99]. This type of ion mirror, if adjusted properly, increases the mass resolution of the spectrometer by removing the contribution to peak broadening caused by the secondary ion emission energy distribution to first order. Both Dr. Chait's spectrum and the spectrum produced by the Manitoba II instrument were made using electrosprayed samples of the material. Dr. Chait's sample was electrosprayed onto aluminum coated Mylar, while our first sample was sprayed onto a boehmite surface. In both cases, dimethylformamide was the electrospray solvent. Dimethylformamide was used because this compound would not dissolve in the more commonly used organic solvents. Due to the presence of quasimolecular ions in both spectra that did not correspond to the expected molecule, the additional dimensionality of HPLC analysis was applied to the problem. A 25 cm long, 0.5 mm i.d. column, packed with 3 μm octyl-coated silica was used. The mobile phase was 45:45:10 dimethylformamide:2-propanol:water, run at a flowrate of 3.00 μl/minute. Approximately 250 ng of the material (that we rather imaginatively dubbed Peptide X) was injected onto the column and the HPLC fractions collected on boehmite. Only one of the fractions appeared to contain a significant amount of material. The mass spectrum of that fraction is shown in Figure 4.39 (upper spectrum).

Comparing the three mass spectra (Figures 4.38 and 4.39), several

Figure 4.38

PDMS spectrum of "Peptide X" sample, prepared by electrospraying a solution using dimethylformamide as the solvent.

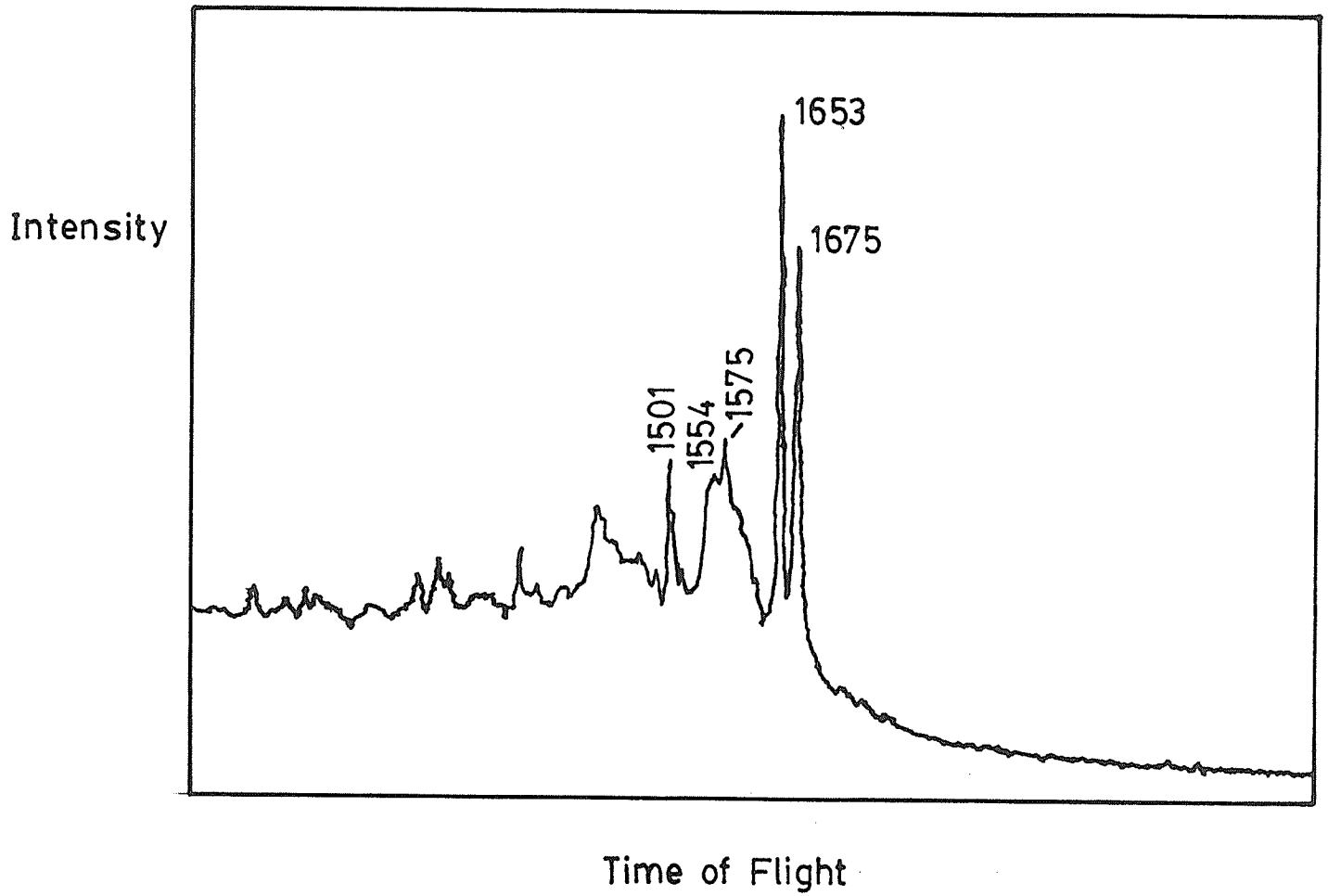
Intensity
1653
1675
1501
1554
1575
Time of Flight

Figure 4.39

SIMS spectra of "Peptide X" prepared in two different ways:

1) Fraction of HPLC run (described in text) sprayed onto boehmite (upper spectrum).

2) Electrospray from dimethylformamide solution onto boehmite (lower spectrum).

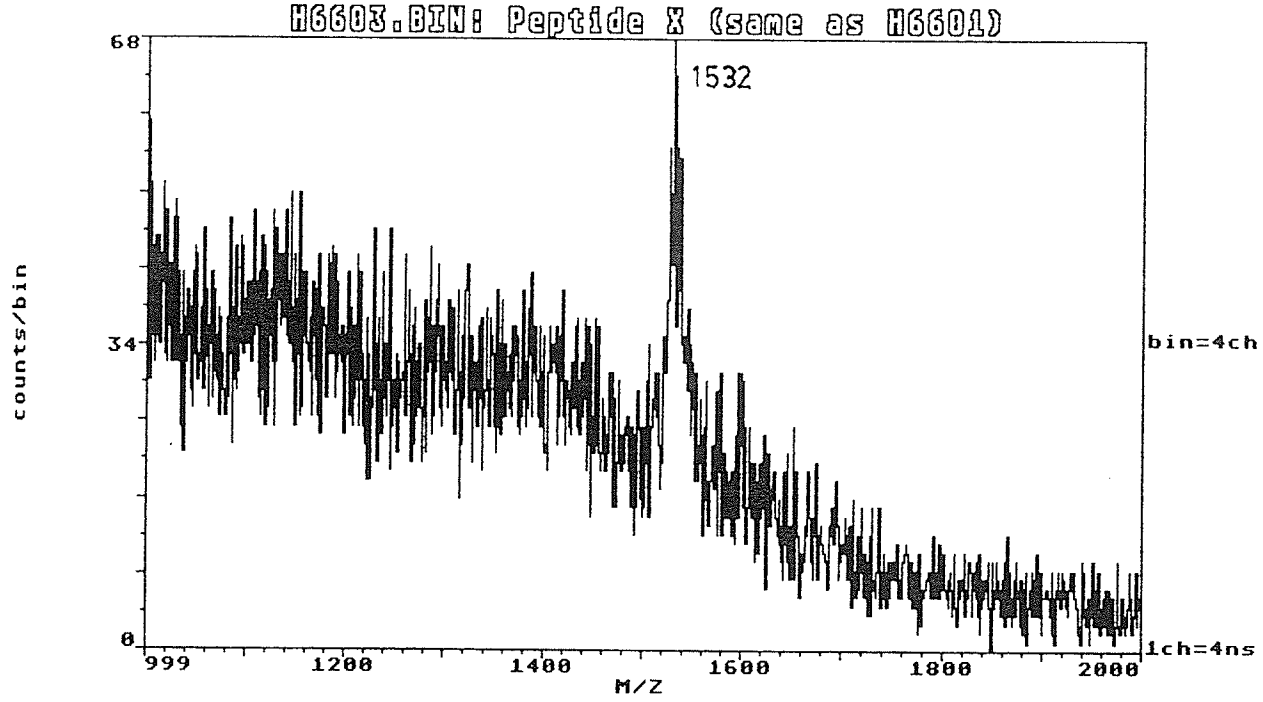
H6603.BIN: Peptide X (same as H6601)
68
34
0
counts/bin
1532
bin=4ch
1ch=4ns
999
1200
1400
1600
1800
2000
M/Z

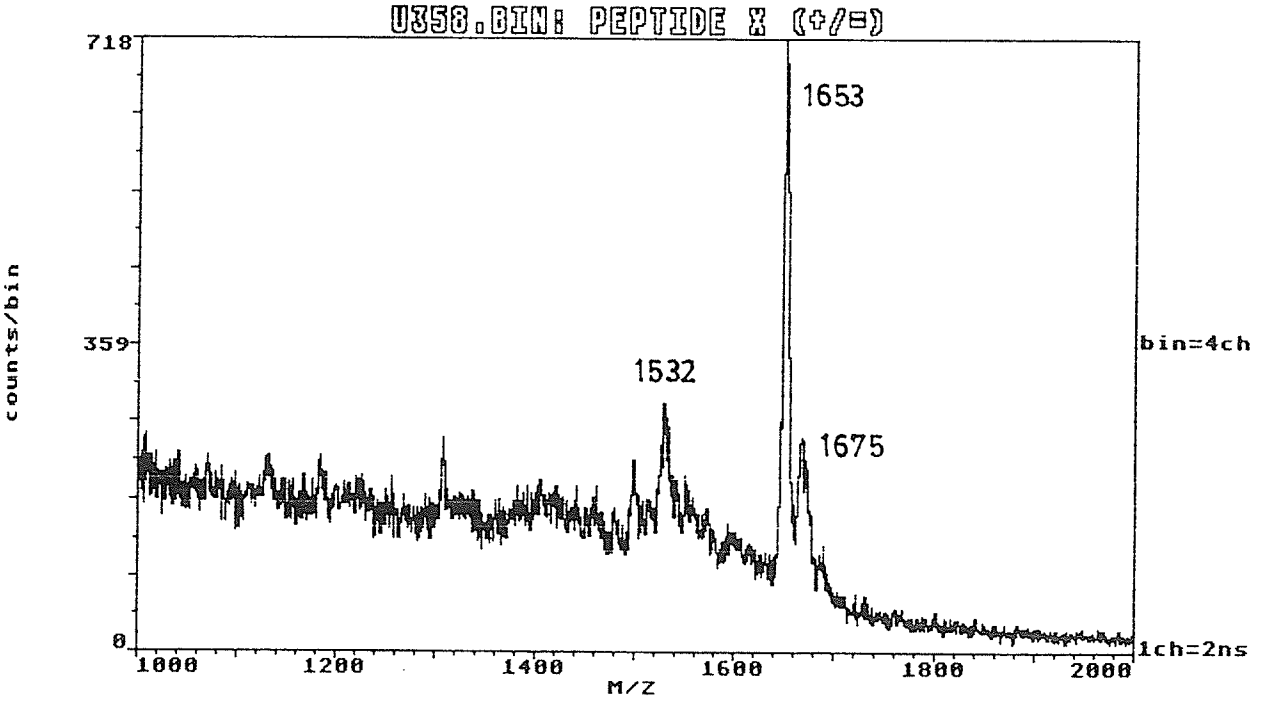
U358.BIN: PEPTIDE X (+/=)
718
359
0
counts/bin
1653
1532
1675
bin=4ch
1ch=2ns
1000
1200
1400
1600
1800
2000
M/Z

interesting features are apparent. In the PDMS spectrum, the putative hydrogen adduct quasimolecular ion was not observed. Sodium contamination made unambiguous mass determination of the molecular species difficult, although ions at m/z = 1554 u and m/z = 1575 u, consistent with sodium adducts (the mass determination of these two peaks is not very exact due to the broad metastable component). Also, there appeared to be another species in the sample, giving rise to ion peaks at m/z = 1653 u and m/z = 1675 u. The sample sprayed onto boehmite (Figure 4.39, lower spectrum) showed a somewhat different pattern. The hydrogen adduct quasimolecular species is present, m/z = 1532 u, and sodium adducts of this species are not present. However, the most intense quasimolecular ions are m/z = 1653 u and m/z = 1675. Therefore, it was assumed that there are at least two components in the sample, the material shown in Figure 4.37 and another compound, either with m = 1630 or m = 1652. There are two possible mass assignments for the second material because it is not clear whether the ion m/z = 1653 u is a hydrogen or sodium adduct. The spectrum shown in Figure 4.39 (upper spectrum) is the molecular ion region of the HPLC fraction containing a visible deposit described above. No spectra, other than background, were obtained from the other fractions. Comparing the upper and lower spectra, clearly the HPLC had removed the additional species at m/z = 1653 u and 1675 u. Only the hydrogen adduct quasimolecular species was present. Unfortunately, the sample appeared to become rapidly damaged by the primary beam; good spectra could only be obtained from the sample for 2 or 3 minutes before the quasimolecular ion yield began to decrease. Therefore, running the spectrum longer to improve the statistics in the high mass region was not possible. Similar behavior had been observed before for fully protected oligonucleotides

using much larger electrosprayed deposits (over 200 $\mu g/cm^2$). Even so, the HPLC results clearly demonstrated that the bulk of the sample was the expected material provided. The other compound, approximately 100 u higher in mass, was not observed by LC-MS and either:

1) was a very minor constituent of the sample that produced intense quasimolecular ions under SIMS analysis of those electrosprayed deposits far out of all proportion to its actual concentration and was present in such small amounts that it was unnoticed in the chromatogram;
2) was held up by the HPLC column for longer than the chromatogram of fractions was collected; or
3) was a SIMS artifact of the sample preparation method used.
4) Underwent chemical change (e.g. solvolysis) during chromatography.

The final class of compounds examined using the LC-MS apparatus was underivatized "involatile" steroid hormones [100]. Dr. F. LaBella (Department of Pharmacology, University of Manitoba) asked us to determine whether our methods could be applied to steroidal sex hormones (Note: The steroids analyzed below could also be examined using electron impact mass spectrometry.). To determine whether it was possible to use our type of LC-MS on these compounds, two common steroids were chosen: progesterone (m.w. = 314) and testosterone (m.w. = 288). The HPLC conditions were: 40:50 2-propanol:water + 0.01% TFA; flowrate = 3.00 µl/minute; and boehmite deposition surface. The spectra obtained from a fraction containing progesterone (0.5 µg injected) and a fraction containing testosterone (0.5 µg injected) are shown in Figure 4.40 (a) and (b). The molecular ion regions of these spectra are shown in Figure 4.41. Clearly, at this level of sample, the hydrogen adduct

Figure 4.40

Mass spectra, taken from HPLC fractions sprayed onto boehmite, of involatile steroid hormones:

a) Progesterone (0.5 µg on column).

b) Testosterone (0.5 µg on column).

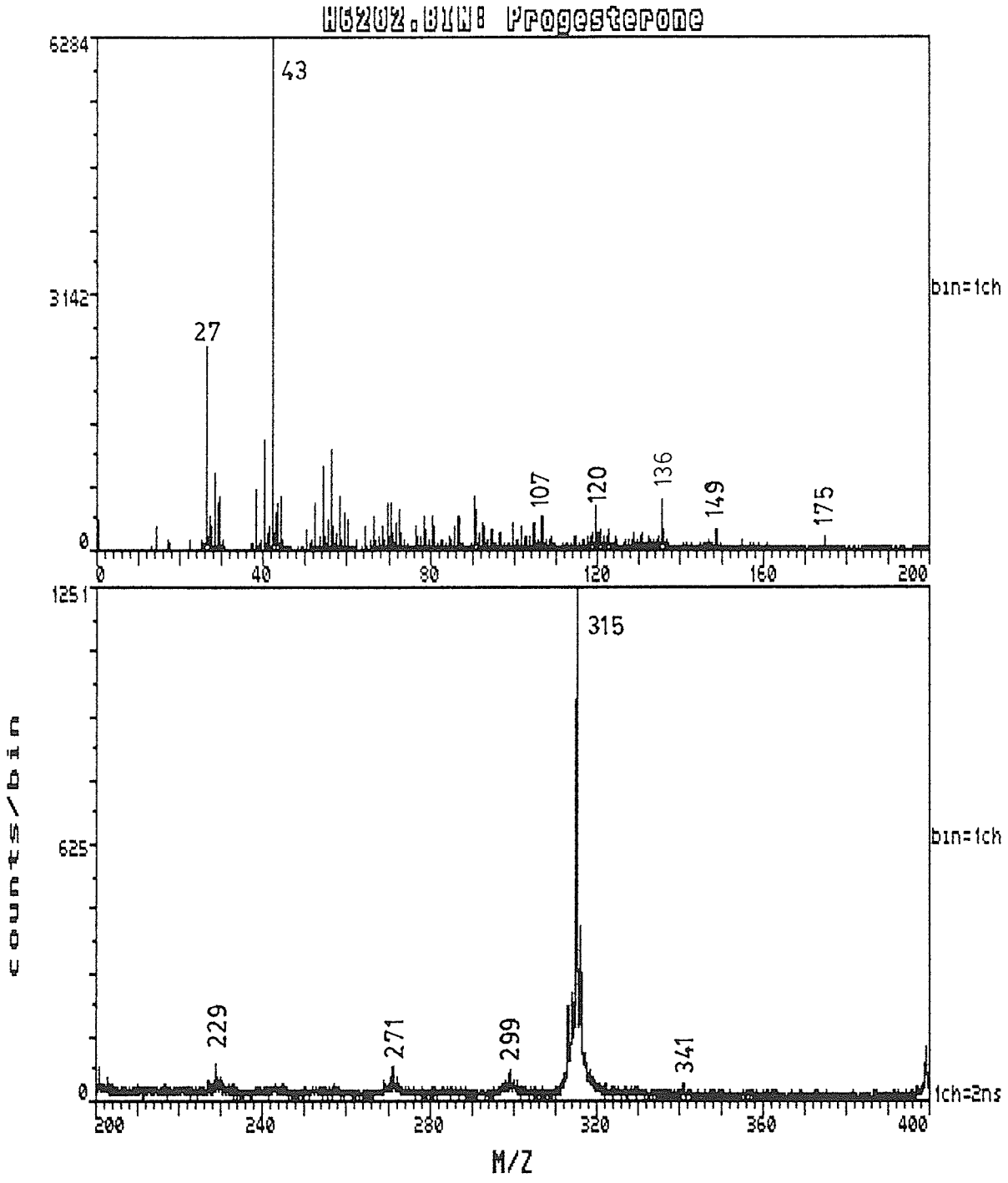
H6ZUZ.BIN: Progesterone
6284
3142
0
43
27
107
120
136
149
175
bin=1ch
0
40
80
120
160
200
1251
625
0
315
229
271
299
341
bin=1ch
1ch=2ns
200
240
280
320
360
400
M/Z
counts/bin

(a)

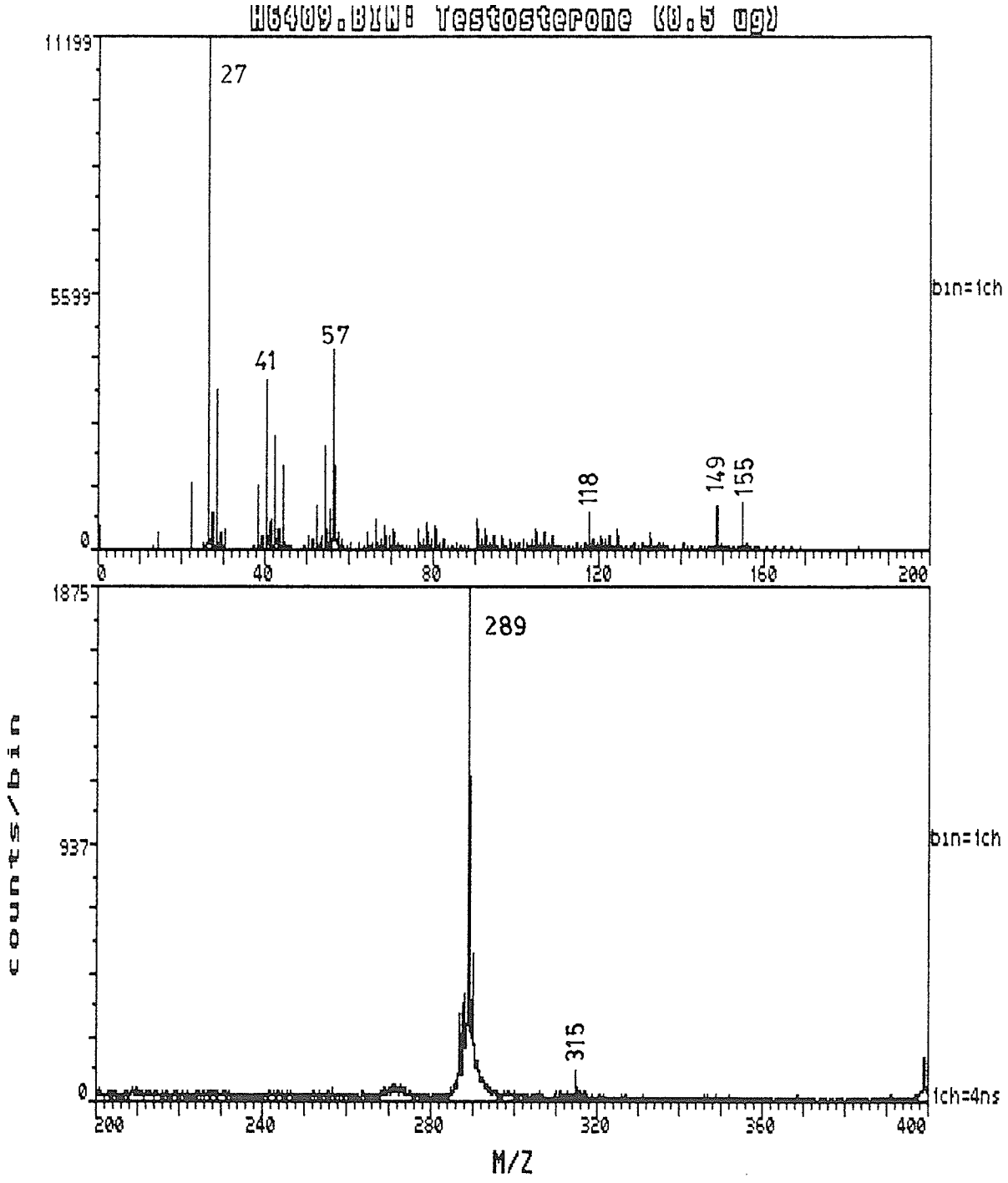
H6409.BIN: Testosterone (0.5 ug)
11199
5599
0
27
41
57
118
149
155
bin=1ch
0
40
80
120
160
200
1875
937
0
289
315
bin=1ch
1ch=4ns
200
240
280
320
360
400
M/Z
counts/bin

(b)

Figure 4.41

Comparison of the hydrogen adduct quasimolecular ion regions of the spectra of progesterone (upper spectrum) and testosterone (lower spectrum).

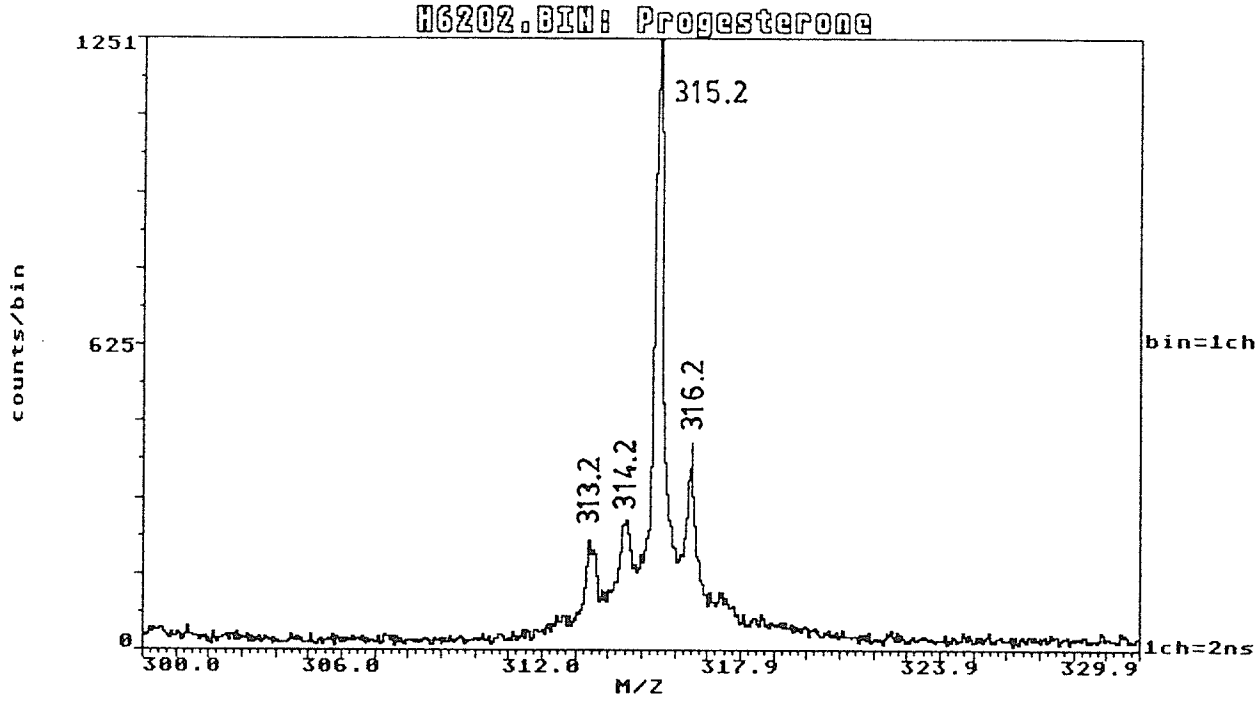
H6202.BIN: Progesterone
1251
625
0
counts/bin
315.2
316.2
313.2
314.2
bin=1ch
1ch=2ns
300.0
306.0
312.0
317.9
323.9
329.9
M/Z

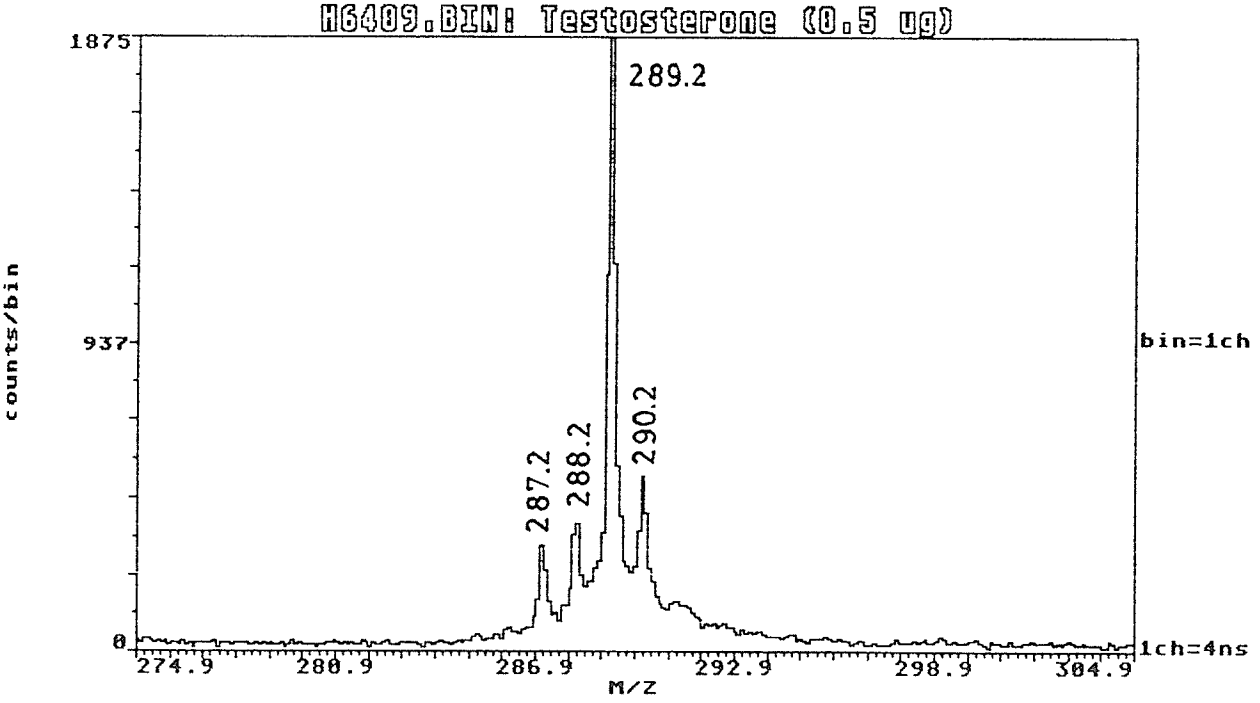
H6409.BIN: Testosterone (0.5 ug)
1875
937
0
counts/bin
289.2
290.2
288.2
287.2
bin=1ch
1ch=4ns
274.9
280.9
286.9
292.9
298.9
304.9
M/Z

Figure 4.42

Mass spectrum of progesterone (25 ng injected on column).

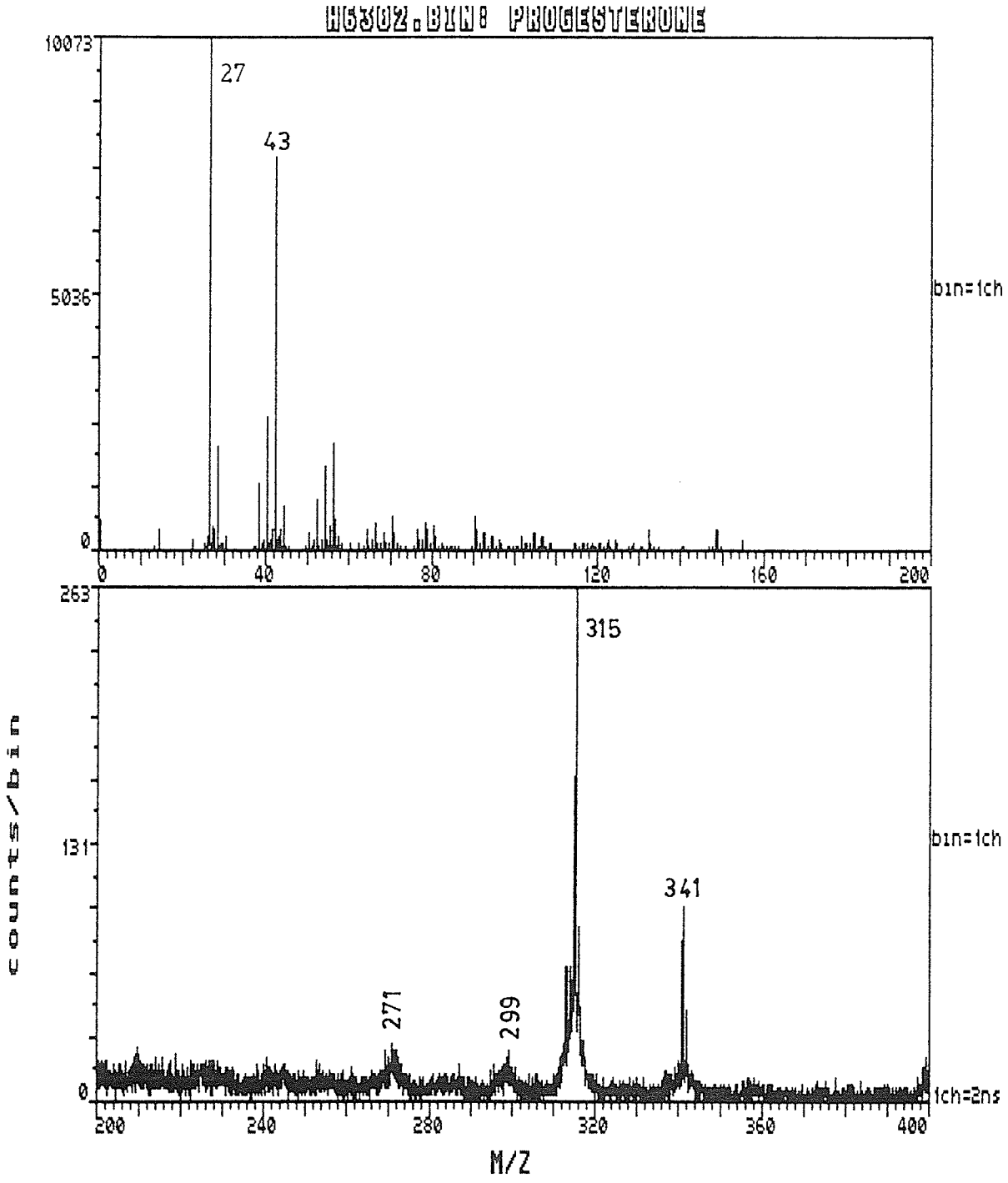
H5302.BIN: PROGESTERONE
10073
27
43
5036
0
0
40
80
120
160
200
bin=1ch
263
315
131
341
271
299
0
200
240
280
320
360
400
1ch=2ns
counts/bin
M/Z

quasimolecular ion is the dominant species, with few abundant fragments of lower mass. Figure 4.42 is the spectrum of fraction from a chromatogram with 25 ng of progesterone (injected on column). This spectrum demonstrates that the sensitivity of the method for determining the molecular weight of a steroid is very good. Also, if the signal-to-noise ratios of the 500 ng and 25 ng samples are compared (i.e. the ratio of the hydrogen adduct ion peak integral to an integral of the same number of channels in the nearby background), the ratio is unchanged. The quasimolecular ions m/z = 341 u (Figure 4.41 (a) and 4.42, progesterone) and m/z = 315 u (Figure 4.41 (b), testosterone) are $(M + 27)^+$ ions and are tentatively assigned to aluminum adduct ions. This assignment is unusual; it would be the first case of an aluminum adduct organic ion in our experience. However, the mass determination of the ions was not reliable enough to make the assignment as aluminum adducts a certainty.

CHAPTER V

Final Discussions and Conclusions

5.1) General Comments

The thesis so far has been broken up into four chapters. Chapter I discussed what had been done in the field of liquid chromatography coupled with mass spectrometry. Chapter II gave the general outline of our plan of research and gave theoretical reasons why this approach was favoured for our particular instrumental requirements. Chapter III dealt with the practical description of the final version of the off-line liquid chromatograph-mass spectrometer interface that was used. Chapter IV dealt with the actual development of the system, starting from initial, rudimentary results and progressing to the interpretation of spectra obtained from HPLC separated peptide mixtures in an effort to sequence the peptides involved. This chapter (Chapter V) attempts to draw the stated goals of the research and the actual results of the research together: to show if the method of LC-MS coupling chosen is practical and if it could produce results that could not be obtained from other, simpler methods.

The approach to evaluating the results of the research was to view the HPLC system as a method of sample preparation for the time-of-flight SIMS instrument. Another equally valid viewpoint would be to consider the time-of-flight SIMS instrument as a detector for the HPLC. So why choose one

over the other? First, in order for the results to be interpreted in an orderly and logical manner, some viewpoint must be selected as a benchmark from which to view the information. Second, the laboratory in which the research was carried out was interested mainly in developing techniques involving static SIMS analysis. Therefore, it would be natural for the automated sample preparation method afforded by the HPLC apparatus to be viewed as just that, an automated sample preparation method.

Applying the eluent deposition apparatus, as a sample preparation method, made it possible to remove one of the major drawbacks of applying the electrospray deposition technique to solid phase SIMS: the variability of results. The spraying of solutions from syringe needles led to deposits that might show high sodium contamination (or not) or high organic contaminant levels (or not) or high quasimolecular ion yields (or not). It was not possible to predict whether a deposit would produce good SIMS spectra or not, even if the sample in question had been analyzed before. The high degree of parameter control available with the HPLC eluent deposition apparatus made the preparation of reproducible samples possible. A good example of this additional parameter control is the flowrate of the spraying solvent. Sections 4.2 and 4.6 clearly demonstrate that the solution flowrate is a critical factor in whether a deposit had a reasonable secondary ion yield. However, in the method normally used for electrospray, regulation of the flowrate is difficult and the flowrate actually changes during deposition; the flow is fastest when the canula is full and slows down as the spraying progress continues (i.e. as the solution's pressure head in the canula decreases). A controlled, well regulated flow, with a well defined amount of sample injected onto the column (the injection volume was always either 1.0 ul or 0.5 ul with a very low variance) made it possible to study the effect

of flowrate on the deposition technique and thereby demonstrate the importance of this parameter. This controlled flow also made it possible to develop a better substrate for electrospray: boehmite. Without the assurance that samples could be sprayed reproducibly, and without the ability to spray samples containing high water concentrations, determining whether an individual substrate was better or worse than another would have been very tedious, because the effect of variable electrospraying parameters could not have been separated from the effects caused by the substrate. Attempts made by several other individuals in our laboratory to demonstrate substrate effects on electrosprayed deposits using the normal needle apparatus were unsuccessful, probably for just this reason.

Another example of the ability to control sample preparation, with the LC-MS system developed, highlighted the added dimension of separation: the removal of unpredictable sample contaminants. A fact that became evident to us when initially applying solid phase SIMS to organic samples was that most samples contained impurities, including those purchased from commercial houses. The sensitivity of solid phase SIMS to impurities has been frequently mentioned above. These impurities, while minor with respect to the sample concentration, were variable from received sample to sample and could be present to such an extent that the sample of interest was not discernible in the mass spectrum. The example in Section 4.8 of a fully protected oligopeptide demonstrates the ability of the HPLC system to separate a molecule of interest from impurities present in the refined form presented to the laboratory for analysis. The spectra presented in Section 4.6, 4.7 and 4.8 demonstrate that only a few impurities were present on the substrate and in the eluent deposit, the most prominent of which was due to a

molecule giving an ion at m/z = 398 u. The introduction of boehmite substrates greatly decreased the importance of alkali metal cation contamination. Therefore, if an impurity is present in the mass spectrum, such as the very high sodium adduct peak present in Figure 4.30 (a), some property of the sample molecule must be causing the impurity to be prominent. The case of the molecule in Figure 4.30 (a) is discussed in detail below.

5.2) Application to Peptide Mixtures

The main goal of the research was to add the ability to separate peptides to our ability to analyze them with time-of-flight SIMS. The results given in Chapter IV support the contention that this goal was achieved using the interface developed. The automated nature of the fraction collection system allowed dozens of fractions to be collected without the supervision of the experimenter. The same deposits could have been prepared from fractions collected in the conventional way from a conventional sized column, but the tedious nature of producing thirty or forty electrospray deposits (without loss of sample) would have made the procedure difficult enough that it would rarely be applied.

A feature of the spectra produced using the final system was the presence of a hydrogen adduct quasimolecular ion in all cases. Many other spectra were recorded (other than those given in this thesis) and the presence of hydrogen adduct ion was indeed common to all of these for amino acids and oligopeptides up to intact alpha-endorphin. The reliable appearance of the hydrogen adduct ion is important, for without it the

unambiguous determination of the molecular weight of the peptide by SIMS is not always possible. If only alkali metal adduct quasimolecular ions are present, as was the case for the peptide spectra obtained before the introduction of boehmite substrates, it would be inferred that the lowest mass quasimolecular ion was a sodium adduct ion. The example of proenkephalin (Figure 4.13) demonstrates that this is not necessarily the case.

The presence of the quasimolecular ions allowed the determination of the mass of the peptide molecules in question, but what additional information is present in the peptide spectra? As was mentioned in Chapter IV, while the exact mass determination of a peptide may allow the experimenter to infer the amino acids present in the molecule (with the exception of distinguishing between isoleucine and leucine residues), it does not give any indication of the order of the residues in the peptide, something that may be more important than the precise determination of the abundance of each type of amino acid residue present in the molecule. Another way to state this is that with only the abundance and identity of amino acid residues known for a decapeptide, the field of possible structures would be narrowed to 10! = 3,628,800 possible peptides (or 7,257,600 if only one isoleucine/leucine residue is present). Clearly, even for small peptides, more information about the molecule must be determined in order for the experimenter to provide a useful characterization of the molecule to other scientists interested in it.

The extra information in the case of SIMS/FAB mass spectra is the fragmentation of the intact molecule into smaller daughter fragment ions. The presence of fragment ions is not sufficient, however. The fragmentation of the parent molecule has to follow a sensible scheme (preferably one that has been previously observed) so that the residue sequence may be inferred

from this fragmentation pattern. The Roepstorff-Folmann (RF) scheme [87] (see Figure 4.28) attempts to do just that, giving a basic nomenclature for single bond-breaking fragmentation along the amide linkage backbone. Fragmentation along these lines has been reported by several groups using FAB [101, 102, 103], although complete sequencing of peptides using single stage mass spectrometers seems to be the exception rather than the rule [104]. Our group's work on oligopeptides [86] has demonstrated that using relatively large amounts of sample, approximately 100 μg, small peptides yield fragments that can be fitted into the RF scheme, with additional fragmentations caused by the loss of favoured portions of amino acid residue sidechains.

The results set out in Section 4.7 demonstrate that much smaller quantities of peptide can be used to produce a significant number of structurally related fragments. As little as 100 ng of a peptide produced fragment ions of sufficient intensity to determine at least a partial peptide structure. Unfortunately, this was not the case for all peptides. Primary ion bombardment of some molecules produced quasimolecular ions so stable that they did not undergo significant fragmentation.

Several observations about the fragmentation of molecules in solid phase static SIMS can be made with reference to the results in Section 4.7. First, as mentioned above, not all peptides fragmented. The prevailing wisdom in the field of particle induced desorption of peptide ions has been that the stability of peptide quasimolecular ions should increase as the size of the molecule increases. The reason for the increase in stability is that for larger molecules, there would be more degrees of freedom associated with molecular vibrations, allowing the initial vibrational energy deposited in the molecule during desorption to partition into a large number of degrees of

freedom. Therefore, assuming that any peptide being desorbed receives approximately the same amount of vibrational energy in the desorption process (a process as yet undefined), larger peptides should have the same amount of energy spread out over more bonds, leading to less energetic individual bond vibrations and therefore a lower probability of fragmentation.

The results displayed in Figure 4.31 indicate that other factors also influence a peptide's stability. The smaller molecule (SQTPLVT) was far less stable than the larger molecule (YGGFMTSEK). What appeared to be far more important in determining the stability of a peptide hydrogen adduct quasimolecular ion was the amino acid sequence of the peptide. Any of the peptides examined that had a C-terminal basic amino acid residue (arginine or lysine) produced very stable hydrogen adduct quasimolecular ions and also had a very low tendency to form sodium adduct quasimolecular ions.

The importance of the actual amino acid sequence in determining fragmentation pathways is nicely demonstrated by the spectra selected for Section 4.7. Of the six peptide spectra shown, only one could be directly sequenced by single bond breaking fragments of the type given by the RF scheme. The molecule that displayed RF type fragmentation, Arg-Pro-Tyr-Ile-Leu (RPYIL), showed only A-type fragments (breaking the alpha C-C bond) with the charge retained on the N-terminus containing fragment. In addition to the single bond breaking fragments, two important fragment ions appear caused by a further bond breaking in the side chain. These are the $(A_5 - 42)^+$ ion, caused by the loss of the terminal isopropyl group from the leucine side chain and the $(A_4 - 28)^+$ ion, caused by the loss of the terminal ethyl group from the isoleucine sidechain. This additional fragmentation pathway made it possible to distinguish between isoleucine and

leucine in the sequence, something not possible from the mass of RF-type fragments alone. The intensity of the fragment ions decreased as the mass of the fragment increased, but all the fragments were observed for this pentapeptide.

The other molecule that could be completely sequenced from the fragmentation pattern, Ser-Gln-Thr-Pro-Leu-Val-Thr (SQTPLVT), had some fragmentation corresponding to the RF scheme, but the dominant set of fragment ions that allowed sequencing was produced by the attachment of a sodium ion followed by two bond breakings. The C-tilde fragmentation pattern was assumed to be caused by the loss of formamide from the end of the glutamine side chain of a C-type fragment with sodium addition to the N-terminal portion. All of the expected fragments of this type were observed, and the intensity of the fragment ions did not diminish to any obvious extent as the mass of the fragment increased (remember that the intensity of the fragment ions decreased for RPYIL). The sodium ion must have added to the molecule near the N-terminal end (complexed between the polar Ser^1 and Gln^2 side chain?) because it was retained in all the fragments up to the glutamine residue. The high abundance of sodiated ions in the spectrum of SQTPLVT was particularly interesting in itself. With the introduction of boehmite substrates, the presence of abundant sodium adduct ions had been effectively suppressed, presumably for the reasons dealt with in Section 4.6. So why, in this case, were the sodium adduct quasimolecular ion and sodiated fragment ions the dominant species? The simplest explanation, an error in the initial experiment, was ruled out because the spectrum in Figure 4.30 (a) was easily reproducible. The elution time of the molecule was k' = 4.2, so any sodium in the original sample should have been removed by the

HPLC volume (the sodium eluting near the void volume), eliminating the explanation of initial sodium contamination. The fact that the other enzymatic cleavage product of alpha-endorphin did not show large amounts of sodium addition also suggested that contamination of the eluent in the HPLC runs of alpha-endorphin cleavage products was not the explanation. The only explanation that fits the facts is that the particular sequence of amino acids in SQTPLVT is the cause of the high level of sodium contamination. The sodium must have been chelated to the peptide molecule and carried down the HPLC column, attached to the molecule. This strong bonding between the peptide and the sodium ion was probably due to a site, or sites, at or near the N-terminal end of the molecule, probably involving the Ser^1 and Gln^2 residue sidechains (which contain polar oxygen functions). The well-controlled nature of the sample deposition method and the ability to compare samples reproducibly prepared in the same manner make it possible to make these statements about sodium chelation. Similar conclusions would have been difficult to support using the typical method of electrospray deposition because of a lack of reproducibility and the inability of the method to separate a sample from its initial contaminants.

The idea of a sodium ion being bound to a peptide molecule via coordination to polar oxygen functions is not new, however. Our laboratory has demonstrated several times, using different time-of-flight methods, that the sodium of the sodium adduct quasimolecular ions can be bound to the peptide backbone or to sidechains, rather than to either the C- or N-terminal ends [105]. Additionally, recent measurements using the Manitoba II instrument, made by Francois Lafortune, indicate that a sodium ion is coordinated between three oxygen atoms in some substituted alkylthymidines [106]. Therefore, the existence of specific coordination sites for sodium

addition to a peptide is not a novel observation, but the apparently strong binding of sodium to these sites in competition with a polar solvent is. It implies that HPLC alone will not be, in general, a completely reliable method of separating peptides from contaminating alkali metal cations, because these cations bind strongly to some types of peptides and can be carried down the HPLC column complexed to the peptide molecule.

Another peptide that produces a reasonable number of sequence ions is pyro-Glu-Leu-Tyr-Glu-Asn-Lys-Pro-Arg (pELYENKPR). The RF-type fragments are X_1, X_2 and Y_2', fragments where the charge is retained by the C-terminal fragment, as mentioned in Section 4.7. The best sequence information was gained from another non-RF-type fragmentation pathway, that yielded W-type fragments. This fragmentation pathway is also a two bond breaking type: first a Z-type fragmentation followed by a breakage at the beta-gamma carbon-carbon bond. Again, the actual sequence of amino acid residues has a large influence on the type of fragmentation pathway followed. The pyroglutamic acid residue on the N-terminal end and the two possible sites for hydrogen attachment at or near the C-terminus (Lys^6 and Arg^8) altered which end of the fragment retains the charge. Also, these W-type fragments decreased in intensity rapidly as the mass of the fragment increases.

Some peptides produced sequence information from their fragmentation pattern, but other peptides did not. Examples of peptides that did not show much fragmentation are: Tyr-Gly-Gly-Phe-Met-Thr-Ser-Glu-Lys (YGGFMTSEK); Tyr-Gly-Gly-Phe-Met-Arg- Gly-Leu (YGGFMRGL); and Tyr-Gly-Gly-Phe-Leu-Arg (YGGFLR). The quasimolecular hydrogen adduct ions of these molecules show that the cations are particularly stable; there is only a minor contribution to the molecular ion peak from metastable unimolecular decay broadening.

There are some obvious similarities about these molecules:

a) all three contain the sequence Tyr-Gly-Gly-Phe;

b) all three contain a basic amino acid residue;

c) the majority of the residues are, at most, weakly polar;

d) the quasimolecular ion region is dominated by the hydrogen adduct cation and only a minor component due to a sodium adduct.

Unfortunately, without many more observations of similar substituted analogs of these molecules, it would not be valid to assign one or more of these similarities as a cause of the lack of fragmentation. However, the lack of fragmentation for these molecules has some very interesting theoretical implications. Assuming that all peptide bonds are created equal (from an energetic standpoint), the lack of fragment ions in the mass spectrum in the field free flight region of the mass spectrometer must imply that these molecules are emitted from the surface with less electronic and/or vibrational energy than the molecules that underwent substantial fragmentation. Therefore, the desorption process, with respect to the amount of energy deposited into the electronic and vibrational modes of the molecule, must depend on the amino acid residue structure of the peptide involved. The size of the peptide does not seem to be the most important variable in the promotion of fragmentation. The modification of leucine enkephalin to $(Arg)^6$-leucine enkephalin was sufficient to suppress fragmentation and produce a very stable hydrogen adduct quasimolecular ion.

These observations on peptide fragmentation have important implications for the use of our LC-MS system and, in general, solid phase SIMS for the sequencing of peptides. The peptides that produced a complete (or nearly complete) family of structurally significant fragments produced only one such family of fragments. It was not necessary to deconvolute the six families of

RF-type fragments possible. The fragmentation pathway that produced structural information could be due to fission of either one or two bond types; i.e. one of the bonds in the peptide backbone of the molecule. The actual pattern of bond fission exhibited was very dependent on the amino acid residue sequence of the peptide. Sufficient data to determine, a priori, which fragmentation pathway would dominate are not available. The second bond fission (if present) is in the sidechains of the peptide, resulting in ions characteristic of the main fragmentation pattern less a favoured side chain group of the residue proximal to the RF fragmentation (e.g. loss of an isopropyl group from the leucine side chain, or the loss of an ethyl group for isoleucine). This may help in the identification of the residue. The fragment favoured to retain the positive charge contains the N-terminus, but this pattern could be altered so that the charge was retained on the C-terminus containing fragment by modification of the amine group of the N-terminal residue. While some peptides were desorbed with sufficient internal energy to break two bonds, there appeared to be a class of peptides that were desorbed with little internal energy, leading to very little fragmentation. These molecules could not be sequenced by solid phase SIMS, using sample deposits prepared in this way.

These conclusions support the validity of our approach to LC-MS. Small quantities of peptide were detectable with the system and many of these peptides could be sequenced at least partially using no other information than the SIMS spectra. The separation dimensionality of the HPLC made it possible to separate and analyze mixtures of peptides. This separation was important. An unexpected pattern of fragmentation, such as shown in Figure

4.30 (a) or 4.33 (b), could not have been unambiguously assigned if more than one quasimolecular ion had been present. Trypsin digestion seemed to be a profitable method of making smaller peptide cleavage products that were more amenable to SIMS fragmentation sequencing.

5.3) Application to Other Classes of Involatile Compounds

The number of non-peptide molecules studied was small. The fully protected oligopeptide sample, separated with a dimethylformamide: 2-propanol:water mobile phase, gave a hydrogen adduct quasimolecular ion using our system, while it gave strong, multiple sodium adduct ions and an unexplained species when the sample was prepared using normal electrospray procedures (sprayed from neat dimethylformamide). This example demonstrated the usefulness of the system in "cleaning up" purified real-world samples.

The preliminary results using involatile steroid hormones showed a great deal of promise. The advantage of using our system over GC-MS would be that for GC-MS, some of these steroids must be derivatized to be put into the gas phase, while in our technique no derivatization is necessary. The other side of this argument would be that the LC-MS would not detect volatile samples - volatile in the sense that the sample would evaporate after 30-60 minutes in a good vacuum.

5.4) Concluding Remarks (Personal and Otherwise)

The work outlined in this thesis took about six years to complete, from

the spring of 1981 to the spring of 1987. The work involving the use of boehmite substrates was all performed between the summer of 1986 and the spring of 1987; boehmite was found (after a determined search) to be useful in the summer of 1986. The pattern of research was laid out in the thesis in very much the same way as it was conducted, although in several cases the order was rearranged to make a more logical progression for literary purposes and several of the lines of research were carried on simultaneously, for example: improvements in the HPLC system and the development of an improved substrate were performed concurrently.

The development of the boehmite substrate was a personal watershed in the research. Without boehmite's property of reducing the effect of the sodium contamination problem, only spectra of poor quality could be obtained, containing dominant sodium adduct ions and very little, if any, structurally significant fragmentation. A system that only produced such spectra could hardly be considered a successful method for peptide analysis. The simplicity and low cost of the substrate material allowed it to be used without regard to how much of the material was used.

The work that has been done with the LC-MS system opened up several interesting possibilities for further research. More work should be done on the effect of the addition of an N-terminal pyroglutamic acid residue to peptides to determine whether this modification of the N-terminal amino group always changes the charge bearing fragment to the C-terminal fragment, rather than the N-terminal fragment. In general, more work should be done to discover what rules determine the effect of amino acid residue sequence on:

1) the main fragmentation pattern;

2) the retention of alkali metal cations on the molecule;

3) the stability of the quasimolecular hydrogen adduct ion.

Also, it would be interesting to know if samples that produce a stable hydrogen adduct ion (i.e. the quasimolecular ion peak shows little metastable broadening) always have few fragment ions in the spectra. The metastable fragmentation pattern of peptides is currently under examination by our group using the MS-MS capabilities of Manitoba II. The comparison of the metastable decay pattern and the fragmentation pattern in the ordinary time-of-flight spectrum could determine whether the fragmentation mechanism in both cases was the same.

Appendix A

Point by point instructions for our most successful method of packing microbore HPLC columns (See Section 3.3 for additional information).

1) Cut the column blank to length.

2) Wash the column blank with hexane, acetone and water to remove any machining oil left in the bore.

3) Swage on the ferrules and bushings for the inlet and outlet ends. Attach the endfitting.

   Note: The ferrule and bushing used must match the fitting they are attached to. eg. a Rheodyne ferrule and bushing must be used to attach the column blank to the Rheodyne injection valve.

4) Fill the column blank-endfitting assembly with methanol.

5) Measure out the appropriate amount of column packing material (roughly 2.5 milligrams per microliter of column blank to be filled) and place the packing material in a small, screw top bottle.

   Example: For a 15 cm length of 0.020" (0.5mm) i.d. column blank, the column volume was approximately 30 microliters, therefore use approximately 75 milligrams of packing.

6) Add 1 milliliter of 2-propanol to the packing material and shake for at least 5 minutes. If possible, place the container in an ultrasonic bath for five minutes.

7) Attach the column blank-endfitting assembly to the reservoir.

8) Charge the Haskel pump with 20 milliliters of methanol and run at least 10 milliliters of methanol through the pump to remove air bubbles in the system.

9) With the packing well suspended, remove the slurry from the bottle using a syringe with a long (4 cm) wide gauge (20 gauge) needle. Make sure that the needle, syringe barrel and syringe plunger have been carefully washed to remove any of the lubricating grease normally present.

10) Inject the slurry into the reservoir.

11) Attach the slurry reservoir-column blank-endfitting assembly to the pump.

12) Slowly increase the gas pressure to the pump until the maximum pressure (80 p.s.i. gas pressure = 10,000 p.s.i. (70 MPa) fluid pressure) has been reached. The rate of solvent flow should decrease as the column packs.

13) Flow 10 milliliters of methanol through the column.

14) Change the solvent to 1:1 chloroform:methanol and flow 10 milliliters through.

15) Change the solvent to methanol and flow 10 milliliters through.

16) Change the solvent to 1:1 methanol:water and flow 10 milliliters through.

17) Change solvent to water and flow 5 milliliters through.

18) Turn off the gas pressure and allow the pressure to slowly drop to zero, i.e. until no liquid flows out.

19) Remove the slurry reservoir-column blank-endfitting assembly from the pump.

20) Clamp the reservoir into a vice.

21) Unscrew the bushing attaching the column blank to the reservoir. If the column does not easily detach from the reservoir, carefully grab the column blank with needle nose pliers and tap the pliers with a small hammer until the column comes free.

22) Quickly attach the column to the injection valve port and pressurize the column with the desired solvent.

23) The column is now ready to equilibrate with the solvent mixture of choice.

Appendix B

Amino Acid Three Letter and One Letter Abbreviations and Physical Masses

Proper Name	Three Letter Abbreviation	One Letter Abbreviation	Physical Name (u)
Alanine	Ala	A	89.04767
Arginine	Arg	R	174.11165
Asparagine	Asn	N	132.05347
Aspartic Acid	Asp	D	134.04531
Cysteine	Cys	C	121.01974
Glumatine	Gln	Q	146.06912
Glutamic Acid	Glu	E	148.06096
Glycine	Gly	G	75.03202
Histidine	His	H	155.06946
Isoleucine	Ile	T	131.09462
Leucine	Leu	L	131.09462
Lysine	Lys	K	146.10551
Methionine	Met	M	149.05104
Phenylalanine	Phe	F	165.07897
Proline	Pro	P	115.06332
Serine	Ser	S	105.04258
Threonine	Thr	T	119.05823
Tryptophan	Trp	W	204.08986
Tyrosine	Tyr	Y	181.07388
Valine	Val	V	117.07897

APPENDIX C

Recent reference material for on-line LC/MS

The following references to recent work in on-line LC/MS are classified by the ionization method used in the mass spectrometer. A separate category is given for reviewed articles.

a) Chemical Ionization

a1) W. Erdahl and O. Privett, JAOCSA 62(1985)786.

a2) J. Van der Greef, L. Nijssen, H. Maarse, M. Ten Noever de Brauw, D. Games and N. Alcock, Dev. Food Sci. 10(1985)603.

a3) T. Covey, E. Lee and J. Henion, Anal. Chem. 58(1986)2453.

b) Direct Liquid Introduction

b1) F. Alderweireldt, E. Esmans and P. Beboes, Nucleosides Nucleotides 4(1985)135.

b2) E. Esmans, P. Geboes, Y. Layton and F. Alderweireldt, Biomed. Mass Spectrom. 12(1985)241.

b3) T. Tsuda, G. Keller and H. Stan, Anal. Chem. 57(1985)2280.

b4) P. Hirter, H. Walther and P. Daetwyler, J. Chromatogr. 323(1985)89.

b5) R. Tiebach, W. Blaas and M. Kellert, J. Chromatogr. 323(1985)121.

b6) P. Arpion and C. Beaugrand, Int. J. Mass Spectrom. Ion Processes 64(1985)275.

b7) W. Niessen and H. Poppe, J. Chromatogr. 323(1985)37.

b8) E. Lee and J. Henion, J. chromatogr. Sci. 23(1985)253.

b9) W. Niessen, Chromatographia 21(1986)342.

c) Thermospray

c1) G. Schmelzeisen-Redeker, M. McDowall, U. Giessmann, K. Levsen and F. Roellgen, J. Chromatogr. 323(1985)127.

c2) D. Watson, S. Murray and G. Taylor, Biochem. Soc. Trans. 13(1985)1224.

c3) M. Vestal and G. Fergusson, Anal. Chem. 57(1985)2373.

c4) P. Games and E. Ramsey, J. Chromatogr. 323(1985)67.

c5) J. Chapman, J. Chromatogr. 323(1985)153.

c6) R. Voyksner, anla. Chem. 57(1985)153.

c7) C. Parker, L. Levy, R. Smith, K. Yagaguchi, S. Gaskell and K. Korach, J. Chromatogr. 344(1985)378.

c8) J. Joyce, R. Ardrey and I. Lewis, Biomed. Mass Spectrom. 12(1985)588.

c9) C. Edmonds, M. Vestal and J. McCloskey, Nucleic Acids Res. 13(1985)8197.

c10) C. Vestal and G. Fergusson, Int. J. Mass Spectrom. Ion Processes 70(1986)185.

c11) G. Schmelzeisen-Redeker, F. Roellgen, H. Wirtz and F. Voegtle, Org. Mass Spectrom. 20(1985)752.

c12) Fong Fu Hsu, C. Edmonds and J. McCloskey, Anal. Lett. 19(1986)1259.

c13) J. Ballard and L. Betowski, Org. Mass Spectrom. 21(1985)575.

d) Fast Atom Bombardment

d1) Y. Ito, T. Takeuchi, D. Ishii and M. Goto, J. Chromatogr. 346(1985)161.

e) Reviews

e1) K. Biemann, J. Chromatogr. Libr. 32(1985)55.

e2) G. Spiteller, Angew, Chem. 97(1985)461.

e3) K. Levsen, Gewaesserschutz, Wasser, Abwasser 72(1984)253.

e4) S. Tsuge, J. Chromatogr. Libr. 30(1985)217.

e5) S. Tsuge and K. Matsumoto, Tanpakushitsu Kakusan Koso 30(1985)1138.

e6) P. Vouros and B. Karger, New Methods Drug Res. 1(1985)45.

e7) A. Gouyette, Drug Fate Metab. 5(1985)247.

e8) R. Browner, P. Winkler, D. Perkins and L. Abbey, Microchem. J. 34(1986)15.

e9) T. Covey, E. Lee, A. Bruins and J. Henion, Anal. Chem. 58(1986)1451A.

REFERENCES

1) H.R. Morris, Nature, 286 (1980) 447.

2) C. Brooks, Phil. Trans, R. Soc. Lond. A, 293(1979)53.

3) R.D. Craig, R.H. Bateman, B.N. Green and D.S. Millington, Phil. Trans. R. Soc. Lond. A293(1979)135.

4) H.D. Beckey, Int. J. Mass Spectrom. Ion Phys. 2(1969)500.

5) W.D. Reynolds, Anal. Chem. 51(1979)283A.

6) K.L. Olson, J.C. Cook and K.L. Rinehart, Biomed. Mass Spectrom., 1(1974)358.

7) R.E. Honig, in Mass Spectrometric Analysis of Solids, ed. A.J. Ahern, Elsevier, (1966)16.

8) P. Sigmund, in Inelastic Ion-Surface Collisions, eds. H.H. Tolk, J.C. Tully, W. Heiland and C.W. White, Academic Press, (1977)121.

9) N. Winograd, Prog. Solid St. Chem., 13(1982)285.

10) D.F. Torgerson, R. Kowronski and R.D. Macfarlane, Biochem. Biophys. Res. Comm., 60(1974)616.

11) R.D. Macfarlane and D.F. Torgerson, Science, 191(1976)920.

12) A. Hedin, P. Hakansson, B. Sundqvist and R.E. Johnson, Phys. Rev. B, 31(1985)1780.

13) S. Della Negra, D. Jacquet, I. Lorthiois, Y. LeBeyec, O. Becker and K. Wien, Int. J. Mass Spectrom. Ion Phys., 53(1983)215.

14) A. Benninghoven and W. Sichtermann, Anal. Chem., 50(1980)1180.

15) M. Barber, R. Bordoli, G. Elliot, R. Sedgwick and A. Tyler, Anal. Chem., 54(1982)645A.

16) D.H. Williams, C. Bradley, S. Santikarn and G. Bojesen, Biochem. J., 201(1982)105.

17) A.M. Buko, L.R. Phillips, and B.A. Fraser, Biomed. Mass Spectrom., 10(1983)324.

18) A.L. Burlingame, J.O. Whitney and D.H. Russell, Anal. Chem., 56(1984)417R.

19) A.L. Burlingame, T.A. Baillie and P.J. Derrick, Anal. Chem., 58(1986)165R.

20) J.L. Gover, Biochem, Mass Spectrom., 12(1985)191/

21) F. Hillenkamp, in Ion Formation from Organic Solids, Springer Series in Chemical Physics, Vol. 25, ed. A. Benninghoven, Springer-Verlag (1983).

22) R.J. Cotter, J. Honovich, J. Olthoff, P. Demirev and M. Alaim, in Ion Formation from Organic Solids (IFOS III), Springer Processings In Physics, Vol. 9, ed. A. Benninghoven, Springer-Verlag, (1986)142.

23) K. Walter, U. Boesl and E.W. Schlag, Int. J. Mass Spectrom. Ion Phys. 71(1986)309.

24) J. Grotemeyer, U. Boesl, K. Walter and E.W. Schlag, JACS, 108(1986)4233.

25) S. Della Negra and Y. LeBeyec, Int. J. Mass Spectrom. Ion Proc., 61(1984)21.

26) L.S. Ettre, in HPLC, Advances and Perspectives, Vol. 1, ed. C. Horvath, Academic Press, (1980)2.

27) B.J. Millard, Quantitative Mass Spectrometry, Heydon and Son (1978).

28) J.C. Giddings, Anal. Chem., 35(1963)2215.

29) B.T. Chait and K.G. Standing, Int. J. Mass Spectrom. Ion Phys., 53(1983)125.

30) K.G. Standing, R. Beavis, G. Bolbach, W. Ens, F. Lafortune, D. Main, B. Schueler, X. Tang and J. Westmore, Anal. Instrum., 16(1987)173.

31) K.G. Standing, B.T. Chait, W. Ens, G. McIntosh and R.C. Beavis, Nucl. Instrum. Methods, 198(1982)33.

32) W. Ens, R.C. Beavis, G. Bolbach, D.E. Main, B. Schueler and K.G. Standing, Nucl. Instrum. Methods, A245(1986)146.

33) B.L. Karger and P. Vouros, J. Chromatogr., 323(1985)13.

34) H.G. Menet, P.C. Gareil and R.H. Rosset, Anal. Chem., 56(1984)1770.

35) R.P.W. Scott, J. Chromatogr.Libr., 11(1977)229.

36) W.H. McFadden, J. Chromatogr, Sci., 18(1980)97.

37) R.D. Smith, J. Burger, and A.L. Johnson, Anal. Chem., 53(1981)1603.

38) J. Stroh, J. Cook, R. Milberg, L. Brayton, T. Kihara, Z. Huang, K. Rinehart, Jr. and I. Lewis, Anal. Chem., 57(1985)985.

39) D.S. Millington, D.A. Yorke and P. Burns, Adv. Mass Spectrom., 8B(1980)1819.

40) P.J. Arpino, in Liquid Chromatography Detectors, ed. T.M. Vickery, Marcel Dekker, (1983)243.

41) P.J. Arpino, P. Krein, S. Vajta and G. Devant, J. Chromatogr., 203(1981)117.

42) R.C. Willoughby and R.F. Browner, Anal. Chem., 56(1984)2625.

43) C.R. Blakley and M.L. Vestal, Anal. Chem., 55(1983)750.

44) C.M. Whitehouse, R.N. Dreyer, M. Yamashita and J.B. Fenn, Anal. Chem., 57(1875)675.

45) M.L. Vestal, Mass Spectrom. Rev., 2(1983)447.

46) M. Bursey, C. Parker, R. Smith and S. Gaskel, Anal. Chem., 57(1985)2597.

47) P.A.Garteiz and M.L. Vestal, LC Mag., 3(1985)334.

48) J. Zeleny, Phys. Rev., 3(1914)69.

49) W.A. Macky, Proc. Roy. Soc. A, 133(1931)565.

50) B. Vonnegut and R.L. Neubauer, J. Colloid Sci., 7(1952)616.

51) D.J. Carswell and J. Milsted, J. Nucl. Energy, 4(1957)51.

52) M.A. Mawab and S.G. Mason, J. Colloid Sci., 13(1958)179.

53) F.R. Krueger, Chromatographia, 10(1977)151.

54) C.J. McNeal, R.D. Macfarlane and E.L. Thurston, Anal. Chem., 51(1979)2036.

55) R.P.W. Scott and P. Kucera, J. Chromatogr., 125(1976)251.

56) D. Ishii, K. Asai, K. Hibi, T. Jonokuchi and M. Magaya, J. Chromatogr., 144(1977)157.

57) J. Gluckman, A. Hirose, V. McGuffin and M. Novotny, Chromatographia, 17(1983)303.

58) V. McGuffin and M. Novotny, J. Chromatogr., 255(1983)381.

59) J.D. Pearson, N.T. Lin and F.E. Regnier, Anal., Biochem., 124(1982)217.

60) K.K. Unger, W. Messer and K.R. Krebs, J. Chromatogr., 149(1978)1.

61) I. Halusz, R. Indele and P. Vogtel, J. Chromatogr., 126(1976)19.

62) N.H.C. COoke and K. Olsen, J. Chromatogr. Sci. 18(1980)512.

63) Metals Handbook, 8th Edition, Vol. 2, American Society for Metals, (1967)621.

64) R. Beavis, W. Ens, and K.G. Standing, 31st Ann. Conf. on Mass Spectrom, and Allied Topics, Boston, Mass. (1983)679.

65) R.P.W. Scott and P. Kucera, J. Chromatogr., 169(1979)51.

66) R.P.W. Scott and P. Kucera, J. Chromatogr., 185(1979)27.

67) S.M. McCown, B.E. Morrison and D.L. Southern, Am. Lab., May(1984)82.

68) M. Ende and G. Spiteller, Mass Spectrom. Rev., 1(1982)29.

69) B.L. Karger, J.N. LePage and N. Tanaka, in HPLC, Advances and Perspectives, Vol. 1, ed. C. Horvath, Academic Press, (1980)113.

70) D.M. Desiderio and M.D. Cunningham, J. Liquid Chromatogr., 4(1981)721.

71) J.L. Meek and Z.L. Rossetti, J. Chromatogr., 211(1981)15.

72) M.T.W. Hearn, in HPLC, Advances and Perspectives, Vol. 3, ed. C. Horvath, Academic Press, (1983)88.

73) R. Beavis, G. Bolbach, W. Ens, D. Main, B. Schueler and K.G. Standing, 33rd Ann. Conf. on Mass Spectrom, and Allied Topics, San Diego, Ca., (1985)202.

74) R. Beavis, G. Bolbach, W. Ens, D. Main, B. Schueler and K.G. Standing, J. Chromatogr., 359(1986)489.

75) R. Beavis, W. Ens, K.G. Standing and J.B. Westmore, Int. J. Mass Spectrom. Ion Phys., 46(1983)471.

76) U. Gubler, P. Seeburg, B. Hoffman, L. Gage and S. Udenfriend, Nature, 295(1982)206.

77) S. Tamaki, W. Sichtermann and A. Benninghoven, Jap. J. Appl. Phys., 23(1984)544.

78) E.a. Jordan, R.D. Macfarlane, .R. Martin and C.J. McNeal, Int. J. Mass Spectrom. Ion Phys. 53(1983)345.

79) E.A. Jordan, C.R. Martin, C.J. McNeil and R.D. Macfarlane, 33rd Ann. Conf. on Mass Spectrom. and Allied Topics, San Antonio, Tx., (1984).

80) G. Jonsson, A. Hedin, P. Hakansson, B. Sundqvist, C. Save, P. Nielsen, P. Roepstorff, K. Johansson, I. Kamensky and M. Lindberg, Anal. Chem., 58(1986)1084.

81) B. Sundqvist, P. Roepstorff, J. Folman, A. Hedin, P. Hakansson, I. Kamensky, M. Lindberg, M. Salehpour and C. Save, Science, 226(1984)696.

82) M. Barber, R.S. Bordoli, R.D. Sedgewick and L. Teller, Org. Mass Spectrom., 16(1981)256.

83) A.M. Buko, L. Philips and B. Frase, Biomed. Mass Spectrom., 10(1983)408.

84) A.L. Lehninger, Biochemistry, Worth, (1975).

85) H. Fasold and G. Gunlack, in Methods of Enzymatic Analysis, Vol. 4, ed. H.U. Bergmeyer, Academic Press, (1974)1625.

86) J.B. Westmore, W. Ens and K.G. Standing, Biomed. Mass Spectrom., 9(1982)119.

87) P. Roepstorff and J. Fohlman, Biomed. Mass Spectrom., 11(1984)569.

88) L.M. Mallis and D.H. Russel, Anal. Chem., 58(1986)1076.

89) S. Della Negra, Y. Le Beyec and J.C. Tabet, Orsay Report IONO-DRE-85-22, Institute de Physique Nucleaire, Orsay, France, (1985).

90) This laboratory, unpublished results.

91) B. Schueler, R. Beavis, W. Ens, D. Main and K.G. Standing, Surf. Sci., 160(1985)571.

92) B.T. Chait and F.H. Field, Int. J. Mass Spectrom. Ion Phys., 41(1981)17.

93) R. Beavis, W. Ens, M.J. Nemer, K.K. Ogilvie, K.G. Standing and J.B. Westmore, Int. J. Mass Spectrom. Ion Phys., 46(1983)475.

94) B.T. Chait and F.H. Field, Int. J. Mass Spectrom. Ion Phys., 41(1981)17.

95) C.F. Ijames and C.L. Wilkins, 32nd Ann. Conf. on Mass Spectrom. and Allied Topics, San Antonio, Tx., (1984)588.

96) D.M. Desiderio, Int. J. Mass Spectrom. Ion Proc., 74(1986)217.

97) J.T. Stults and J.T. Watson, Biomed. Environ. Mass Spectrom., submitted (1987).

98) R.S. Johnson, S.A. Martin and K. Biemann, Anal. Chem., submitted (1987).

99) X. Tang, R. Beavis, W. Ens, B. Schueler and K.G. Standing, 34th Ann. Conf. on Mass Spectrom. and Allied Topics, Cincinnati, Ohio, (1986)171.

100) M. Briggs and J. Brotherton, Steriod Biochemistry and Pharmacology, Academic Press. (1970).

101) D.F. Hunt, W.M. Bone, J. Shabanowitz, J. Rhodes and J.M. Ballard, JACS, 53(1981)1704.

102) I. Katakuse and D.M. Desiderio, Int. J. Mass Spectrom. Ion Proc., 54(1983)1.

103) K. Rinehart, Jr., L. Gaudioso, M. Moore, R. Pandey, J. Cook, Jr., M. Barber, R. Bordoli, R. Sedgewick, A. Tyler and B. Green, JACS, 103(1981)6517.

104) P. Roepstorff, P. Hojrup and J. Moller, Biomed. Mass Spectrom. 12(1985)181.

105) W. Ens, R. Beavis, G. Bolbach, B. Schueler, K.G. Standing and J.B. Westmore, 33rd Ann. Conf. on Mass Spectrom. and Allied Topics, San Diego, Ca., (1985)253.

106) F. Lafortune, J.B. Westmore, X. Tang and K.G. Standing, in preparation.